Identification of disease causing genes in families with skeletal and ophthalmological disorders

By

Rana Muhammad Kamran Shabbir

Human Genetics Lab

Department of Zoology

Faculty of Biological Sciences

Quaid-i-Azam University, Islamabad, Pakistan

2020

Identification of disease causing genes in families with skeletal and ophthalmological disorders

PhD Dissertation

A dissertation submitted in partial fulfilment of requirements for degree of Doctor of Philosophy in Human Genetics

Supervised by:

Professor Dr. Sajid Malik

Conducted by

Rana Muhammad Kamran Shabbir

Human Genetics Lab

Department of Zoology

Faculty of Biological Sciences

Quaid-i-Azam University, Islamabad, Pakistan

2020

Author's Declaration

I **Mr. Rana Muhammad Kamran Shabbir** hereby state that my PhD thesis titled "Identification of disease causing genes in families with skeletal and ophthalmological disorders" is my own work and has not been submitted previously by me for taking any degree from Quaid-i-Azam University, Islamabad, Pakistan.

At any time if my statement is found to be incorrect even after my Graduate the University has the right to withdraw my Ph.D. degree.

Mr. Rana Muhammad Kamran Shabbir

Date: 11-08-2021

Certificate of Approval

This is to certify that the research work presented in this thesis, entitled "Identification of disease causing genes in families with skeletal and ophthalmological disorders" was conducted by **Mr. Rana Muhammad Kamran Shabbir** under the supervision of **Prof. Dr. Sajid Malik**. No part of this thesis has been submitted anywhere else for any other degree. This thesis is submitted to the Department of Zoology of Quaid-i-Azam University, Islamabad in partial fulfillment of the requirements for the degree of Doctor of Philosophy in Field of Human Genetics.

Student Name: **Mr. Rana Muhammad Kamran Shabbir** Signature:

Examination Committee:

a) External Examiner 1: Signature:

Dr. Afsar Mian
Professor (Retd.)
House No. 1273, Street No. 59
Sector II, Gulshan Abad, Adayala road,
Rawalpindi

b) External Examiner 2: Signature:

Dr. Naeem Akhtar
Professor /Dean
Rawalpindi Medical University and
Allied Hospital, Rawalpindi

Supervisor Name: **Prof. Dr. Sajid Malik** Signature:

Name of HOD: **Prof. Dr. Sajid Malik** Signature:

Date: 11-08-2021

QUAID-I-AZAM UNIVERSITY
DEPARTMENT OF ZOOLOGY

No. Zoo (PhD)-2021/ Dated:

Ph.D. Examination
Defence of Thesis

Name of student: **Mr. Rana Muhammad Kamran Shabbir**

Title of thesis: "Identification of disease causing genes in families with skeletal and ophthalmological disorders"

Supervisor: **Prof. Dr. Sajid Malik**

Date of Viva-Voce: 11-08-2021

The candidate has/~~has not~~ **successfully** defended his thesis.

The candidate is **recommended**/~~not recommended~~ for the award of Ph.D. degree.

EXTERNAL EXAMINERS

1. **Dr. Afsar Mian**
   Professor (Retd.)
   House No. 1273, Street No. 59
   Sector II, Gulshan Abad, Adayala road,
   Rawalpindi

2. **Dr. Naeem Akhtar**
   Professor /Dean
   Rawalpindi Medical University and
   Allied Hospital, Rawalpindi

11/8/2021

3. **Prof. Dr. Sajid Malik**
   Research Supervisor

Prof. Dr. Sajid Malik
Chairman

Controller of Examinations

QUAID-I-AZAM UNIVERSITY
DEPARTMENT OF ZOOLOGY

No. Zoo (PhD)-2021/ Dated:

CERTIFICATE

This is to certify that **Mr. Rana Muhammad Kamran Shabbir,** Ph.D. scholar has incorporated typographic corrections and suggestions as required by the External Examiners in the thesis.

The title of his thesis is as under:

"Identification of disease causing genes in families with skeletal and ophthalmological disorders"

Dr. Afsar Mian
Professor (Retd.)
External Examiner

11/8/24

Dr. Naeem Akhtar
Professor
External Examiner

Prof. Dr. Sajid Malik
Research Supervisor and Chairman

Controller of Examinations

Plagiarism Undertaking

I solemnly declare that research work presented in the thesis titled "Identification of disease causing genes in families with skeletal and ophthalmological disorders" is solely my research work with no significant contribution from any other person. Small contribution / help wherever taken has been duly acknowledged and that complete thesis has been written by me.

I understand the zero tolerance policy of the HEC and Quaid-i-Azam University towards plagiarism. Therefore I as an Author of the above titled thesis declare that no portion of my thesis has been plagiarized and any material used as reference is properly referred/cited.

I undertake that if I am found guilty of any formal plagiarism in the above titled thesis even after award of Ph.D degree and that HEC and the University has the right to publish my name on the HEC/University Website on which names of students are placed who submitted plagiarized thesis.

Student / Author Signature: _____

Name: **Mr. Rana Muhammad Kamran Shabbir**

Dedicated To

Holy Prophet Muhammad ﷺ

&

My Loving Parents

(Naseem Akhtar and Muhammad Shabbir)

&

Family Members

Acknowledgment

I offer my humblest and sincere thanks to Almighty ALLAH, Who bestowed me with potential and ability to make a solid contribution to already existing ocean of knowledge and I also feel pleasure to offer thanks for Holy Prophet Hazrat Muhammad (PBUH), Who showed us the right path and enabled us to recognize our creator.

This work would not have been possible without the support and encouragement of my teacher Dr. Sajid Malik, under whose supervision I chose this topic and began the thesis. When I registered at QAU, I was nothing but today I am able to submit this thesis. He always has been a continuous source of encouragement for me.

I am grateful to Dean Faculty of Biological Sciences; Prof. Dr. Muhammad Shahab and chairman department of Zoology; Prof. Dr. Sajid Malik for providing pre-requisites for this work and thus facilitating this task.

I am very thankful to Prof. Dr. Jan Marshal Friedman and his team at the University of British Columbia, Vancouver, Canada, for giving me training in state of Next Generation Sequencing Data Analysis and facilitating me during my stay in Canada. I would also extend my thanks to the Higher Education Commission of Pakistan, for providing me funding for this visit through IRSIP scheme.

I am highly indebted to our collaborator Prof. Dr. Aslihan Tolun and her entire team at the Molecular Genetics Laboratory, Istanbul technical University and Bogazici University Istanbul, Turkey. She guided me throughout my studies and provided substantial contribution to my research. She is unique in her scientific understanding, support, and work ethics.

Clerical and technical assistant in scientific research is an undeniable important element. So, I am righteous in thanking Syed Mujahid Hussain Shah (Lab. assistant), Naeem Masih (Senior Clerk) and Samiullah (Junior Clerk) for their thorough and in time assistance.

I am highly thankful to my senior Dr. Muhammad Afzal for his help in terms of polite behavior, positive criticism and moral support that he provides me whenever I need at any time at any occasion during the field work and compilation of thesis and he never disappointed me.

I am highly grateful to all those families and subjects whose gave their consent and participated in the study. I am also thankful to all those people who helped and facilitated me during field work.

I also want to pay special thanks to my PhD lab fellows/juniors Ms. Rehana Yasmin, Ms. Syeda Farwa Naqvi, Ms. Qandeel Zahra, and Anisa Sahar. All these respected ones assist and helped me in blood samples processing.

I am thankful to the M. Phil colleagues at my Lab of Human Genetics, for their cooperation and nice company, especially, Mr. Salman Ahmad, Ms. Rabbiya Fareed, Ms. Aqeela Nawaz, Ms. Sadia Saleem, Ms. Anoosha Hassan, Mr. Qazi Waheed, Ms. Saba Rafiq, Ms. Summaya, Ms. Sapna Usman, Mr. Muhammad Naeem, Ms. Muqadssa Naureen, Ms. Filza and others.

In the end I owe my gratitude to my parents whose countless love, prays and encouragement and I achieved this academic task only because of their efforts and sacrifices that they done for me.

Rana Muhammad Kamran Shabbir

List of Table

List of Figures

List of Acronyms

Abbreviation	Elaboration
AMP	Adenosine monophosphate
AP	Anterior posterior
AR	Autosomal recessive
BACs	Bacterial artificial chromosome
BAM	Binary Alignment Map
BMs	Basement membrane
BWA	Burrows-Wheeler Aligner
CA	Congenital anomalies
CACP	Camtodactyly arthropathy coxa-vara pericarditis
CGH	Comparative genomic hybridization
CHD	Congenital heart defects
CNVs	Copy number variations
CT	Computer topography
DNA	Deoxy ribose nucleic acid
dNTP	Deoxy Nucleoside triphosphate
ECM	Extracellular matrix
EORD	European Organization of Rare Diseases
FISH	Fluorescence in situ hybridization technique
FSA	Fetus structure anomalies
GAGs	Glycosaminoglycans
GHIS	Growth hormone insensitivity syndrome
GHR	Growth hormone receptor
GUS	Genes of unknown significance
ICD	International Classification of Diseases

IGF	Insulin like growth factor
IHH	Indian hedgehog
IRB	Institutional Review Boards
JTS	Japanese Teratology Society
KNO1	Knobloch syndrome 1
LOD	Logarithm of odds
LS	Laron syndrome
MCH	Mean corpuscular hemoglobin
MCP	Metacarpophalangeal
MCV	Mean corpuscular volume
MPS	Massively parallel sequencing
NGS	Next generation sequencing
OMIM	Online Mendelian Inheritance in Man
PCR	Polymerase chain reaction
PGs	Proteoglycans
PIJ	Proximal interphalangeal joints
PSB	Phospho-sulfate binding site
RFLPs	Restriction fragment length polymorphism
RNA	Ribo nucleic acid
SAM	Sequence Alignment/Map
SDs	Skeletal dysplasias
SNVs	Single nucleotide variant
SSCP	Single strand conformation polymorphism
SULTs	Substrate specific sulfotransferases
TLC	Total leukocytes
TSH	Thyroid stimulating hormone;
UCSC GB	University of California Santa Cruz genome browser

UPD	Uniparental disomy
USG	Ultra-sonography
WBCs	White blood cells
WHO	World health organization
YACs	Yeast artificial chromosome

Table Contents

Abstract

Hereditary and congenital anomalies are common in Pakistan and are a significant cause of morbidity and mortality. Generally, the monogenic disorders occur due to heterozygous dominant or homozygous recessive mutations. Here, the recessive mutations causing rare diseases usually appear due to increased inbreeding. The current study was aimed to identify the causative variants segregating with autosomal recessive malformation in Pakistani families. Five families with rare hereditary skeletal and ophthalmological disorders were recruited from Southern Punjab, Pakistan. DNA of the available affected and unaffected subjects was extracted from peripheral blood for molecular study. SNP genotyping carried to find the candidate chromosomal region and exome sequence was done to find candidate variants causing diseases in the recruited families and identified mutations validated by Sanger sequencing. These families were resolved by identifying five different mutations: (i) In family 1, a novel homozygous deletion c.463-477del p.(155-159del) in *CHST11* was observed to cause osteo-chondrodysplasia with malformed digits and skeletal defects. This finding confirms the role of *CHST11* in skeletal morphogenesis but also indicate that *CHST11* mutation has variable manifestations and includes a range of digit malformations and skeletal defects. (ii) In family 2, a homozygous deletion encompassing *MYADML2* and *PYCR1* genes was observed to causes new syndromic phenotype with unusual skeletal malformation with features of cutis laxa. The unusual clinical features included lack of cranial symmetry, displaced fused sagittal sutures, maxillary hypoplasia, mandibular prognathia, teeth abnormalities, delayed bone maturity, multiple joints dislocation, malformed patellae, intracondylar fissures in hummers, scapular dyskinesis, lumbar lordosis, protruding chest, clavicles were prominent clevicles, long, limbs, reduced 5th digital rays, and transvers creases in digits. Additionally, features of cutis laxa were present in all affected sibs. Mutations in *PYCR1* caused autosomal recessive cutis laxa (ARCL) and all patients had common features of ARCL whereas *MYADML2* is a gene of unknown function and has not been associated with disease. This study reported a possible phenotype related to mutation in *MYADML2* gene that causes impaired bone patterning and maturation. The study findings provide a start point for future studies on the function of MYADML2 protein. Discovery of new patients requires confirming the *MYADML2* mutation related

phenotype. (iii) In family 3, a homozygous variant in *GHR* gene c.442G>C was implicated in proportionate dwarfism Laron type. This molecular report confirmed the diagnosis of Laron syndrome and suggestive for to develop the diagnostic tests for carrier testing, prenatal and premarital screening for genetic counselling of the families. (iv) In family 4, a homozygous two-base pair deletion c.4054_4055delCT in *COL18A1* was implicated in Knobloch syndrome with unusual features like chest abnormality, low sweating, slow bleeding in wounds, low sensitivity to pain and abnormal skin pigmentation. However, the range of clinical symptoms evident in the present family is surprising and taken together with other studies; this study further expands the phenotypic manifestation of KNO1. (v) In family 5, a homozygous deletion C.2861_2862delAA in coding region of *PRG4* was detected in patients that had camptodactyly-arthropathy-coxa vara-pericarditis syndrome with new clinical features like brachydactyly, small nails, scoliosis, and barrel shaped chest. Conclusively, the study results might be helpful to establish genotype-phenotype correlation of the CACP. In conclusion, the study results may prove helpful for understanding the puzzling nature of the inherited malformation. This understanding may lead to novel strategies by which the rare disorders can be promptly diagnosed, reduced or prevented. Study could be beneficial for clinicians and it would be highly informative to setup the centers for genetic counseling as well as equally useful for various medical centers and institutions.

CHAPTER 1

INTRODUCTION

Chapter 01 Introduction

1.1: Genes and Genetic disorders

A genome is a complete set of genetic information, including protein-encoding genes and other DNA sequences (Lewis 2009). Any dysfunction in the genome leads to genetic disorder. This dysfunctioning may be single base change, chromosomal aberrations, i.e., deletion or addition of segment of chromosomes or whole chromosomes and change in chromosome sets and number. These genetic disorders categorize as monogenic, chromosomal irregularities, multifactorial and can be transmitted from parents to offspring(Lewis 2009).

Any part of the genome can be affected by the mutation, including sequences that control transcription or encode proteins; repeats in introns and exon splicing sites critical for intron removal. Mutations can change function and may be harmful, have no effect, or may be beneficial. Most of the mutations are loss-of-function mutations which are involved in the cause of human disorders (Collins *et al.* 2004).

1.2: Congenital anomalies

Congenital anomaly (CA) includes any morphological, functional, biochemical or molecular defects that may develop in the embryo and fetus from conception until birth that is present at birth, whether detected or not (Cardoso-dos-Santos *et al.* 2020). CA is permanent change with varying cosmetic consequences due to defective development in body structures during prenatal life. These can cause lifelong physical, mental, visual, and auditory disabilities to its carrier if not managed properly that has negative impact on human and economic life to the affected person, their families, and communities (Singh *et al.* 2014). Parental emotional response (denial, feelings of guilt, worry, grieving and shame) occurs with the birth of an infant with major anomalies. So their meaningful counseling is very important (Singh & Gupta 2009).

Congenital anomalies responsible for high morbidity and infant mortality. Their etiology is associated with physical, chemical, biological, or genetic and environmental factors (de Almeida Brasil & D'Angeles 2014). Anomalies based on the severity of symptoms are divided into two categories: major and minor. Major anomalies are defined as anatomical anomalies that affect an individual's life and natural performance. Minor anomalies are referred to structural changes that do not require treatment or can be improved through simple methods (Vatankhah *et al.* 2017). The most common congenital anomalies include the neural tube defects, cardiovascular and musculoskeletal defects (El Koumi *et al.* 2013). The prevalence rate of congenital anomalies is high in middle- and low-income countries. It is estimated that approximately 95% of the children die in low income countries from birth defects due to limited health resources (KIng 2008). The incidence and spectrum of congenital morbidities vary among geographical variations, sampling and analyzing methods and different population structures and matting patterns (ICBDSR 2014; Morris *et al.* 2018).

Congenital anomalies mostly involve central nervous system, musculoskeletal, limbs, cardiovascular system, gastrointestinal system, with least affected urogenital system (Taye *et al.* 2019). About 60% cases of congenital malformations have unknown origin, 20% have genetic cause involving single gene mutation and chromosomal abnormalities, 8% due to environmental factors (drugs, chemical

exposures and maternal factors) while rest of anomalies result from multifactorial inheritance (Redin *et al.* 2017).

Worldwide, the congenital anomalies are the major cause of infant morbidity and mortality. Every year, during the first 28 days of life approximately, 270,000 newborns die due to congenital anomalies (Organization 2009). The 5-year mortality reported by world Health Organization in 2005, describe that within the first month of life >300000 newborns die due to congenital malformation (Janghorban & Azarkish 2016). About, 7.9 million children are born every year with a serious congenital anomaly, 3.3 million children (under five years) die from these severe defects, and 3.2 million who survive may develop a disability later in life (Ndibazza *et al.* 2011). The percentage of worldwide neonatal mortality due to congenital anomalies has increased from 3% in 2008 to 4.4% in 2013(Oestergaard *et al.* 2011; Liu *et al.* 2015).

1.3: Causes and risk factors

About 25% of congenital anomalies are multifactorial, which involves a complex interaction between genetic and environmental risk factors (Moore *et al.* 2013). During pregnancy, the exposure to drugs such as thalidomide, alcohol, certain environmental chemicals and high doses of radiation also involve in the cause of congenital anomalies. The advanced maternal and paternal age, parental consanguinity and low birth weight has also been associated with occurrence of congenital anomalies (Taksande *et al.* 2010).

1.4 Global prevalence of congenital anomalies

The prevalence of birth defects varies in different geographical regions of the world, depends on the different environment factors and socioeconomic status. It has been estimated that 3-7% of children are born with birth defects (Sekhobo & Druschel 2001). This difference explains an important information on the prevalence, pattern and risk factors for congenital anomalies in different areas of world (Ekwere *et al.* 2011).

The incidence of congenital anomalies is 2.5% in India and 1.3% in China (Parmar *et al.* 2010). In the Middle East, there is 2–2.5%, prevalence of major congenital anomalies and the highest prevalence (7%) reported in consanguineous

marriages (Malla 2007). In the United States of America, 2-5% of all live births are affected by congenital anomalies (Sekhobo & Druschel 2001).

1.5: Consanguinity and congenital anomalies

About, 60% of congenital anomalies have no known origin (Moore *et al.* 2013). Parental consanguinity is as a recognized risk factor for congenital anomalies (Rittler *et al.* 2001). It has been estimated, the risk for birth defects in the children of first-cousin mating increase rapidly compared to non-consanguineous marriages (Stoll *et al.* 1999).

Consanguineous marriage means a union between biologically related individuals (Modell & Darr 2002). The overall rate of consanguineous marriages is 38% in Iran, 40% in Middle East and above 50% in Pakistan (Bittles & Black 2010; Iqbal & Van Bokhoven 2014). It has been estimated worldwide that consanguinity influences some reproductive health parameters such as postnatal mortality and rates of congenital malformations. The rate of homozygotes increases due to consanguinity and results in autosomal recessive genetic disorders (Tadmouri *et al.* 2009). Generally, the highest rates of consanguinity reported in rural areas and in society where people are less educated and poverty rate is high (Bittles *et al.* 1993).

The rate of consanguineous marriages is higher among parents of offspring with congenital birth defects as compared to general population (Dawodu *et al.* 2005). First cousin marriage mostly associated with an increased risk of congenital heart defects (CHD) (Khalid *et al.* 2006). It is reported that the rate of consanguinity high in parents of children with congenital hydrocephalus and neural tube defects (Rajab *et al.* 1998). Within *baradari* marriage and consanguinity increasing the rates of genomic homozygosity and that results the highest expression of autosomal recessive genetic disorders (Small *et al.* 2016).

1.6: How to classify human congenital anomalies?

Prenatal fetal developmental diseases whether visible or invisible, are termed congenital anomalies (CA), and they include the malformation of physical disabilities, neuro-motor loss of functions, inborn error of metabolism, etc. (Silva *et al.* 2018). The synonyms of CA include birth defect of malformations (CA due to abnormal body parts), disruption (CA due to disruptive process), dysplasia (CA due to abnormal

organization), and genetic defects (CA due to gene alterations). These birth defects are taken into account with prevalence of rate in the range of 2-5% out of all total live births in a general populations (Campos *et al.* 2018; Morris *et al.* 2018). According to European Organization of Rare Diseases (EORD), the anomalies with prevalence rate of 1/2000 live births are called rare diseases (RD) that may be neonatal with progressive and prolonged nature (Mazzucato *et al.* 2018). The more recently in 58th annual gathering of Japanese Teratology Society (JTS) with main theme "congenital anomalies as variants" mean everyone has genetic variants which cause inborn disorders in some situations (Numabe 2018).

International Classification of Diseases (ICD) is the foundation that monitors standard protocols to report the health and diseases globally. Its 11th version the succeeded version of ICD-10 has been released on 06/2018 and members countries are preparing for its implementations and the partner countries will start its use in 2022 after the submission in 72nd world health assembly in 2019 by WHO (Chute 2018).

From ICD-10 version 2016, the congenital malformations, deformations, and chromosomal abnormalities are classified into 11 groups (Table 1.1).

Table 1.1. Major group of congenital anomalies

Sr. No	*Congenital malformation of*	*ICD-10 codes*
1	Nervous system	Q00-Q07
2	Eye, ear, face, and neck	Q10-Q18
3	Circulatory system	Q20-Q28
4	Respiratory system	Q30-Q34
5	Cleft lip/palate	Q35-Q37
6	Digestive system	Q38-Q45
7	Genital organs	Q50-Q56
8	Urinary system	Q60-Q64
9	Musculoskeletal system	Q65-Q79
10	Other organs e.g skin	Q80-Q89
11	Unclassified chromosomal anomalies	Q90-Q99

Source: http://apps.who.int/classifications/icd10/browse/2016/en#/XVII.

Most of these Mendelian phenotypic variations are monogenic traits which are caused by different genetic, and environmental factors (Hamosh *et al.* 2005). These anomalies may be nonsyndromic (isolated anomalies), sequence (multiple anomalies due to defects in pathologic cascade pathway), associated (anomalies that developed altogether always), and syndromic (complex of different kinds of anomalies) (Bermejo-Sánchez *et al.* 2018).

1.7: Patho-mechanism of congenital anomalies

The searching and understanding for molecular genetic causes of Mendelian phenotypes is the basic focus of human genome project to develop the genotypic-phenotypic correlation in addition to study about the gene functions, regulation, and biological process that may prove helpful to develop the therapeutics against different human diseases (Chong *et al.* 2015). Several genetic forces are involved in establishment various diseased conditions given below.

1. According to latest OMIM statistics (11th Sep. 2020), there are 16,348 described genes, 6732 total phenotypes with known genetic basis, 4326 total number of genes with phenotype causing mutation, and 1536 described phenotype with unknown molecular basis.

2. In genome changes in repeated sequences trinucleotide repeats/copy number variants have lethal effects on expressions of genes, RNA and proteins. It means changes in these repeat sequences led to onset of diseases pathology by inducing somatic mutations, unstable metabolic pathways, oxidative DNA breaks, etc (McMurray & Vijg 2014).
3. Central to life is genes control mechanism, which work in precise manners but there is gap between occurrence of human diseases and gene control. It means there are some regulating mediums/factors that act through this gap and are very important for the normal development of embryo or fetus (Karnuta & Scacheri 2018). Human embryo/fetus growth is complicated dynamic developmental process whose work is dependent on genes, hormones, nutrients, and different environmental agents (Argente & Pérez-Jurado 2018). Therefore, if developmental plan is deteriorated due to illegal involvement of the regulatory components then normal growth failure resulted in different clinical disorders in fetus. The fetus structure anomalies (FSA) create problems in 3% of pregnancies and these are main cause of disability and mortality among the children all over the world (Vatankhah *et al.* 2017).
4. Enhancers are *cis*-acting regulatory sequences, which bridge the gap between gene control and anomalies development. These regulatory sequences are the parts of non-coding nucleic acid and are in large numbers as compared the exons the protein coding part of DNA. Many enhancers in combine way regulate the single gene control mechanism. So if any alteration occurs in the enhancers then it resulted in different type of disorders in human. The possible ways by which enhancers altered are recently reviewed (Karnuta & Scacheri 2018). The armed biotechnologies uncovered the changed enhancer-gene control mechanism with emphasis on genetic diseases due to germline and somatic mutations in the non-protein coding region.

Apart from the genetic causes, consanguinity is another important factor that influences the genetic burden of diseases over a population. About 10% of the congenital disorders are associated with traditional consanguinity (Yan *et al.* 2015). Inbreeding is major subject of clinical study and boosting autosomal recessive human disease by increasing the numbers of homozygotes in a specific human population. This aspect is stimulated by cultures, ethnicity, religions, geographic location, and

socio-economic status of the families/populations. The consanguineous unions among blood relatives are also susceptible factor to occur the human diseases (Fareed & Afzal 2017). So the populations of Pakistan, India, and Bangladesh are useful for the discovery and study of recessive genes (Yan *et al.* 2015).

1.8: Understanding disease causing mechanisms

Advance genetic analyses enable us to understand the pathomechanism of the congenital anomalies. The invention of next generation sequencing (NGS) technologies accelerates the rate of identification of disease causative genes. This technology includes different modules (Table 1.2) for molecular elucidation FSA at gene level by linkage mapping and genome sequencing of (Chitty 2014). The NGS is productive and cost-effective techniques, which are being in use robustly. These technologies have been utilized in large number of studies and their blessing were also reviewed by different researchers (Gulati & Somlo 2018; Mone *et al.* 2018).

Table 1.2: Description of different techniques of NGS

Sr. No	Modules of NGS	Description
1	Whole Genome Sequencing (WGS)	To sequence the coding and non-coding regions of DNA.
2	Whole Exome Sequencing (WES)	To sequence the amino acids coding regions of genome.
3	Targeted Exome Sequencing (TES)	To sequence panel of known candidate genes to a specific phenotype.
4	Trio-Whole Exome Sequencing (tWES)	Identification of mutations in cases of two normal parents with single affected children.

1.9: Advancement in Genetic Techniques

1.9.1: Conventional cytogenetics techniques

DNA structure was proposed by Watson and Crick in 1952 and they share a noble prize for this discovery (Watson & Crick 1953). Human chromosome number

were identified with the peripheral leucocyte culture incorporation with fixation and staining method. This makes possible to identify the abnormalities on chromosomal level (Moorhead *et al.* 1960). Genetic technique on prenatal samples were applied by developing the Amniocentesis to check the aberrations in the fetus. After that high-resolution banding technique was developed for better visualization and more accurate results (Yunis 1976). Although, high resolution banding technique helped in identification of unknown chromosomal aberrations and syndromes but the submicroscopic aberrations that were not visible at 500-1000X remained undiagnosed.

1.9.2: Molecular cytogenetic techniques

To overcome the drawbacks of high-resolution banding technique fluorescence in situ hybridization technique (FISH) was developed. The first application of FISH was established in 1980 in which RNA was directly labelled with fluorophore was used as a probe for specific DNA sequences (Bauman *et al.* 1980). Human Genome Project revealed the accurate map of human genome, more and more probes from cloned and map segments (cosmids, BACs and YACs) become available for diagnosis purposes. Being time consuming and expensive to evaluate chromosomal rearrangements in whole genome by FISH led the development of new techniques such as array-based comparative genomic hybridization (CGH). CGH based on competitive hybridization of amplified tumor DNA and normal DNA hybridized on normal metaphase slide to detect genomic imbalances in tumor cells. For the identification of deletions and duplications at high resolution copy number variations (CNVs) technique was developed (Kallioniemi *et al.* 1992).

Array-CGH may fail to detect the recessive disease genes, mosaic aneuploidy, uniparental disomy (UPD), or heterochromatic rearrangements. Due to this advantage, it was considered to combine it with SNP array for better resolution of array-CGH (de Leeuw *et al.* 2012). These arrays have the highest resolution of all the available array-based platforms. The major drawback of array-CGH was that it can only detect the unbalanced rearrangements and is unable to detect balanced aberrations such as chromosome translocations, inversions and insertions. To overcome this problem translocation CGH (tCGH) was developed to address the recurrent translocations breakpoints (Greisman *et al.* 2011).

1.9.3: Molecular genetics

Larger genomic changes such as translocations, duplications and deletions can be detected by conventional karyotyping, FISH or array-CGH methods but detection of single nucleotide change is not possible. Discovery and automation of PCR greatly facilitated and simplified the detection of genomic mutations. PCR was used in restriction fragment length polymorphism (RFLPs) and single strand conformation polymorphism (SSCP). Both RFLP and SSCP were widely used in laboratories but were unable to detect every mutation. Un identification of mutations urged the discovery of new method Sanger sequencing that works on the chain termination method (Sanger *et al.* 1977). Introduction of first-generation automated DNA sequencer has improved the Sanger Sequencing method (Metzker 2005).

Advancement in the molecular genetics make it possible to launch the Human Genome Project. Human genome project not only revealed the complete the DNA sequence but also improved the sequencing technologies. Although Sanger sequencing was good, but it was still not time and cost effective. New technology massively parallel sequencing (MPS) erasing these technologies was developed by Lynx Therapeutics (Brenner *et al.* 2000). This technology using reads of multiple reactions simultaneously and generating large amounts of sequence data for exome sequencing, whole genome sequencing and transcriptome and methylation profiling. The high-throughput technology that is called next generation sequencing (NGS) technology reduced the cost of sequencing of a human genome to less than $1000. This technology is projected to sequence a human genome in 1 hour for $100 after new technological improvements in the near future. NGS technology is widely used for a variety of clinical and research applications, such as detection of rare genomic variants by whole genome resequencing or targeted sequencing for disease diagnosis (Marian 2012).

1.10: Sequencing technologies used in this study

Homozygosity mapping is wonderful strategy to hunt the genes various disorders with different modes of inheritance. *De-novo* variants are genes of unknown significance (GUS) in the genome. They, in particular with loss of functions, have paternal origin with genomic alteration ranging from to single nucleotide variant

(SNVs) to large structural variations through small insertions-deletions caused different genetic anomalies e.g neuro-developmental, skeletal disorders, etc. Such variants can be easily identified by using trio WES/WGS approach by using this approach, Thiffault et al. (2018) found 21 *de-novo* variants from samples of 971 sporadic cases. The reporting of de-novo variants in GUS may offer cost effective reanalysis.

Komlosi et al. (2018) suggested the use of NGS to find the lethal autosomal recessive genes by screening of heterozygous couples who carry at least one affected child or more affected individuals. The lethal recessive alleles do not appear in the general population due to mortality of fetus/newborn in prenatal/postnatal life. In such situations families advised to take prenatal and preimplantation diagnosis incases of more pregnancies and most effective method is non-invasive exome sequencing (NIES) (Best *et al.* 2018). But a number of limitations are linked to prenatal identification of molecular cause of FSAs (Mone *et al.* 2018).

On other hands, different NGS techniques are still depending on conventional sequencing method for the mutation validation. The conventional method of sequencing is direct polymerase chain reaction (PCR) based Sanger sequencing to elucidate the molecular bases of different hereditary human disorders. This method is very suitable in cases when we are sure about the type of the phenotype on the bases of clinical diagnosis. The Sanger sequencing is early and cost effective differential diagnostic molecular method and this method is successfully applied in the study (Afzal *et al.* 2017).

In summary, the genetic disorders caused by genetic instability which triggered by point mutations, copy number variants (CNVs), chromosomal alterations, DNA breaks, epigenetic changes, mobile genetics elements, telomere deterioration, mitochondrial damages (Maizels & Lupski 2013). So the diseases classification is in its developing procedure and it helps the geneticist and clinicians in diagnosis, prediction, counselling, controlling, and in explanation of disease etiology (Amberger *et al.* 2011).

1.11: Aim and objectives

The study was aimed at the understanding of underlying molecular basis of rare hereditary anomalies in Pakistani families. The specific objectives of the study were to identify variants segregating in families afflicted with autosomal recessive skeletal and ophthalmological disorders. For this purpose, modern techniques of SNP genotyping, exome sequencing and Sanger sequencing were utilized in five inbreeding families recruited from Punjab province, Pakistan.

CHAPTER 2

MATERIALS AND METHODS

Chapter 02 Materials and Methods

2.1 Study Approval and Families Recruitment

The current study protocols were approved by the Institutional Review Boards (IRB) of Quaid-i-Azam University, Islamabad and Bogazici University Istanbul, Turkey. Different families afflicted with genetic disorders were identified with the help of resource personals. Research team accompanied with medical doctors traveled to the residence areas of families. The resource personals were generally local notables, teachers, close family associates and community influential persons.

Written consent for clinical and genetic/molecular analysis were obtained according to Helsinki II protocol from all members who participated in the study. For complete diagnosis, the affected individuals from different families were brought to the hospitals for detailed clinical examination.

2.2 Pedigree Construction and Blood Sampling

Clinical and genetic assessment of five families were carried out in different areas of South Punjab, Pakistan. All the well-informed members of each family were interviewed, and pedigrees were generated based upon the information provided. Detailed medical histories, photographs, roentgenograms, ultra-sonography (USG), computed topography (CT) scan, hormonal and biochemical test depending upon family phenotype, were obtained from available family individuals. For genetic study, peripheral blood samples, up to 10 ml were collected in vacutainers by using 10 ml syringe from all participants.

2.3 Chemicals

All liquids and solid chemicals used in this study were purchased from Biochar, Riedel-de-Haen, Merck (Germany), Sigma (USA), Carlo Erba (Italy).

2.4. Solutions

2.4.1. List of solutions used in different methods

Solutions	Reagents
Cell Lysis Buffer	• 0.32m Sucrose • 1M Tris HCl (pH 7.5) • 1M Mgcl2
Nucleus Lysis Buffer	• 1M Tris HCl (pH 7.5) • 1M NaCl • 1M EDTA (pH 8)
Proteinase K Enzyme	• 20 mg/ml Proteinase K • dH_2O
Sodium dodecyl sulfate (SDS)	• 20% SDS (weight/volume) • dH_2O
Phenol	• 100g phenol • 100ml 50 mM Tris-HCl (pH 8.0)
Tris-HCL	• 121g Tris base • 800 ml dH_2O
Chloroform	• 99+ extra pure
Isoamyl alcohol	• 99+ extra pure
Ethanol	• Absolute Ethanol
TE Buffer	• 20 mM Tris-HCL • 1 mM EDTA (pH 8.0)

2.4.2 Polymerase Chain Reaction

Reagent	**Final Concentration**	**Quantity for 25µl of reaction mixture**
DNA	50ng/µl	1 µl
PCR buffer	2mM	2.5 µl
Forward Primer	10 Pico Mol	0.5 µl
Reverse Primer	10 Pico Mol	0.5 µl
dNTPs	25mM	0.5 µl
$MgCl_2$	-	1.5 µl
Taq Polymerase	5U/µl	0.4 µl
PCR Water		18 µl

2.4.3 Agarose gel electrophoresis

Solutions	Reagents
Agarose	• 2% Agarose • 0.5 X TBE buffer
10 X TBE Buffer	• 20 mM EDTA • 0.89 M Boric acid • 0.89 M Trizma base (pH 8.3)
6 X Loading Buffer	• 10 mM Tris-HCL (pH 7.6) • 50% Glycerol • 60 mM EDTA • 2.5 mg/ml Bromophenol Blue
Ethidium Bromide	• 10 mg/ml • dH_2O

2.4.4 Sanger sequencing

Solutions	**Reagents**
Reaction mixture	• 5.5µl of deionized water • 1 µl 5X sequencing buffer • 1.1µl DNA template (200ng) • 1µl primer (forward/reverse) • 1.5µl BigDye terminator
Stock solution	• 1µl of 3M sodium acetate (pH5.2) • 1µl of 100M sodium EDTA (pH5.2) • 0.5µl of 20 µl mg/ml glycogen
Absolute ethanol	• 70 µl
70% ethanol	• 150µl
Hi-Di Formamide (HDF)	• 20 µl

2.5 Enzyme

Important ingredient of PCR, DNA *Taq* Polymerase supplied with PCR buffer was used and purchased from Roche (Germany).

2.6 Oligonucleotide primers

The goal of oligonucleotide primer designing was achieved with the help of Primer3 software. To evaluate the secondary structures and self-annealing sites, OligoCalc was used. Primers were purchased from Macrogen. 1 ml dH_2O was used for the liquification of lyophilized primers. In order to use in PCR reactions 10 µM dilutions were prepared.

2.7 DNA commercial kits and molecular weight markers

Name	**Company (Country)**
Dream*Taq* PCR kit	Thermo Fisher Scientific (USA)
Gel Extraction kit	Qiagen (Germany)
PCR Purification kit	Qiagen (Germany)

2.8 Equipment and apparatus

Equipment	Company (Country)
-20°C Deep Freezer	Arcelik (Turkey)
480 LightCycler	Roche (Switzerland)
-80°C Ultra Freezer	Thermo Scientific (USA)
Allegra X-22R Centrifuge	Beckman Coulter (USA)
AMB430T Autoclave	Astell (South Korea)
DCode Universal Mutation Detection System	BioRad (USA)
Electronic Balance	Precisa (Switzerland)
Electrophoresis Gel Equipment	Thermo Scientific (USA)
Fotoforce 250 Electrophoresis Power Supply	Fotodyne (USA)
Gel Doc Documentation System	BioRad (USA)
Grant LTD 6G Thermostatic Water Bath	Grant (UK)
Horizontal DNA Electrophoresis Equipment	BioRad (USA)
Incubator HEPA	Thermo Scientific (USA)
J2-MC Centrifuge	Beckman Coulter (USA)
KD 200 Oven	Nuve (Turkey)
Lab Dancer Vario Vortex	Roth (Germany)
Micropipettes	Gilson (France)
MiniSpin Plus Centrifuge	Eppendorf (Germany)
MR3001 Magnetic Stirrer	Heidolph (Germany)
NanoDrop 1000 Spectrophotometer	Thermo Scientific (USA)
Orbital Incubator	Gallenkamp (UK)

P250A Power Supply	Sigma-Aldrich (Germany)
Power Pac Model 3000	BioRad (USA)
PTC-200 Thermal Cycler	MJ Research (USA)
Reax vortex mixer	Heidolph (Germany)
Rotamax 120 Minishaker	Heidolph (Germany)
T100 ThermalCycler	BioRad (USA)
Ultra-Pure Water Purification system	Hach-Lange (USA)
Universal 16R Centrifuge	Hettich (Germany)

2.9 Electronic databases

Following databases mentioned in Table 2.1 were approached during research study.

Table 2.1: List of databases approached during the study:

Database	Description	Homepage
1000 Genome	The detailed catalogue of human genetic variation and project designed for the sequence of 1000 anonymous individuals with different ethnic groups and.	http://www.internationalgenome.org/1000-genomes-browsers
Database of Genomic Variants (DGV)	A detailed catalogue of human genomic structural variations	http://dgv.tcag.ca/dgv/app/home
ENSEMBL Genome Browser	Scientific project at European Bioinformatics Institute to provide a centralized resource for studying the genome of our and different species.	https://asia.ensembl.org/index.html
Exome Sequencing Project (ESP6500)	The database was designed to discover the new genes contributing to blood, heart and lung disorders.	https://evs.gs.washington.edu/EVS/
Gene Cards	The database that provides genomic, transcriptomic, proteomic, genetic and functional information on all	https://www.genecards.org/

	known and predicted human genes.	
GeneDistiller	Tool that is used to query, select and project genes from within a linkage interval.	http://www.genedistiller.org/
Gene Ontology (GO)	Bioinformatics tool to unify the gene and gene products across all species.	http://geneontology.org/
Genome Aggregation Database (gnomAD)	Resource developed by the international collaborations with the goal aggregation and harmonizing both exome and genome sequencing data.	http://gnomad.broadinstitute.org/
Genome Data Viewer	Genome browser supporting the exploration and analysis of eukaryotic RefSeq genome assemblies.	https://www.ncbi.nlm.nih.gov/genome/gdv/
HomoloGene	Tool designed for the automated detection of homologs among the annotated genes of completely sequenced eukaryotic geomes.	https://www.ncbi.nlm.nih.gov/homologene
HomozygosityMapper	Tool used to obtain the homozygosity intervals across the genome.	http://www.homozygositymapper.org/
Human Splicing Finder 3.1	An online bioinformatic tool designed to predict the	http://umd.be/Redirect.html

	splicing signals.	
KEGG (Kyoto Encyclopedia of Genes and Genomes)	Resource database for understanding high levels of functions and utilities of the biological systems.	https://www.genome.jp/kegg/
Mendelian Clinically Applicable Pathogenicity (M-CAP)	First pathogenic tool used for classification of rare missense variant in the human genome.	http://bejerano.stanford.edu/mcap/
Mutation Taster2	Web based tool to evaluate the DNA sequence variants for their disease-causing potential.	http://www.mutationtaster.org/
NCBI PubMed	Database comprised of more than 29M citations for biomedical literature from MEDLINE, life science journals and online books.	https://pubmed.ncbi.nlm.nih.gov/
NCBI-BioProject	Collection of biological data related to a single initiative, originating from a single organization or form a consortium.	https://www.ncbi.nlm.nih.gov/bioproject/
OligoCalc (Oligonucleotide Properties Calculator)	OligoCalc, a web-based tool for calculating the physical properties of DNA and RNA oligonucleotides.	http://biotools.nubic.northwestern.edu/OligoCalc.html
Online Mendelian Inheritance in Man	OMIM is an online continuously updating database with human genes and genetic traits with focus on	https://www.ncbi.nlm.nih.gov/omim

(OMIM)	genotype-phenotype relationship.	
Polymorphism Phenotyping (PolyPhen-2)	The tool that predicts the possible impact of an amino acid on the structure and function of protein.	http://genetics.bwh.harvard.edu/pph2/
Primer3 software	Computer program that suggests PCR primers for a variety of applications e.g. creation of sequence tag sites for radiation hybrid mapping.	https://bioinfo.ut.ee/primer3-0.4.0/
Protein Variation Effect Analyzer (PROVEAN)	Software that is used to predict whether amino acids substitution or indels has an impact on the biological function of a protein.	http://provean.jcvi.org/index.php
Reactome	Tool that aimed to provide bioinformatic tools for visualization, interpretation and analysis of pathway knowledge to support basic research, genome analysis, modelling, system biology and education.	https://reactome.org/
SIFT (Sorting Intolerant from Tolerant)	Tool that predicts the potential impact of amino acids substitution on protein function.	https://sift.bii.a-star.edu.sg
SNPs 3D	Tool that assigns molecular functional effects of non-synonymous SNPs based on structure and sequence analysis.	http://www.snps3d.org/

UCSC Genome Browser	Online genome browser that provides access to genomic sequence data of vertebrate and invertebrates species.	https://genome.ucsc.edu/
UniProt (Universal Protein Resource)	Database that provides comprehensive, high quality and freely accessible resource of protein sequence.	https://www.uniprot.org/

2.10 Bioinformatics Tools

For the analysis of whole exome sequencing data few bioinformatics programs were used which are freely available on internet. These programs are mentioned below (Table 2.2):

Table 2.2: Bioinformatics tools used in whole exome analysis

Program Name	Description	Homepage
BWA (Burrows-Wheeler Aligner)	Software package for the alignment of short read against a reference genome, such as human genome.	http://bio-bwa.sourceforge.net/
SAMTools (Sequence Alignment/Map)	Package used for operating the large nucleotide sequences alignments in the SAM format including sorting, indexing and variant calling	http://samtools.sourceforge.net/
GATK (Genome Analysis Tool Kit)	A program used for discovery of SNPs/indels, Copy Number Variations (CNVs) and Structural Variations (SV).	https://gatk.broadinstitute.org/hc/en-us
Picard	Java based command line tool for manipulating the next-generation sequencing data in the format	https://broadinstitute.github.io/picard/

	of SAM/BAM files.	
BEDTools	A package for comparing large data sets genomic features with public and custom genome annotation tracks.	https://sourceforge.net/projects/bedtools/
IGV (Integrative Genomics Viewer)	Java based application used for visualizing the read alignment data stored in BAM files.	http://software.broadinstitute.org/software/igv/
ANNOVAR	A tool available for the functional annotations of genomic variants resulted from next-generation sequencing data. Annotation could be filter base, region based, or gene based.	https://annovar.openbioinformatics.org/

2.11 Isolation of genomic DNA from peripheral blood samples

In case of DNA extraction, 500µl blood was taken in sterile eppendorf tube. Pre-chilled cell lysis buffer (Solution A) was added in the tube and was mixed and the mixture in tube was left at room temperature for 15-20 minutes for osmotic swelling. After this incubation, the tube centrifuged at 13000 rpm and white blood cells pellet separated by discarding the supernatant and this step was repeated two times. After that, solution B, 20 µl SDS, and 15 µl PK were added in the tube containing the pellet and the overnight incubation was done at 37°C. After incubation, 500µl of fresh mixture of equal volume of Solution C (Phenol + Tris-HCl (4:1 ratio)) and Solution D (Chloroform + Isoamyl alcohol (24:1 ratio)) were added in the tube and was centrifuged at 6000rpm for 13 minutes. Transparent upper layer was collected in new eppendorf tube, added 500µl Solution D in that tube and was centrifuged at 6000rpm for 13 minutes. In the result of centrifugation, upper layer was placed in 15ml falcon tube, 55µl of Sodium acetate (3M, pH6) and 3 volumes of chilled absolute ethanol were added. Tube was gently inverted several times for DNA precipitation. The floating white thread of DNA was fished with the help of micropipette tip, washed in 70% Ethanol and was transferred to a new eppendorf tube. The tube was left open at room temperature until the ethanol evaporated. DNA was rehydrated by adding 150µl of TE Buffer and was stored at -4°C in freezer.

2.12. SNP genotyping

Whole-genome SNP genotype data of the affected individuals were generated at Macrogen Inc (South Korea) by using Illumina Human OmniExpress-24 BeadChip. Details about SNP genotyping performed from each family as given in the respective chapters (Chapter 3, 4, and 5) of the families as described in the following publications (Shabbir *et al.* 2018; Bölükbaşı *et al.* 2020).

2.12.1. Linkage Analysis and Homozygosity mapping

Linkage analysis, a statistical test calculates the LOD (logarithm of odds) score that associates the disease genes with a locus. Linkage analysis were performed

by using tool easyLinkage_v5.02. Family pedigree, SNP genome of family members and genetic map of the markers are necessary for the parametric linkage analysis.

Homozygosity Mapper (www.homozygositymapper.org) was used to perform the homozygosity mapping in autosomal recessive (AR) families and >100 kb homozygous regions were detected in patients. ALLERGO was used to construct the haplotypes for the identification of homozygous regions identical by descent (IBD). Homozygosity comparison in Excel (HCiE) developed by our collaborator in Turkey, was also used. HCiE is an MS Excel macro in which three different types of SNP genotypes AA, BB and AB in the individuals are differently color while markers are arranged according to their locations. In this way, homozygous intervals are detected among the affected subjects as well as observed whether they have same genotype within homozygous shared intervals.

ALLERGO, GeneHunter and Marline programs were used to calculate the multipoint LOD score. In case of AR inheritance, 0.0001 frequency was set, and full penetrance was assumed. Markers were selected at 0.01cM spacing and used in set of 30. MacroGen Inc provided the physical and genetic maps of markers. ALLERGO program was used to construct the haplotypes. Homozygosity was confirmed at the candidate loci by HCiE.

2.13 Whole exome sequencing

MacroGen Inc (South Korea) and Yale Centre for Genome Analysis paid services were utilized for exome sequencing. DNA sample of only one individual from each family was subjected to exome capture with Illumina TruSeq Exome Capture kit (Illumina, USA). Massively parallel paired-end sequencing with Illumina HiSeq 2500 was performed (Illumina, USA). TruSeq Exome Capture kit features are as follows (table 2.3):

Multiple steps are involved in obtaining the sequence information from exome sequencing and results in a list of variants within or near the coding regions of genome. From the Illumina TruSeq DNA Sample Preparation kit (Illumina, USA), sample library was prepared. In order to generate the sample library, 5-10µg of

genomic DNA was used as a starting material. Generation of multiplexed paired-end sequencing libraries by adding the adapter sequences to the DNA fragments is the basic goal of this step. In this step, genomic DNA is sheared to obtain the double stranded DNA fragments of 300-400 base pairs in average and overhangs are converted to blunt ends. 3′ ends are sealed with a single nucleotide "A" to prevent the ligation of blunt fragments. Adapters having "T" nucleotide at the 3′ ends are used for ligation of blunt fragments. Biotinylated capture probes of targeted regions are hybridized with blunt fragments soon after the ligation of adapters while unbound fragments are washed off. Fragments are hybridized onto the flow cell as the streptavidin beads pull out the biotinylated capture target. Flow cell is a solid surface containing forward and reverse adapters in spatially separated clusters. The capture target is amplified by bridge PCR with the help of the adapters and subsequent reaction takes place and data is stored in the sequencer (Fig. 2.1).

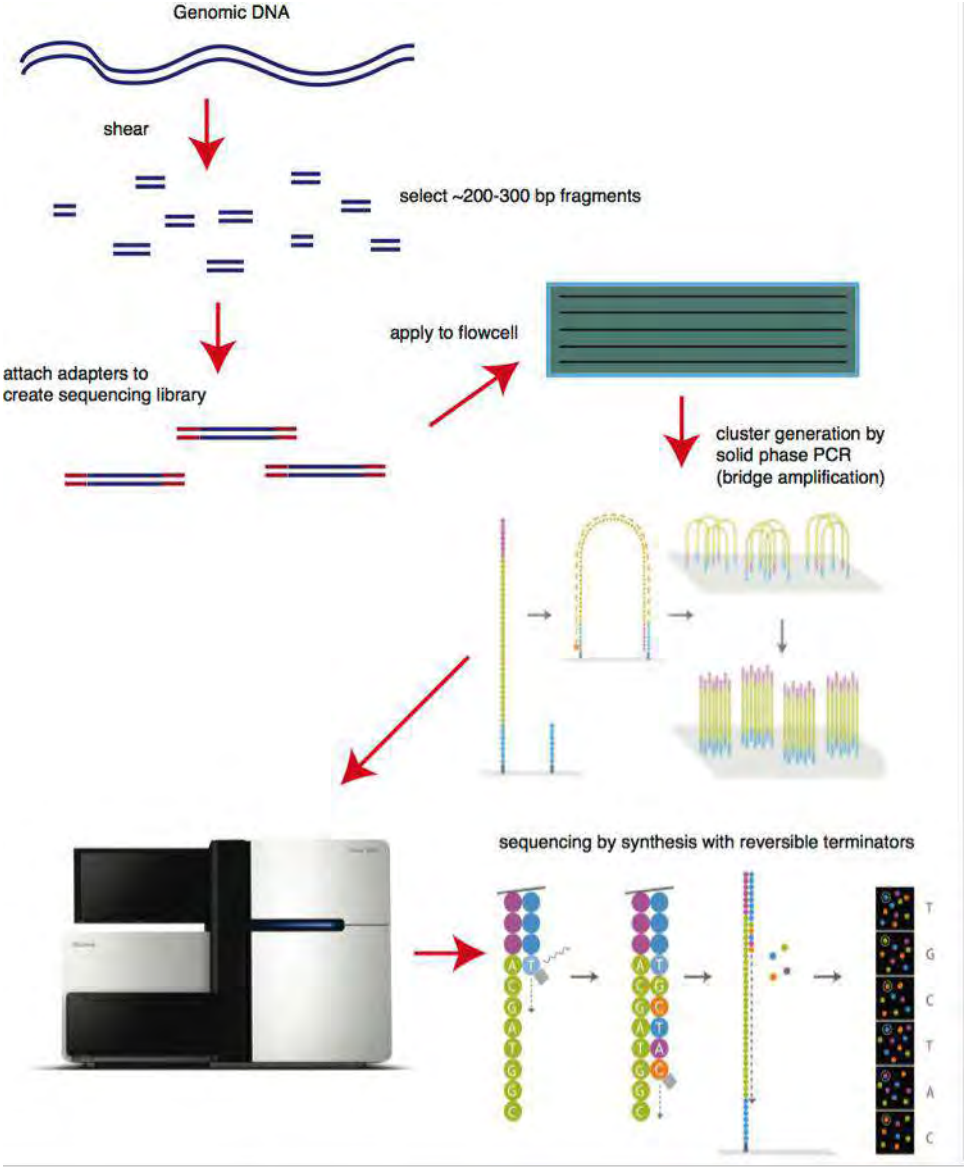

Figure 2.1: Illumina Sequencing Technology (Sequencing-by-Synthesis)

(The picture was adopted from: Sigma-Aldrich® Advanced Genomics)

2.13.2 Analysis of the exome sequencing file

Macrogen provided standard bioinformatics analysis services of exome sequencing data analysis with standard parameters by using packages such as BWA and SAMTools. Company provided an annotated list of variants in MS Excel file. However, in order to avoid the false negative calls and validate the results, bioinformatics analysis was performed again. For this purpose paired end ".fastq" files were obtained from company.

UCSC Genome Bioinformatics site was retrieved for the downloading of human reference genome sequence (assembly GRCh37/hg19). The downloaded assembly was unzipped; individually assembled chromosomes were concatenated to each other and were indexed. BWA (Burrows-Wheeler Aligner) program was used to align the pair-end reads to the reference genome and the final alignment was generated in SAM (Sequence Alignment/Map) format. SAMTools package was used to convert the SAM file into BAM (Binary Alignment Map) format. The resulting file was sorted, indexed and subjected to VCF (Variant Calling File) by using GATK (Genome Analysis Tool Kit), which outputs a list of variants that were different from the reference genome. ANNOVAR was used to annotate the list of variants which denotes the chromosomal location, dbSNP ID, region of the nucleotide change, exonic nucleotide change or splicing mutation. Regions of the exonic nucleotide change includes exonic, intronic, UTR, non-coding RNA or intergenic while type of exonic nucleotide change includes synonymous, non-synonymous, frameshift, stop gain or stop loss. Integrative Genomic Viewer (IGV) was used for the visualization of alignments. Commands used for the analysis and their purposes are given in table 2.3.

Table 2.3. Command line used in bioinformatics analysis of exome sequencing data and their purposes

Purpose	Command
To download the reference genome assembly from UCSC	http://hgdownload.soe.ucsc.edu/goldenPath/hg19/bigZips/hg19.fa.gz
To unzip the file	gunzip file.fa
Concatenates all chromosomes of the reference genome sequence	cat file.fa > file.fasta
Indexes the references genome	bwa index -a bwtsw file.fasta
Aligns paired end reads to the reference genome	bwa mem -M -t 8 file.fasta File_1.fastq File_2.fastq > file.sam
Cleans up unusual FLAGs such as read pairing information in the sam records created by BWA	samtools fixmate -O bam file.sam file.bam
Sorts the bam file with chromosomal coordinates	samtools sort -O bam -o file.sorted.bam file.bam
For adding or replacing the Read Groups	java -jar picard.jar AddOrReplaceReadGroups I=file_sorted.bam O=file_sorted.RG.bam RGID=1 RGLB=lib RGPL=illumina RGPU=index RGSM=file_sorted.RG.bam
To create the .fai file	samtools faidx hg19.fasta
To generate the .dict file	java -jar picard.jar CreateSequenceDictionary R=hg19.fasta O=hg19.dict
To generate the .idx file	java -jar gatk-package-4.0.4.0-local.jar IndexFeatureFile -F dbsnp_138.hg19.vcf
To generate the .idx file	java -jar gatk-package-4.0.4.0-local.jar IndexFeatureFile -F 1000G_phase1.indels.hg19.sites.vcf
For Base Recalibrator	java -Xmx4g -jar gatk-package-4.0.4.0-local.jar BaseRecalibrator -R

For Base Quality Score Recalibration	hg19.fasta --known-sites dbsnp_138.hg19.vcf --known-sites 1000G_phase1.indels.hg19.sites.vcf -I file_sorted.RG.bam -O file_recal_data.table java -Xmx4g -jar gatk-package-4.0.4.0-local.jar ApplyBQSR -R hg19.fasta -I file_sorted.RG.bam --bqsr-recal-file file_recal_data.table -O file_sorted.realigned.recal.bam
For marking and removing the duplications	java -Xmx4g -jar picard.jar MarkDuplicates REMOVE_DUPLICATES=TRUE INPUT=file_sorted.realigned.recal.bam OUTPUT=file_sorted.realigned.recal.rmdup.bam METRICS_FILE=file_marked_dup_metrics.txt
For Bam Indexing	java -jar picard.jar BuildBamIndex I=file_sorted.realigned.recal.rmdup.bam O=File_sorted.realigned.recal.rmdup.bam.bai
For generation of ".vcf" file	java -jar gatk-package-4.0.4.0-local.jar HaplotypeCaller --genotyping-mode DISCOVERY -R hg19.fasta -I file_sorted.realigned.recal.rmdup.bam --dbsnp dbsnp_138.hg19.vcf -stand-call-conf 30 -O alam_raw_variants-new.vcf
For annotation	Upload the data at http://wannovar.wglab.org/

2.14 Candidate genes and mutation screening

Mutations within genes/loci that emerged as the best candidates as a result of exome sequence analysis were selected. Candidates with high coverage, high-quality scores and predicted adverse impact on the protein were considered on top priority among the selected candidates. Minimum quality score accepted was 40 and threshold for enough coverage was assumed as four reads. Variants not falling in these criteria were assumed more likely as false positives. Nonetheless, all variants were taken in consideration. The variants that were reported in gnomAD and 1000 Genomes databases were removed if their frequency was equal to or more than 0.001. With respect to severity of mutation, expression in the tissues, gene functions and indication in animal models rare and novel variants were prioritized. Among the rare variants, the exome sequencing results was validated by Sanger Sequencing.

2.14.1 PCR amplifications

As a result of exome sequencing filtering, sites of strong candidate variants were subjected to PCR amplifications and then DNA sequencing for relevant individuals. PCR for each primer pair was performed using 30 ng genomic DNA, 0.2 U *Taq* DNA polymerase, 1X PCR buffer, 0.2 µM of each dNTP, 0.4 µM of each primer and water adding up to 25 µl.

2.14.2 Analysis of PCR products

The efficiency and the size of the products were checked on 2% agarose gel containing ethidium bromide for all the PCR reactions. PCR product (5 µl) was mixed with loading dye (1 µl) and was loaded on agarose gel. For electrophoresis 0.5X TBE was used as a running buffer at 10 volts/cm for 20 minutes. UV light was used in BIORAD Universal Hood II and Quantity One 4.6.9 software for the visualization of DNA fragments.

2.14.3 DNA sequence analysis

All the regions were amplified by PCR in 50 µl reactions in order to be analyzed with Sanger sequencing. 50-200 µl volume per sample was available depending upon the efficiency of reaction. All the samples were sent to MacroGen Inc (South Korea), where the sequence analysis was performed for all our projects.

CHAPTER 3

FAMILY I

Chapter 3. Novel homozygous variant c.463_477del p.(L155_N159del) in CHST11 cause osteo-chondrodysplasia with malformed digits and skeletal defects

3.1: Abstract

CHST11 is important for skeletal morphogenesis and its expression regulates Indian hedgehog (IHH) signaling in the developing growth plate. Up-till now, only 55-kb homozygous deletion encompassing the first coding exon of the *CHST11* was found in a woman with short stature, hand/foot malformation encompassing brachydactyly, campto-clinodactyly, hyperphalangy, and malignant lymphoproliferative disease and her deceased sister was similarly affected. Aside from this single report, there is no other pathogenic variant known to cause *CHST11* with a skeletal malformation. A six generations pedigree with autosomal recessive inheritance pattern of disease was recruited from Southern part of the Punjab. Physical and clinical assessment done by taking photographs and X-rays. Blood samples taken from nineteen subjects (7 affected and 12 unaffected) for DNA extraction to perform SNP and Exome sequencing. Sanger sequencing used to validate the mutation. Through SNP genotyping and exome sequencing, a novel homozygous in-frame deletion of 15 nucleotides in *CHST11* was identified. This mutation c.463_477del p.(L155_N159del) deduced to lead to the deletion of five highly conserved amino acids. In silico analysis predicted the mutation as protein damaging. The identified mutation caused an autosomal recessive phenotype, not described in OMIM database, in extended consanguineous Pakistani kindred. In the family, patients had an unusual combination of a limb malformation with variable expressivity accompanied by skeletal defects. The limb abnormalities were brachydactyly of certain fingers and toes, crossed-fingers/toes, clino-symphalangism of certain digits and syndactyly and polydactyly in feet whereas skeletal defects were mild short stature, scoliosis, dislocated patella and fibula, and pectus excavatum. Our findings confirm the vital role of *CHST11* in skeletal morphogenesis but also indicate that *CHST11* mutation has variable manifestations and includes a range of digit malformations and skeletal defects.

3.2: Introduction

Proteoglycans (PGs) are macromolecules on the surface of the cell and in the extracellular matrix and are responsible for specific mechanical, biochemical, and physical properties to tissues like growth plate, cartilage, and bones (Paganini *et al.* 2020). PGs are characterized by a core protein to which linear polysaccharides chains, glycosaminoglycans (GAGs) are linked (Iozzo 1998). For the proper functions of PGs, the sulfate groups that found on GAGs, are very crucial (Bowman & Bertozzi 1999). Therefore, the maintenance of correct sulfate groups' metabolism is important for tissue development and for their functions, particularly in cartilage where PGs are fundamental and abundant components of extracellular matrix (Paganini *et al.* 2019). In chondrocytes, the main source for sulfate is the extracellular matrix where sulfate donors processed during sulfotransferase reactions (Monti *et al.* 2015). Therefore, any alteration in the metabolism of sulfate can affect macromolecular sulfation that may lead to the onset of diseases that affect cartilage and bone (Geister & Camper 2015). Therefore, the mutations in genes that regulate the molecular sulfation lead to a different type of skeletal dysplasia (Krakow & Rimoin 2010).

In all kind of mammalian tissues, for the sulfation of PGs, there is a universal sulfate donor for various substrate specific sulfotransferases (SULTs). The universal sulfate donor includes 3′-phosphoadenosine-5′-phosphosulfate (PAPS). Hence, intracellular sulfate is activated to PAPS through sulfate activation pathway which catalyzed by different SULTs (Klaassen & Boles 1997). Generally, during sulfate metabolism, the intracellular level of sulfate is dependent on its extracellular uptake by different membrane transporters like solute carrier family 26 member 2 (SLC26A2). A small proportion of sulfate comes from the catabolism of sulfur containing amino acid and thiols or also from sulfate metabolic reactions in lysosomes. After activation of sulfate into the universal sulfate donor, PAPS in the presence of PAPS synthetase (PAPSS). The PAPS is used to adenosine monophosphate (AMP) by cytosolic SULTs for sulfation of hormones or by Golgi sulfotransferases for sulfation of PGs by the involvement of solute carrier family 35 member B2 and B3 (SLC35B2 and SLC35B3)(Paganini *et al.* 2020) (Figure 1).

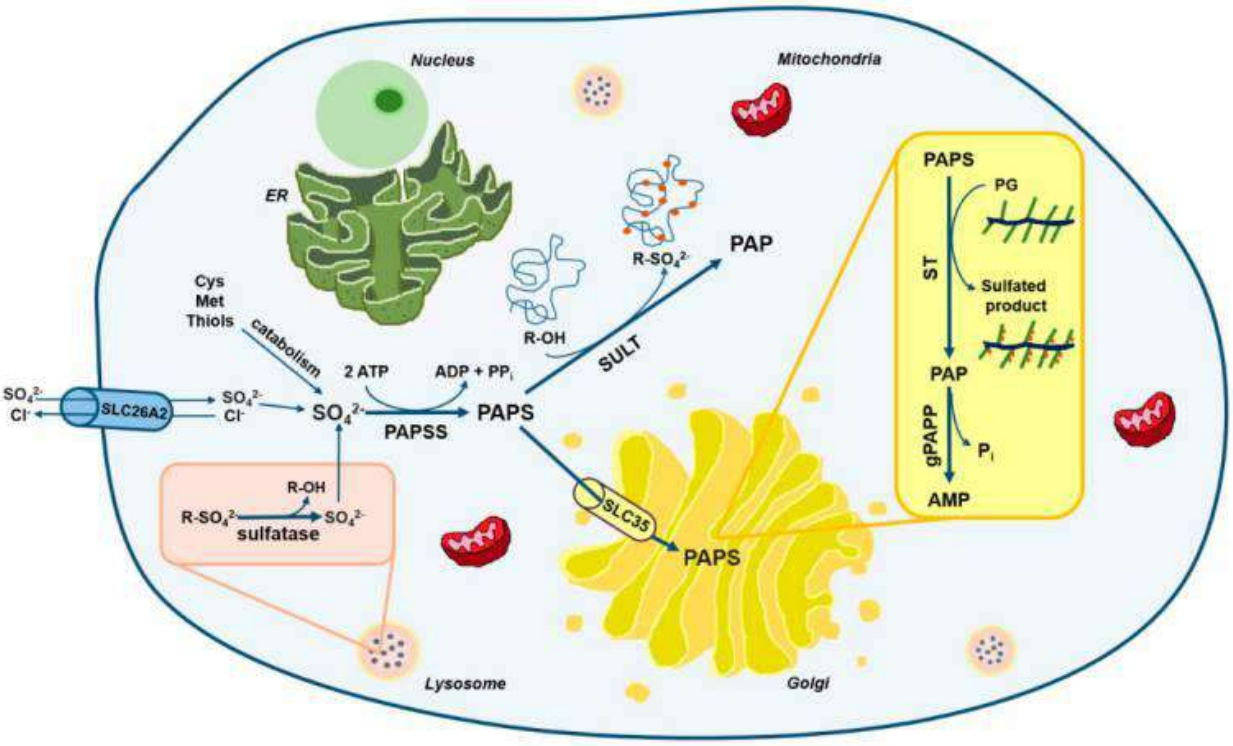

Figure 3.1: Summary of intracellular sulfate metabolism.

The diagram was taken from the following publication "Paganini, C., C. Gramegna Tota, et al. (2020). "Skeletal Dysplasias Caused by Sulfation Defects." International Journal of Molecular Sciences 21(8): 2710."

Abnormal biosynthesis of PGs results in a huge number of genetic disorders due to abnormal defects of cartilage and bone. The cartilage based phenotypes might be due to the high amount of sulfated PGs in the cartilage extracellular matrix (Paganini *et al.* 2019). Various genetic diseases involving the uptake of sulfate, metabolic acrtivation, and sulfation of GAGs. The errors in PGs biosynthesis results in several types of skeletal dysplasia which include achondrogenesis type 1B (ACG1B), atelosteogenesis type 2 (AO2), diastrophic dysplasia (DTD), recessive multiple epiphyseal dysplasia (EDM4), spondyloepimetaphyseal (SEMD), brychyolmia type 4 (BCYM4), brchyolmia type 1A (BCYM1A), brachyolmia type 1B (BCYM1B), spondyloepiphyseal dysplasia with congenital joint dislocation (SEDCJD), Ehlers-Danlos syndrome musculocontractural type 1 (EDSMC1), osteo-chondrodysplasia, brachydactyly, and overlapping malformed

digits (OCBMD, presented phenotype). The schematic defective pathway for these skeletal disorders shown in Figure 3.2 (Paganini *et al.* 2020).

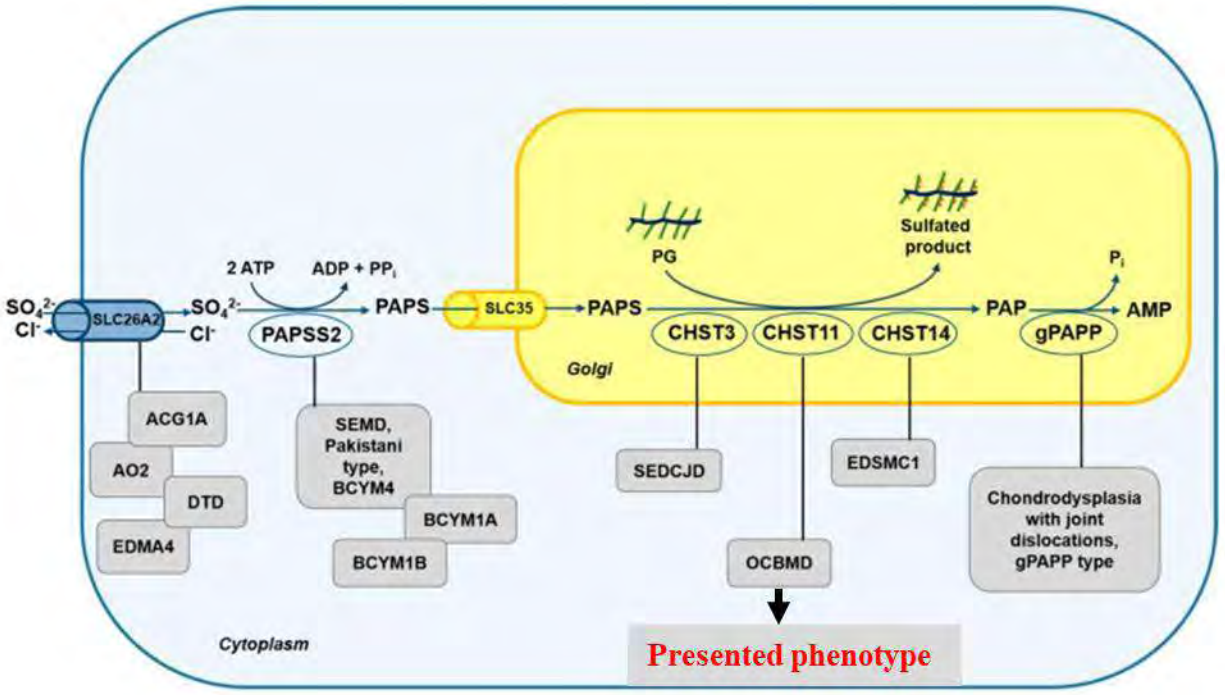

Figure 3.2: General presentation of the defects due to abnormal sulfation pathway causing several skeletal dysplasias.

The diagram was taken from the following publication "Paganini, C., C. Gramegna Tota, et al. (2020). "Skeletal Dysplasias Caused by Sulfation Defects." International Journal of Molecular Sciences 21(8): 2710."

Skeletal dysplasias (SDs) are a complex heterogeneous group of genetic disorders that mainly involve defects of cartilage and bone. Other secondary complications include neurological, auditory, visual, cardiac, pulmonary, and renal problems. This indicates that causative genes for SDs have a functional role in skeleton and tissue development. Relevant to SDs, at least 461 disorders have described on the bases of clinical and molecular data and for these 437 causative genes/proteins have identified (Krakow & Rimoin 2010; Mortier *et al.* 2019; Paganini *et al.* 2020).

Among these genes/proteins, carbohydrate sulfotransferases (CHSTs) is a family of 15 transporter proteins (CHST1-15). CHSTs catalyze the transfer of sulfate groups

from a donor to the sugar of the repeating disaccharide chains on GAGs and the GAGs chondroitin sulfate (CS) attached to the surface of certain cells. The proper sulfation of the molecules plays essential roles in intercellular communication, cellular adhesion and maintenance of extracellular matrix. *Carbohydrate sulfotransferase* (*CHST11*; OMIM: 610128) gene that codes a primary enzyme for 4-O-sulfation of N-acetylgalactosamine residues in CS (Mikami & Kitagawa 2013). The function of *CHST11* is important for skeletal morphogenesis and its expression regulates Indian hedgehog (IHH) signaling in the developing growth plate (Cortes *et al.* 2009).

Up-till now, there is only a single report of 55-kb homozygous deletion encompassing the first coding exon of the *CHST11* and the embedded microRNA MIR3922 was detected in a woman with short stature, hand/foot malformation encompassing brachydactyly, campto-clinodactyly and hyperphalangy, and malignant lymphoproliferative disease and her deceased sister was similarly affected (Chopra *et al.* 2015). Aside from this single report, there is no known other pathogenic variant that implicating *CHST11* in a skeletal malformation.

The current study is aimed to report unusual phenotype due to mutation in *CHST11* gene in Pakistani kindred, which segregated in autosomal recessive inheritance pattern.

3.3: Subjects and methods

All information obtained according to the Helsinki-II declaration and the protocols of the ethical review committee of Quaid-i-Azam University, Islamabad and the Boğaziçi University Institutional Review Board for Research with Human Participants. This part of the study was supported by the Scientific and Technological Research Council of Turkey (114Z829; to AT), URF-QAU Pakistan.

3.3.1: Family origin

The family recruited from Southern Punjab, Pakistan. The six-generation pedigree was drawn by interviewing heads of the family and information about pedigree and disease phenotypes were crosschecked from other family relatives. The pedigree indicated autosomal recessive inheritance pattern (Figure 3.3). Upon inspection of the kindred, ten affected members (8 male and 2 female) were observed in the family. Overall, twenty-two relatives (10 affected and 12 unaffected) were examined physically with the help of local physicians. Photographs of all ten (401, 509, 516, 518, 519, 521, 525, 601, 602, and 603) and roentgenograms of three affected subjects (401, 509, and 519) were obtained to write the clinical report. Nineteen of those individuals (7 affected and 12 unaffected) participated to find the molecular cause of the phenotype.

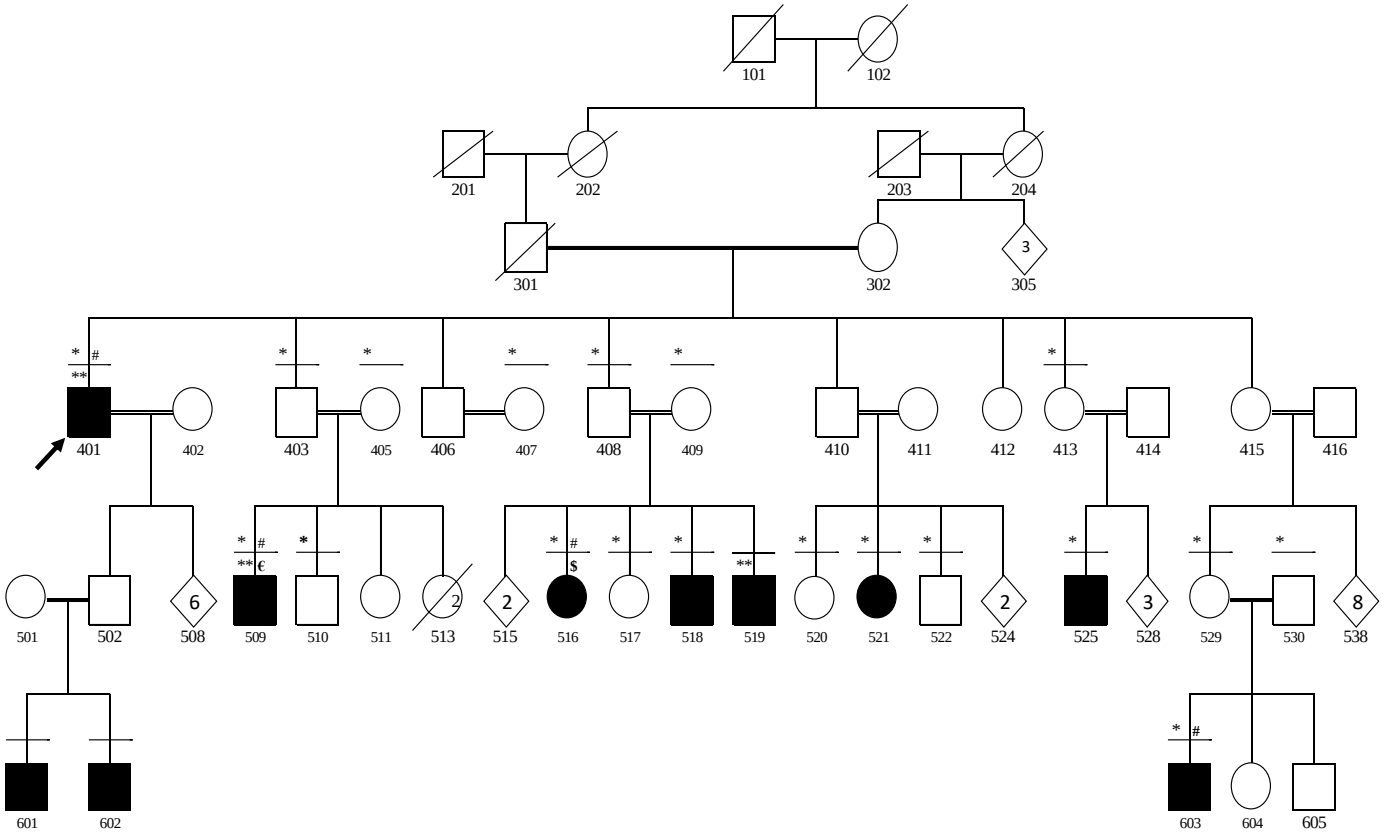

Figure 3.3: Pedigree of Pakistani kindred with digital and skeletal malformation.

Symbol with arrow: propositus; symbol with above horizontal line: physically observed; symbols with oblique line: deceased; *: blood samples; **: X-rays; #: SNP genotyping; $: exome sequence; €: sanger sequence

3.3.2: Genetic study

3.3.3: SNP genotyping

Whole-genome SNP genotype data of the four affected individuals (401, 509, 516 and 603) were generated by using Illumina Human OmniExpress-24 BeadChip and Homozygosity Mapper (www.homozygositymapper.org) used to find shared homozygosity regions. Genomic deletions and duplications were detected through cnvPartition (v3.2.0) CNV Analysis Plug-in for Genome Studio. Genotypes were compared on MS-Excel to verify that all patients shared the homozygosity in the region detected and that the homozygosity was possibly due to identity by descent.

3.3.4: Exome sequencing

Exome sequencing library for affected individual 516 was prepared using IDT xGen Exome Research Panel V.1.0 that targets 98% of bases in RefSeq database and sequencing was performed using Illumina HiSeq2500. The generated reads were aligned to reference sequence GRCh37/hg19 using BWA-0.7.12-r1039. Exome sequencing yielded a mean depth of 104X with approximately 99.68% of the targeted bases read with at least 20X depth. Variants were called with SAMtools-1.6. After annotation of the variants by ANNOVAR, we considered those variants that are novel or have frequencies 0.5 and possibly damaging to protein. Sanger sequencing was carried out to validate the single candidate variant detected, and its segregation in 18 family members was investigated by electrophoresis on an 8% polyacrylamide gel to resolve fragments for wild-type allele (283bp) and variant allele (268bp). Sequences of the primers for PCR amplifications are F: CATCTACTGCTACGTGCCCA and R: GTACCGCTTGTGGAAGGAGA. The variant is submitted to ClinVar with submission number SUB3259126.

3.3.5: *In silico* analysis

Human reference sequence GRCh38 was retrieved from NCBI database (https://www.ncbi.nlm.nih.gov). Conservation of the genomic region of interest across

species was visualized by HomoloGene (https://www.ncbi.nlm.nih.gov/homologene). Computational algorithms Mutation Taster and Protein Variation Effect Analyzer (PROVEAN) were used to predict the effect of the identified deletion on the protein. Predict Protein Server (https://www.predictprotein.org) was utilized to predict and compare the secondary structures of the reference and variant proteins. To visualize the effect of the deletion on *CHST11*, we predicted tertiary (three-dimensional (3D)) structures for the reference and variant proteins encoded by the two splice variants by using I-TASSER predicting the 3D structures based on threading approach and assembling the structural fragments using Monte Carlo simulations. For evaluation and overlay of 3D models, RAMPAGE (http://mordred.bioc.cam.ac.uk/~rapper/rampage.php) and VMD tools were used.

3.4: Results

The predominant clinical features among the patients include brachydactyly, overriding digits, and mild short stature shortening of lower legs. In hands, the digital defects included adducted thumbs, overlapping fingers, ulnar inclination of index fingers, camptoclinodactyly of fingers 3 > 5. In feet, the toes anomalies are valgus inclination of broad halluces, overriding of 2nd toe to 3rd toe, short 5th toes, and post-axial polydactyly. The other associated skeletal features are pectus excavatum, scoliosis, displaced patellae and fibulae. We reported the findings in the publication (Shabbir *et al.* 2018). The current study work described that the functions of *CHST11* are important for digits and skeletal morphogenesis.

3.4.1: Clinical findings

The physical examination of all ten patients (401, 503, 506, 508, 509, 511, 513, 601, 602 and 603) was carried out with the help of local clinicians whereas as radiographs were taken of three patients (401, 509, and 519). The phenotype showed variable expression among the affected individual in the family. The physical and radiographic findings given in Table 3.1 and 3.2, respectively.

All affected individuals have bilateral and symmetrical skeletal defects that affect the limbs and skeleton. The short stature was evident due to the shortening of bones in the lower legs (Table 1, 2). Primarily, hand/foot malformation was short and adduced thumbs, overriding of 3rd finger over 4th finger in most of the patients, short 2nd fingers with ulnar curvature and short and campto-clinodactylous 3-5 fingers. In feet, there were short and broad hallux with varus inclinations, 2nd toe overriding the 3rd toe, short 5th toe, and postaxial polydactyly (Table 3.1). Secondary associated features were scoliosis, pectus excavatum, and polydactyly (Table 3.1).

Three index patients (401, 509, and 603) complained of fatigue and exhausting easily and not being able to carry heavy loads. Additionally, two index patients (401 and 509) complain about joints pain that is indicative of osteoarthritis, but their knee and

ankle X-rays did not show any kind of degenerative symptoms for osteoarthritis. All patients had normal mental status while asymmetrical facial appearance was in one subject (603). One patient (525) and his two siblings (526 and 527) did not show skeletal defects except deafness.

Table 3.1: Morphological features of limbs and skeletal elements in physically examined affected subjects

Pedigree ID	***401***	***509***	***516***	***518***	***519***	***521***	***525***	***601***	***603***
Gender/age (years)	M/50	M/20	F/10	M/8	M/4	F/13	M/24	M/6	M/18
					Limbs defects				
Upper limbs									
Short hands	+	–	+	–	+	–	–	–	–
Thumb: adducted, short	+, broad	–	+	+, R	+	–	–	–	–
Index finger: ulnar curved	+, short	+, short	+, short	+, short	+, short, overriding the 3rd finger	+, short	+	+	+
Middle finger: ulnar curved	+, short	+	-, elongated, camptodactyly, radial curved	–	+, overriding the 4th finger	-, radial curved	+	+	+, short
Ring finger: campto-clionodactylous	+, ulnar curvature	+, radial curved	+, radial curved	–	+, radial curved	+	+, radial curved	+	No campto-clino; ulnar curved
Fifth finger: campto-clinodactylous	+, short	+, short	+, short, radial curved	+	–	+	+	+	+, ulnar curved
Cross-finger	–	+, 3-4	+, 2-3	–	+, 3-4; 2-3	–	+, 3-4	+, 3-4	–
Missing few flexion	+	+	Extra flexion	Missing	Extra	Extra	Extra flexion	Extra flexion	+; extra flexion

creases on fingers			creases	on thumb, Extra on fingers	flexion creases	flexion creases	creases	creases	creases
Lower limbs									
Size short	+	–	+	–	–	–	–	–	–
Hallux: varus inclination	+, short, broad	+	+, short, broad	+	+	–	+	+, short, broad	–
Second toe overriding third	+	–	+	–	+; cross-toes	–	+	+	+
Third toe: campto-clinodactyly	–	+	+	–	–	–	–	–	+
Fourth toe: short	–	–	–	–	–	–	–	+, camptodactylous	+, camptodactylous
Fifth toe: short	+	+	-	+	-	-	+	+	+
Postaxial polydactyly	+; B	–	–	–	–	–	+, synpolydactyly (L)	–	+, synpolydactyly (R)
Wide-space between 1-2 toes	–	–	–	+	–	–	+	+	+
Skeletal defects									
Short stature	+	+	+	–	–	+	+	+	+
Scoliosis	+	+	NA	+	NA	NA	+	NA	+
Lumber lordosis	+	–	NA	+	NA	NA	–	NA	+
Pectus excavatum	–	+	–	–	–	–	–	–	+

Prominent clavicle	+	–	NA	–	–	NA	+	–	+
Pain in running	+	+	–	+	–	–	–	–	+
Others	prominent ear (L); cannot carry heavy objects	cutaneous fusion of 1-2 toes (L); cannot carry heavy objects	–	digestive problems	–	–	deaf-mute	–	mildly asymmetric face; prominent scapula; cannot carry heavy objects; digestive problems

Abbreviations: +, feature present; −, feature absent; NA, not assessed; B, bilateral; R, right limb; and L, left limb

Table 3.2: Radiographic findings in three index patients (401, 509, and 519)

Ped ID	***401***	***509***	***519***
Investigated Variables		***Radiographic features***	
Upper limbs			
Radius and ulna	Shortened	Shortened, narrow spaces	Wide spaces
Humerus curved	–	+	–
Hypertrophic first digital ray	+	–	–
Short proximal phalanx 2-4 fingers	+	+	–
Hypoplastic distal phalanx	+	–	+
Extra osseous elements in fingers	4 and 5	2, 3 and 4	2-4; delta phalanx in 2nd-3rd
Symphalangism in fingers	4	5	–
Fifth finger with two phalanges	+	+	–
Carpals	Crowding	Crowding	Immature /missing
Lower limbs			
Hypertrophic first digital ray	+	+	+
Dysmorphic and short proximal and distal phalanx	+	+	+
Duplication of 5^{th} phalanx	+	–	–
Crowding of tarsals	+	+	–
Laterally displaced calcaneous	+	–	+
Narrow aligned femur and tibia	+	+	NA

Thinning of tibia-fibula	+	+	–
Dislocated patella	+	+	NA
Latero-ventrally displaced fibula	+	+	–
Skeletal abnormalities			
Scoliosis	Thoracic and lumbar vertebrae	Thoracic vertebrae	NA
Sacroiliac joint gap	+	–	NA

+, features present; -, features absent; and NA, not assessed

3.4.1.1: Index Subject 401

The index patient 401 was a 50-year-old man who had short stature due to short pelvic girdle and lower leg bones. The patient had slightly short hands and feet. In hands, he had odd shaped fingers, short, broad and abducted thumbs, short index & middle fingers, campto-clinodactyly and extra osseous elements found at the distal phalangeal joints (DPJ) of fourth and fifth fingers. All fingers showed ulnar inclination (Table 3.1; Figure 3.4). Through anterio-posterior (AP) view of radiographs, we found short dysplastic proximal phalanges and hypoplastic distal phalanges in 2-4th fingers. Symphalangism at proximal phalangeal joint (PPJ) were observed in 4th fingers. There were only two phalanges in 5th fingers, with enlarged proximal phalanges. The first digital rays appeared hypertrophic. Radii and ulnae were mildly short with overlapping of carpals. The radiographs of axial skeleton revealed prominent clavicle and mild scoliosis in the thoracic and lumbar region with an impression of lumbar lordosis (Table 3.2; Figure 3.4).

In feet, there were short halluces with varus inclination, overriding of the second toe over third, fifth and extra postaxial toes were short. Whereas, 4th toes appeared normal. Radiographs of feet indicated hypoplastic ends of all metatarsals, dysmorphic and dwarf proximal and distal phalanges in all toes, halluces were hypertrophic, overriding and accreted tarsals, laterally displaced calcanei. Radiographs of middle

segments of lower limbs revealed posterior dislocation of fibulae, narrow spaces between femurs and tibiae/fibulae, and left femur was with slight curve Table 3.1-3.2; Figure 3.4.

Physiologically, the patient 401 informed that he had difficulty in running. Additionally, the index subject 401 complained about pain, rapid fatigue, and joint stiffness at morning. The left ear was protruding. Ultra-sonographic examination of chest & abdomen and biochemical examination of blood & urine did not show any kind of structural and metabolic abnormality in the rest of the body parts and systems. Moreover, the patients were mentally normal and were engaged in manual jobs.

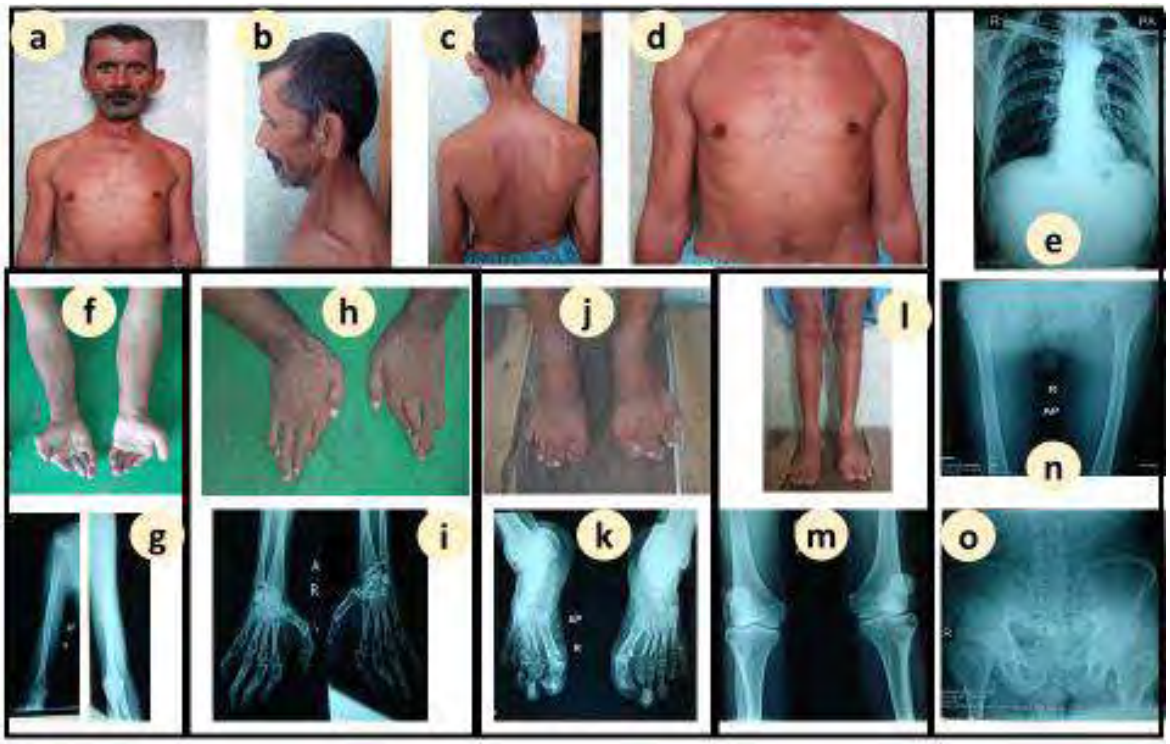

Figure 3.4: Morphological and anatomic features of index patient 401. Short stature (a), large ear and prominent clavicle bones (b), protruding scapula bones and lumber lordosis (c), chest abnormality (d), scoliosis (e), brachydactyly of hands (f, h), abnormal feet and knees (j, l), X-rays of hands and arms (g, i), X-rays of feet (k), dislocated patella (m) and abnormal pelvis with narrow femur angle (n, o).

3.4.1.2: Subject 509

The patient 509 was 20 years old male who had bilateral brachydactyly of 2nd index fingers, a characteristic cross-finger appearance of 3rd and 4th fingers, and campto-clinodactyly of little 5th fingers (Table 3.1; Figure 3.5). Radiographs of hands revealed short proximal phalanges in 2-4 fingers, hypoplastic terminal phalanges in 2-5 fingers and symphalangism of 5th fingers in both hands. In the feet, campto-clinodactyly of 3rd toes and shortening of 5th toes were observed (Table 3.2; Figure 3.5). The skeletal findings were mild short stature, scoliosis and pectus excavatum (Table 3.1; Figure 3.5).

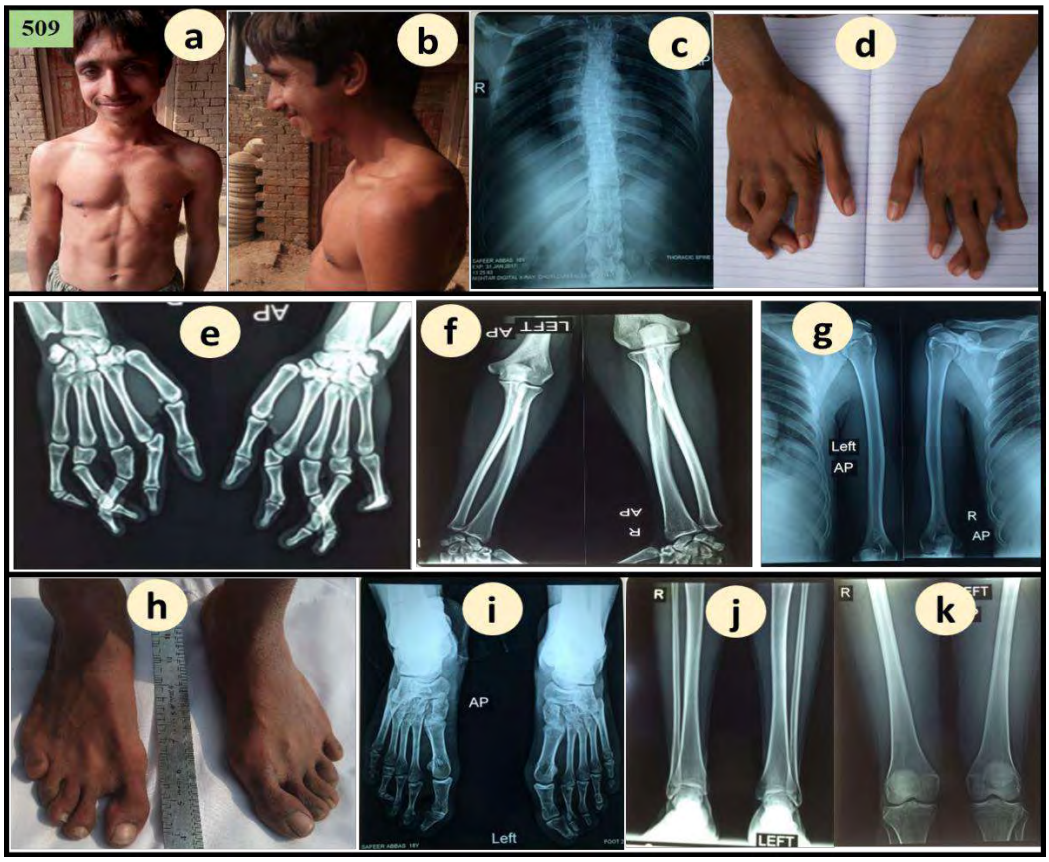

Figure 3.5: Phenotypic expression and radiographic features of patient 509. Pectus excavatum (a), cranio-facial lateral view (b), scoliosis (c), overlapping fingers in hands (d), X-rays of hands and arms (e-g), abnormal feet (h), X-rays of feet (i), narrow space between tibia and fibula (j) and dislocated patella bone (k).

3.4.1.3: Subject 516 and 518

Patient 516 was a 10-year-old girl who had short stature. In the hands, thumbs were short and abducted, second fingers were short with ulnar curvature, camptodactyly of 2-3 fingers and radial curvature of 2-4 fingers were found. She also had second fingers overriding the third, whereas the third fingers were elongated. Short and broad halluces with varus inclination, second toes overriding third, and camptodactyly of the third toe were observed in the feet (Table 3.1; Figure 3.6a-c).

Patient 518 was an 8-year-old boy who had short stature. Skeletal deformities include scoliosis and lumbar lordosis. The patient complained of difficulty whilst running. The appearance of the hands was as follows: thumb of right hand was short and abducted, second fingers were short with ulnar curvature, 3-5 fingers were oddly shaped with swollen tips, and campto-clinodactyly was observed on the fifth fingers. Similarly, the appearance of the feet was as follows: halluces with varus inclination were observed, the fifth toes were short, wide spaces being evident between 1-2 toes (Table 3.1; Figure 3.6d-f).

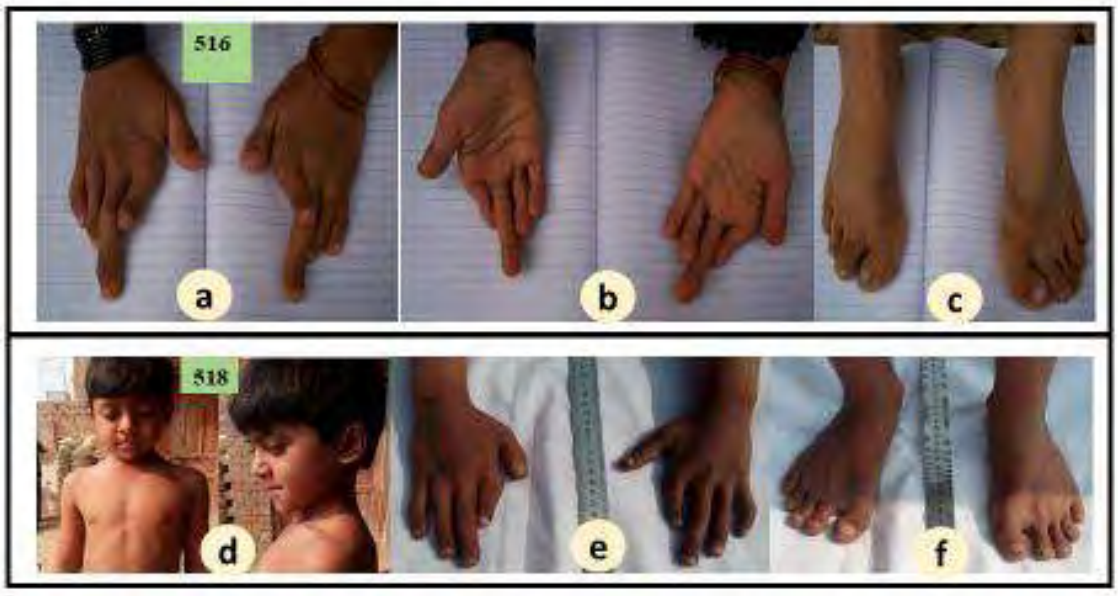

Figure 3.6: Morphological features of patient 516 and 518. Dorsal and ventral view of abnormal hands with brachydactyly, short and abducted thumbs and camptodactyly, (a, b). Short and broad halluces

with varus inclination (c). cranio-facial view of 518 (d), short and abducted thumb with fingers ulnar curvature (e) and halluces with varus inclination (f).

3.4.1.4: Index patient 519

A four-year-old boy with short stature, wide forehead and prominent right ear. Upon examining the hands, it was found that the thumbs were short and abducted, the index fingers being short, 2-3 fingers had ulnar curvature while fourth fingers had radial curvature with campto-clinodactyly. It had been observed that halluces with varus inclination were present in the feet (Table 3.1; Figure 3.7a-c). Radiographical examination revealed: hypoplastic distal phalanges, 2-4 fingers with extraosseous elements and 2-3 delta phalanges. Carpals were immature and missing. Widely spaced radii and ulnae were evident. The radiographical appearance of the lower limbs: hypolastic first digital rays, dysmorphic and short proximal and distal phalanges. Calcanie were laterally displaced (Table 3.2; Figure 3.7d-e).

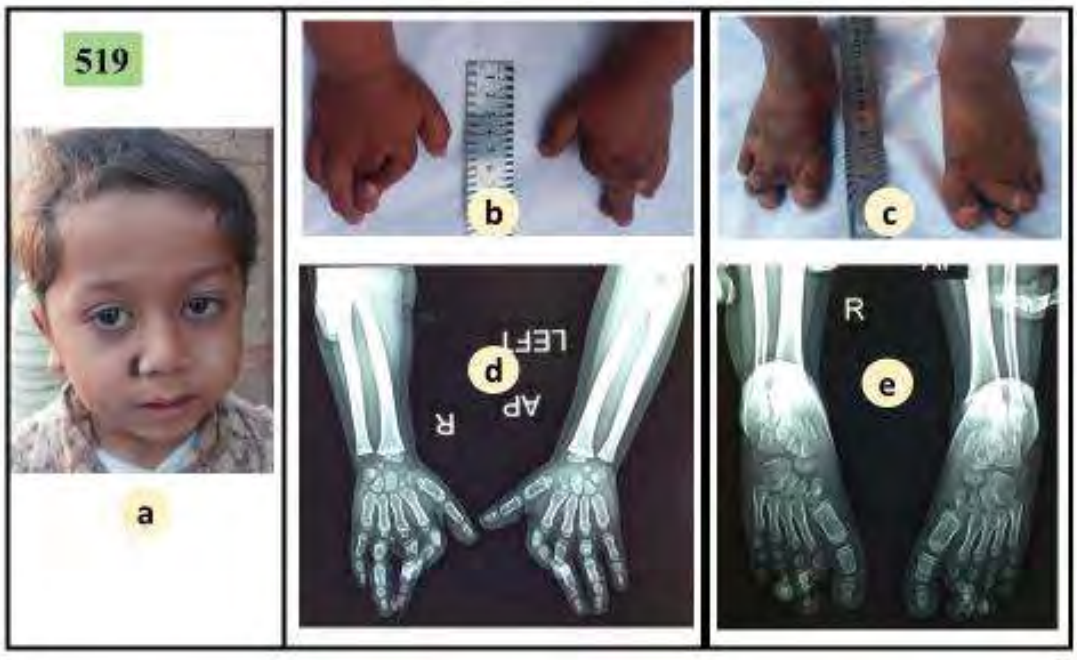

Figure 3.7: Morphological and radiographic features in patient 519. Broad forehead and large ears (a), short, abducted thumb and over lapping fingers (b), halluces with varus inclination in feet (c), hypoplastic distal phalanges with extraosseous elements in hands and feet (d, e).

3.4.1.5: Subjects 521 and 525

The patient 521 was a 13 years old girl and she had short stature. Second fingers were short with ulnar curvature, however third fingers had radial curvature, and 4-5 fingers were camptodactylous in the hands and halluces with varus inclination in feet (Table 3.1; Figure 3.8a-c).

The affected subject 525 was a 24-year-old man with normal stature, scoliosis and prominent clavicles. In the hands: 2-3 fingers had ulnar curvature whilst third and fourth fingers had radial curvature, 4-5 fingers had campto-clinodactyly. In the feet: halluces with varus inclination were observed, second toes were overriding the third, fifth toes were short, 1-2 toes being widely spaced. Postaxial polydactyly and synpolydactyly of the left foot were evident (Table 3.1; Figure 3.8d-i).

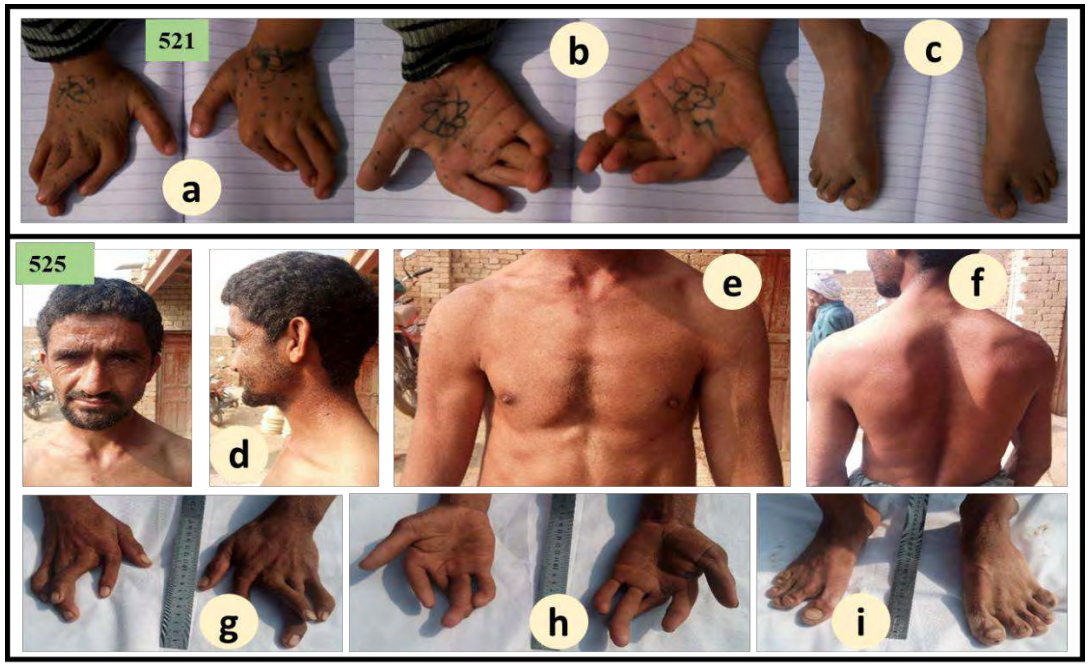

Figure 3.8: The morphological features of the disease in the affected subjected 521 and 525. Short and radial curvature fingers in hands (a, b) and halluces with varus inclination in feet (c). Cranio-facial features (d), prominent clavicles (e), scoliosis (f), fingers with ulnar curvatures and campto-clinodactyly (g, h) and halluces with varus inclination, overriding toes, postaxial polydactyly and synpolydactyly (i).

3.4.1.6: Subject 601

A 6-year-old boy with short stature. The appearance of the hands consisted of 2-3 fingers having ulnar curvature, 3-4 fingers with camptodactyly. In the feet, short and broad halluces with varus inclination, camptodactyly of the fourth toe, short 4-5 toes, and wide spacing between 1-2 toes were examined (Table 3.1; Figure 3.9a-b).

3.4.1.7: Subject 602

The patient was a 5-year-old boy with short stature. 2-4 fingers were overriding, also 3-4 fingers had ulnar inclination. In the feet: thumbs were short and abducted, second toes overriding the third, and 1-2 toes had cutaneous fusion (Table 3.1; Figure 3.9c-d).

3.4.1.8: Subject 603

Affected subject 603, 18 years old male who had disproportionate and short fingers, with a camptodactylous and symphalangous presentation. There were missing and/or additional flexion creases in the fingers, indicative of symphalangism and hyperphalangism, respectively. In the feet, there was a shortening of 2nd and 5th toes, campto-clinodactylous 3rd toe, and synpolydactyly in the right foot. The individual additionally had a mildly asymmetric face, mild short stature, scoliosis, pectus excavatum, prominent clavicle and scapula, and lumbar lordosis (Table 3.1; Figure 3.9e-i).

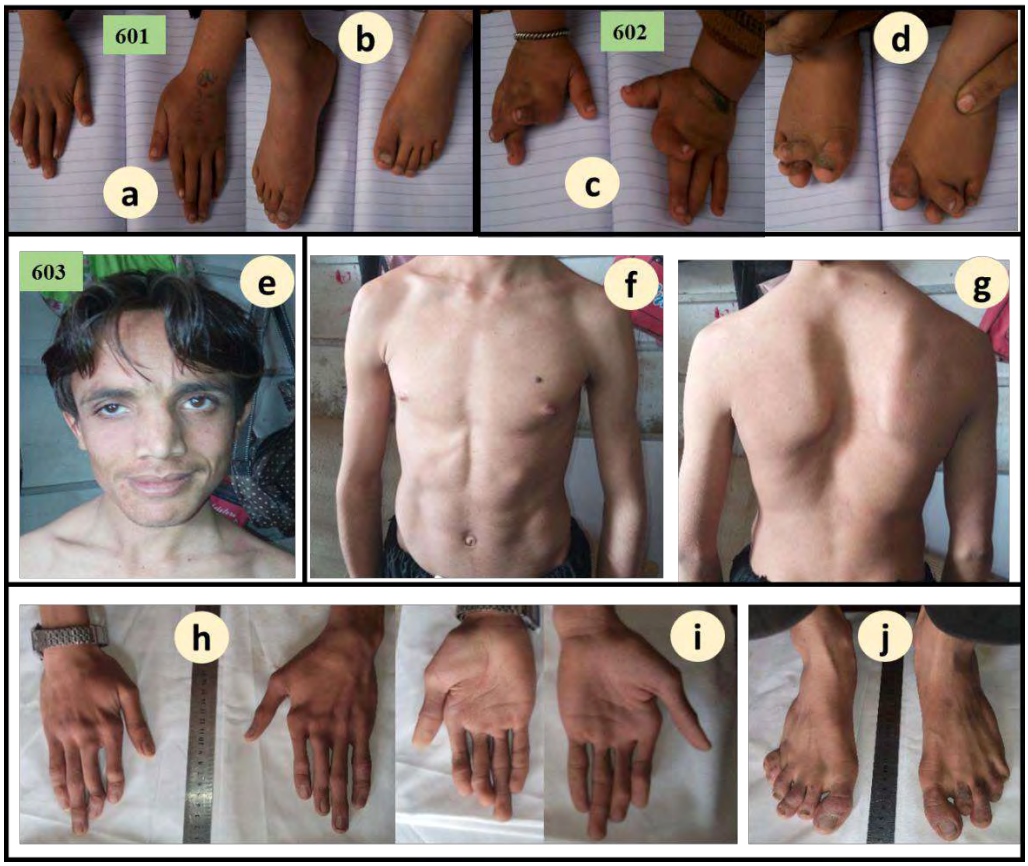

Figure: 3.9: Phenotype in three affected subjects 601, 602, and 603. Fingers with ulnar curvature, camptodactyly (a), short and broad halluces with varus inclination (b), overriding fingers with ulnar inclination (c), short abducted thumb and overriding toe (d), mild asymmetric face (e), pectus excavatum (f), scoliosis (g), camptodactylous and symphalangous fingers (h), symphalangism and hyperphalangism (i), campto-clinodactylous and synpolydactyly in feet (j).

3.4.2: Genetic findings

By using SNP genotype data, homozygosity mapping detected two loci > 1Mb at 12q23.3. The maximal shared homozygosity in the larger region (at 12q23.3) was of 1.6 MB, between rs1922261 (104,854,011 nucleotides) and rs6539247 (106,459,902 nucleotides). The homozygosity in the region was identical in four patients (401, 509, 516, 603) as shown in Figure 3.10.

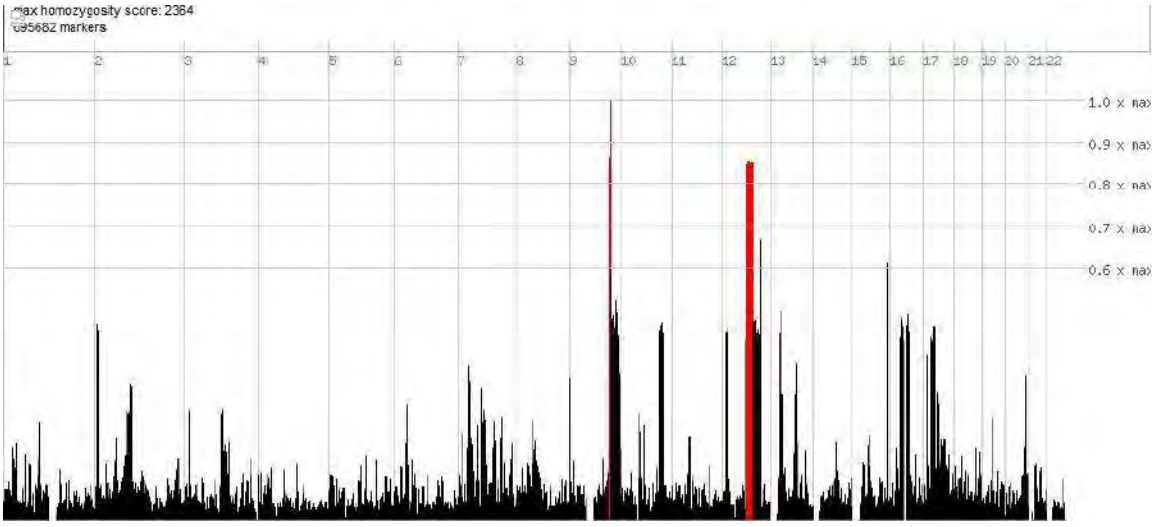

Figure 3.10. Graphical representation of homozygosity intervals obtained by HomozygosityMapper with default parameters. Red bars depict the longer stretches of homozygous genotypes on chromosomes and black bars revealed short intervals with homozygous genotypes.

At the time of this study, there was no report of any relevant phenotype on OMIM and therefore, exome sequencing was launched. In the exome file of the patient (516), a rare and novel variant within the linked region at 12q23.3 was selected, and the exome sequence analysis is shown in Table 3.3. Exome sequence complete summary is briefly explained in figure 3.11. The identified variant possibly underlies the bone malformations in the family. The mutation was an in-frame deletion of 15 nucleotides in *CHST11* exon 3 (NM_001173982:c.463_477del:p.Leu155_Asn159del). The mutation was possibly protein damaging and the variant was not reported in databases ExAc, 1000

Genome or ESP6500. The unaffected relatives were heterozygous or non-carrier for the identified variant.

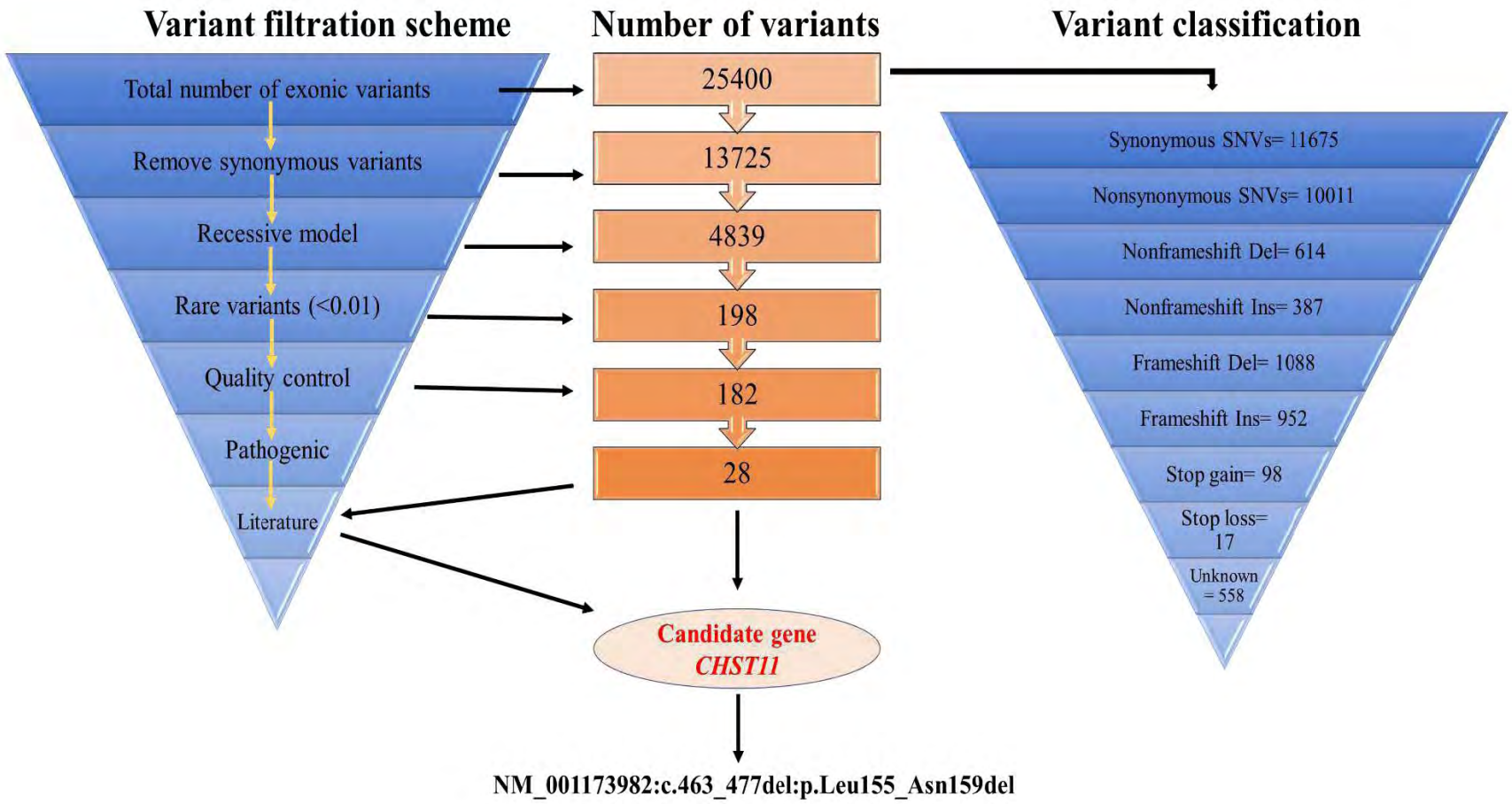

Figure 3.11. Summary of exome filtration scheme

Table 3.3: List of candidate variants at ch. 12 that fall in homozygous interval

Chr	Start	End	Ref	Alt	Region	Gene	Change	Exon/ transcript	Mutation	Effect on protein	Frequency (ExAC)		Prediction (resulting prediction)	
											World wide	South Asian	PROVEAN	Mutation Taster
12	104995811	104995811	-	TG	intronic	*CHST11*	.	.	.	.	.	.	.	polym
12	105150998	105151012	CCAACCTGAAGACCC	-	Exonic	*CHST11*	nonfrmdel	3/NM_018413	c.476_490del	p.159_164del			Del	disease causing
12	105151000	105151014	AACCTGAAGACCCTG	-	Exonic	*CHST11*	nonfrmdel	3/NM_018413	c.478_492del	p.160_164del			Del	disease causing
12	105151014	105151014	-	CC	Exonic	*CHST11*	frmins	3/NM_018413	c.492_493insCC	p.L164fs		.	NA	disease causing
12	105260158	105260159	GT	-	intronic	*SLC41A2*	.	.	.	.	.	.	.	polym
12	105260161	105260168	ACACACAC	-	intronic	*SLC41A2*	.	.	.	.	.	.	.	polym
12	105260165	105260165	-	GT	intronic	*SLC41A2*	.	.	.	.	0.00006	0	.	polym
12	105260362	105260365	AATT	-	intronic	*SLC41A2*	.	.	.	.	.	.	.	disease causing
12	105260363	105260365	ATT	-	intronic	*SLC41A2*	.	.	.	.	.	.	.	disease causing
12	105260364	105260364	T	-	intronic	*SLC41A2*	.	.	.	.	0.04729	0	.	disease causing
12	105260365	105260366	TA	-	intronic	*SLC41A2*	.	.	.	.	.	.	.	polym

12	105260383	105260383	G	-	intronic	*SLC41A2*	.	.	.	.	.	.	.	polym
12	105432058	105432063	ACACAC	-	Intronic	*ALDH1L2*	.	.	.	.	.	.	.	polym
12	105454605	105454605	-	AA	intronic	*ALDH1L2*	.	.	.	.	.	.	.	polym
12	105454605	105454605	-	AAAA	intronic	*ALDH1L2*	.	.	.	.	.	.	.	polym
12	105526566	105526571	GTGTGT	-	intronic	*KIAA1033*	.	.	.	.	.	.	.	polym
12	105538268	105538270	CTC	-	intronic	*KIAA1033*	.	.	.	.	.	.	.	polym
12	105538270	105538270	C	-	intronic	*KIAA1033*	.	.	.	.	.	.	.	polym
12	105538271	105538271	T	-	intronic	*KIAA1033*	.	.	.	.	0.00370	0.00530	.	polym
12	105538287	105538287	A	-	intronic	*KIAA1033*	.	.	.	.	.	.	.	polym
12	105538422	105538423	TT	-	intronic	*KIAA1033*	.	.	.	.	.	.	.	polym
12	105538425	105538425	T	-	Intronic	*KIAA1033*	.	.	.	.	.	.	.	polym
12	105742197	105742198	AA	-	Intronic	*C12orf75*	.	.	.	.	.	.	.	polym
12	105769567	105769568	AG	-	Intergenic	*C12orf75,CASC18*	.	.	.	.	.	.	.	polym
17	58733814	58733814	A	-	Intronic	*PPM1D*	.	.	.	.	.	.	.	polym
17	59001877	59001877	-	T	Intronic	*BCAS3*	.	.	.	.	0.00004	.	.	polym
17	59001896	59001898	TTG	-	Intronic	*BCAS3*	.	.	.	.		.	.	polym
17	59147701	59147701	A	C	Intronic	*BCAS3*	.	.	.	.	0.00010	0.00070	.	disease causing

In last, the study rule-out all variants in known genes *BMP2, BMPR1B, CHSY1, GDF5, HOXD13, IHH, NOG, PRMT7, PTHLH, ROR2, RUNX2* and *TRPV4* for brachydactyly types. No variants with frequency < 0.01, number of reads to total reads ratios >0.25 and predicted to be possibly damaging to the protein were found.

Through Sanger sequencing, the identified candidate variant was validated in 18 family members and the mutation was homozygous in affected whereas the normal subjects were normal or heterozygous for the identified mutation (Figure 3.12). The deleted amino acids were conserved across the vertebrate species (Figure 3.13).

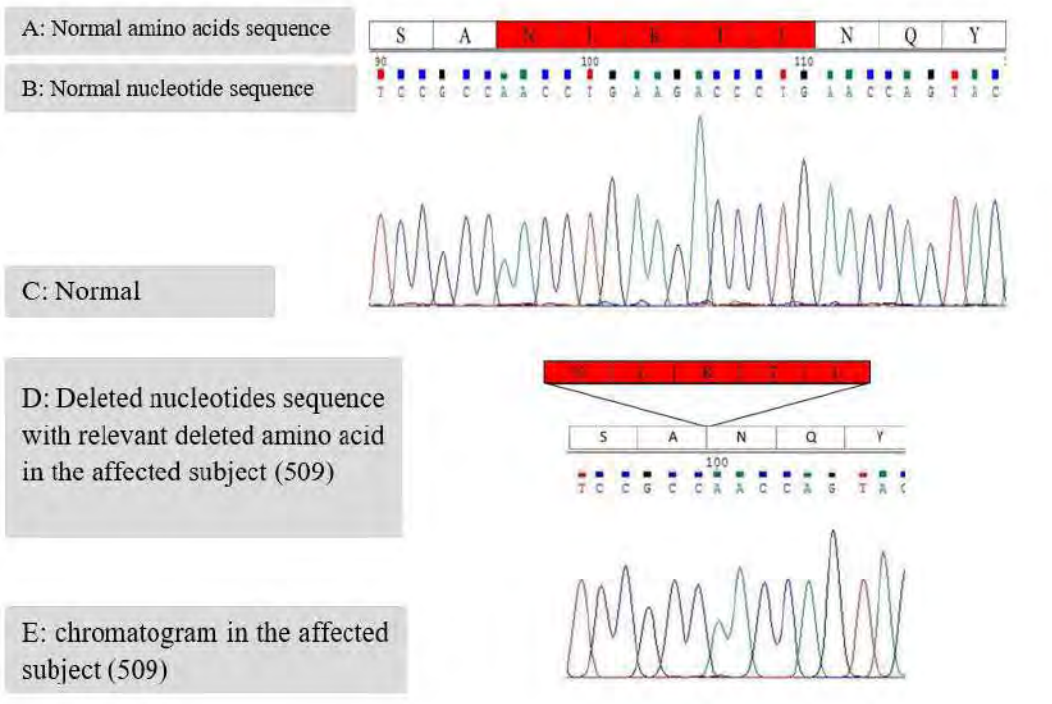

Figure 3.12. Electrophoretograms for reference and affected individual 509 showing mutation *CHST11* c.463_477del (p.155_159del; NM_001173982).

Species	Start	Aminoacid Sequences	End
H.sapiens	148	M E I P A N E A H V S A N L K T L N Q Y S I P E I N H R L K S	178
P.troglodytes	143	M E I P A N E A H V S A N L K T L N Q Y S I P E I N H R L K S	173
M.mulatta	143	M E I P A N E A H V S A N L K T L N Q Y S I P E I N H R L K S	173
C.lupus	148	M E I P A N E A H V S A N L K T L N Q Y S I P E I N H R L K S	178
B.taurus	148	M E I P A N E A H V S A N L K T L N Q Y S I P E I N H R L K S	178
M.musculus	148	M E I P A N E A H V S A N L K T L N Q Y S I P E I N H R L K S	178
R.norvegicus	148	M E I P A N E A H V S A N L K T L N Q Y S I P E I N H R L K S	178
G.gallus	148	M E I P A N E A H V S S N L K T L N Q Y S I P E I N H R L K N	178
D.rerio	148	M E I P S N E A H V P S N L K T L N Q Y S I P D I N H R L K N	178
X.tropicalis	143	M E I P A N V A H V S S N L K T L N Q Y S I P E I N H R L K N	173

Figure 3.13: Conservation of the deleted amino acid sequences across the vertebrate species.

3.4.3: Protein analyses

The detected mutation resulted in the deletion of five amino acids in the luminal domain of the protein CHST11. CHST11 encoded as a 352 or 347 amino acid containing protein by two transcripts isoform. It has three domains like cytoplasmic domain, transmembrane domain, and a luminal domain (Kahsay *et al.* 2005). The luminal domain has phospho-sulfate and phosphate binding site and acts as catalytic domain (Figure 3.14). The identified mutation lies in that domain in a region where amino acid sequence is highly conserved across the species (Figure 3.15).

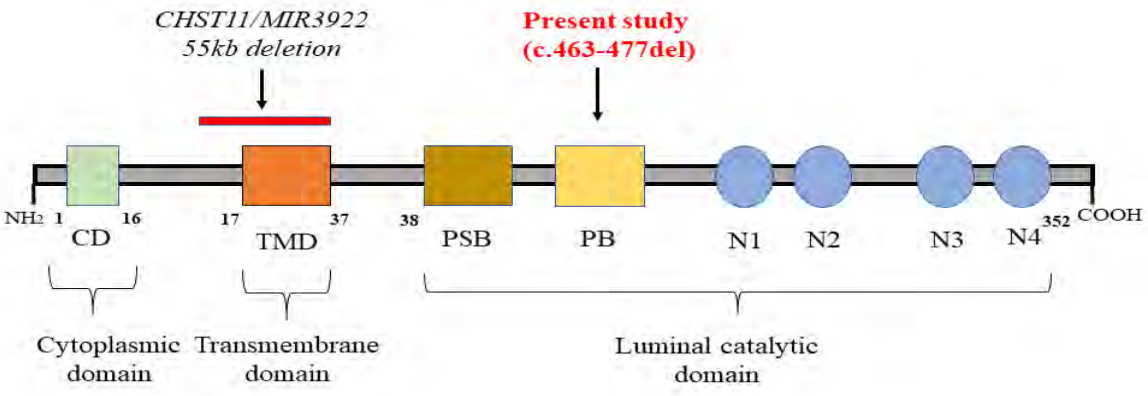

Fig 3.14: Schematic representation of CHST11 protein and its domain. Cytoplasmic domain (CD) consists of 1-16 amino acids (aa). Transmembrane domain (TD) consists of 17-37 aa. Luminal domain is subdivided in three parts: phospho-sulfate binding site (PSB), phosphate binding site (PB), four N-linked glycosylation sites (N1 to N4).

To investigate whether the variant is protein damaging or not, we first employed online computational algorithms. Mutation Taster predicted that the variant is disease-causing (score 0.98) and PROVEAN as highly deleterious (score -20.03). Next, we applied protein modeling using a threading approach. I-TASSER predicted five models for each version of the protein, and for comparison, one model was selected for each version, based on the C-score, Exp. TM-score and Exp.RMSD. The values of these parameters for selected models were given in Table 3.4.

Table 3.4. Tertiary structure evaluation parameters of selected CHST11-3D models based on I-Tasser predictions.

Structure Model	**C-Score**	**Exp. TM Score**	**Exp. RMSD**
Reference CHST11 splice variant 001	-1.05	0.33±0.15	10.0±4.6
Mutant CHST11 splice variant 001	-2.31	0.44±0.14	12.0±4.4
Reference CHST11 splice variant 002	-1.65	0.51±0.15	10.3±4.6
Mutant CHST11 splice variant 002	-1.98	0.48±0.15	11.1±4.6

Comparison of reference and variant protein models using RAMPAGE revealed differences in the number of favored and outlier regions (Table 3.5).

Table 3.5: Structural comparison of reference and mutant CHST11 proteins as evaluated by RAMPAGE

Protein	**Favoured region**	**Allowed region**	**Outlier region**
Reference CHST11-001	209 (60.6%)	76 (22.0%)	60 (17.4%)
Mutant CHST11-001	226 (65.5%)	75 (21.7%)	44 (12.8%)
Reference CHST11-002	239 (68.3%)	76 (21.7%)	35 (10.0%)
Mutant CHST11-002	221 (65.0%)	72 (21.2%)	47 (13.8%)

The superimposed structures of the reference (NP_060883.1; NP_001167453.1) and variant protein models for both splice variants showed differences in protein folding, especially in the cytoplasmic and transmembrane domains (Figure 3.14).

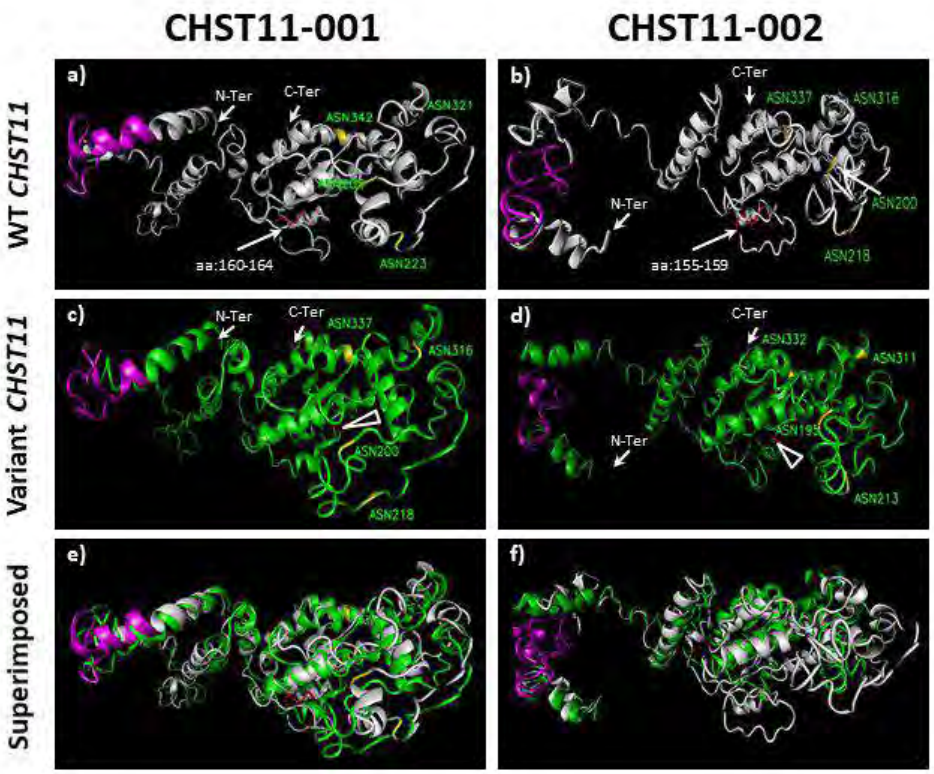

Figure 3.15: Predicted tertiary structure of wild-type CHST11 splice variant 001 (a), variant 002 (b) and respective Variant CHST11 (c,d). Position of 05 deleted amino acids in respective wild-type variants are shown in red color and are indicated with an arrow; aa: 160-164 for CHST11-001 and aa: 155-159 for CHST11-002. Superimposed structure of wild type and mutant CHST11-001 (e) and CHST11-002 (f) are shown in white and green color respectively. The N- and C-terminus are indicated with an arrow; the membrane domain is represented in magenta color. The four N-Glycosylation sites are marked with yellow color and labeled as amino acid name and position.

3.5: Discussion

Carbohydrate sulfotransferases is a family of 15 transporter proteins (CHST1-15). Carbohydrate sulfotransferases catalyze the transfer of sulfate groups from a donor to the sugar of the repeating disaccharide chains. The GAGs chondroitin sulfate (CS) attached to the surface of certain cells, and proper sulfation of the molecules is essential for their roles in intercellular communication, cellular adhesion and maintenance of extracellular matrix. Carbohydrate sulfotransferase 11 (CHST11), also known as chondroitin-4-sulfotransferase-1 (C4ST-1), is the primary enzyme for 4-O-sulfation of N-acetylgalactosamine residues in CS (Mikami & Kitagawa 2013).

The vital role of CHST11 in skeletal morphogenesis has been elucidated in various studies. CHST11 is a membrane protein of Golgi apparatus and catalyses the transfer of sulphate to position 4 of the N-acetylgalactosamine residue of chondroitin. This catalytic modification is crucial for proper Indian hedgehog signaling in the developing growth plate (Cortes et al. 2009). Studies on animal models have shown that Chst11 is required for proper chondroitin sulfate localization, modulation of distinct signaling pathways and cartilage growth plate morphogenesis (Kluppel et al. 2005). The mice mutant for Chst11 show substantial phenotypic overlap with the malformation observed in humans. Further, the absence of C4st1 leads to osteoarthritis-like symptoms in mice (Kluppel et al. 2005). Not surprisingly, genome-wide association studies have shown that CHST11 is a susceptibility locus associated with osteoarthritis in certain populations and rs835487 SNP in CHST11 has been significantly associated with knee osteoarthritis (Yau et al. 2017). A further clue to an important role of CHST11 in skeletal development was provided by Bhattacharyya et al. (2015) who showed that the expression of *CHST11* is regulated by opposing effects of arylsulfatase B on *BMP4* and *Wnt9A*.

Different studies on animal models have shown that Chst11 is required for proper chondroitin sulfate localization, modulation of distinct signaling pathways and cartilage growth plate morphogenesis (Klüppel *et al.* 2005). The mice mutant for *Chst11* show substantial phenotypic overlap with the malformation observed in humans. Further, the absence of C4st1 leads to osteoarthritis-like symptoms in mice (Klüppel *et al.* 2005). Not surprisingly, genome-wide association studies have shown that CHST11 is a

susceptibility locus associated with osteoarthritis in certain populations and rs835487 SNP in CHST11 has been significantly associated with knee osteoarthritis (Yau et al. 2017). A further clue to an important role of CHST11 in skeletal development was provided by Bhattacharyya et al. (2015) who showed that the expression of CHST11 is regulated by opposing effects of arylsulfatase B on BMP4 and Wnt9A.

We reported clinical and molecular findings in large Pakistani kindred affected with digital and skeletal malformation. The digital anomalies include brachydactyly, overriding fingers, campto-clinodactyly, whereas skeletal findings were scoliosis, dislocated patella & fibulae, and pectus excavatum due to deletion of five amino acids in the catalytic luminal domain of CHST11.

Up-till now, a single 55-kb homozygous deletion encompassing the first coding exon of the *CHST11* and the embedded microRNA *MIR3922* was detected in a woman with short stature, hand/foot malformation encompassing brachydactyly, campto-clinodactyly and hyperphalangy, and malignant lymphoproliferative disease and her deceased sister was similarly affected (Chopra *et al*. 2015). Beyond this single report implicating *CHST11* with a skeletal malformation, no other pathogenic variant is known.

The study reported a small homozygous in-frame deletion in the topological domain of the transmembrane protein in a Pakistani family afflicted with skeletal malformations that affect vertebrae, leg bones, hands and feet with highly variable phenotype, indicating that the *CHST11* mutation has a variable expressivity. The combination of features like short stature, scoliosis, pectus excavatum, prominent clavicle, crossed-fingers/toes, polydactylous toes, and clino-symphalangous digits, witnessed in our family were not reported for the previous family.

3.5.1. Differential Diagnosis

The pattern of short fingers evident in our family was not fully concordant with any of the well-characterized brachydactyly types (Temtamy and Aglan, 2008; Mundlos, 2009). Moreover, the identified feature in our patient did not overlap in any other type of skeletal dysplasia's (SDs) (Table 3.4).

However, brachydactyly type C (BDC) appeared to be clinically closer to the limb malformation in our family. BDC is characterized by shortening of the 2nd, 3rd and 5th fingers due to the shortening of first metacarpal and the middle phalanges, while 4th finger is least affected. BDC may additionally exhibit other features like hyperphalangism 2nd and 3rd fingers with ulnar deviation of the 2nd fingers, and occasionally mildly short stature (Castriota-Scanderberg et al., 2005; Gutierrez-Amavizca et al., 2012). Mutations of *GDF5* (growth and differentiation factor 5 protein) have been implicated in this dominantly segregating condition.

Table 3.6: Comparison of molecular and biochemical features of the presented phenotype with other phenotypes of skeletal dysplasia

Phenotypes	MIM	MOI	Gene	Protein Product and Function	Biochemical features	References
Achondrogenesis type 1B	600972	AR	*SLC26A2*	Sulfate/chloride antiporter present on cell membrane.	Severe cartilage PG undersulfation; reduced sulfate uptake in fibroblasts.	(Hästbacka *et al.* 1994)
Atelosteogenesis type 2	256050	AR	*SLC26A2*			(Superti-Furga *et al.* 1999)
Diastrophic dysplasia	222600	AR	*SLC26A2*		Cartilage PG undersulfation; reduced sulfate uptake in fibroblasts; in mice altered sulfate uptake in chondrocytes, and osteoblasts; altered Ihh signaling; reduced chondrocytes proliferation.	(Rossi & Superti-Furga 2001)
Recessive multiple epiphyseal dysplasia	226900	AR	*SLC26A2*		Reduced sulfate uptake.	(Karniski 2001)
Spondyloepimetaphyseal dysplasia, Pakistani type	612847	AR	*PAPSS2*	PAPS synthetase 2, enzyme that synthesizes the universal sulfate donor (PAPS).	Macromolecular undersulfation; signs of androgen excess (in a minority of patients); very low DHEAS levels and increased androgen levels (in one patient).	(Ahmad *et al.* 1998)
Brachyolmia type 1	271530	AR	*PAPSS2*		Undersulfation of CS; low activity of PAPS-CS sulfotransferase; signs of androgen excess (in a minority of patients).	(Mourão *et al.* 1981)
	271630	AR				
Chondrodysplasia with joint dislocations	614078	AR	*BPNT2*	Golgi resident PAP phosphatase, enzyme that hydrolyzes PAP to	In mice impaired CS and HS sulfation.	(Vissers *et al.* 2011)

				AMP and phosphate.		
Spondyloepiphyseal dysplasia with congenital joint dislocations	143095	AR	*CHST3*	Carbohydrate sulfotransferase-3, enzyme that transfers sulfate to GalNAc residues of CS.	Depletion of 6-O-sulfated GalNAc residues in CS chains in fibroblasts and urine.	(Unger *et al.* 2010)
Ehlers-Danlos syndrome musculocontractural type 1	601776	AR	*CHST14*	Carbohydrate sulfotransferase-14, enzyme that transfers sulfate to GalNAc residues of DS.	Reduction of 4-O-sulfation in GalNAc residues in DS chains; decrease of DS and increase of CS chain synthesis.	(Janecke *et al.* 2016)
Osteochondrodysplasia, brachydactyly and overlapping malformed digits	618167	AR	*CHST11*	Carbohydrate sulfotransferase-11, enzyme that transfers sulfate to GalNAc residues of CS.	In mice abnormal CS localization; strong up-regulation of TGF-β signaling and down-regulation of BMP signaling; altered morphology of the growth plate.	Presented Study; (Shabbir *et al.* 2018)

AR: autosomal recessive; MIM: Mendelian inheritance in man; MOI: mode of inheritance

The limb anomalies witnessed in our family were more complex and comprised a combination of brachydactyly, crossed-fingers/toes, campto-clino-symphalangous digits, and polydactylous and syndactylous toes, in addition to other skeletal findings. Interestingly, Al-Qattan et al. (2015) reported an Arab family with a homozygous mutation in *GDG5* and a wider spectrum of limb anomalies, bringing it closer to the phenotype in our family. There were abducted thumbs, mild shortening of the middle phalanges of the 2nd, 3rd and 4th fingers, hyperphalangism in the 2nd and 3rd, and ulnar deviation of the 2nd and 3rd fingers. In addition to encompassing most of the features reported in the Arab family, our family is presented with a more extended phenotypic manifestation.

As a differential diagnosis, the phenotype was also considered like preaxial brachydactyly syndrome (TPBS; MIM 605282), which is an autosomal-recessive congenital syndrome of the limb with additional features (Temtamy et al. 1998). The features shared between our kindred and TPBS include brachydactyly, abducted thumbs clinodactyly, symphalangism, phalangeal duplication and syndactyly, scoliosis, pectus excavatum, and short stature. However, other features witnessed in TPBS but not shared with the condition in our family include lateral/medial deviation of thumbs, radioulnar synostosis, generalized osteoporosis, plagiocephaly, hypertelorism, micro-/retrognathia, microdontia, deafness, developmental delay, mental retardation, and optic atrophy. Further, the unique features in our family are crossed-fingers/toes, mild facial asymmetry, dislocation of patella, and malaligned fibula (Table 1). Curiously, TPBS is known to be caused by mutations in chondroitin synthase 1 (CHSY1), which is a mediator of BMP signaling and has vital role in developmental pathways (Li et al. 2010).

The study results compared with an apparently novel phenotype of hand and foot abnormalities and severe pectus excavatum in a mother and daughter (Low et al. 2013). The daughter was presented with a limb phenotype characterized by short broad thumbs, short deviated index fingers with associated clinodactyly of the fifth fingers, broad valgus deviated halluces and a laterally deviated overlapping 2nd toe on the right. The other features were brachycephaly, tracheomalacia, congenital heart disease, and pectus excavatum. She had recurrent respiratory infections and poor weight gain. Facial features

included a low anterior hairline, flat supraorbital ridges, telecanthus, small mouth, and posteriorly rotated ears. The authors showed that this dominant phenotype overlapped with TPBS and Catel–Manzke syndrome phenotypes. In both the mother and daughter, a 227 kb duplication was observed within 15q26.3 which encompassed *TM2D3* (OMIM 610014).

In a recent report, Chopra et al. (2015) presented a Turkish family with a deletion of 55-kb that encompasses *CHST11* exon 2 and the embedded microRNA *MIR3922*. The subject had brachydactyly with disproportionately short index fingers and radial or ulnar deviations of fingers and toes at the interphalangeal (IP) joints, long proximal phalanx in 2nd finger, a fused distal phalanx and subluxation of the index metacarpophalangeal (MCP) joint, third digit with four phalanges and a horizontal articulation at the base of the proximal phalanx, the 4-5 fingers had long proximal phalanges; and the 5th finger middle phalanx had a curved articulation distally. The features in these patients shared with our family were brachydactyly, hyperphalangy, and radial and ulnar deviation of fingers and toes. However, unlike our family the Turkish patients also had symphalangism of 1st toe, shortening of middle phalanges of 2-3 toes, loss of toes in 4th toe, and normal thumbs and wrist bones. Additionally, those patients developed the malignant lymphoproliferative disease. On the other hand, our family had additional features like adducted thumbs, cross-fingers, campto-clinodactyly of 3-4 figners, missing or extra flexion creases in certain fingers, hallux varus, cross-toes, postaxial polydactyly in toes, in addition to other skeletal findings, but no history of cancer.

Mice knockout for *Chst11* have severe dwarfism and died shortly after birth (Kluppel et al. 2005). Severe chondrodysplasia in the mutant mice was characterized by a disorganized cartilage growth plate as well as specific alterations in the orientation of chondrocyte columns. The phenotype in the mutant embryos ranged from severely shortened limbs, small rib cage, kinked vertebral column, and dome-shaped skull. Phalanges two and three was absent in both the fore- and hindlimbs, an impaired segmentation of cartilage in digits, the vertebrae of mutant embryos were misshapen with poorly formed dorsal arches, reduced scapula, severely shortened facial bones that included the maxilla, mandible and nasal bones.

Further studies showed that Chst11 is required for proper chondroitin sulfate localization, modulation of distinct signaling pathways and cartilage growth plate morphogenesis. The authors concluded that Chst11 mutation led to strong upregulation of TGFB signaling with concomitant downregulation of BMP signaling, while Indian hedgehog (Ihh) signaling was unaffected. It is of note that the absence of C4st1 leads to osteoarthritis-like symptoms in mice.

The phenotype of our patients is on a milder end compared to that of knockout mice, except for marked facial dysmorphology in mice. Those mice died within hours of birth and were severely dwarfed (Klüppel et al. 2005). The woman with a deletion of 55-kb that encompasses *CHST11* exon 2 and the embedded microRNA *MIR3922* has similar findings as our patients but with also with malignant lymphoproliferative disease. Her deceased sister was similarly affected. The sisters developed lymphoproliferative disease by the age of 36 and 17 years, respectively, and so did their father at the age of 59. The family we present has no cancer history, verifying the hypothesis that if *CHST11* has a role in cancer, the role is the suppression of the proliferation of tumor and not its development.

Nonetheless, our findings confirm that human phenotype is variable and can be rather like the mouse model. Alternatively, it is quite likely that that the additional symptoms evident in the Ireland family like lipoproliferative disease are caused by the deletion of MIR3922 while the deletion mutation in *CHST11* is responsible for limb/skeletal phenotype. This hypothesis, however, requires the functional characterization of these genes in animal models.

This study reports a novel autosomal recessive phenotype characterized by bilateral symmetrical limbs and skeletal defects in the affected individuals, was described as Osteo-chondrodysplasia-bracydactyly-malformed-digits (OCBMD; OMIM: 618167) in OMIM, in extended consanguineous Pakistani kindred due to homozygous deletion in *CHST11* gene on chromosomes 12q23.3 (Shabbir *et al.* 2018).

CHAPTER 4

FAMILY II

Chapter 4. Homozygous deletion encompassing *MYADML2* and *PYCR1* genes causes new syndromic phenotype with unusual skeletal features and cutis laxa

4.1: Abstract

Mutations in a gene that encodes a specific enzyme/protein and leads to the production of an inactive enzyme or no enzyme at all are known as null mutations. Therefore, such mutations are crucial to describe phenotypic features of a disease and uncover the unique functions of null mutated genes. This study reports a homozygous deletion mutation in contiguous genes *MYADML2* and *PYCR1*, which causes a new syndrome with an unusual combination of skeletal anomalies in five sibs of a consanguineous family originated from Southern Punjab, Pakistan. The unique clinical characteristics were lack of cranial symmetry, displaced fused sagittal sutures, maxillary hypoplasia, mandibular prognathia, teeth abnormalities, delayed bone maturity, multiple joints dislocation, malformed patellae, intracondylar fissures in hummers, scapular dyskinesis, lumbar lordosis, protruding chest, clavicles were prominent clavicles, long, limbs, reduced 5^{th} digital rays, and transvers creases in digits. Additionally, features of cutis laxa were present in all affected sibs. The disease gene locus was 3.62-Mb region that mapped at 17q25.3. In the locus, a homozygous deletion of maximal 7.3 kb assumed to cause complete inactivation of *MYADML2* and *PYCR1* genes. Mutations in *PYCR1* cause autosomal recessive cutis laxa (ARCL). All patients had common features of ARCL but did not carry the rare features of ARCL. Therefore, the attributed anomalies were not typical for ARCL to *MYADML2* deficit, because no other genetic defect was present in the identified gene region. *MYADML2* is a gene of unknown function and has not been associated with any disease. This study reported a possible phenotype related to mutation in *MYADML2* gene that causes impaired bone patterning and maturation. The study findings provide a start point for future studies on the function of MYADML2 protein. Discovery of new patients requires confirming the *MYADML2* mutation related phenotype.

4.2: Introduction

There are 5704 known genetic phenotypes out of 25,923 genes covered by OMIM database. This indicates many of our genes not listed in different databases. Similarly, there is lack of reports on some genes like *MYADML2* (PubMed) indicating that the gene has not been studied much. To unravel the function the function of the protein/gene, identification of a null mutation in a gene as the molecular basis of a disease defines the clinical manifestation of the deficit of the encoded protein is one way to explore the functions of gene or protein of unknown nature. There are many cases of hereditary disorders of connective tissues do not fit the current classification systems (Alazami *et al.* 2016). Consanguinity and double recessive gene pathology of inherited disorders making the clinical diagnosis more challenging especially in case of consanguineous pedigrees. However, precise molecular diagnosis through next generation sequencing technology improved the diagnosis of such disorders (Onoufriadis *et al.* 2019).

The current study identified homozygous deletion in five affected sibs born to inbreed parents and the patients afflicted with cutis laxa apart from unusual combination various skeletal and other malformation. In affected siblings, the identified deletion encompassed two genes (*PYCR1* and *MYADML2*) and mutation deduced to complete inactivation of both genes. The *PYCR1* encodes pyrroline-5-carboxylate reductase1 enzyme in which homozygous mutation causes cutis laxa (Guernsey *et al.* 2009; Reversade *et al.* 2009; Alazami *et al.* 2016).

Cutis laxa is an inherited autosomal recessive skin disease featured by inelastic wrinkled skin due to inborn errors of elastic formation and physical malformation of extracellular protein matrix led to sagging skin with an appearance of progeria (premature aging) (Morava *et al.* 2009). In other words, it is skin anomaly of loose, redundant skinfolds and abnormal elasticity of skin (MEHREGAN *et al.* 1978). Autosomal recessive cutis laxa (ARCL) has highly heterogeneous clinical spectrum by considering severity and organ involvement. The clinical spectrum of different type of recessive cutis laxa is given in Table 4.1.

Table 4.1: Clinical spectrum of different recessive hereditary syndrome with cutis laxa.

Phenotypic variables	**Types of Cutis laxa**						
	ARCL-I	***ARCL-II****	***DBS***	***XRCL***	***WSS****	***GO***	***CS***
OMIM	219100	219200	222448	304150	278250	231070	218040
Skin							
Generalized cutis laxa	++	++	++	++	+	−	+
Facial cutis laxa	++	++	++	++	+	−	−
Pathognomonic skin histology	++	++	+	+	−	+	−
Cranio-facial							
Large anterior fontanel	−	++	++	++	+	+	−
Late closure of the fontanel	−	++	++	++	+	+	−
Microcephaly	−	+	+	−	+	−	−
Facial dysmorphy	+	++	++	++	+	+	+
Downslanting palpebral fissures	−	++	++	+	+	−	+
Central nervous system							
Delayed motor development	+	++	++	++	+	+	++
Mental retardation	−	+	++	+	+	+	++
CNS anomalies	−	+	+	+	−	−	+
Skeletal							
Severe short stature/dwarfism	−	+	+	+	−	++	+
Spontaneous	++	+	−	−	−	++	−

fractures							
Joint laxity, subluxation	++	++	+	−	+	+	−
Miscellaneous							
Dystonia/cataract	−	−	++	−	−	−	−
Hernias	++	+	+	++	+	−	−
Significant CV abnormalities	++	+	−	++	−	−	++
Abnormal N- and O-glycosylation	−	+/−	−	−	+/−	−	−
Mutated genes	*FBLN4,5*	*ATP6V0A2*	−	*ATP7A*	*ATP6V0A2*	*SCYL1BP*	*HRAS, KRAS2*
Genetically unsolved cases	+	+	+	−	+	+	+

+: feature present; ++: feature strongly present; -: feature absent; CNS: central nervous system; CV: cardiovascular; ARCL: autosomal recessive cutis laxa; DBS: De Barsy Syndrome; XRCL: X-linked recessive cutis laxa; WSS: wrinkled skin syndrome, GO: geroderma osteodysplastica, CS: Costello syndrome.

Adapted from (Morava *et al.* 2009).

Cutis laxa is highly heterogenetic. For example, ARCL 2B (MIM 612940) and ARCL 3B (MIM 614438) resulted due to biallelic mutations in *PYCR1* with different phenotypic features as compared to and had overlapping features of cutis laxa. Therefore, they are considering *PYCR1* related ARCL. *PYCR1*-related ARCL involves wrinkled skin, intrauterine growth retardation (IUGR), premature aging, visible veins over surface of body, joint hyper-extensibility, hypotonia, and intellectual disability (ID) (Morava *et al.* 2009; Kariminejad *et al.* 2017). Whereas less occurring symptoms are postnatal development delay, osteopenia, and microcephaly.

The current study reports very unusual features for cutis laxa due to deleted parts of *MYADML2* and *PYCR1* genes. The *MYADML2* is protein-coding gene that encodes myeloid-associated differentiation marker-like 2 (MYADML2) protein which contains 307 amino acids in human. This protein has seven transmembrane domains and each domain contains 21 amino acid residues. The MYADML2 protein is integral part of cell membrane but its function is unknown and is not listed in OMIM, PubMed, and in ClinVar no mutation is reported. This is first molecular report of *MYADML2* that caused new syndromic condition with overlapping features of cutis laxa in a Pakistani family.

4.3: Subjects and Methods

4.3.1: **Family** Recruitment

The family was located from remote area of Southern Punjab, Pakistan. The study was approved by Ethical Review Committee of Quaid-i-Azam University, Islamabad, Pakistan (DAS-1070) and the Istanbul Technical University Human Research Ethical Committee (MBG. 22/2014) The detailed pedigree was drawn after taking informed and written consent (Figure 4.1).

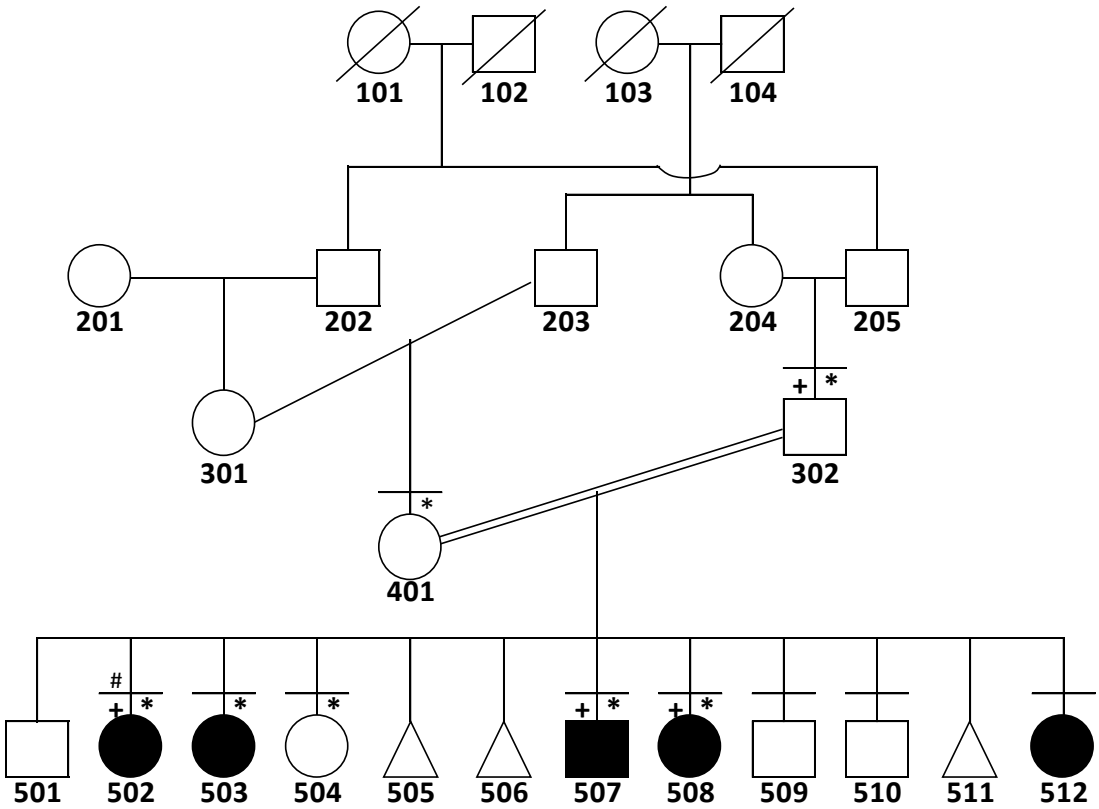

Figure 4.1: Pedigree of family afflicted with cutis laxa like new syndromic condition. Symbols with above horizontal line: physically observed; symbols with oblique line: deceased; *: blood samples available; +: SNP genotyped; #: exome sequence.

△ indicates miscarriages

The family elders told about three prenatal deaths with unknown reasons. Overall, ten subjects (five affected: 502, 503, 507, 508 and 512; five unaffected: 302, 401, 504, 509, and 510) participated in study. All participated subjects were physically examined along with team of local physicians at the residential site of the family.

4.3.2: Molecular Methods

4.3.3: SNP Genotyping and linkage analysis

Peripheral blood samples were drawn from seven subjects (four affected and three normal). DNA was extracted from each sample to perform molecular genetic study. SNP genotyping was done to find the disease gene locus. For SNP genotyping, samples of normal father and three affected subjects were used. The genotype data of 710K SNP markers was generated by using Illumina Human OmniExpress-24 BeadChip. By assuming autosomal recessive inheritance pattern and a disease allele frequency of 0.001, multipoint linkage analysis was performed using Allegro in easyLINKAGE v.5.08.

4.3.4: Exome Sequencing

In order to find the causative gene, exome sequencing was performed for patient 502. The Agilent SureSelect Target Enrichment System was used for exome capturing and the Illumina HiSeq2000 platform for sequencing. Exome file was analyzed to search for the candidate causative mutation. Rare variants with frequencies <0.01 in all populations in ESP6500, 1000 Genomes and gnomAD that includes 10,000 Pakistani exomes in the South Asian samples were selected. The variants which assessed as possibly homozygous predicted as damaging to the protein and is in a possibly relevant gene were considered as candidates to underlie the disease. Hg19 genome assembly at UCSC was used throughout the study.

4.3.5: Polymerase chain reaction

In order to validate the homozygous deletion identified in patients and in addition to test whether *MYADML2* exon 2 was also deleted, PCR amplification

performed by targeting exons 2 and 3 of both deleted genes involved. The primers sequences for respective exons of respective gene given in Table 4.2.

Table 4.2: List of primers sequences to validate the mutation in deleted genes

Mutated Genes	**Amplified exons for mutation validation**	
MYADML2	**Exon 2**	**Exon 3**
F	AACCCTGTGAACCCCAGG	CTGGCCACCCTGCTATG
R	CCCAACATTTATCTCACCCCT	AAGGCCTGGACGATCTTG
PYCR1		
F	CCTAACTTGCTCTCGATCCT	AAGAACTGAAGAGGAACTGTTT
R	GCCAGTCTCTCCCACTG	GTCTCCTTTCTCCCTTTCATC

4.4: RESULTS

4.4.1: Clinical Report

Five normal subjects (father, mother and 3 sibs (302, 401, 504, 509 and 510)), clinically examined had no skeletal malformation, facial dysmorphic features or skin anomaly. Physical examination and X-rays images indicated that five affected subjects had similar phenotypic features (Tables 4.3-4.4 and Figures 4.2-3). The clinical symptoms were cranial asymmetry, mandibular prognathia, hypoplastic maxilla, mal-positioned and crowded teeth in all patients. The cranial CT-scan of patient 503 showed skull anomalies like partially fused sagittal sutures deviating from the medial axis, depressed frontal and occipital bones of the skull (Figure 4.3). X-ray films revealed osteopenia, and general skeletal abnormalities affecting cranio-facial, axial and appendicular bones. In case of axial skeleton, there was variable scoliosis of thoracic and lumber areas. In case of appendicular skeleton, in upper limbs, clavicles were hypoplastic and dislocated, dyskinesis of scapula, intracondylar fissures in humor, proximal end of ulna was dislocated, 5^{th} digital rays were short, and radii and ulnae were narrowly aligned (508). In lower limbs, pelvic girdle was underdeveloped, and asymmetric, proximal femoral heads were dislocated, fibulae were dislocated malformed patellae, and expanded tarsal bones. Bilateral malformation of acetabulum. Additionally, there was lack of bone maturation as depicted by the metaphyseal lines which were unfused and poor bone mineralization.

Table 4.3: Clinical features in five affected sibs compared with *PYCRI*-associated phenotype

Features	**502**	**503**	**507**	**508**	**512**	***PYCR1*-ARCL**
Gender, age (years)	F, 18	F, 16	M, 12	F, 10	F, 4	
Prenatal						
IUGR	+	+	+	+	+	+
Skin						
Loose wrinkled skin	+	+	+	+	+	+
Translucent skin appearance	+	+	+	+	+	+
Mildly low IQ	+	+	+	+	NA	+
Low hairline	+	+	+	+	+	+
Sparse hair	+	+	+	+	+	+
Extra flexion creases on fingers	+	+	+	+	+	−
Skull and orofacial						
Cranial asymmetry	+	+	+	+	+	−
Mandibular prognathia	+	+	+	+	+	−
Maxillary hypoplasia	+	+	+	+	+	−
Misaligned/crowded teeth	+	+	+	+	NA	−
Elongated and triangular face	+	+	+	+	NA	+
Protruding forehead	+	+	+	+	+	+
Splayed eyebrows	+	+	+	+	+	+
Down slanting eyes	+	+	+	+	+	+
Ears were large and prominent	+	+	+	+	+	+
Strabismus	+	+	+	+	−	+
Alternative esotropia	+	+	+	+	−	+
Musculoskeletal						
Hypotonia	+	+	+	+	+	+
Short stature	+	+	+	+	NA	+

Gait problem	+	+	+	+	NA	+
Joint dislocations	+	+	+	+	NA	+
Joint hyperlaxity	+	+	+	+	+	+
Scoliosis	+	+	+	+	NA	–
Lumbar lordosis	+	+	+	+	NA	–
Protruding sternum	+	+	+	+	NA	–
Prominent clavicles	+	+	+	+	NA	–
Hypoplastic pelvic girdle	+	+	+	+	NA	+
Dislocated proximal femoral heads	+	+	+	+	NA	+
Posteriorly dislocated fibulae	+	+	+	+	NA	–
Hypoplastic / malpositioned patellae	+	+	+	+	NA	–
Splayed tarsal bones	+	+	–	–	NA	–
Dislocated / hypoplastic clavicles	+	+	+	+	NA	–
Scapular dyskinesis	+	+	+	+	NA	–
Humeral intracondylar fissures	+	+	+	+	NA	–
Dislocation of proximal ulnar heads	+	+	+	+	NA	+
Shortening of 5th digital rays	+	+	+	+	NA	–
Lack of maturation of tubular bones	+	+	+	+	NA	+
Flat feet	+	+	+	+	+	+
Cylindrical and elongated digits	+	+	+	+	+	+

+, feature present; -, feature absent; NA, could not be assessed due to too young age

Table 4.4: Summary of radiological and anatomic features in patients

Variables	**502**	**503**	**507**	**508**
Gender, age (years)	F, 18	F, 16	M, 12	F, 10
Skull and orofacial				
Mandibular prognathia	+	+	+	+
Maxillary hypoplasia	+	+	+	+
Dental crowding	+	+	+	+
Cranial asymmetry	+	+	+	+
Axial skeleton				
Protruding chest	+	+	+	+
Scoliosis	+	+	+	+
Hypoplastic and asymmetrical pelvic girdle	+	+	+	+
Hip dislocation	+	+	+	+
Hypoplastic iliac shaft	+	+	+	+
Femoral head hypoplasia/dislocation	+	+, left	+	+
Hypoplastic and posteriorly dislocated fibulae	+	+	+	+
Hypoplastic and malpositioned patellae	+	+	+	+
Appendicular skeleton				
Splayed tarsal bones	+	+	–	–
Dislocated and hypoplastic clavicle	+	+	+	+
Scapular dyskinesis	+	+	+	+
Humeral intracondylar fissure	+	+	+	+
Dislocation of proximal ulnar heads	+	+	+	+
Narrow spaces between radii and ulnae	–	–	–	+
Brachydactyly of 5^{th} finger	+	+	+	+
Generally delayed bone age	+	+	+	+

+, feature present; -, feature absent. Features are present bilaterally unless mentioned otherwise.

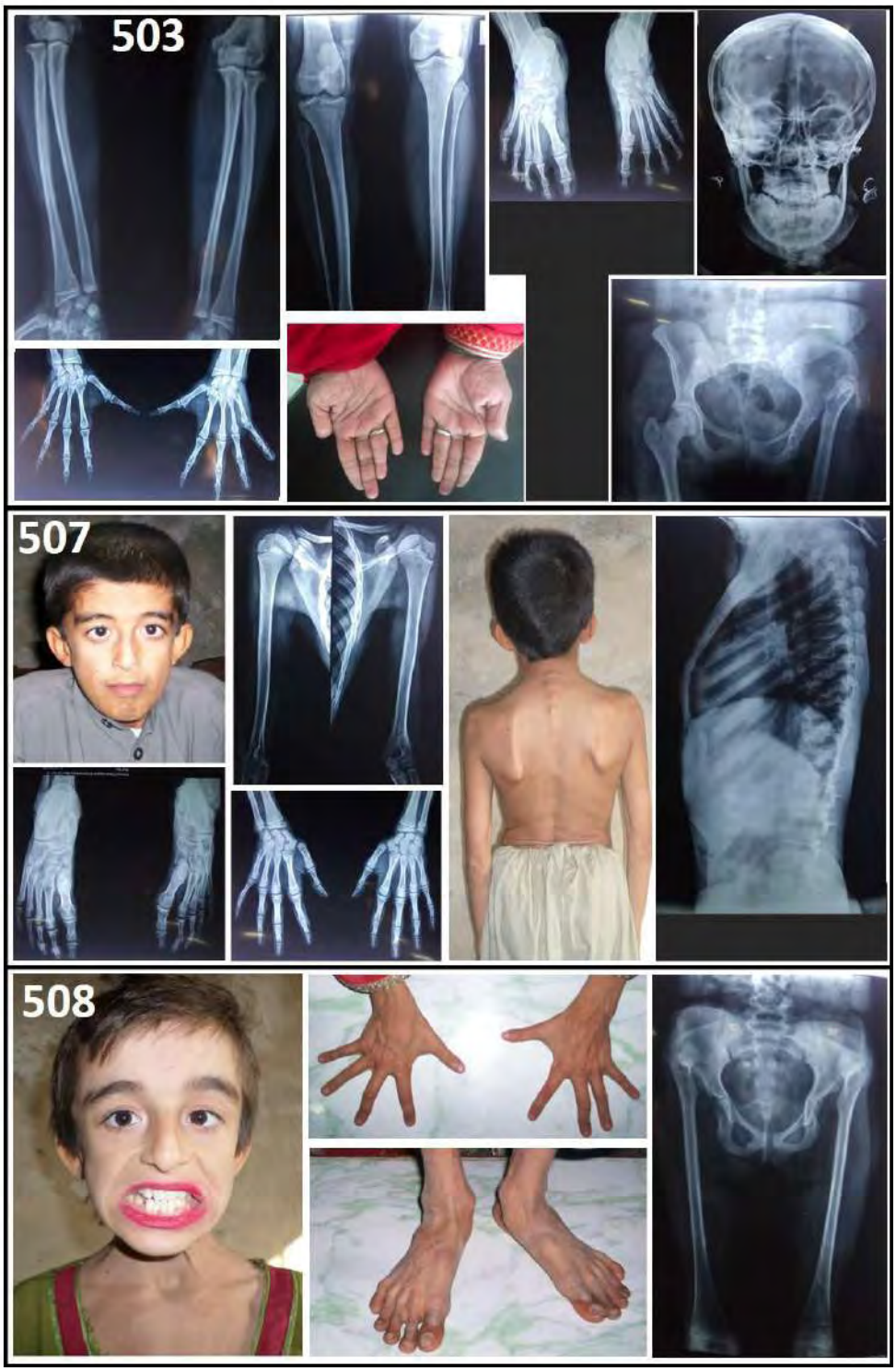

Figure 4.2: Phenotype in three affected subjects (503, 507, and 508). Osteopenia, and general skeletal abnormalities affecting cranio-facial, axial and appendicular bones (503). Cranial asymmetry, mandibular prognathia, hypoplastic maxilla, scoliosis, lumbar lordosis and dyskinesis of scapula (507). Misaligned/crowded teeth, long digits, asymmetric underdeveloped pelvic girdle, proximal femoral heads were dislocated, fibulae were dislocated malformed patellae, lack of bone maturation and poor bone mineralization (508).

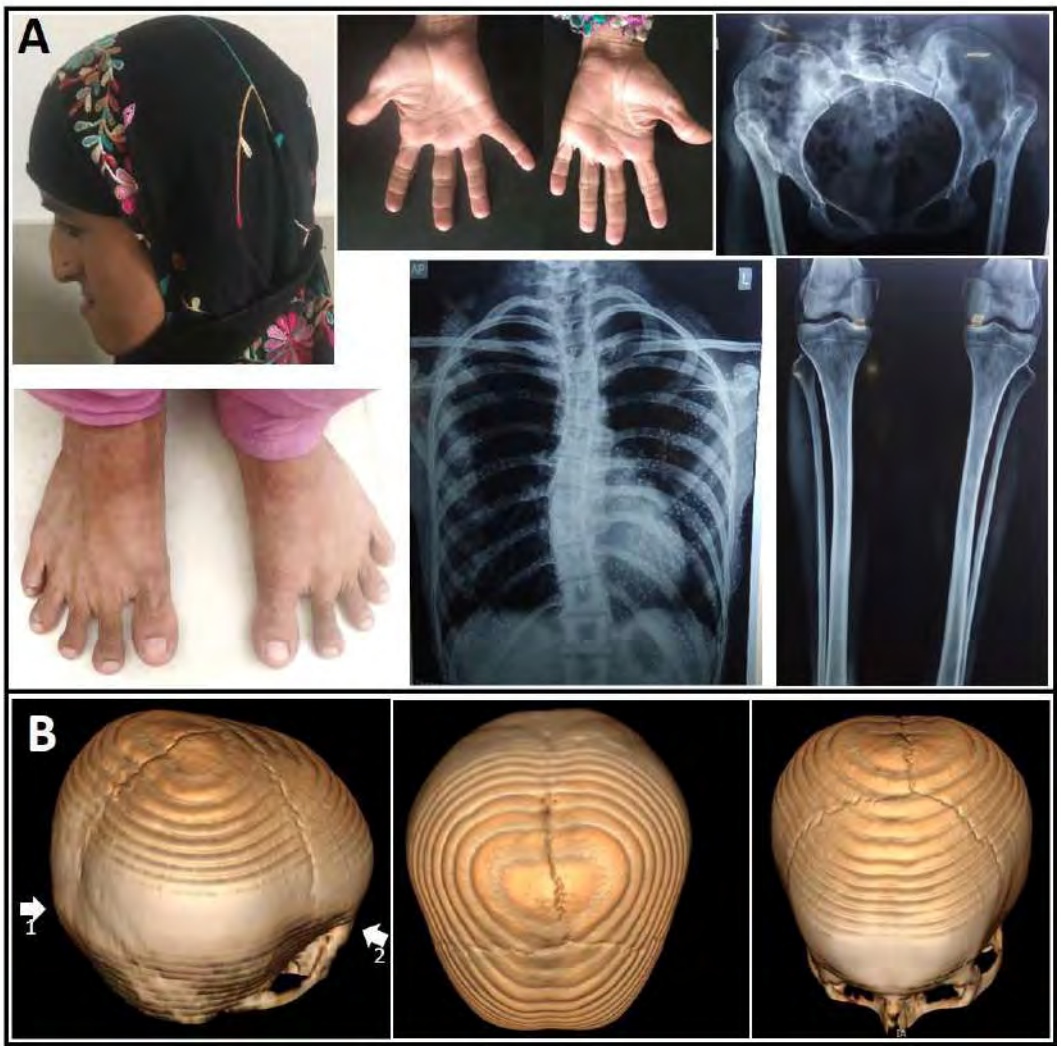

Figure 4.3: Phenotypic in affected patient 502. Pictures and X-ray images of affected sib 502. Mandibular prognathia, maxillary hypoplasia, and prominent nose bridge; thin cylindrical fingers with extra ventral phalangeal creases and shortening of fifth fingers; hypoplasia of pelvic girdle with short iliac wings, malformation of acetabula and asymmetrically and posteriorly dislocated femoral heads that articulated with the posterior aspects of iliac crests; narrowly aligned tibiae and fibulae, and hypoplastic and malpositioned patellae; general osteopenia and lack of maturation of tubular bones as evidenced by visible metaphyseal lines, unfused metaphyseal lines and poor bone mineralization; general delayed bone age indicated by the epiphyseal gaps at the end of long bones and delayed closure of epiphyseal lines; scoliosis of thoracic and lumbar spines and dislocated and hypoplastic clavicles; splayfoot; b 3D reconstructions of cranial CT of 503, showing cranial anomalies including incompletely fused sagittal sutures deviating from the medial axis, and asymmetry evident as depressions in the frontal and occipital aspects of the skull (arrows).

Invariant skeletal malformations were short stature, hyperlaxity in joints, scoliosis, lumber lordosis, keel like sternum, prominent clavicles, scapular dyskinesis, elongated and cylindrical fingers and toes, and flat feet. On some fingers extra ventral transverse digital creases were found apart from the normal flexion creases. Parents reported intrauterine growth retardation for all five patients. Anthropometric measurements were taken of four patients, showed poor development. The microcephaly was present only in one patient 508 (Table 4.5). Affected sibs had mild low IQ because patients attend normal school but with low performance. First four elder patients had developed strabismus in late childhood.

Table 4.5: Comparison of anthropometric measurements of affected (502, 503, 507, and 508) and normal subjects (302, 509, and 510)

Variables	**502**	**503**	**507**	**508**	**302**	**509**	**510**
Gender, age (years)	F,18	F, 16	M, 12	F, 10	M, 45	M, 9	M, 8
Affection status	A	A	A	A	UA	UA	UA
OFC (cm) ‡	52 (25)	53 (50)	50 (>10)	47 (<1)	58 (>85)	50 (<10)	50 (<25)
Arm span (cm) §	149 (>95)	145 (>30)	121 (>30)	110 (>30)	155 (>30)	120 (>30)	120 (>30)
Standing height (cm)*	138 (<1)	143 (<1)	124 (<1)	118 (<1)	159 (<3)	122 (<3)	119 (<10)
Sitting height (cm) †	67 (<1)	68 (<1)	63 (<1)	61 (<1)	80 (<3)	58 (<1)	57 (<1)
Weight (kg)*	33 (<1)	56 (>25)	23 (<1)	19 (<1)	NA	NA	NA

A, affected; UA, unaffected; NA, not assessed; OFC, occipitofrontal circumference

‡ Chirita-Emandi A, Doros G, Simina IJ, Gafencu M, Puiu M. Head circumference references for school age children in Western Romania. Rev Med Chir Soc Med Nat Iasi. 2015; **119**:1083-91.

§With reference to height. Chen WY, Lin YT, Chen Y, Chen KC, Kuo BI, Tsao PC, Lee YS, Soong WJ, Jeng MJ. Reference equations for predicting standing height of children by using arm span or forearm length as an index. *J Chin Med Assoc.* 2018; **81**:649-56.

*Percentiles are from WHO Growth Reference: http://www.who.int/growthref/who2007_height_for_age/en/

†Kelly AM, Shaw NJ, Thomas AM, Pynsent PB, Baker DJ. Growth of Pakistani children in relation to the 1990 growth standards. *Arch Dis Child*. 1997; **77**:401-5.

The features of cutis laxa (with clear progeria) were loose wrinkled skin, dysmorphic facial features, and skeletal defects, joint dislocation, abnormal gait, triangular elongated face with protruding forehead, splayed eyebrows, down slanting eyes (Figure 4.2), ears were large and prominent, low hairline, sparse hairs, thin translucent wrinkled skin (Table 4.3). Veins were visible and prominent all over the body, hypotonia, osteopenia, shortness of breath, and early fatigue during physical activity. Ocular examination indicated esotropia with normal refractive errors & normal vision. Computed tomography scan of brain of affected subject 503 showed normal gyri, sulci, grey matter differentiation, brain parenchyma density, ventricles, posterior fossa, paranasal sinuses, orbits, and mastoid. Therefore, CT-scan declared normal brain development without structural defects in brain.

4.4.2: Molecular findings

In summary, clinical findings were not typical to any known phenotype, hence, molecular tests launched to find disease gene. Linkage analysis performed to map gene defect causing disease in the family (Figure 4.4). Through SNP analysis, those regions which yield multipoint LOD score >2 and with shared homozygosity were considered as candidate regions to harbor the disease gene. Shared homozygosity regions >1Mb were considered as candidate regions to harbour the putative gene defect (Figure 4.5). Multipoint LOD score graphs for all chromosomes (Figure 4.6).

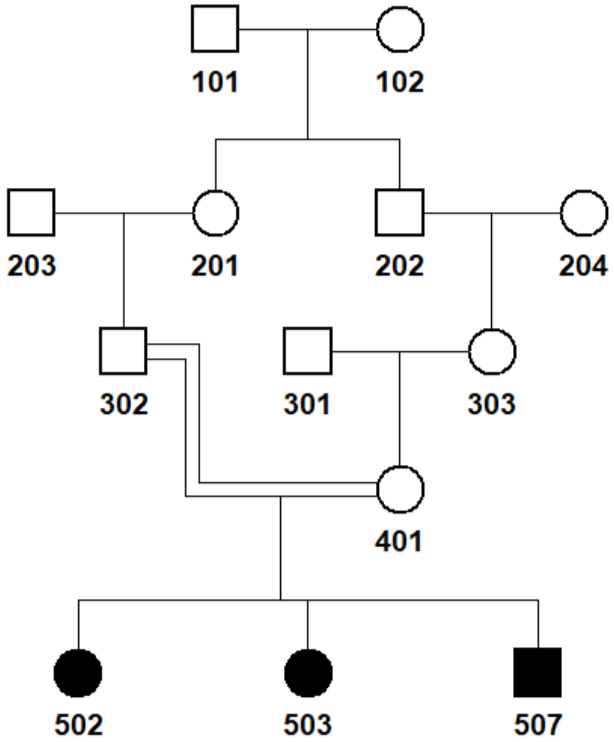

Figure 4.4: Simplified pedigree used for linkage analysis

Among candidate regions, only one region of 3.62 Mb at 17q25.3 between rs2612778 (nucleotide 77,150,807) and rs2677919 (80,774,148) was opted while other regions which were selected as candidate regions were neglected because of their small size < 1Mb. Later, unaffected sister 504 without SNP data was not homozygous for the deletion in the region whereas patient 503 was homozygous, increasing the LOD score from 2.69 to 3.43. Therefore, this region was considered as disease gene locus in the family and the homozygosity in the candidate region shown in Figure 4.5 and the chromosomes wise linkage analysis given in Figure 4.6.

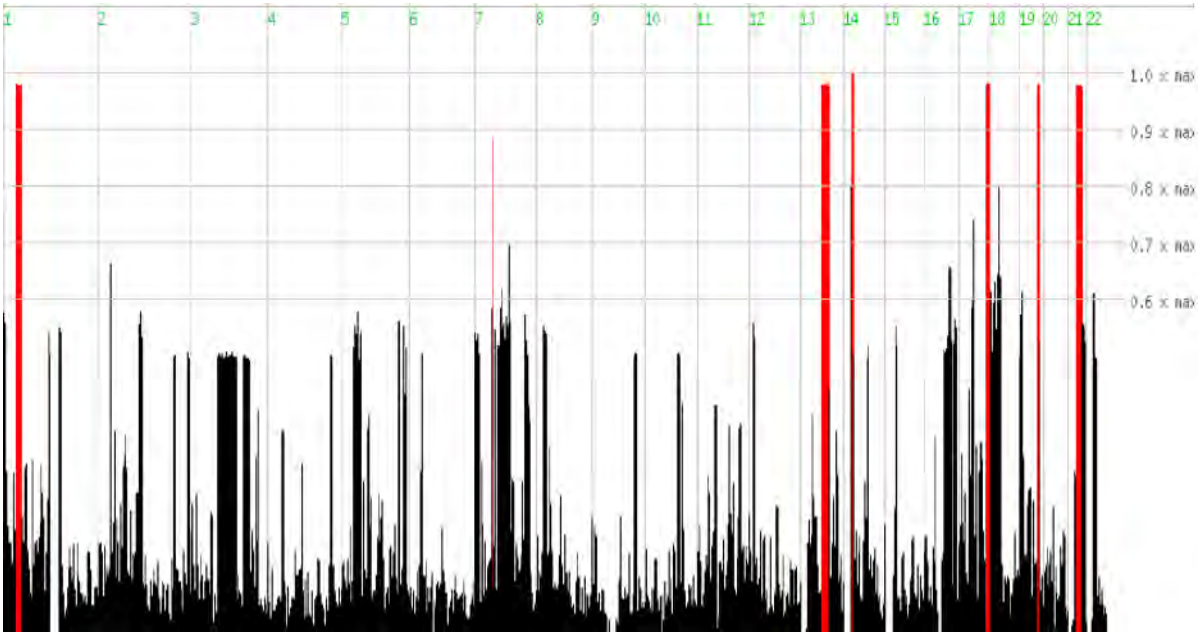

Figure 4.5: Graphical representation of homozygosity intervals obtained by HomozygosityMapper with default parameters. Red bars depict the longer stretches of homozygous genotypes on chromosomes and black bars revealed short stretches of homozygous genotypes.

Chromosome 1

Project:	FAM38-SNP FILES FOR LINKA	Inheritance:	Recessive
Family name:	TOTALS	Common allele:	99.90 %
Used map:	730k Mb (sex-averaged)	Disease allele:	0.10 %
Marker positions:	14500 ok / 29 ? / 0 outside	LC1 PCOPY rate:	0.00 %
Allele frequencies:	Codominant	LC1 PENET wt/mt:	0.00 %
		LC1 PENET mt/mt:	99.00 %

Marker	CHR	cM	LOD	ALPHA	HLOD
1.rs4651288	1	185.79	2.6983	0.0000	2.6983
2.rs13375391 - rs17448230	1	185.80	2.6983	0.0000	2.6983
3.rs13375391 - rs17448230	1	185.81	2.6983	0.0000	2.6983
4.rs13375391 - rs17448230	1	185.81	2.6983	0.0000	2.6983
5.rs13375391 - rs17448230	1	185.82	2.6983	0.0000	2.6983

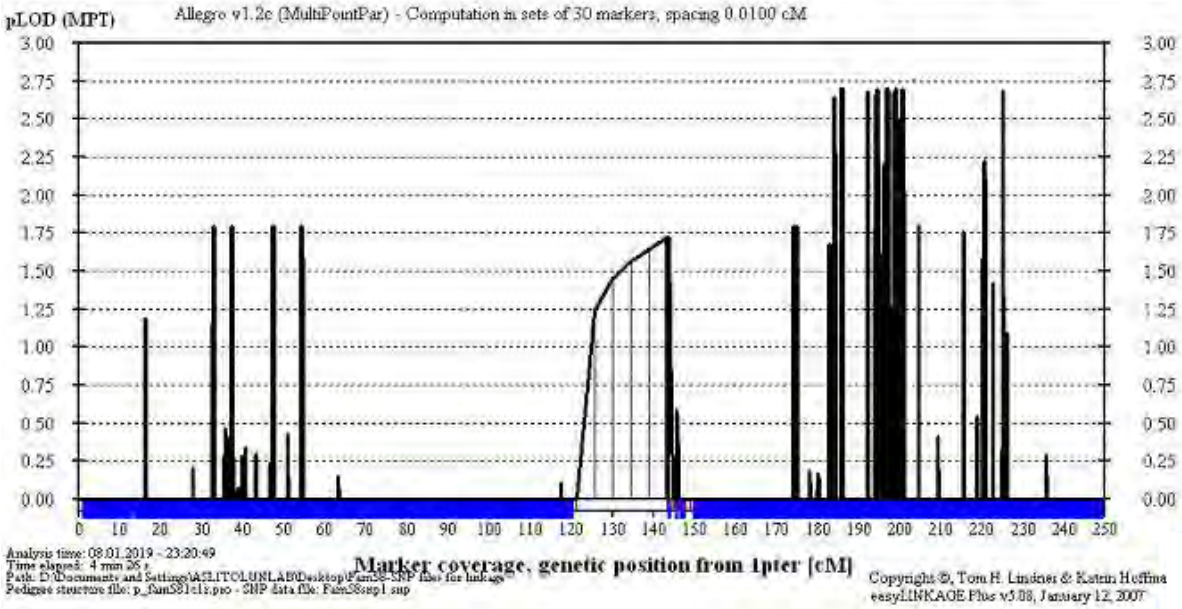

Figure 4.6: Chromosome wise results of linkage analysis; graphical output of easyLinkage.

Chromosome 2

Project:	FAM38-SNP FILES FOR LINKA	Inheritance:	Recessive
Family name:	TOTALS	Common allele:	99.90 %
Used map:	730k Mb (sex-averaged)	Disease allele:	0.10 %
Marker positions:	14807 ok / 25 ? / 0 outside	LC1 PCOPY rate:	0.00 %
Allele frequencies:	Codominant	LC1 PENET wt/mt:	0.00 %
		LC1 PENET mt/mt:	99.00 %

Marker	CHR	cM	LOD	ALPHA	HLOD
1.rs12712328	2	32.65	2.6983	0.0000	2.6983
2.rs12712328 - rs12992095	2	32.66	2.6983	0.0000	2.6983
3.rs12712328 - rs12992095	2	32.66	2.6983	0.0000	2.6983
4.rs12992095 - rs6747906	2	32.66	2.6983	0.0000	2.6983
5.rs12992095 - rs6747906	2	32.66	2.6983	0.0000	2.6983

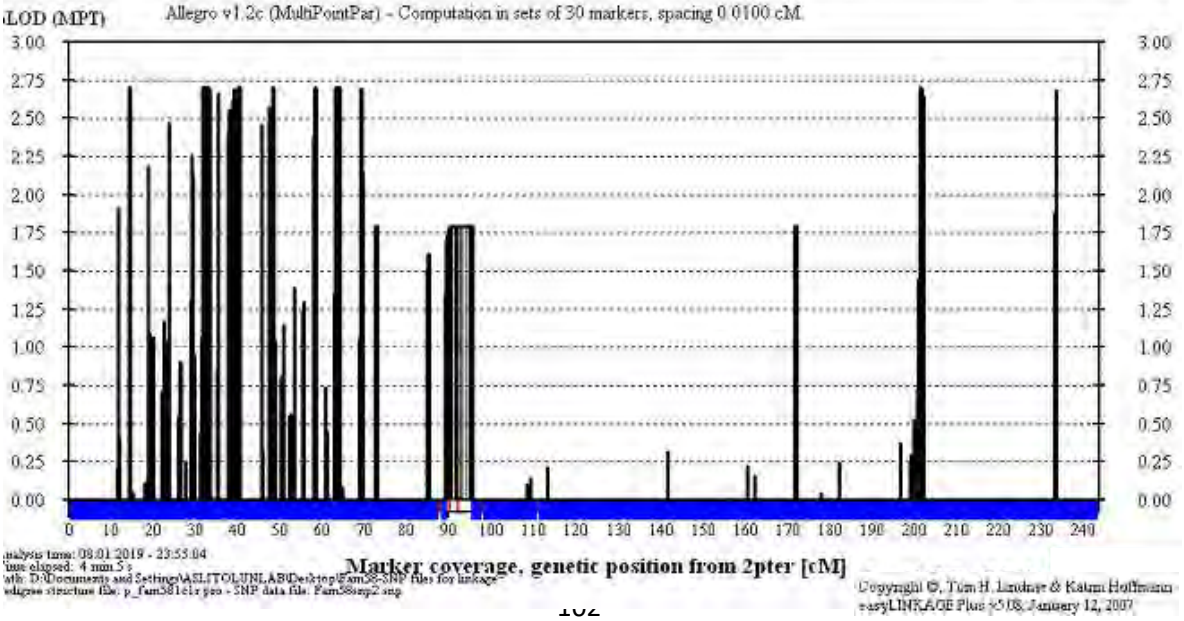

Figure 4.6: continued

Chromosome 3

Project:	FAM38-SNP FILES FOR LINKAGE	Inheritance:	Recessive
Family name:	TOTALS	Common allele:	99.90 %
Used map:	730k Mb (sex-averaged)	Disease allele:	0.10 %
Marker positions:	11804 ok / 16 ? / 0 outside	LC1 PCOPY rate:	0.00 %
Allele frequencies:	Codominant	LC1 PENET wt/mt:	0.00 %
		LC1 PENET mt/mt:	99.00 %

Marker	CHR	cM	LOD	ALPHA	HLOD
1.rs2289303	3	27.30	2.0265	0.0000	2.0265
2.rs9833074 - rs4973868	3	27.30	2.0265	0.0000	2.0265
3.rs9833074 - rs4973868	3	27.30	2.0265	0.0000	2.0265
4.rs9833074 - rs4973868	3	27.31	2.0265	0.0000	2.0265
5.rs9833074 - rs4973868	3	27.31	2.0265	0.0000	2.0265

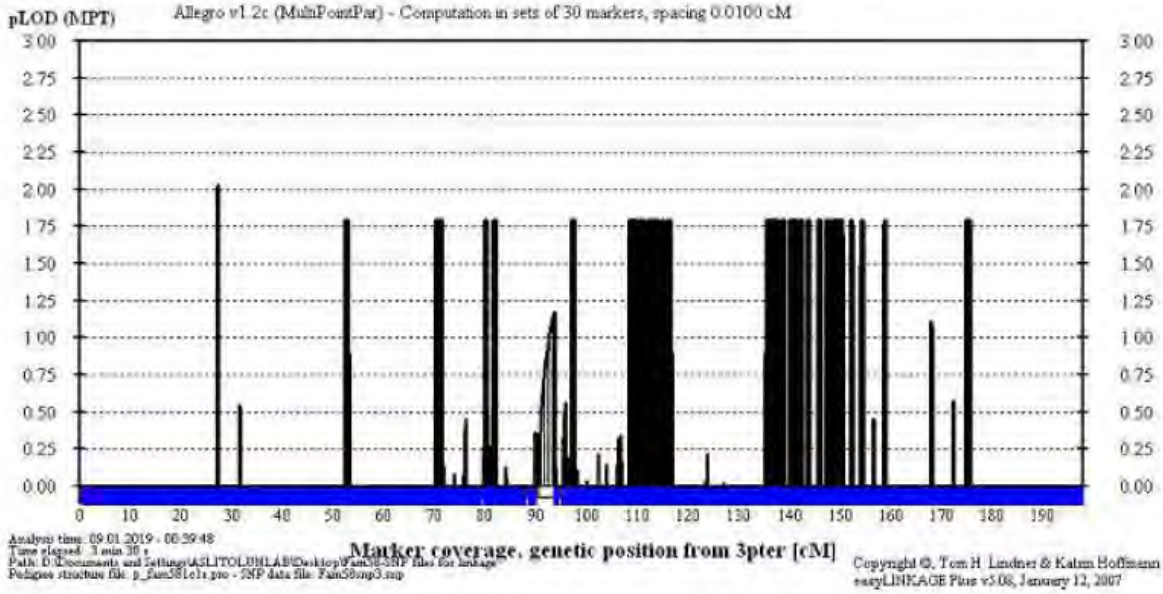

Chromosome 4

Project:	FAM38-SNP FILES FOR LINKAGE	Inheritance:	Recessive
Family name:	TOTALS	Common allele:	99.90 %
Used map:	730k Mb (sex-averaged)	Disease allele:	0.10 %
Marker positions:	10812 ok / 19 ? / 0 outside	LC1 PCOPY rate:	0.00 %
Allele frequencies:	Codominant	LC1 PENET wt/mt:	0.00 %
		LC1 PENET mt/mt:	99.00 %

Marker	CHR	cM	LOD	ALPHA	HLOD
1.rs10009466 - rs6851779	4	45.48	2.6981	0.0000	2.6981
2.rs6851779	4	45.49	2.6981	0.0000	2.6981
3.rs6851779 - rs17595063	4	45.49	2.6981	0.0000	2.6981
4.rs17595063 - rs990676	4	45.49	2.6981	0.0000	2.6981
5.rs990676 - rs16858591	4	45.50	2.6981	0.0000	2.6981

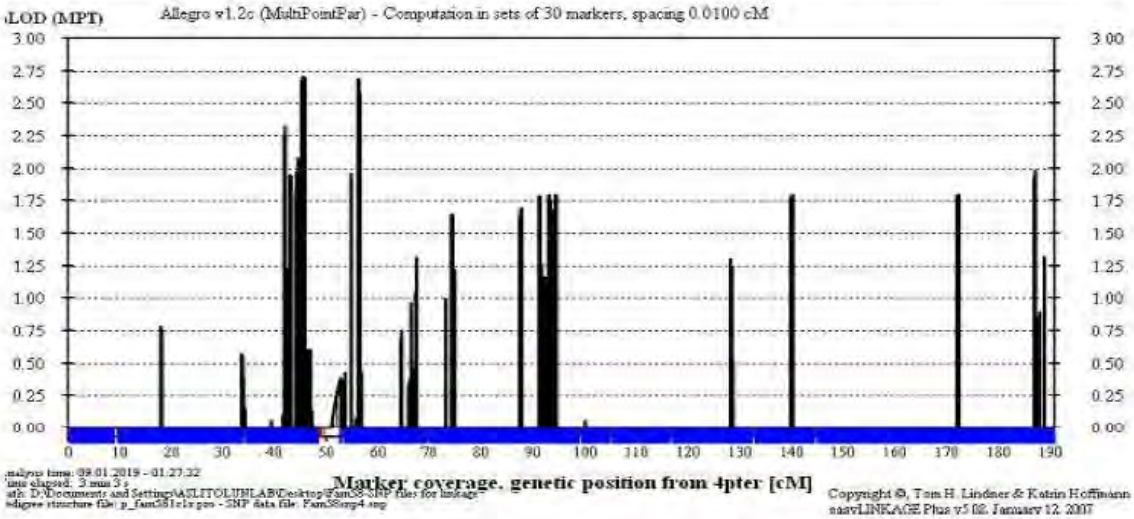

Chromosome 5

Project:	FAM58-SNP FILES FOR LINKA	Inheritance:	Recessive
Family name:	TOTALS	Common allele:	99.90 %
Used map:	730k Mb (sex-averaged)	Disease allele:	0.10 %
Marker positions:	10515 ok / 15 ? / 0 outside	LC1 PCOPY rate:	0.00 %
Allele frequencies:	Codominant	LC1 PENET wt/wt:	0.00 %
		LC1 PENET mt/wt:	99.00 %

Marker	CHR	cM	LOD	ALPHA	HLOD
1 rs10941412	5	30.92	1.7952	0.0000	1.7952
2 rs2278328 - rs2278329	5	30.92	1.7952	0.0000	1.7952
3 rs157291 - rs6892496	5	30.92	1.7952	0.0000	1.7952
4 rs6892496 - rs2749737	5	30.93	1.7952	0.0000	1.7952
5 rs6892496 - rs2749737	5	30.93	1.7952	0.0000	1.7952

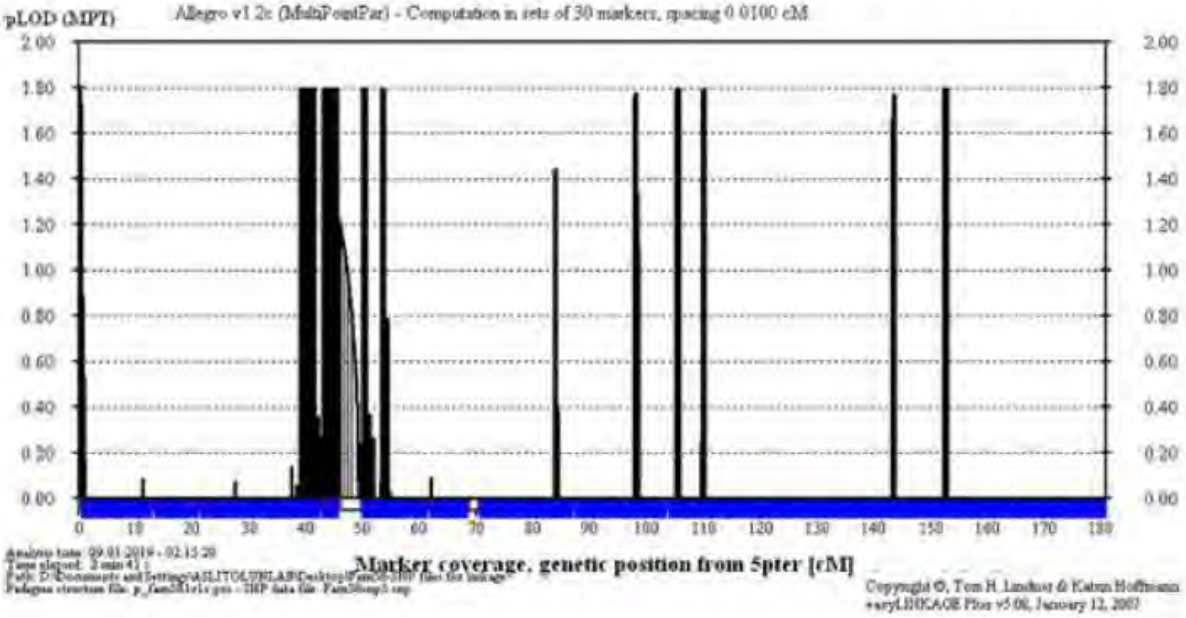

Chromosome 6

Project:	FAM58-SNP FILES FOR LINKA	Inheritance:	Recessive
Family name:	TOTALS	Common allele:	99.90 %
Used map:	730k Mb (sex-averaged)	Disease allele:	0.10 %
Marker positions:	10575 ok / 54 ? / 0 outside	LC1 PCOPY rate:	0.00 %
Allele frequencies:	Codominant	LC1 PENET wt/wt:	0.00 %
		LC1 PENET mt/wt:	99.00 %

Marker	CHR	cM	LOD	ALPHA	HLOD
1 rs1936899	6	19.70	1.8370	0.0000	1.8370
2 rs9460400 - rs9465496	6	19.70	1.8370	0.0000	1.8370
3 rs9465496 - rs9358265	6	19.70	1.8370	0.0000	1.8370
4 rs9465496 - rs9358265	6	19.71	1.8370	0.0000	1.8370
5 rs17547572 - rs6926312	6	19.71	1.8370	0.0000	1.8370

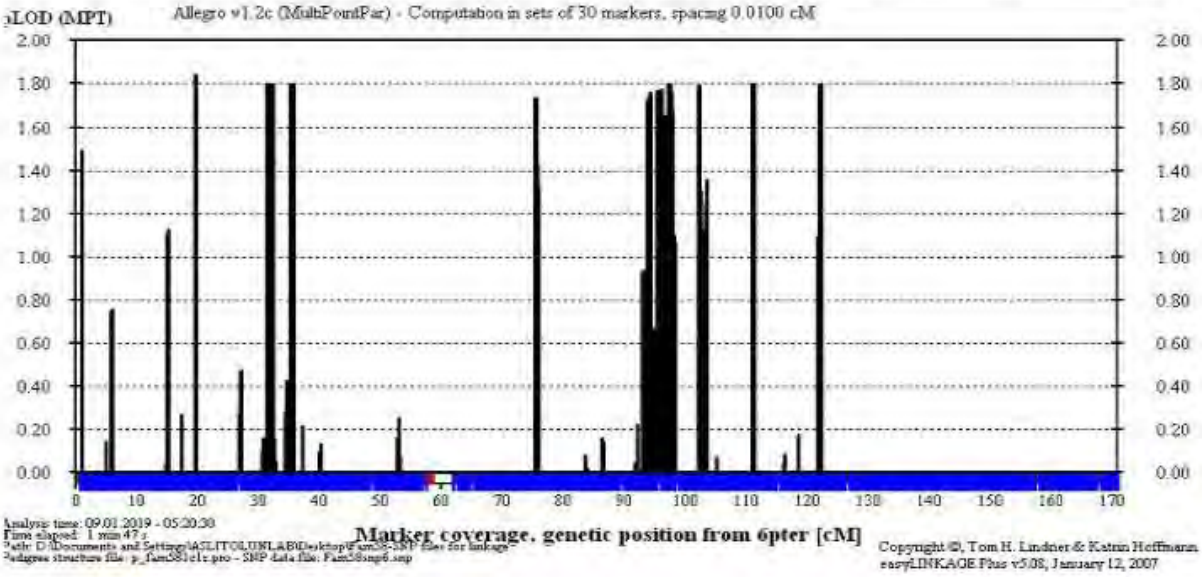

Chromosome 7

Project:	FAM58-SNP FILES FOR LINKA	Inheritance:	Recessive
Family name:	TOTALS	Common allele:	99.90 %
Used map:	730k Mb (sex-averaged)	Disease allele:	0.10 %
Marker positions:	9539 ok / 22 ? / 0 outside	LC1 PCOPY rate:	0.00 %
Allele frequencies:	Codominant	LC1 PENET wt/wt:	0.00 %
		LC1 PENET mt/mt:	99.00 %

Marker	CHR	cM	LOD	ALPHA	HLOD
1 rs10279856	7	43.64	2.6983	0.0000	2.6983
2 rs10279856 - rs10215478	7	43.65	2.6983	0.0000	2.6983
3 rs10279856 - rs10215478	7	43.65	2.6983	0.0000	2.6983
4 rs10279856 - rs10215478	7	43.65	2.6983	0.0000	2.6983
5 rs10279856 - rs10215478	7	43.65	2.6983	0.0000	2.6983

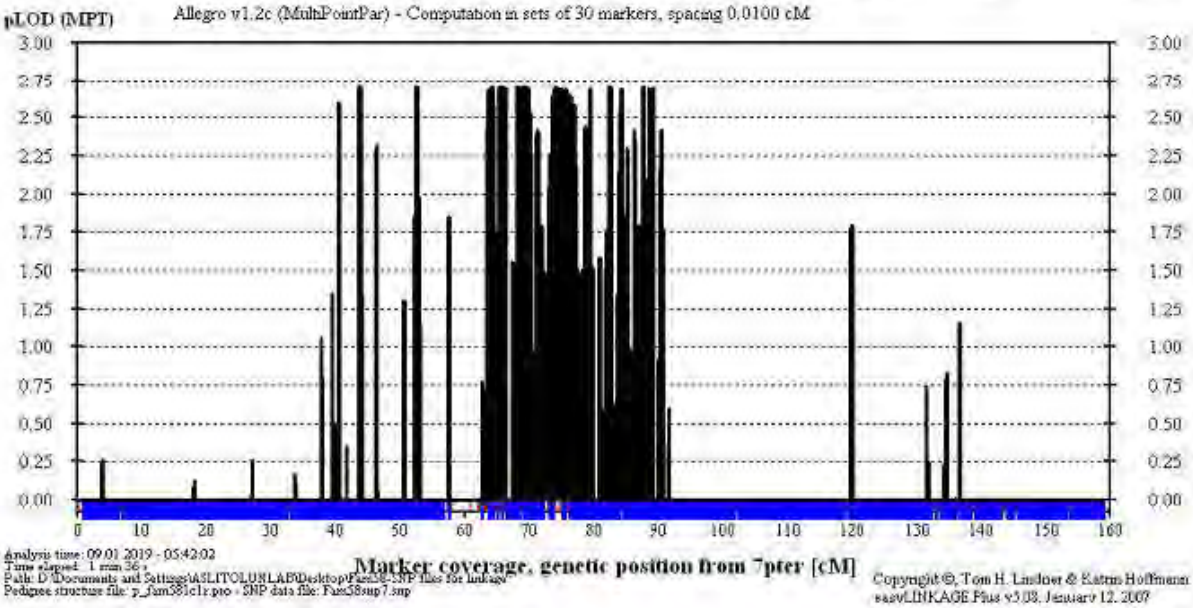

Analysis time: 09.01.2019 - 05:42:02
Time elapsed: 1 min 36 s
Path: D:\Documents and Settings\ASLITOLUNLAB\Desktop\Fam58-SNP files for linkage
Pedigree structure file: p_fam58c1r.pro - SNP data file: Fam58snp7.snp

Chromosome 8

Project:	FAM58-SNP FILES FOR LINKA	Inheritance:	Recessive
Family name:	TOTALS	Common allele:	99.90 %
Used map:	730k Mb (sex-averaged)	Disease allele:	0.10 %
Marker positions:	8673 ok / 9 ? / 0 outside	LC1 PCOPY rate:	0.00 %
Allele frequencies:	Codominant	LC1 PENET wt/wt:	0.00 %
		LC1 PENET mt/mt:	99.00 %

Marker	CHR	cM	LOD	ALPHA	HLOD
1 rs2298423	8	37.83	1.7952	0.0000	1.7952
2 rs2298423 - rs28813686	8	37.84	1.7952	0.0000	1.7952
3 rs2298423 - rs28813686	8	37.85	1.7952	0.0000	1.7952
4 rs2298423 - rs28813686	8	37.86	1.7952	0.0000	1.7952
5 rs2298423 - rs28813686	8	37.87	1.7952	0.0000	1.7952

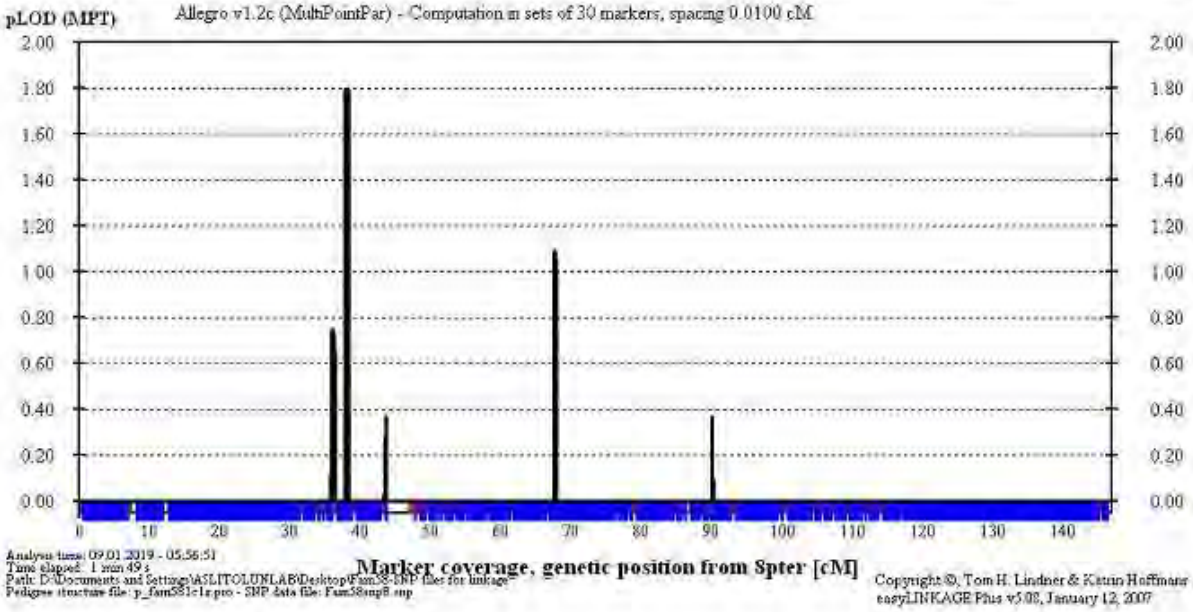

Analysis time: 09.01.2019 - 05:56:51
Time elapsed: 1 min 49 s
Path: D:\Documents and Settings\ASLITOLUNLAB\Desktop\Fam58-SNP files for linkage
Pedigree structure file: p_fam58c1r.pro - SNP data file: Fam58snp8.snp

Chromosome 9

Project:	FAM58-SNP FILES FOR LINKA	**Inheritance:**	Recessive	**Marker**	**CHR**	**cM**	**LOD**	**ALPHA**	**HLOD**
Family name:	TOTALS	**Common allele:**	99.90 %	1.rs10441737	9	114.30	2.6983	0.0000	2.6983
Used map:	730k Mb (sex-averaged)	**Disease allele:**	0.10 %	2.rs10441737 - rs10759501	9	114.30	2.6983	0.0000	2.6983
Marker positions:	7162 ok / 28 ? / 0 outside	**LC1 PCOPY rate:**	0.00 %	3.rs10759501 - rs12341420	9	114.31	2.6983	0.0000	2.6983
Allele frequencies:	Codominant	**LC1 PENET wt/mt:**	0.00 %	4.rs10759501 - rs12341420	9	114.31	2.6983	0.0000	2.6983
		LC1 PENET mt/mt:	99.00 %	5.rs10759501 - rs12341420	9	114.31	2.6983	0.0000	2.6983

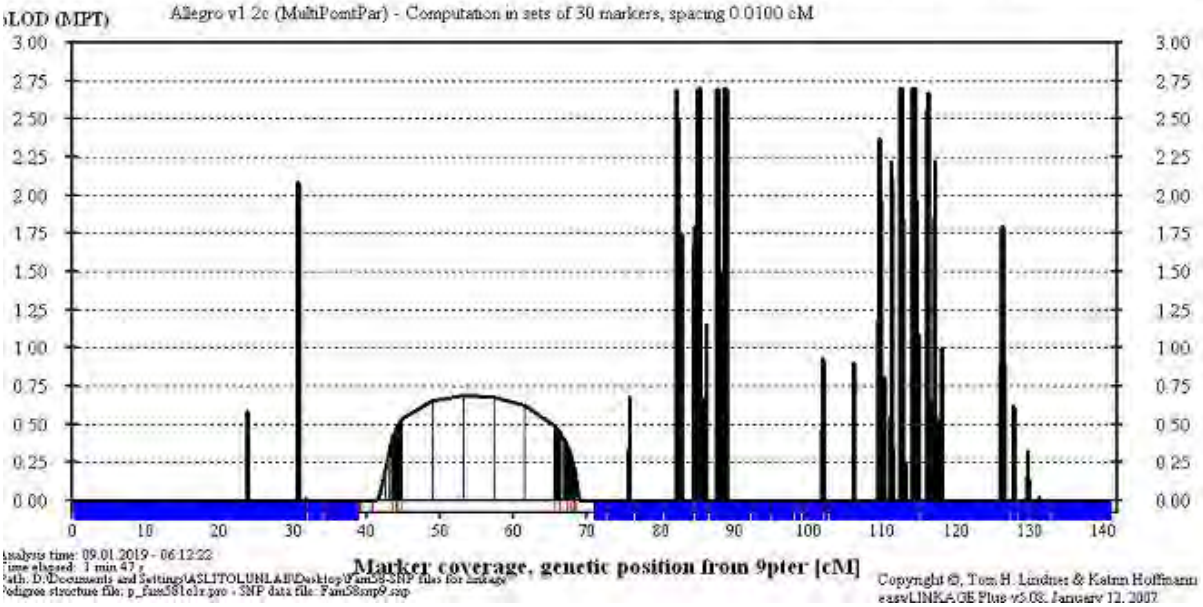

Chromosome 10

Project:	FAM58-SNP FILES FOR LINKA	**Inheritance:**	Recessive	**Marker**	**CHR**	**cM**	**LOD**	**ALPHA**	**HLOD**
Family name:	TOTALS	**Common allele:**	99.90 %	1.rs2277207	10	113.92	2.6277	0.0000	2.6277
Used map:	730k Mb (sex-averaged)	**Disease allele:**	0.10 %	2.rs17129557 - rs2277207	10	113.92	2.6274	0.0000	2.6274
Marker positions:	8630 ok / 27 ? / 0 outside	**LC1 PCOPY rate:**	0.00 %	3.rs17129557 - rs2277207	10	113.92	2.6270	0.0000	2.6270
Allele frequencies:	Codominant	**LC1 PENET wt/mt:**	0.00 %	4.rs17129557 - rs2277207	10	113.91	2.6267	0.0000	2.6267
		LC1 PENET mt/mt:	99.00 %	5.rs2792740 - rs12146169	10	113.91	2.6262	0.0000	2.6262

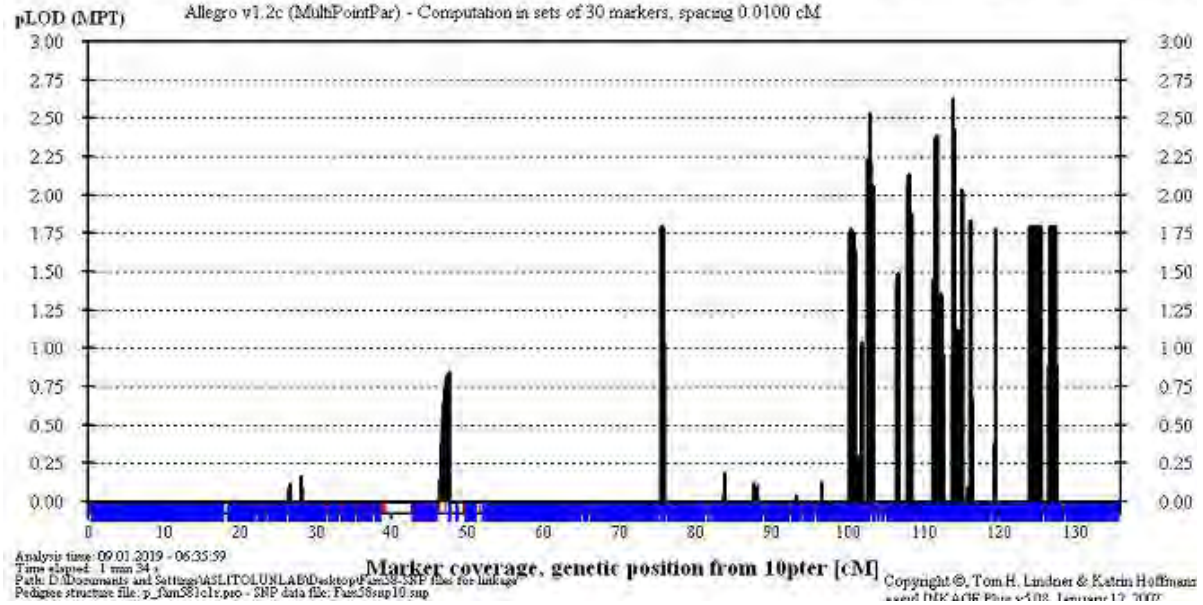

Chromosome 11

					Marker	CHR	cM	LOD	ALPHA	HLOD
Project:	FAM58-SNP FILES FOR LINKA	**Inheritance:**	Recessive							
Family name:	TOTALS	**Common allele:**	99.90 %		1 rs11230729	11	126.90	2.6908	0.0000	2.6908
Used map:	730k Mb (sex-averaged)	**Disease allele:**	0.10 %		2 rs11230729 - rs7931141	11	126.90	2.6892	0.0000	2.6892
Marker positions:	8154 ok / 12 ? / 0 outside	**LC1 PCOPY rate:**	0.00 %		3 rs11230729 - rs7931141	11	126.91	2.6876	0.0000	2.6876
Allele frequencies:	Codominant	**LC1 PENET wt/mt:**	0.00 %		4 rs11230729 - rs7931141	11	126.91	2.6860	0.0000	2.6860
		LC1 PENET mt/mt:	99.00 %		5 rs7931141 - rs516926	11	126.91	2.6844	0.0000	2.6844

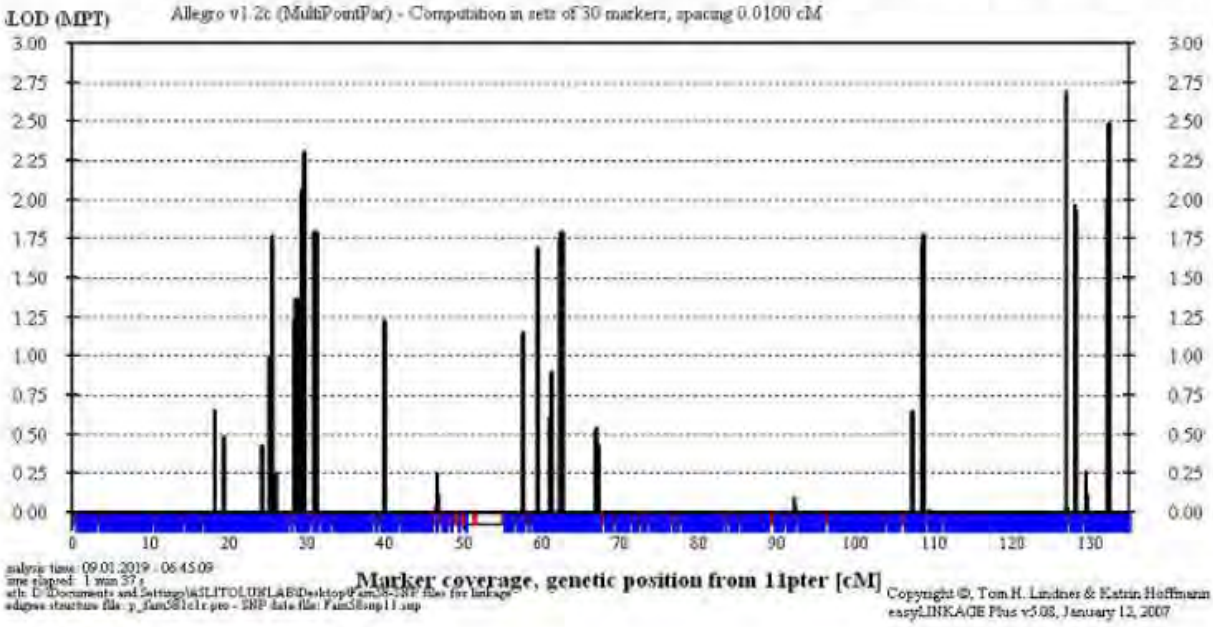

Chromosome

12

					Marker	CHR	cM	LOD	ALPHA	HLOD
Project:	FAM58-SNP FILES FOR LINKA	**Inheritance:**	Recessive							
Family name:	TOTALS	**Common allele:**	99.90 %		1 rs2306182	12	10.53	2.6983	0.0000	2.6983
Used map:	730k Mb (sex-averaged)	**Disease allele:**	0.10 %		2 rs2617151 - rs7989985	12	10.53	2.6983	0.0000	2.6983
Marker positions:	8373 ok / 39 ? / 0 outside	**LC1 PCOPY rate:**	0.00 %		3 rs7989985 - rs7954052	12	10.54	2.6983	0.0000	2.6983
Allele frequencies:	Codominant	**LC1 PENET wt/mt:**	0.00 %		4 rs7989985 - rs7954052	12	10.54	2.6983	0.0000	2.6983
		LC1 PENET mt/mt:	99.00 %		5 rs7989985 - rs7954052	12	10.54	2.6983	0.0000	2.6983

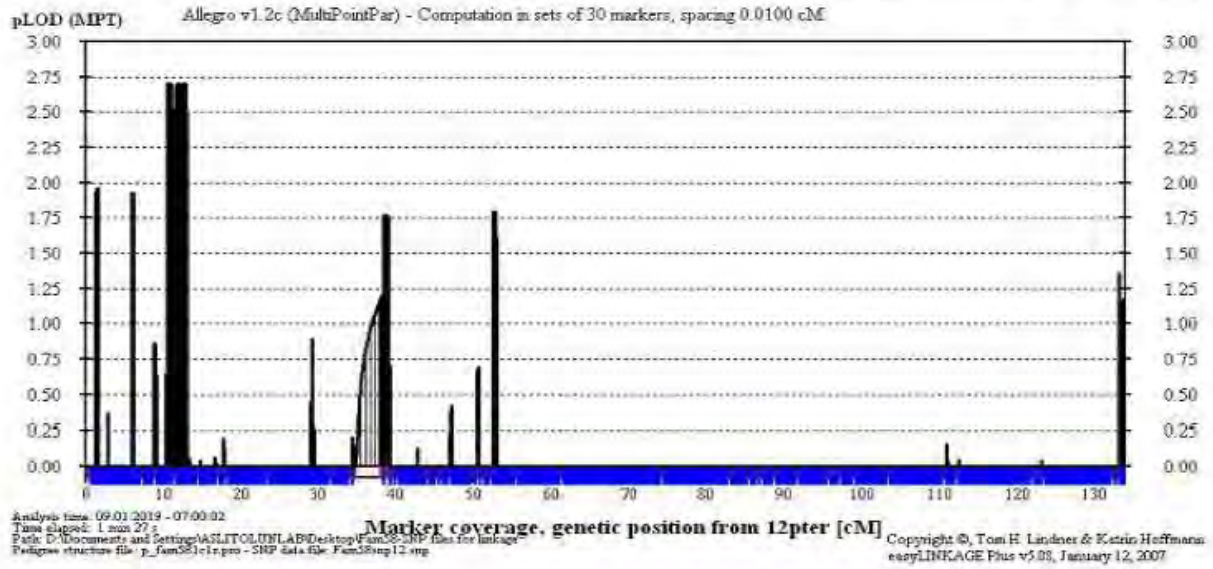

Chromosome 13

Project:	FAM58-SNP FILES FOR LINKAGE	Inheritance:	Recessive
Family name:	TOTALS	Common allele:	99.90 %
Used map:	730k Mb (sex-averaged)	Disease allele:	0.10 %
Marker positions:	6173 ok / 3 ? / 0 outside	LC1 PCOPY rate:	0.00 %
Allele frequencies:	Codominant	LC1 PENET wt/mt:	0.00 %
		LC1 PENET mt/mt:	99.00 %

Marker	CHR	cM	LOD	ALPHA	HLOD
1.rs429397 - rs9592177	13	62.90	2.6983	0.0000	2.6983
2.rs9592177	13	62.91	2.6983	0.0000	2.6983
3.rs9593835	13	84.45	2.6983	0.0000	2.6983
4.rs9531519 - rs3737193	13	84.45	2.6983	0.0000	2.6983
5.rs3737193 - rs9593836	13	84.45	2.6983	0.0000	2.6983

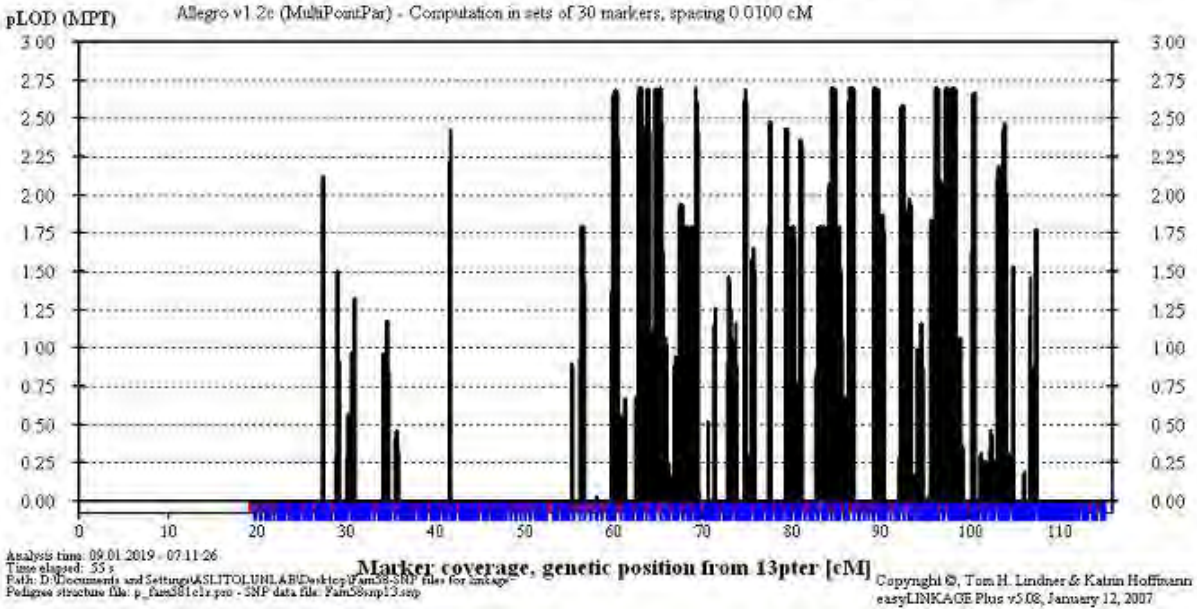

Chromosome 14

Project:	FAM58-SNP FILES FOR LINKAGE	Inheritance:	Recessive
Family name:	TOTALS	Common allele:	99.90 %
Used map:	730k Mb (sex-averaged)	Disease allele:	0.10 %
Marker positions:	5360 ok / 3 ? / 0 outside	LC1 PCOPY rate:	0.00 %
Allele frequencies:	Codominant	LC1 PENET wt/mt:	0.00 %
		LC1 PENET mt/mt:	99.00 %

Marker	CHR	cM	LOD	ALPHA	HLOD
1.rs4981925	14	20.75	1.7952	0.0000	1.7952
2.rs4981925 - rs7159007	14	20.75	1.7952	0.0000	1.7952
3.rs4981925 - rs7159007	14	20.75	1.7952	0.0000	1.7952
4.rs4981925 - rs7159007	14	20.75	1.7952	0.0000	1.7952
5.rs4981925 - rs7159007	14	20.76	1.7952	0.0000	1.7952

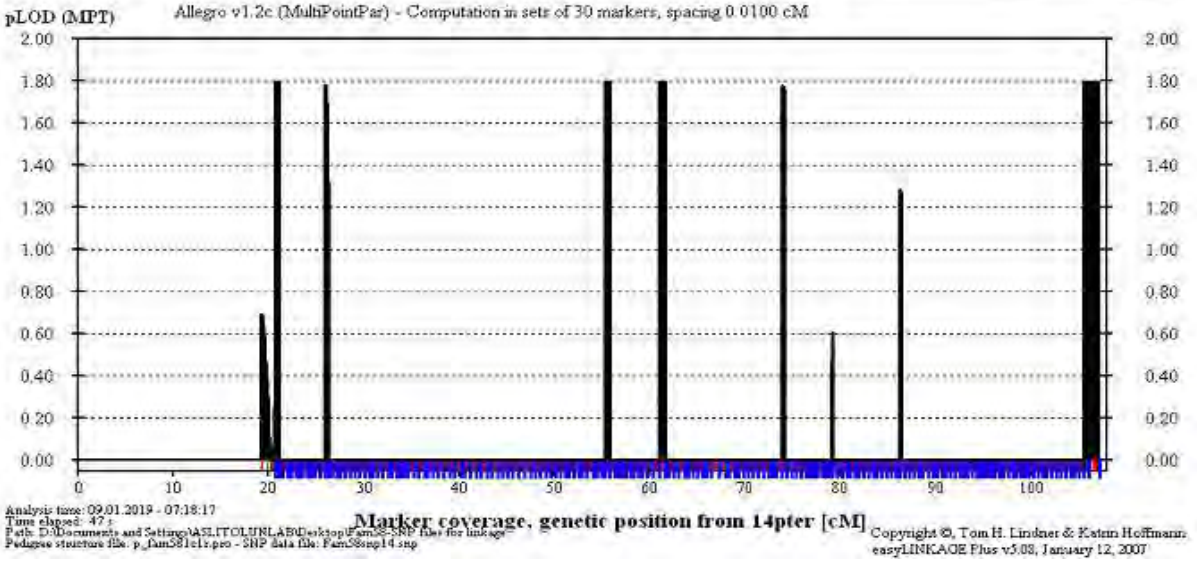

Chromosome 15

Project:	FAM38-SNP FILES FOR LINKAGE	Inheritance:	Recessive
Family name:	TOTALS	Common allele:	99.90 %
Used map:	730k Mb (sex-averaged)	Disease allele:	0.10 %
Marker positions:	4796 ok / 8 ? / 0 outside	LC1 PCOPY rate:	0.00 %
Allele frequencies:	Codominant	LC1 PENET wt/wt:	0.00 %
		LC1 PENET mt/mt:	99.00 %

Marker	CHR	cM	LOD	ALPHA	HLOD
1.rs1021800 - rs7164866	15	44.61	2.6983	0.0000	2.6983
2.rs1021800 - rs7164866	15	44.62	2.6983	0.0000	2.6983
3.rs1021800 - rs7164866	15	44.63	2.6983	0.0000	2.6983
4.rs1021800 - rs7164866	15	44.63	2.6983	0.0000	2.6983
5.rs7164866	15	44.64	2.6983	0.0000	2.6983

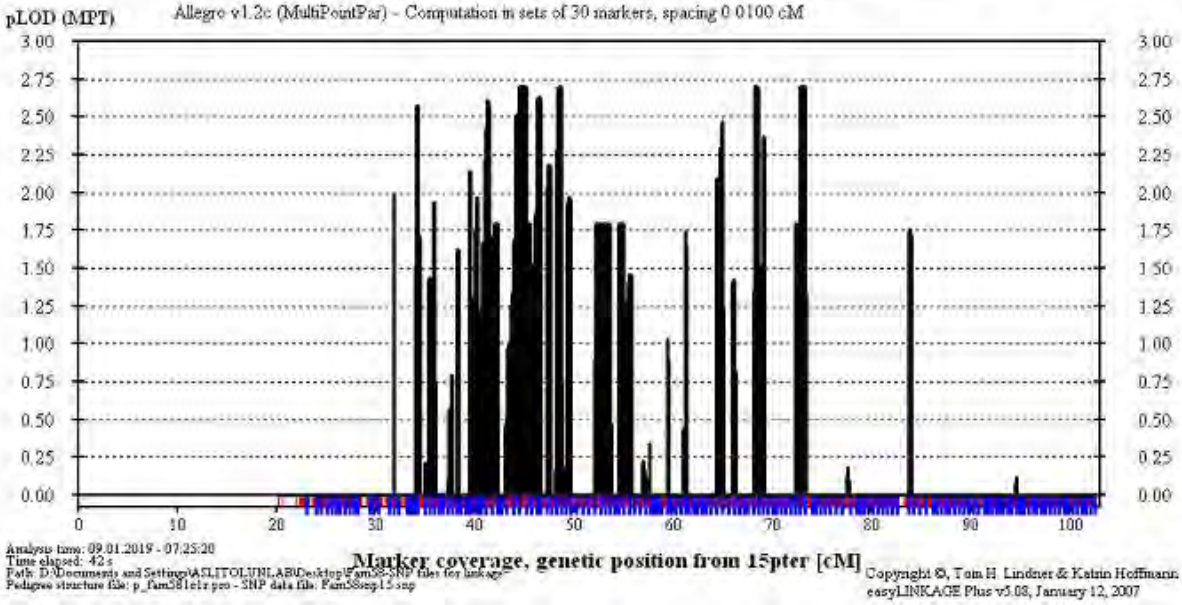

Chromosome 16

Project:	FAM38-SNP FILES FOR LINKAGE	Inheritance:	Recessive
Family name:	TOTALS	Common allele:	99.90 %
Used map:	730k Mb (sex-averaged)	Disease allele:	0.10 %
Marker positions:	4929 ok / 18 ? / 0 outside	LC1 PCOPY rate:	0.00 %
Allele frequencies:	Codominant	LC1 PENET wt/wt:	0.00 %
		LC1 PENET mt/mt:	99.00 %

Marker	CHR	cM	LOD	ALPHA	HLOD
1.rs3785109	16	68.12	2.3844	0.0000	2.3844
2.rs2418740 - rs7201742	16	68.09	2.3844	0.0000	2.3844
3.rs2418740 - rs7201742	16	68.09	2.3844	0.0000	2.3844
4.rs2418740 - rs7201742	16	68.09	2.3844	0.0000	2.3844
5.rs2418740 - rs7201742	16	68.10	2.3844	0.0000	2.3844

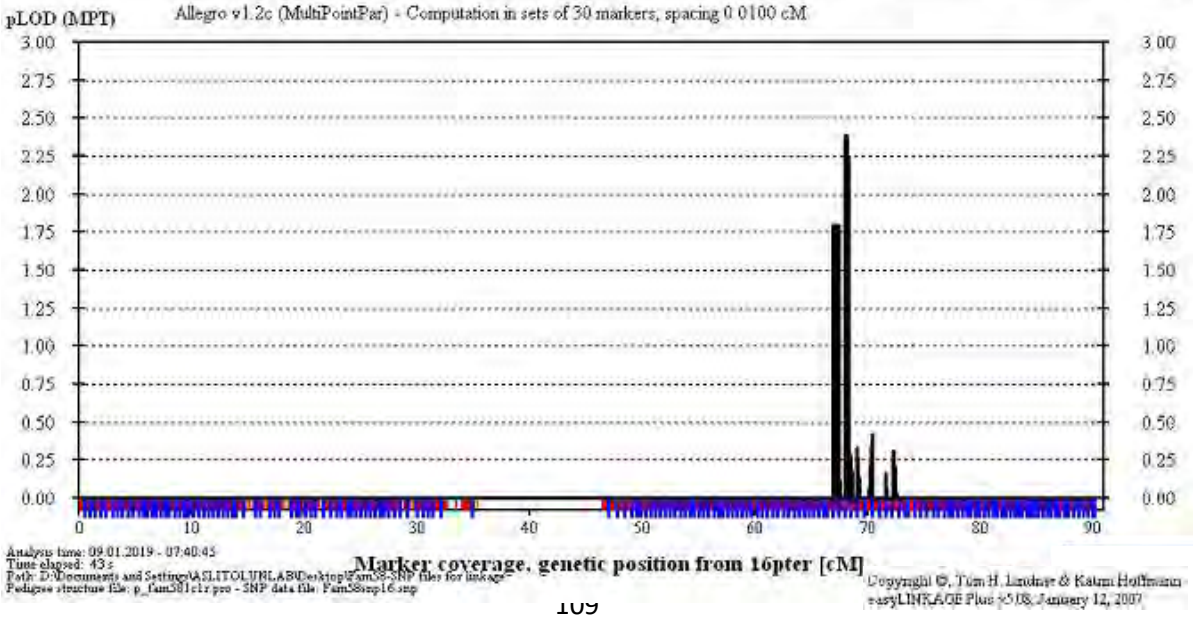

Chromosome 17

Project:	FAM58-SNP FILES FOR LINKA	Inheritance:	Recessive
Family name:	TOTALS	Common allele:	99.90 %
Used map:	730k Mb (sex-averaged)	Disease allele:	0.10 %
Marker positions:	4623 ok / 11 ? / 0 outside	LC1 PCOPY rate:	0.00 %
Allele frequencies:	Codominant	LC1 PENET wt/mt:	0.00 %
		LC1 PENET mt/mt:	99.00 %

Marker	CHR	cM	LOD	ALPHA	HLOD
1.rs4073995 - rs4074469	17	77.59	2.6983	0.0000	2.6983
2.rs4073995 - rs4074469	17	77.61	2.6983	0.0000	2.6983
3.rs4073995 - rs4074469	17	77.63	2.6983	0.0000	2.6983
4.rs4074469	17	77.66	2.6983	0.0000	2.6983
5.rs4074469 - rs4889936	17	77.66	2.6983	0.0000	2.6983

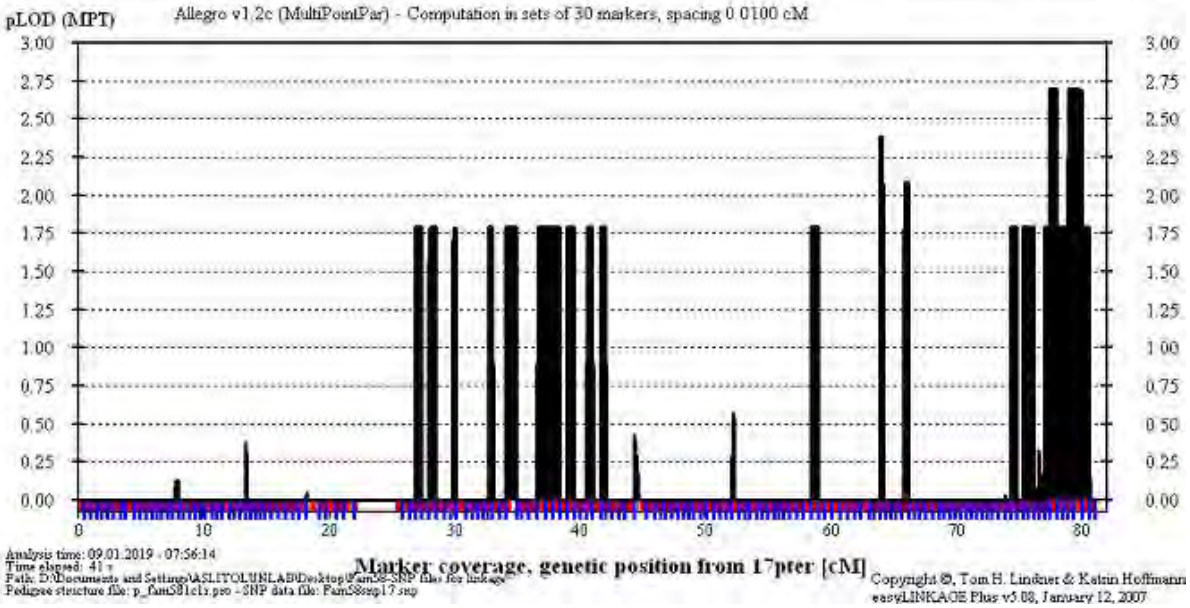

Chromosome 18

Project:	FAM58-SNP FILES FOR LINKA	Inheritance:	Recessive
Family name:	TOTALS	Common allele:	99.90 %
Used map:	730k Mb (sex-averaged)	Disease allele:	0.10 %
Marker positions:	3073 ok / 5 ? / 0 outside	LC1 PCOPY rate:	0.00 %
Allele frequencies:	Codominant	LC1 PENET wt/mt:	0.00 %
		LC1 PENET mt/mt:	99.00 %

Marker	CHR	cM	LOD	ALPHA	HLOD
1.rs2941386	18	66.30	2.1691	0.0000	2.1691
2.rs9555540 - rs7236251	18	66.30	2.1690	0.0000	2.1690
3.rs7236311 - rs2941386	18	66.30	2.1690	0.0000	2.1690
4.rs2941386 - rs12232586	18	66.30	2.1690	0.0000	2.1690
5.rs2941386 - rs12232586	18	66.31	2.1690	0.0000	2.1690

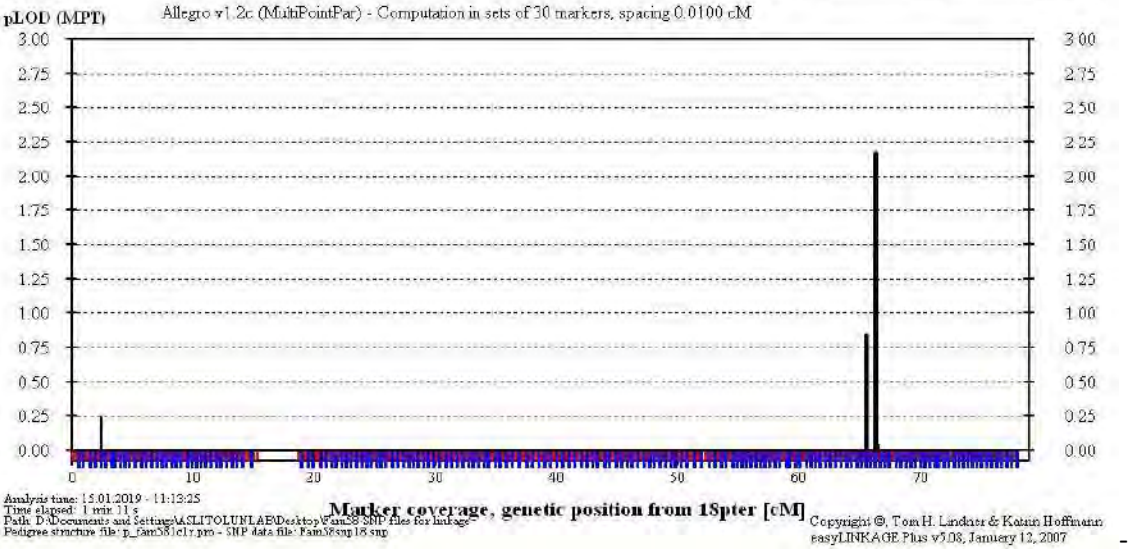

Chromosome 19

Project:	FAM58-SNP FILES FOR LINKA	Inheritance:	Recessive
Family name:	TOTALS	Common allele:	99.90 %
Used map:	730k Mb (sex-averaged)	Disease allele:	0.10 %
Marker positions:	3683 ok / 2 ? / 0 outside	LC1 PCOPY rate:	0.00 %
Allele frequencies:	Codominant	LC1 PENET wt/mt:	0.00 %
		LC1 PENET mt/mt:	99.00 %

Marker	CHR	cM	LOD	ALPHA	HLOD
1.rs2198978	19	27.83	2.6983	0.0000	2.6983
2.rs2198978 - rs365344	19	27.84	2.6983	0.0000	2.6983
3.rs2198978 - rs365344	19	27.84	2.6983	0.0000	2.6983
4.rs2198978 - rs365344	19	27.85	2.6983	0.0000	2.6983
5.rs2198978 - rs365344	19	27.86	2.6983	0.0000	2.6983

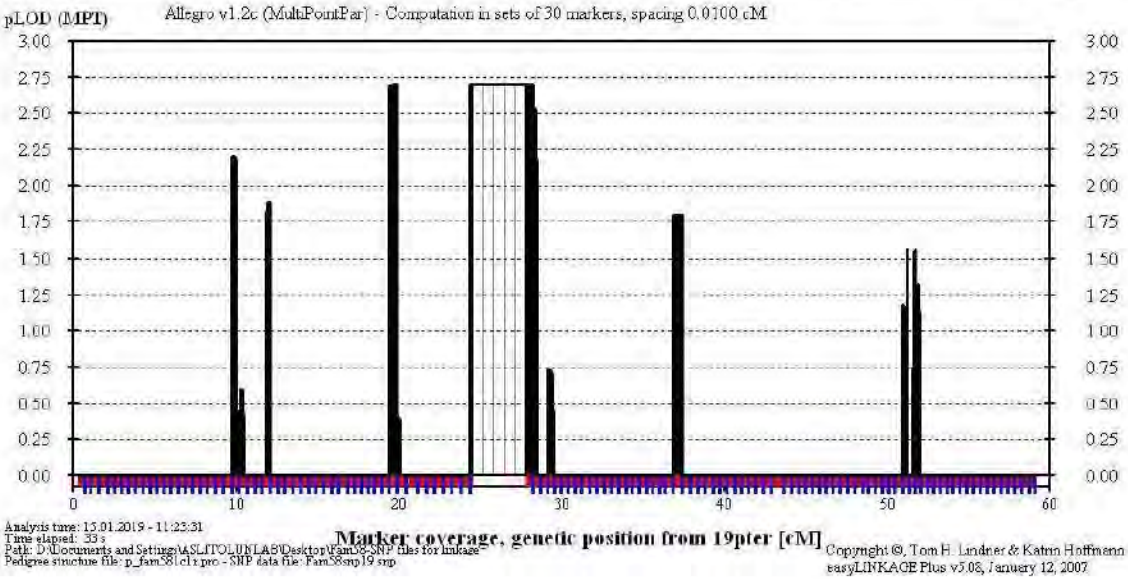

Chromosome 20

Project:	FAM58-SNP FILES FOR LINKA	Inheritance:	Recessive
Family name:	TOTALS	Common allele:	99.90 %
Used map:	730k Mb (sex-averaged)	Disease allele:	0.10 %
Marker positions:	4130 ok / 59 / 0 outside	LC1 PCOPY rate:	0.00 %
Allele frequencies:	Codominant	LC1 PENET wt/mt:	0.00 %
		LC1 PENET mt/mt:	99.00 %

Marker	CHR	cM	LOD	ALPHA	HLOD
1.rs232636	20	7.08	1.4600	0.0000	1.4600
2.rs232636 - rs368007	20	7.08	1.4600	0.0000	1.4600
3.rs232636 - rs368007	20	7.08	1.4600	0.0000	1.4600
4.rs368007 - rs2207719	20	7.09	1.4600	0.0000	1.4600
5.rs368007 - rs2207719	20	7.09	1.4600	0.0000	1.4600

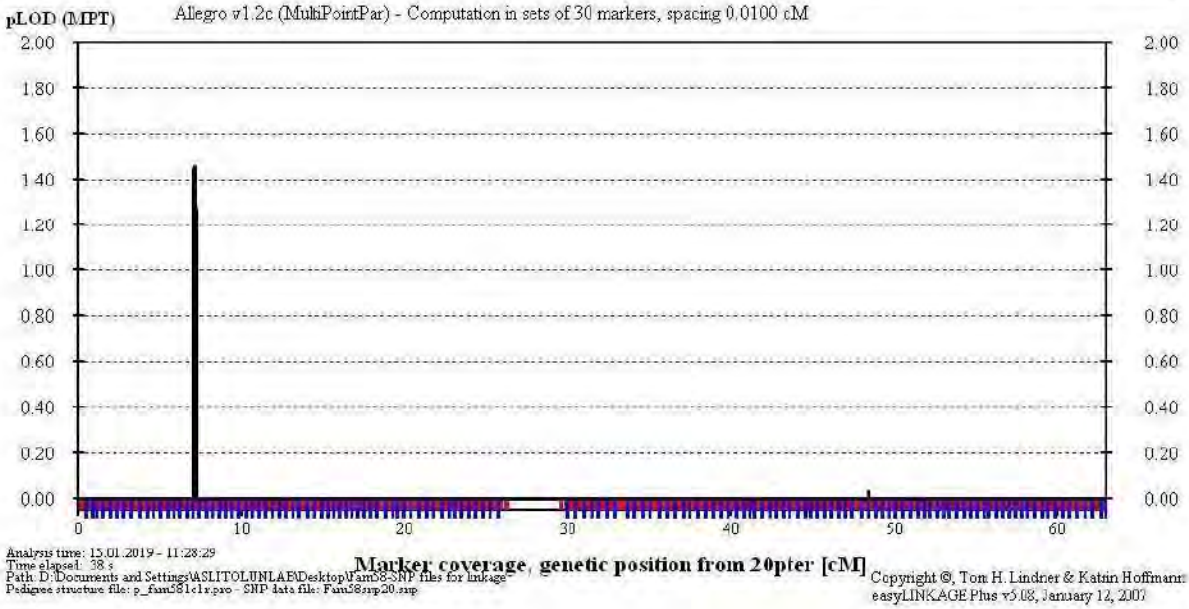

Chromosome 21

Project:	FAM58-SNP FILES FOR LINKA	Inheritance:	Recessive
Family name:	TOTALS	Common allele:	99.90 %
Used map:	730k Mb (sex-averaged)	Disease allele:	0.10 %
Marker positions:	2290 ok / 12 ? / 0 outside	LC1 PCOPY rate:	0.00 %
Allele frequencies:	Codominant	LC1 PENET wt/mt:	0.00 %
		LC1 PENET mt/mt:	99.00 %

Marker	CHR	cM	LOD	ALPHA	HLOD
1.rs12627009	21	41.82	0.7433	0.0000	0.7433
2.rs2837629 - rs2837636	21	41.82	0.7433	0.0000	0.7433
3.rs2837629 - rs2837636	21	41.82	0.7433	0.0000	0.7433
4.rs2837629 - rs2837636	21	41.82	0.7433	0.0000	0.7433
5.rs2837629 - rs2837636	21	41.82	0.7433	0.0000	0.7433

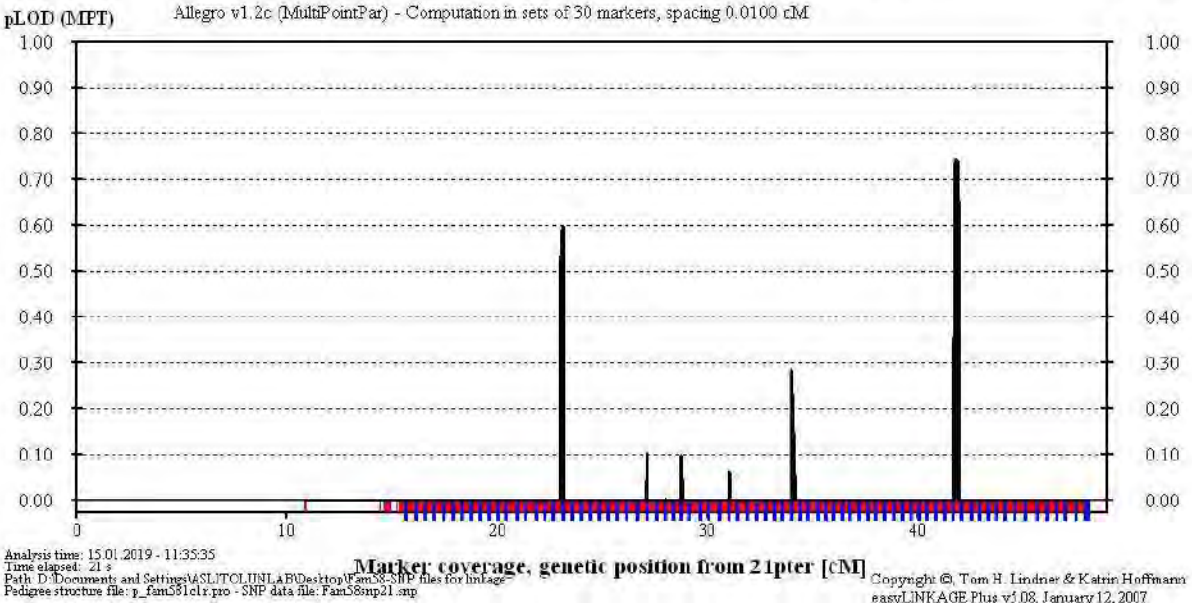

Chromosome 22

Project:	FAM58-SNP FILES FOR LINKA	Inheritance:	Recessive
Family name:	TOTALS	Common allele:	99.90 %
Used map:	730k Mb (sex-averaged)	Disease allele:	0.10 %
Marker positions:	2174 ok / 75 ? / 0 outside	LC1 PCOPY rate:	0.00 %
Allele frequencies:	Codominant	LC1 PENET wt/mt:	0.00 %
		LC1 PENET mt/mt:	99.00 %

Marker	CHR	cM	LOD	ALPHA	HLOD
1.rs3788684	22	46.84	2.0442	0.0000	2.0442
2.rs3747250 - rs3788684	22	46.83	2.0441	0.0000	2.0441
3.rs3747250 - rs3788684	22	46.83	2.0441	0.0000	2.0441
4.rs3747250 - rs3788684	22	46.83	2.0441	0.0000	2.0441
5.rs3747250 - rs3788684	22	46.83	2.0441	0.0000	2.0441

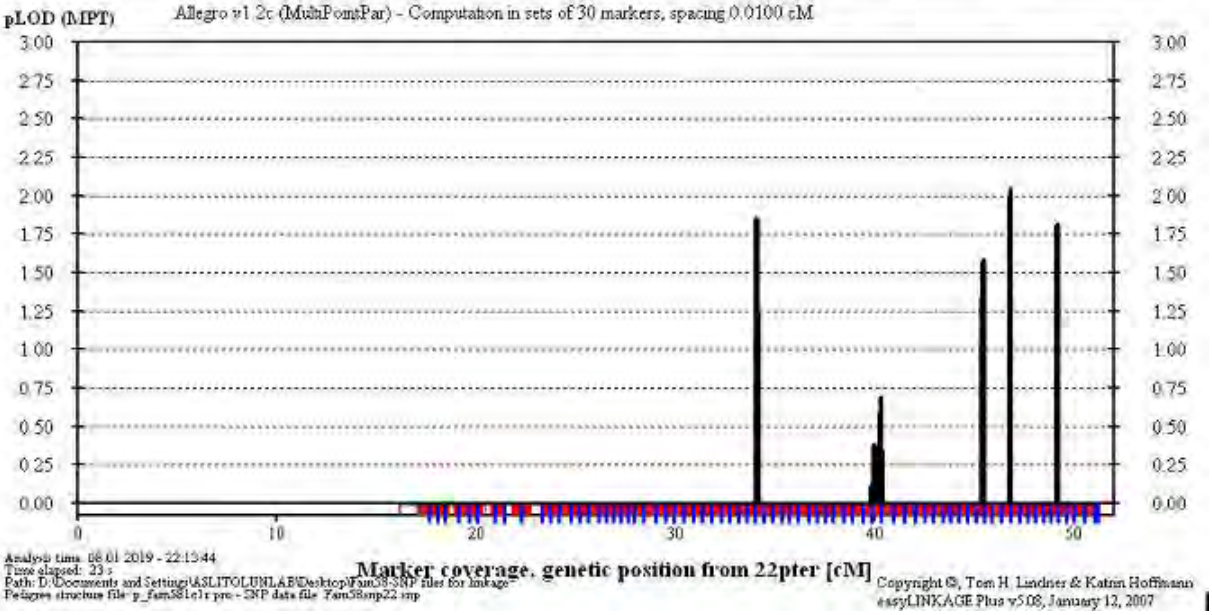

Chromosome X

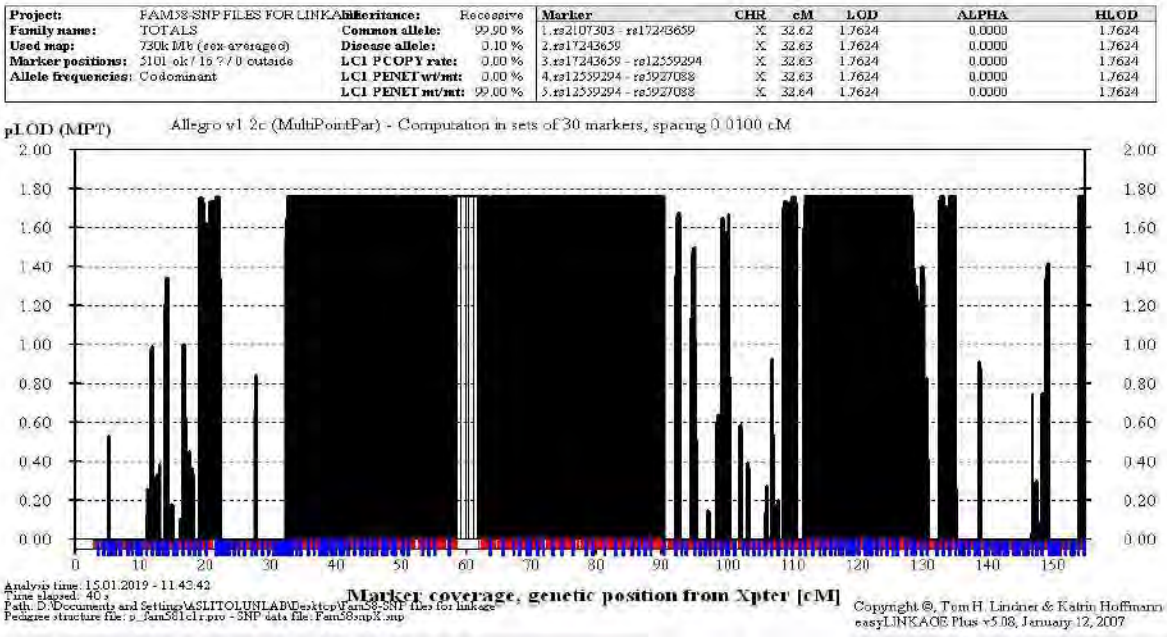

Chromosome XY

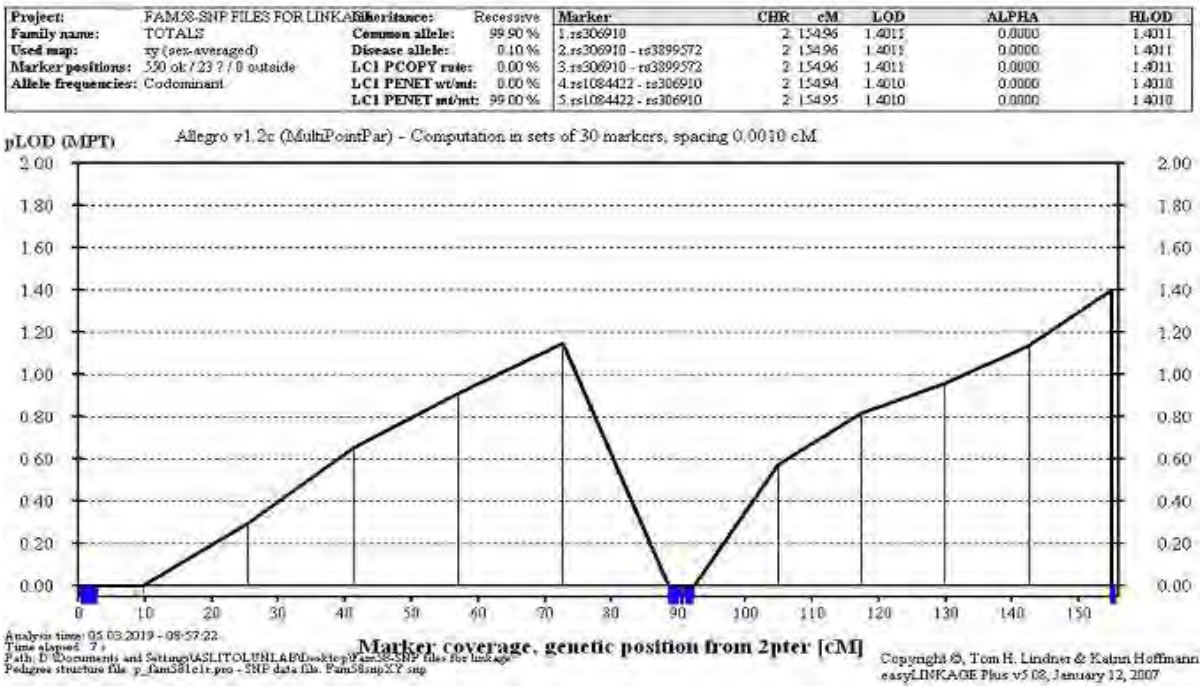

Figure 4.6: Multipoint LOD score graphs for all chromosomes. Later regions yielding maximal multipoint LOD scores of ~2.7 were investigated for shared homozygosity in patients. Shared homozygosity regions >1Mb were considered as candidate regions to harbour the putative gene defect.

Through exome sequence analysis, rare candidate variants with frequency < 0.01 were selected. Such variants were not found in the small regions less than 1Mb. In the selected locus at 17q25.3, there was only single variant in 3' UTR c.*1453A>T (rs574027014; NM_017450.2) of brain specific angiogenesis inhibitor 1 associated protein 2 (BAIAP2) gene with frequency of 0.0074 in non-Finnish Europeans. It is 40 nucleotides upstream of the polyadenylation signal and low CADD score of 4.669 revealed that the identified variant was not highly deleterious. Therefore, this variant did not cause the disease in the family.

In the selected identified gene region, SNP genotype data aligned in Microsoft excel and SNP analysis indicated two homozygous SNPs in father and no-call in affected sibs. This is suggestive for homozygous deletion in the all patients. The no call SNPs were rs36101864 (nucleotide 79,898,644) and rs34319293 (79,899,900). Both these were flanked by following two SNPs rs34575645 (79,891,184 bp) and rs35810039 (79,901,665 bp). These two flanking SNPs were present in all SNP genotype files (table 4.6).

Table 4.6: SNP genotypes of unaffected (302) and affected (502, 507, 508) subjects at the candidate locus

Genomic coordinates			Unaffected	Affected Siblings		
SNP ID	**Chr**	**SNP Position**	**302**	**502**	**507**	**508**
rs35953598	17	79680353	BB	BB	BB	BB
rs6565625	17	79681370	BB	BB	BB	BB
rs13912	17	79687893	BB	BB	BB	BB
rs12449687	17	79693136	AA	AA	AA	AA
rs9319620	17	79697383	BB	BB	BB	BB
rs9709386	17	79702833	BB	BB	BB	BB
rs2070871	17	79805134	BB	BB	BB	BB
rs35138785	17	79819954	AA	AA	AA	AA
rs34185514	17	79828248	BB	BB	BB	BB
rs2230474	17	79862604	AA	AA	AA	AA
rs8069388	17	79862824	AA	AA	AA	AA
rs35291429	17	79872241	BB	BB	BB	BB
rs35589179	17	79891156	BB	BB	BB	BB
rs34575645	17	79891184	AA	AA	AA	AA
rs36101864	17	79898644	AA	NC	NC	NC
rs34319293	17	79899900	AA	NC	NC	AB
rs35810039	17	79901665	BB	BB	BB	BB
rs35935560	17	79908807	AB	AA	AA	AA
rs34600945	17	79915035	AB	BB	BB	BB
rs34725780	17	79915442	AB	BB	BB	BB
rs34996156	17	79915509	AB	AA	AA	AA
rs4239275	17	79923718	AB	AA	AA	AA
rs34480725	17	79924431	AB	BB	BB	BB
rs35290415	17	79925150	AB	BB	BB	BB
rs4796860	17	79943475	AA	AA	AA	AA
rs9912517	17	79946373	BB	BB	BB	BB

The analyses of the intervals through Integrative Genome Viewer (IGV) showed that two no-call SNPs within the deletion did not read. Between the flanking SNPs, there were present exons of *PYCR1* and *MYADML2*. In the selected locus, exome sequence data analyzed. Analysis with IGV revealed that no reads had been aligned to coding exons 2 and 1 of *PYCR1* (NM_001282281) and the upstream regulatory regions of the gene as well as to coding exon 3 of *MYADML2* (NM_001145113). The two non-coding exons 1-2 of MYADML2 were not covered by exome sequencing (Figure 4.7).

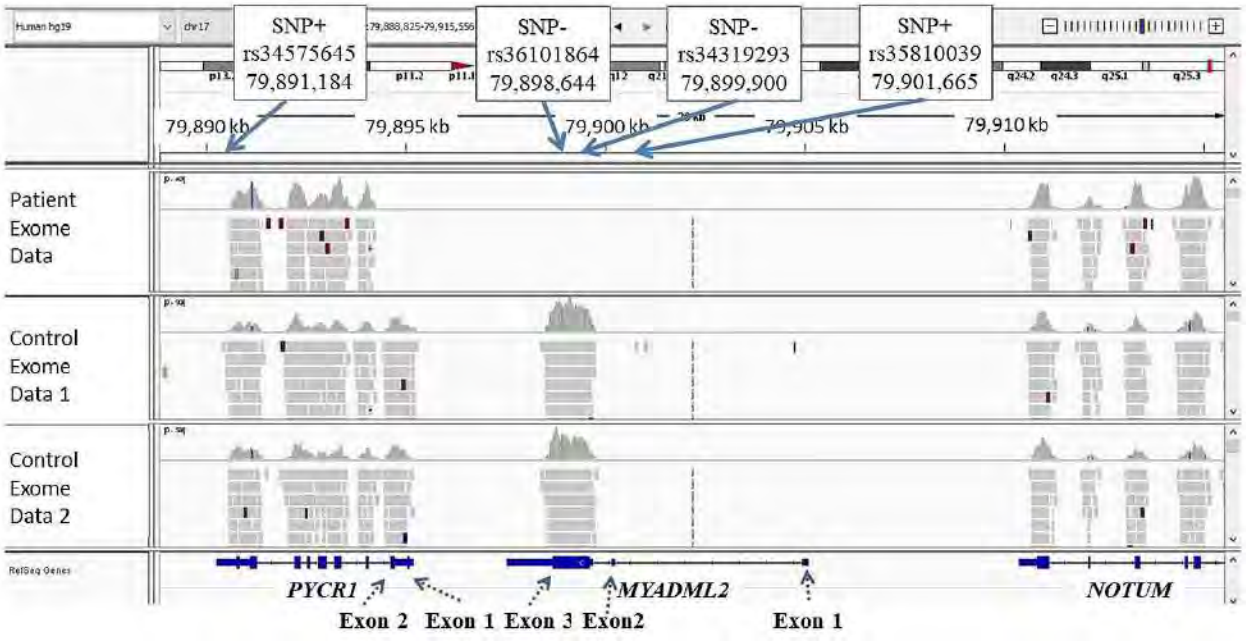

Figure 4.7: Analysis with Integrative Genome Viewer (IGV)

Therefore, these two non-coding exons of *MYADNL2* not captured in any exome file including the control exome files of two unrelated individuals. Exons 3-8 of *PYCR1* had been covered in the patient exome file, 20X to 36X. The three exons (exon 2 & 1 of *PYCR1* and exon 3 of *MYADNL2*) included in the exome sequencing had been covered 20X to 70X in the control exome files but not read in the affected sib sample.

To identify the breakpoints, the deletion junctions amplified. However, only a few oligo primers for long range PCR reaction designed around the deletion region using computational tool PrimerQuest Tool (Integrated DNA Technologies). However, the amplification across the deletion junction failed. Later, validation of deletion carried by PCR amplification, for exons 2 and 3 of the *PYCR1* and *MYADML2* genes. The amplification products obtained for all those exons for the DNA samples of father, unaffected sister and control individuals whereas for patient samples, PCR amplification products obtained for exon 3 of PYCR1 but not for the other three exons, validating the deletion and showing that it encompasses also exon 2 of *MYADML2*.

Hence, the SNP genotype and exome data plus the PCR amplification results together indicated that the deletion extended maximally from 79,894,278 (where exome reads in patient file end) to 79,901,665 bp (rs35810039) and minimally again from 79,894,278 to 79,900,249 (*MYADML2* exon 2 reverse primer starts), with a length of 7.3 kb and 5.9 kb, respectively (table 4.6).

Exome data analysis also for any possibly homozygous or compound heterozygous variants in other progeria-related genes *BANF1, LMNA, SLC25A24, ZMPSTE24, ERCC8, NAT10, SUN2*, *ALDH18A1*, *B4GALT7, FOXM1*, *NAMPT, PIK3R1, SOD2, PTDSS1* and *GH1*) and telomere genes *TERT, TERC*, *RTEL1, PARN, DKC1 and TINF2*, biallelic mutations of which can cause progeria or progeria-like syndromes. None of the rare (frequency <0.01) variants was possibly damaging, i.e., nonsynonymous, truncating or splicing.

4.5: Discussion

In the family, the five affected subjects had a similar presentation of an unusual combination of skeletal abnormalities apart from overlapping features of cutis laxa. SNP and exome sequence analysis revealed novel homozygous deletion of exons 1-2 of *PYCR1* and exon 2 of *MYADML2*. Mutation validated by PCR amplification didn't revealed results and exons deletions were supposed to deduced the synthesis of proteins from both mutated genes. Before this, *MYADML2* has not been associated with any kind of human phenotype but mutations in *PYCR1* caused ARCL.

In order to determine the clinical symptoms of *MYADML2* insufficiency, clinical features of >100 reported cases of *PYCR1*-related ARCL were compared with the clinical symptoms in the studied family and it indicated that non-concordant skeletal findings were due to deletion in *MYADML2*. The non-concordant skeletal findings included multiple joint dislocation, delayed bone maturation, asymmetry of cranium, intracondylar fissures in humorae, scapular dyskinesis, and lack of spaces between radii and ulnae. Out of these findings, only multiple joints dislocations reported in cases of *PYCR1*-related ARCL (Onoufriadis *et al.* 2019).

In the investigated affected siblings, toes elongation, cylindrical & long digits, winged scapula, protruding sternum, scoliosis, and lumbar lordosis all were overlapping features with *PYCR1*-related ARCL(Guernsey *et al.* 2009; Lin *et al.* 2011; Scherrer *et al.* 2013; Alazami *et al.* 2016). However, these overlapping features were very less occurring in case of *PYCR1*-related ARCL. Therefore, in the family, these features attributed due to deletion in *MYADML2* gene.

It could be hypothesized that *MYADML2* is involved in maturation and pattern formation of bones. Perhaps cranial asymmetry, joints dislocations, lumber lordosis, and prominent clavicles might be due to anomalous or disproportionate bone growth. In contrary to this, the rare extra transverse creases on fingers could be due to deletion in *PYCR1* that is responsible skin anomalies. Perhaps it could be true but there is no report of such creases for any *PYCR1* reported mutation.

By evaluation of patients from 50 families, researchers could not find that all related patients had same features, but they had variable clinical features. In contrary to this the patients of current study have same common features like wrinkled skin, IUGR, hyperlaxilty of joints, early aging, visible veins on body, hypotonia, postnatal growth delay (Reversade *et al.* 2009; Dimopoulou *et al.* 2013; Kariminejad *et al.* 2017; Ritelli *et al.* 2017).

The study results indicated that *MYADML2* gene encodes a protein that involves in bone maturation and morphogenesis and deficit of that protein manifests with a novel skeletal phenotype. Computational bioinformatics analysis showed that the deletion was novel and deleterious. Moreover, amino acid sequence of the gene conserved across the species and previous studies did not showed homozygous loss of function mutation in families with consanguineous parents (Ioannidis *et al.* 2016; Narasimhan *et al.* 2016; Saleheen *et al.* 2017).

The gnomAd does not list any variant with loss of function in homozygous state and the frequencies of all such variants are <0.00038. Moreover, there is no evidence for irrelevance of the gene in bone development. It is suggestive that *MYADML2* deficit can be deleterious rather than inactivation of some genes without obvious effect on phenotype. Additionally, gnomAD reports a pLI of 0 for the gene, its mean it is tolerant to loss of function mutations and only 5 missense variants predicted as deleterious with frequencies ranging from 0.00098-0.0347 and reported in homozygous state in various individuals. But the predictions for missense mutations by computational algorithms are not always reliable because some such variants are responsible to cause diseases (Jagadeesh *et al.* 2016; Rentzsch *et al.* 2019).

PYCR1 protein has conserved amino acid sequence across the species. Human PYCR1 showed homology with chimpanzee (99.9%), macaque (95.4%), and mouse (91.6%) [HomoloGene]. At least, there are 29 reported biallelic *PYCR1* variants known to cause ARCL. Some mutation in *PYCR1* are severe like 22bp deletion (c.617_633+6del) (Kretz *et al.* 2011; Scherrer *et al.* 2013) but there is no reported deletion up to *MYADML2*. However, there is lack of genotype-phenotype correlation. (Kretz *et al.* 2011). Moreover, the *MYADML2* gene is telomeric to exon 1 of *PYCR1*. Its

sequence is highly conserved in jawed vertebrates; sequence homology of human *MYADML2* with chimpanzee is 99.7%, macaque 97.1%, mouse 91.5%, bird 73.4%, frog 62.8% and zebrafish 62.3%. The gene is highly expressed in skeletal muscles and weakly in brain (Genotype Genome Expression-GTEx; the Human Protein Atlas), but bone tissue is not included in the databases. *MYADML2* is not involved in any of the reported pathways in KEGG, Reactome or GO databases (Aranda *et al.* 2011; Kanehisa *et al.* 2017; Fabregat *et al.* 2018; Consortium 2019). Paralog protein MYADM has a role in cell spreading and migration (Aranda *et al.* 2011).

Conclusively, this is the first report of homozygous deletion encompassing the coding sequences of *MYADML2* together with deletion in coding sequence of *PYCR1*. The five affected siblings had rare similar clinical symptoms not common to *PYCR1* related ARCL. The study findings providing a start point for further studies to investigate the function of *MYADML2*. Testing the individuals with skeletal features similar to our patients for *MYADML2* mutation could validate the pathology of *MYADML2* to delineate its clinical manifestation.

CHAPTER 5

FAMILY III

Chapter 5. Homozygous variant in *GHR* c.442G>C (p.D148H) implicated in proportionate dwarfism Laron type in inbred Pakistani kindred

5.1: Abstract

Mutations in the Growth Hormone Receptor (*GHR*) gene are associated with the pathogenesis of Laron Syndrome (LS) or growth hormone insensitivity syndrome (GHIS). LS is an autosomal recessive disorder characterized by severe short stature of proportionate type and truncal obesity. Biochemically, it is characterized by the high GH levels, low level of IGF-1 and IGFBP-3 in blood stream. The study represents an inbred Pakistani family in which three subjects were afflicted with Laron syndrome. All the available family members were examined with the help of local physician in order to obtain the clinical information. Serological and endocrinological tests were performed. SNP and exome sequencing were carried out for the identification of genetic cause in the family. Clinical examination revealed short stature, truncal obesity, frontal bossing and large ears. The analyses of SNP data revealed 70 autosomal regions >1Mb that were homozygous. The largest interval 1.02 Mb resided on chromosome 5. Exome sequencing revealed a pathogenic variant *GHR*:NM_001242460:c.442G>C:p.Asp148His. This variant is already known to cause LS in another Pakistani family; however, the clinical and phenotypic features of that family were not presented. The present molecular study confirmed the diagnosis of the clinical condition segregating in the family. Medical test like carrier testing, prenatal testing, premarital screening and preimplantation genetic diagnosis would be easy to perform for this syndrome.

5.2: Introduction

Genetics plays a vital role in determining the individual height because 80% of variations in height are under the genetic control. Additionally, genome wide association studies indicated 697 variants clustered in 423 loci involved in growth (Huang *et al.* 2018). Growth of an individual is a multifactorial trait and is regulated by numerous factors like growth hormones and growth regulators (genetic factors), race, life style, nutritional, cultural and socio-economic aspects (environmental factors) (Yadav & Dabas 2015).

Growth hormone (GH) also known as somatotropins is secreted from anterior pituitary gland. It is peptide hormone and responsible for growth, cell progression and renewal (Conway-Campbell *et al.* 2008; Lin *et al.* 2012). GH exerts its widespread actions on the human body by its binding to growth hormone receptor (GHR). GH influences metabolism of carbohydrates, lipids, and proteins, shapes body composition, influences cardiovascular profile and quality of life (Guevara-Aguirre *et al.* 2018). It has crucial role in the regulation of brain and different human systems, e.g., skeletal, cardiovascular, metabolism, immune and reproductive (Waters 2016; Martínez-Moreno *et al.* 2018). However, the action of GH is regulated by growth hormone receptor (GHR) and insulin like growth factor 1 (IGF-1) directly and indirectly. The GH released in pulsatile nature and influenced by variety of hormones such as GH-releasing hormone (GHRH), ghrelin and sex steroids, inhibitory somatostatin, IGF-1, and glucocorticoids.

Short stature is a pediatric endocrine disorder that means the height below the 3rd percentile of an individual (Dauber *et al.* 2014). There are different types of short stature. The most prevalent type of short stature is achondroplasia which occurs in about 1 in almost 25,000-30,000 people but short stature due to mutation in *GHR* is very rare (Wit *et al.* 2016).

Generally, *GHR's* mutations resulted in Laron syndrome with prevalence rate 1-9/1000000 in a population (Somale & Ahmed 2016). Nearly, more than 350 people are reported in literature with Laron syndrome. Among these people two third belongs to Jewish Semitic origin and the rest are from Mediterranean or South Asian descent. The

most genetically homogenous group lives in Southern Ecuador (Guevara-Aguirre *et al.* 2018).

Laron syndrome (LS, OMIM # 262500), is characterized by short stature, truncal obesity, sparse hairs, small head circumference, frontal bossing, sunset sign, crowded defected teeth, acromicria, small gonads or genitalia, high pitched voice, retarded skeletal maturation and slow motor development (Laron 2015). Additional symptoms include protruding forehead, weak muscles, delayed puberty, saddle nose and blue sclera (Guevara-Aguirre *et al.* 1993; Laron *et al.* 2017). First time it was observed in 1958 and was reported in 1966 (Laron *et al.* 1993; Laron & Klinger 1994; Laron 2002). At biochemical level it is diagnosed with hypoglycemia in infancy, high serum hGH, low level of IGF, low IGFBP-3, serum GHBP (- or +) and progressive hyperlipidemia (Laron *et al.* 2017).

The LS is also known as hormone insensitivity syndrome which inherits in an autosomal recessive genetic disorder pattern due to mutation in the human Growth hormone receptor (*GHR*) gene. There are more than 90 mutations reported in *GHR* (Lin *et al.* 2018). These mutations affect ligand binding, GHR dimerization or signal transduction which ultimately halts the body growth (Fassone *et al.* 2007; Gennero *et al.* 2007). These mutations include deletion, RNA processing defects, translational stop codons and missense mutations. Mostly mutations are reported in the extracellular domain followed by intracellular domain and least in intronic regions.

GHR has vital role in the GH-GHR-IGF-1 axis and individual growth. In the interaction of GH-GHR-IGF-1, GHR as an important cytokine, introduces the GH signal into the cell and then regulates the expression of IGFs which controls the individual growth. Consequently, GH physiological activity is directly dependent upon the expression level and functioning of GHR in cells and tissues (Porto *et al.* 2017; Guevara-Aguirre *et al.* 2018; Lin *et al.* 2018). People afflicted with dysfunctional *GHR* are very short as they experience a loss or malfunctioning in the *GHR* response. Such people have low bone mineral density and increased adiposity which leads to increased risk of osteoporosis, lipid malformations and cardiovascular diseases (Rosenbloom 2016).

Human GHR cDNA translates 638 amino acids which includes the signal sequence of 18 amino. Extracellular domain is consisting of 246 amino acids (19-264), is encoded by exon 2-7 of GHR. Transmembrane domain is encoded by exon 8 consisting of 24 residues (265-288), while Intracellular domain consist of 350 residues (289-638) which is encoded by exon 9 and 10. Extra cellular domain of the GHR is divided into two functional sub-domains based on their function. Subdomain 1 consisting of 19-141 residues is responsible for growth hormone binding while subdomain 2 consist of 146-264 is responsible for receptor dimerization and GH-induced receptor rotation (Derr *et al.* 2011).

This study reports detailed clinical finding of a family afflicted with LS. The family has typical features of LS with minor peculiarity. Molecular genetic study of this condition led to the detection of a known mutation in *GHR*. These results further strengthen the clinical feature and molecular diagnosis of LS in Pakistani families.

5.3: Subjects and methods

5.3.1: Study approval

Study was part of international collaboration and approved by institution review board of Quaid-i-Azam University, Islamabad, Pakistan and Bogazici University, Istanbul, Turkey. All Information collected after taking informed and written consent according to declaration of Helsinki II.

5.3.2: Clinical Methods

Family was recruited from remote area of Southern Punjab, Pakistan. A detailed pedigree was drawn, and the pedigree indicated autosomal recessive inheritance pattern of the disease (Figure 5.1).

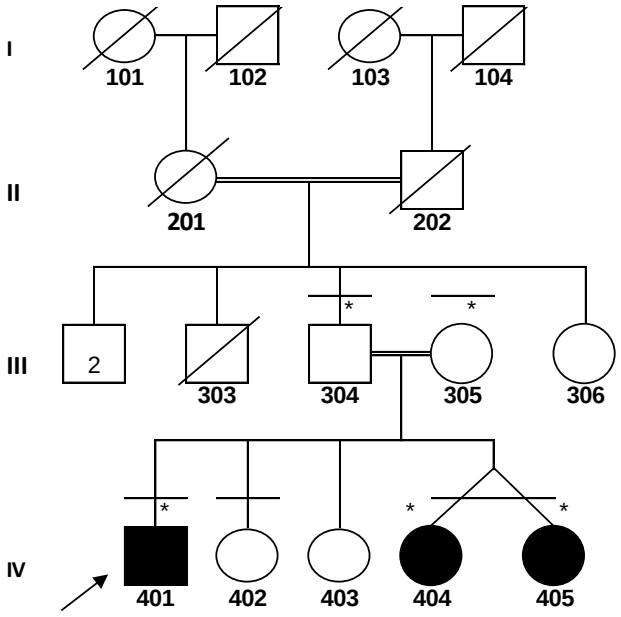

Figure 5.1: Pedigree of the family with Laron syndrome which segregated in three subjects in the last generation. *, individual involved in clinical and molecular study; individual with an arrow was proband; individual

with horizontal line above were physically examined; individual with oblique lines have been deceased.

Overall, five subjects (two normal parents 304 and 305 and three affected; 401, 404, and 405) participated in the study. Physical and clinical examination of all affected subjects was performed, photographs and anthropometric measurements were taken. Anterio-posterior view of X-rays was taken for affected subject 401.

5.3.3: Molecular Methods

The whole peripheral blood samples were taken from all participated subjects. The nucleic acid was extracted from the nuclei of lymphocytes to perform molecular study. SNP data of pooled DNA of three affected subjects were generated by using Illumina Human OmniExpress-24 BeadChip and the data was analyzed with help of Homozygosity mapper (www.homozygositymapper.org). The data were also analyzed by MS-Excel to verify the homozygous region. Exome sequencing for one affected subject 401 was prepared by using IDT xGen Exome Research Panel v.1.0 that targets 98% of bases in RefSeq database and sequencing performed using Illumina HiSeq2500. The generated reads aligned to reference sequence GRXh37/hg19 using BWA-0.7.12-r1039. After alignment SAMtools was used for variant calling. Variants were annotated by ANNOVAR. After annotation, variants were filtered by their frequency <0.001 in genomic databases.

5.4: Results

5.4.1: Clinical Findings

Three patients examined for clinical findings like short stature, sparse hairs, midface hypoplasia, truncal obesity, crowded defective teeth, blue sclera, compromised elbow extension, short pitched voice, and hypo-muscularity, fatigue, large ears, delayed puberty, no menarche, and small genitalia. Patients reported that they have conditional heart pain when involved in rigorous activities or lift heavy objects. Parents told that all the affected subjects had attention deficit. Additionally, patients 403 and 404 cannot lift more than 2 kg of weight (Table 5.1). The phenotypic expression of the disease in patients in comparison to normal father and X-rays of hands of one patient 401 are shown in Figure 5.2.

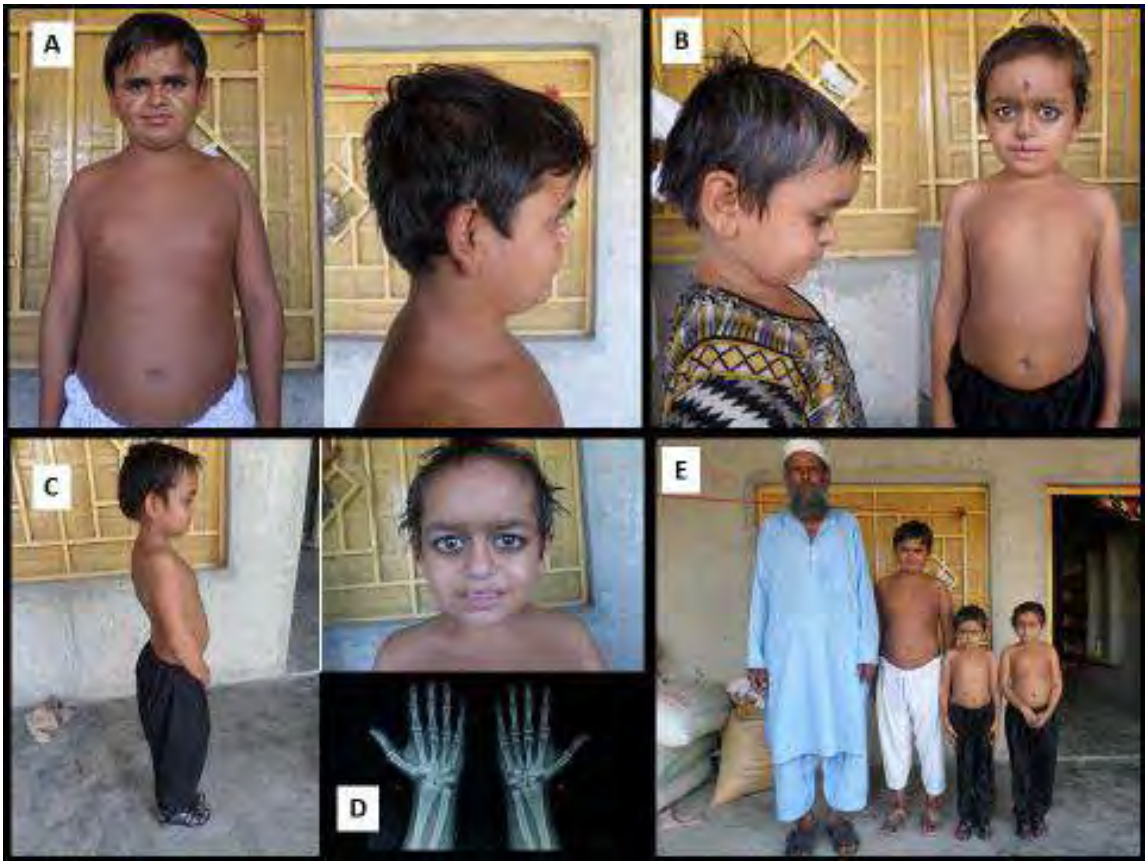

Figure 5.2: Phenotypic representation of Laron syndrome A) 401 with short stature and truncal obesity; Lateral view of face with protruding forehead, depressed nose and large ears. B) 404 truncal obesity, protruding forehead, large ears and sparse hair. C) Short stature in lateral view, blue sclera with crowded malformed teeth. D) X-ray of hands depicting the delayed bone age and late epiphyseal closure at the age of 19 of subject 401. E) A complete family picture depicting short stature with the normal person of family.

Table 5.1: Physical and clinical features of affected family members with Laron syndrome

Patients Ped. ID	**401**	**404**	**405**
Gender/Age	M/19	F/10	F/10
Clinical Features			
Skeletal/ limbs			
Short stature	+	+	+
Short limbs	+	+	+
Hypo-muscularity	+	+	+
Limited elbow extensibility	+	+	+
Truncal adiposity	+	+	+
Delayed bone age	+	N/A	N/A
Facial features			
Protruding forehead/ frontal bossing	+	+	+
Saddle nose	+	+	+
Blue sclerae	+	+	+
Shallow orbits of eye	–	+	+
Large ears	+	+	+
Defected crowded teeth	+	+	+
Skin			
Thin and prematurely age skin	+	+	+
Sparse hairs	+ in childhood	+	+
Decrease sweating	+	+	+
Reproductive symptoms			
Menarche	+	N/A	N/A
Micro-penis and small testicles	+	N/A	N/A
Others			
High-pitched voice	+	+	+

Delay in walking	+	+	+
Heart problem	+	N/A	N/A
Early fatigue	+	+	+
Weakness of muscles	+	+	+
Laboratory diagnosis			
Hypoglycemia	–	+	+
GH levels	Low	N/A	High
Macrocytic anemia	+	+	+

+, feature present; -, feature absent; N/A, not assessed

Patients also underwent hematological and hormonal examinations. Reports of all affected individuals revealed that glucose levels in the male patient showed normal levels while the other two female patients were hypoglycemic. Blood CP test revealed that mean corpuscular hemoglobin (MCH) and white blood cells (WBCs) values were higher in affected individuals while other variables were unremarkable (Table 5.2). Hormonal examination of affected individuals revealed that the growth hormone (hGH) level was lower in male and higher in female. Triiodothyronine (T3), Tetra iodothyronine (T4) and thyroid stimulating hormone (TSH) levels were normal (Table 5.2).

Anthropometric measurements for the all the affected individuals were obtained. Standing height for all the affected individuals showed short stature (Table 5.3).

Table 5.2: Hematological and hormonal results of affected subjects 401, 404, and 405.

ID	**401**	**404**	**405**	**Reference Range**
Gender /Age	M/19	F/10	F/10	
Diagnostic Variables				
Blood Glucose Fasting	76	**59**	**52**	60-100 mg/dl
Hematological Report				
Hb	14.5	11.5	12.1	13-18 (M); 11.5-14.5 (F) mg/dl
Total RBC	5.7	4.9	5	4.5-6.5 (M); 4-5.3 (F) x 10^12/l
Hct	48	39	40	38-52 (M); 33-43 (F)%
MCV	85	79	80	75-95 (M); 76-90 (F)
MCH	**25**	**23**	**24**	26-32 (M); 25-31 (F) pg
MCHC	30	30	30	30-35 g/dl
Platelet Count	326	393	198	150-400 x ^10^9/l
WBC Count (TLC)	**12.3**	**14.1**	**12.1**	4-11 x ^10^9/l
Neutrophils	54	60	60	40-75%
Lymphocytes	28	35	33	20-50%
Monocytes	8	4	5	2-10%
Eosinophils	**10**	1	2	1-6%
Hormonal profiles				
GH	**1.5**	**9.91**	-	2.0-5.0 (M); < 6.0 (F) ng/mL
T3	127.15	120.77	-	80-210 (M); 94-241 (F) ng/dl
T4	7.48	8.98	-	4.6-10.5 (M); 6.4-13.3 (F) ug/dl
TSH	2.716	2.6179	-	0.51-5.27 (M); 0.55-5.46 (F) uIU/ml

Hb, Hemoglobin; RBC, Red blood cells; Hct, hematocrit; MCV, mean corpuscular volume; MCH, mean corpuscular hemoglobin; MCHC, mean corpuscular hemoglobin concentration; WBC, white blood cells; TLC, total leukocytes count; GH, Growth hormone; T3, triiodothyronine; T4, tetraiodothyronine; TSH, thyroid stimulating hormone; mg/dl, milligrams per deciliter; M, male; F, female; pg, picogram; g/dl, grams per deciliter; ng/mL, nanogram per milliliter; ng/dl, nanograms per deciliter; µg/dl, micrograms per deciliter; µIU/ml, micro-international units per milliliter.

Table 5.3: Anthropometric measurements of affected individuals

Ped. ID	**401**	**404**	**405**
Age	M, 19	F, 9	F, 9
Head circumference	52	47	46
Neck circumference	32	23	23
Chest circumference	78	51	50
Arm span	146	105	102
Sitting height	75	52	49
Standing height	139 (<0.1)	102 (<0.1)	100 (<0.1)

(all measurements are in cm)

5.4.2: Genetic Findings

SNP based whole genome data of pooled DNA of three affected sibs were analyzed in order to obtain the homozygous intervals on each chromosome. For this purpose, HomozygosityMapper and MS-Excel were used for data analysis. HomozygosityMapper revealed the homozygosity in the whole genome as shown in figure 5.3. The data were imported in the Excel and the genotype status with heterozygous and homozygous were marked with different colors. During the data analysis by visual inspection, large homozygous intervals were marked. Homozygous regions having a length of ≥ 1Mb were selected and 45 autosomal homozygous intervals were identified as candidate regions. These regions were selected as they were of larger size, and there could be high likelihood to find the defective gene(s) in these regions. The boundary SNPs and their corresponding nucleotide positions of these regions were obtained. In this way, every chromosome was analyzed from upper telomere to lower telomere. Finally, all the information obtained from analysis were tabulated chromosome wise and the candidate interval highlighted in red rectangle through (Table 5.4).

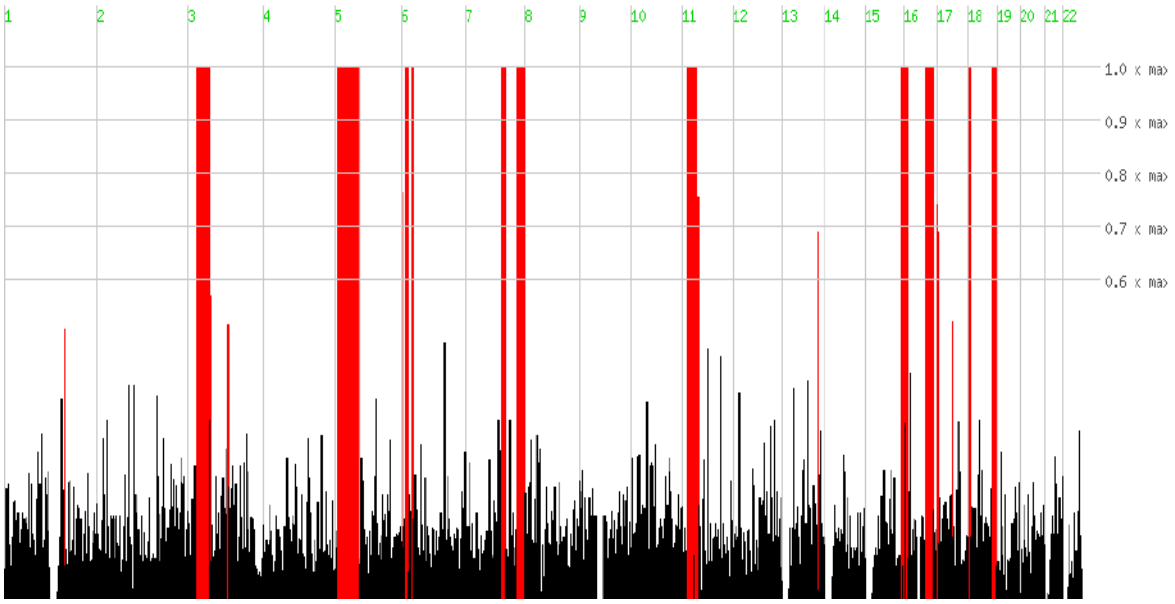

Figure 5.3: Graphical representation of homozygosity intervals obtained by HomozygosityMapper with default parameters. Red bars depict the longer stretches of homozygous genotypes on chromosomes and black bars revealed short intervals of homozygous genotypes.

Table 5.4: SNP analysis indicated following 45 autosomal homozygous intervals ≥1Mb

S. No.	Chr	Start SNP	End SNP	Start position	End position	Interval length	Mb
1	1	rs10489636	rs2840310	160651750	161700827	1049077	1.05
2	2	rs12470303	rs890682	24619883	25948600	1328717	1.33
3	2	rs6436290	rs267993	157148002	158314418	1166416	1.17
4	3	rs9310681	rs7647724	22153897	29725062	7571165	7.57
5	3	rs7647724	rs6800757	29725062	31980606	2255544	2.26
6	3	rs6800757	rs2564926	31980606	53094730	21114124	21.11
7	3	rs2564926	rs3924042	53094730	57020736	3926006	3.93
8	3	rs9828514	rs4855586	107722014	108989277	1267263	1.27
9	4	rs7434819	rs7660477	158731019	159948180	1217161	1.22
10	5	rs2930059	rs30364	10753399	55829376	45075977	45.08
11	5	rs12943234	rs4796691	38861655	39883789	1022134	1.02
12	5	rs30364	rs317969	55829376	66686570	10857194	10.86
13	5	rs299099	rs7732361	68720419	70749745	2029326	2.03
14	6	rs7750580	rs1772987	1211523	2512075	1300552	1.3
15	6	rs1990665	rs4712274	13755585	16036551	2280966	2.28
16	6	rs4712274	rs10946363	16036551	20163330	4126779	4.13
17	6	rs9374450	rs10485113	114588786	116147191	1558405	1.56
18	7	rs17168173	rs10953348	96725713	101169691	4443978	4.44
19	7	rs10953348	rs39334	101169691	103453099	2283408	2.28
20	7	rs39334	rs2893638	103453099	106055504	2602405	2.6
21	7	rs12056021	rs17520243	118489794	119672864	1183070	1.18
22	7	rs17520243	rs10251692	119672864	120714700	1041836	1.04
23	7	rs10435433	rs11771946	138494588	140432893	1938305	1.94
24	7	rs11771946	rs929289	140432893	144112357	3679464	3.68
25	7	rs929289	rs826790	144112357	147027426	2915069	2.92
26	8	rs7388463	rs2945251	6974050	8094406	1120356	1.12
27	8	rs10105616	rs7003452	33906372	35021424	1115052	1.12
28	9	rs7853023	rs4275319	38772575	68513625	29741050	29.74

29	10	rs10751387	rs11259820	46141837	47588324	1446487	1.45
30	11	rs6486167	rs1792537	14114334	15168799	1054465	1.05
31	11	rs12275191	rs1532286	24087672	25818836	1731164	1.73
32	11	rs10767859	rs224612	30571347	32063229	1491882	1.49
33	11	rs10836878	rs4755505	37883072	39283877	1400805	1.4
34	11	rs687558	rs260864	102833618	103876114	1042496	1.04
35	14	rs9671696	rs6576199	105932544	107124500	1191956	1.19
36	15	rs4508392	rs748385	97218758	99143471	1924713	1.92
37	16	rs4485340	rs2279868	7959642	10539413	2579771	2.58
38	16	rs9929017	rs9674439	31838156	33836510	1998354	2
39	16	rs9930089	rs8048667	59208069	71048669	11840600	11.84
40	16	rs8048667	rs11859772	71048669	78965188	7916519	7.92
41	17	rs3999623	rs3785859	58308456	59379738	1071282	1.07
42	18	rs9948893	rs7235529	5190554	7369572	2179018	2.18
43	18	rs9946136	rs7239116	18249729	19486725	1236996	1.24
44	18	rs2156439	rs4464167	64724538	73303404	8578866	8.58
45	19	rs10413586	rs775883	59071321	60143609	1072288	1.07

Overall, exome sequencing captured 23934 exonic variants > 12363 nonsynonymous variants > 4689 homozygous variants > 96 variants with less than 0.001 frequency in 1000G > 62 variants with less than 0.001 frequency in ExAC and ESP6500 > 53 Quality control > 2 pathogenic variants > single *GHR* was final candidate variant. The identified mutation was *GHR*:NM_001242460:c.442G>C:p.D148H. Exome analysis filtration scheme is given in figure 5.4. Amino acids conservation across different species is given in Figure 5.5.

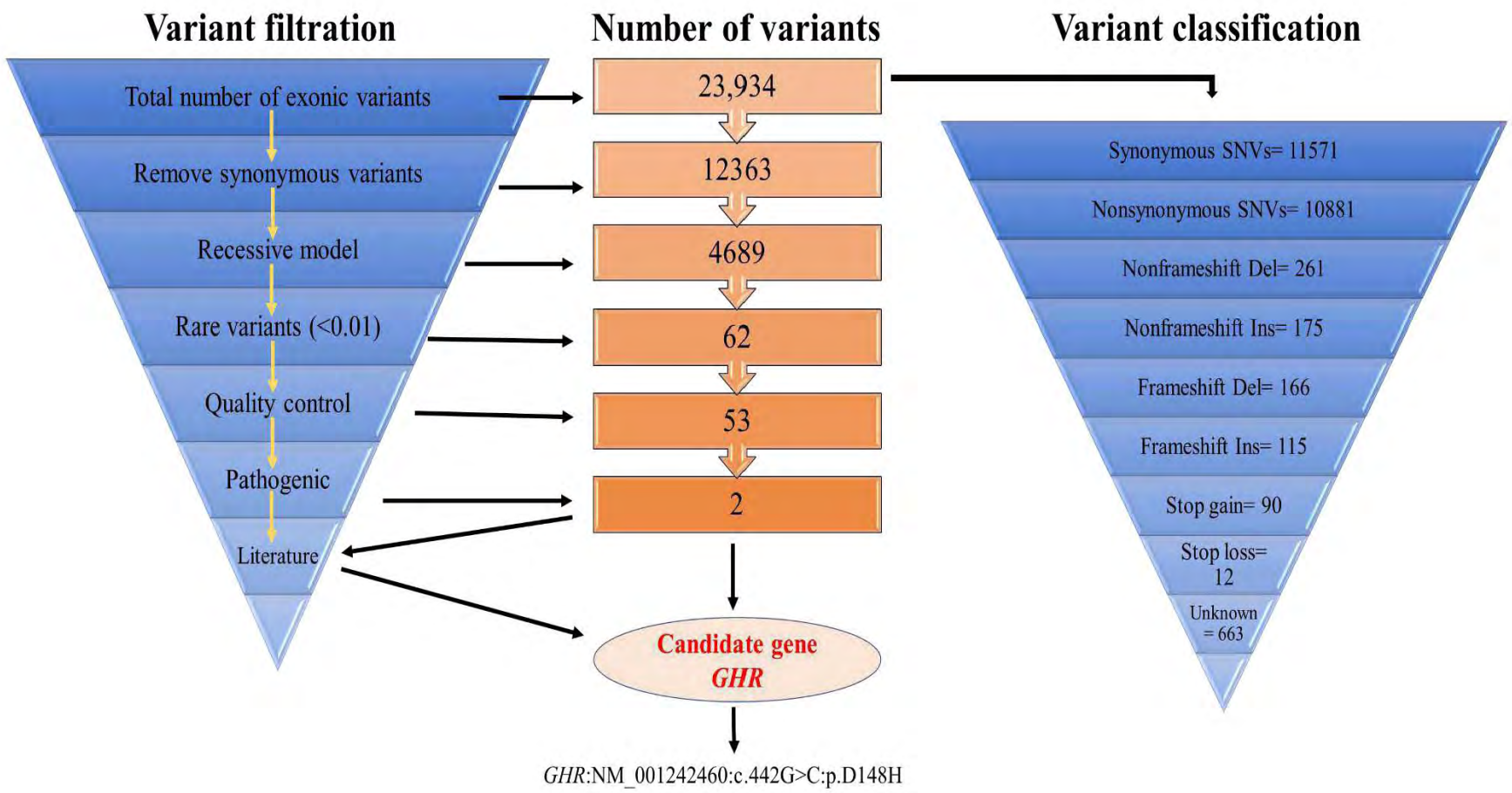

Figure 5.4. Summary of exome filtration scheme

Species	Amino acid sequence												
Mutated *H. sapiens*	L	T	G	I	H	A	H	I	Q	V	R	W	E
H. sapiens	L	T	G	I	H	A	D	I	Q	V	R	W	E
P. troglodytes	L	T	G	I	H	A	D	I	Q	V	R	W	E
M. mulatta	L	T	G	I	H	A	D	I	Q	V	R	W	E
F. catus	L	T	G	I	Q	A	D	I	Q	V	R	W	E
M. musculus	L	T	G	I	R	G	D	I	Q	-	-	-	-
G. gallus	Q	T	G	I	H	G	D	I	Q	V	R	W	D
T. rubripes	-	-	-	-	S	Y	D	V	I	V	N	W	E
D. rerio	R	S	G	L	H	F	D	V	L	V	R	W	T
X. tropicalis	L	T	R	M	R	V	D	I	Q	L	S	W	E

Figure 5.5. Amino acids conservation across species

5.5: Discussion

Short stature may be proportionate or disproportionate like achondroplasia, hypo-achondroplasia, and multiple epiphyseal dysplasia (Hasegawa & Tanaka 2014; Saengkaew *et al.* 2017). Etiological factors for short stature include nutritional, gastrointestinal, endocrinal, and genetic factors (Yadav & Dabas 2015). Endocrinal factors like GH deficiency causes short stature, e.g., LS (Collett-Solberg *et al.* 2019).

Globally, there are 300 reported patients afflicted with LS that mostly found in consanguineous families. The typical features of LS include short stature, low birth weight, protruding forehead, saddle nose, small hand and feet with short limbs, and hypoglycemia due to deficiency of IGF-1 (Laron 2015; Moia *et al.* 2017). Similar features had observed in the presented family. The female patients had hypoglycemia in early child hood whereas male patients have normal glucose level (Laron & Kauli 2016). Atypical symptoms include delayed fontanel closure, shallow eye orbits, sun set sign of eyes, sparse hairs, and blue sclera (Laron 2004). From the atypical features, the shallow eye orbits, sparse hairs, blue sclera, large ear, early fatigue during normal activities, muscle weakness, and macrocytic anemia found in the patients of studied family.

Additionally, LS has common feature with GH-gene deletion syndrome due to identified mutation in the deletion syndrome (Moseley & Phillips III 2000). The common features include acromicria, organomicria, reduced development of skeletal and muscular systems, oro-facial abnormalities, and obesity (Ahmad *et al.* 2011; Somale & Ahmed 2016). In both cases, the major biochemical similarity, IGF-1 is undetectable. In contrary to this, the discriminative feature between these two syndrome involves high level of GH in case LS and lack of GH in case of GH-gene deletion syndrome (Ahmad *et al.* 2011). In the studied family, the high level of GH confirms the LS.

In the present study, a transversion mutation c.442G>C identified in exon 4 of *GHR* gene was already reported and was responsible for the phenotype. Extracellular domain of *GHR* is encoded by 2-7 exons so this mutation occurs in this encoded region. GHR functionally divided in two sub-domains. Sub-domain 1 consists of 19-141 amino acids and responsible for growth hormone binding while sub domain 2 consist of 146-264 amino acids and is responsible for receptor dimerization and GH-

induced receptor rotation. Mutation in the receptor sub-domain 2 stops the dimerization and GH-induced receptor rotation. Consequently, GH-GHR-IGF-1 axis is stopped, and inactivation of IGF-1 occurs which ultimately results in growth failure of an individual. Several mutations have been identified to cause dwarfism. For example mutation c.G62V in exon 4 of GH (El Kholy *et al.* 2011), a heterozygous mutation V1441 in exon 6 of *GHR*, a dinucleotide deletion in exon 7 of *GHR* (Pagani *et al.* 2014), and GT-repeat microsatellite in the 5 UTR of *GHR* gene (Dias *et al.* 2019) result in dwarfism.

Study reported detailed clinical and molecular findings of LS in consanguineous kindred from Pakistan. Shallow eye orbits, sparse hairs, blue sclera, large ear, early fatigue during normal activities, muscle weakness, and macrocytic anemia were unique features. Mutation in sub-domain 2 of *GHR* stops the dimerization of GH-GHR and consequently results in growth failure. These unique features described variability in the family from the other reported studies. This study expands the clinical spectrum of LS and confirm the molecular diagnosis of this rare anomaly. These findings would be very useful in the genetic counseling of the family.

CHAPTER 6

FAMILY IV

Chapter 6. Homozygous deletion c.4054_4055del (p.L1352Vfs*72) in *COL18A1* further delineates the phenotypic spectrum of Knobloch syndrome

6.1: Abstract

Basement membranes (BMs) are specialized extracellular matrix (ECM) structures that provide structural support and influence cell behavior and signaling pathways. BMs contain 60-200 proteins and require collagens for their proper functions. These include collagens IV, VI, VII, XV, XVII, and XVIII and mutations in these collagens result in rare multisystem disorders. Knobloch syndrome 1 (KNO1; MIM 267750) is an autosomal recessive hereditary condition caused by mutations in *COL18A1*, which codes for alpha chain of type XVIII collagen. KNO1 is characterized by the co-occurrence of vitreoretinal and macular degeneration, and occipital encephalocele. The ocular abnormalities range from severe myopia, lens subluxation, retinal detachment and blindness. The affected subjects may also exhibit cutis aplasia, patent ductus arteriosus, pyloric stenosis, midface hypoplasia, epilepsy, and abnormalities of lungs, cardiac and renal systems. This study was aimed to present clinical and molecular investigations of an inbred Pakistani family afflicted with KNO1. The affected individuals had lens dislocation and high myopia, chorio-retinal atrophy, complex cataract, nystagmus, occipital encephalocele, and cutis aplasia. There was complete blindness in late ages and progressive intellectual disability in few subjects. The unusual features evident in the patients were low sweating slow bleeding in wounds, low pain sensation, anterior chest wall defect, and early fatigue. Further, there had been six postnatal mortalities with multiple organ-systems deformities. Through linkage mapping and exome sequencing, homozygous two-base pair deletion c.4054_4055delCT was detected. This mutation is predicted to form a truncated protein, which may profoundly impair its normal function. The range of clinical symptoms evident in the present family is surprising and taken together with other studies, this study further expands the phenotypic manifestation of KNO1.

6.2: Introduction

Basement membranes (BMs) are specialized extracellular matrix (ECM) structures that provide structural support and influence cell behavior and signaling pathways. BMs contain 60-200 proteins and require collagens for their proper functions. In vertebrates, there are 28 different types of collagens, which grouped into five classes on the base of protein domain structure and supramolecular assembly. The classes are fibrillar (collagen I), network forming (collagen IV), beaded microfibril (collagen VI), multiplexin (collagen XV and XVIII), and FACIT (fibril-associated collagens with interrupted triple helices; collagen VII and XVII). All these collagens processed in and secreted from endoplasmic reticulum (Ishikawa *et al.* 2016). Mutations in these BMs associated collagens result in different rare multisystem disorders (Randles *et al.* 2017; Gatseva *et al.* 2019).

Knobloch syndrome 1 (KNO1; MIM 267750) is a rare hereditary disorder due to mutations in collagen XVIII. Its major clinical features include vitreoretinal, macular degeneration, and occipital encephalocele. The minor features may be ocular or skeletal. Its ocular secondary features include myopia, congenital cataract, iris abnormalities, lens subluxation, vitreoretinal degeneration with retinal detachment, and macular abnormalities (which lead to bilateral blindness) (Czeizel *et al.* 1992; Wilson *et al.* 1998). The secondary abnormalities involve cutis aplasia, anomalous pulmonary return in lung, flat nasal bridge, patent ductus arteriosus, a single umbilical artery, pyloric stenosis, flat nasal bridge, midface hypoplasia, bilateral epicanthic folds, cardiac dextroversion, generalized hyperextensibility of the joints, unusual palmar creases, unilateral duplication of the renal collecting system, and epilepsy (Suzuki *et al.* 2002; Keren *et al.* 2007). Some patients have early onset night blindness and progress to total blindness before 20 years of age. Cognitive decline has been reported also in some patients (Caglayan *et al.* 2014). The clinical variability of KNO1 is due to different types of mutations in *COL18A1* gene that codes for collagen XVIII. This type of collagen is found in the basement membranes of various body tissues, including some parts of the eye such as the vitreous and retina.

COL18A1 is located at 21q22.3 and has 43 exons. The encoded collagen XVIII is an important component of basement membranes (Fukai *et al.* 2002). *COL18A1* has three

isoforms; and these isoforms arise through the use of at least two promoters and alternative splicing in the third exon (Passos-Bueno *et al.* 2006). Studies have shown that collagen XVIII has an important role in determining the retinal structure as well as closure of the neural tube (Sertié *et al.* 2000). This protein is vital for normal eye development and is an essential component of the basement membrane of the iris, vitreous and retina. It also plays important functional roles in neuronal cell migration and as a component of the basement membrane of kidney as well as teeth development (Passos-Bueno *et al.* 2006; O'CONNELL *et al.* 2009).

Consistent with its roles in these developmental pathways, the mutations in *COL18A1* result in phenotypes associated with ocular abnormalities ranging from early-onset severe myopia, congenital cataract, iris abnormalities, lens subluxation, vitreoretinal degeneration with retinal detachment, macular abnormalities and blindness, neural migratory defects and abnormalities of the renal system (Czeizel *et al.* 1992; Kliemann *et al.* 2003).

There are at least seventeen mutations leading to KNO1 have been described in the *COL18A1* gene (Li *et al.* 2017). Variants in *COL18A1* are also known to cause predisposition to prostate cancer (Iughetti et al. 2001), and Down-syndrome-associated atrioventricular septal defect (Ackerman et al. 2012). However, there is no report of skeletal abnormality in KNO1 families.

This study reports a Pakistani family with 26 members afflicted with KNO1 with unusual features of skeletal and integumentary systems for KNO1.

6.3: Subjects and methods

6.3.1: Family history and data collection

The inbred family is from Southern Punjab region of Pakistan. A six-generation pedigree constructed with the help of family elders. Twenty-six (15 males and 11 females) members were affected (Figure. 6.1). Nine affected individuals underwent thorough physical and medical examination with the help of local physicians at Nishter Hospital, Multan. Three subjects underwent roentgenographic evaluation. Peripheral blood samples of three affected and four unaffected subjects were available for molecular analyses. In accordance with the regulations of the Ethical Review Committee of Quaid-i-Azam University and the Bogazici University Institutional Review Board for Research with Human Participants, written informed consent was obtained from all participants.

6.3.2: Molecular Methods

DNA samples from three affected and five unaffected members of the family were available for the genetic study. In order to find the causative gene, exome sequencing was performed for patient 521. The Agilent SureSelect Target Enrichment System was used for exome capturing and the Illumina HiSeq2000 platform for sequencing. Exome file was analyzed to search for the candidate causative mutation. Rare variants with frequencies <0.01 in all populations in ESP6500, 1000 Genomes and gnomAD that includes 10,000 Pakistani exomes in the South Asian samples were selected. The variants which assessed as possibly homozygous predicted as damaging to the protein and is in a possibly relevant gene were considered as candidates to underlie the disease.

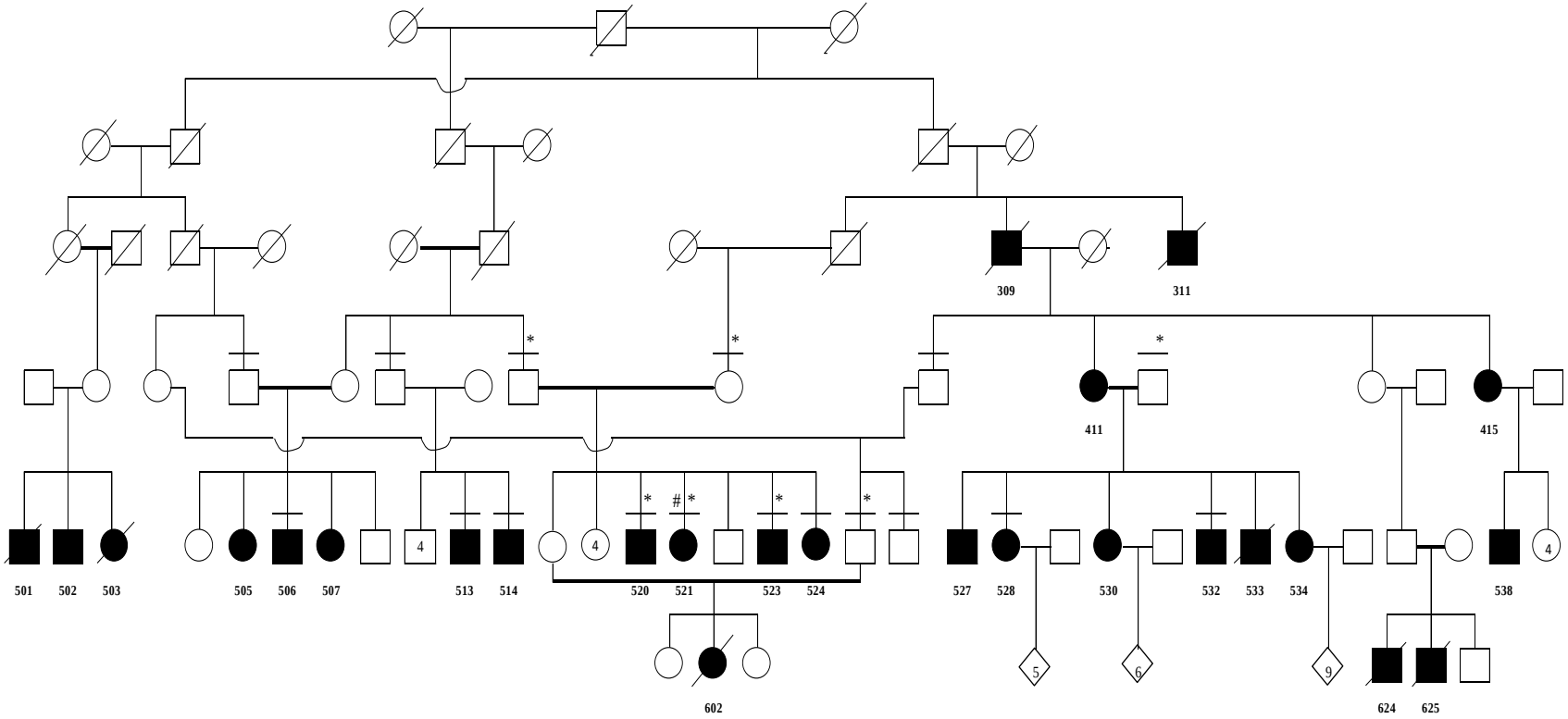

Figure 6.1: Pedigree of large Pakistani kindred with features of Knobloch syndrome.

Symbols with above horizontal lines: physically observed; symbols with oblique lines: deceased; *: blood samples available; and #: exome sequence.

6.4: Results

6.4.1: Clinical Report

The primary feature in the affected individuals was lens dislocation and high myopia. Additional symptoms included chorio-retinal atrophy, complex cataract and nystagmus with squint eyes. The condition was either congenital or early onset leading to progressive loss of vision (Table 6.1). Complete blindness developed at the ages of 50 to 60 years. Occipital encephalocele was reported as a birth presentation in five of the studied affected subjects. However, none of them had undergone surgical corrections and the protuberances, generally ranging ≤ 6 cm in size recessed in few months postnatally. Cutis aplasia and/or remnant scars of encephalocele were evident at the dorsal or posterior aspect of skulls in six of the subjects. According to family elders, the skin there appeared as a thin, transparent membrane in newborn, but the scar healed up slowly and later developed into skin without hair (Figure. 6.2A-D). In the adulthood, sparse hair-follicles appeared gradually, and the scar diminished. Cutis aplasia was restricted to the skull and did not affect any other part of the body.

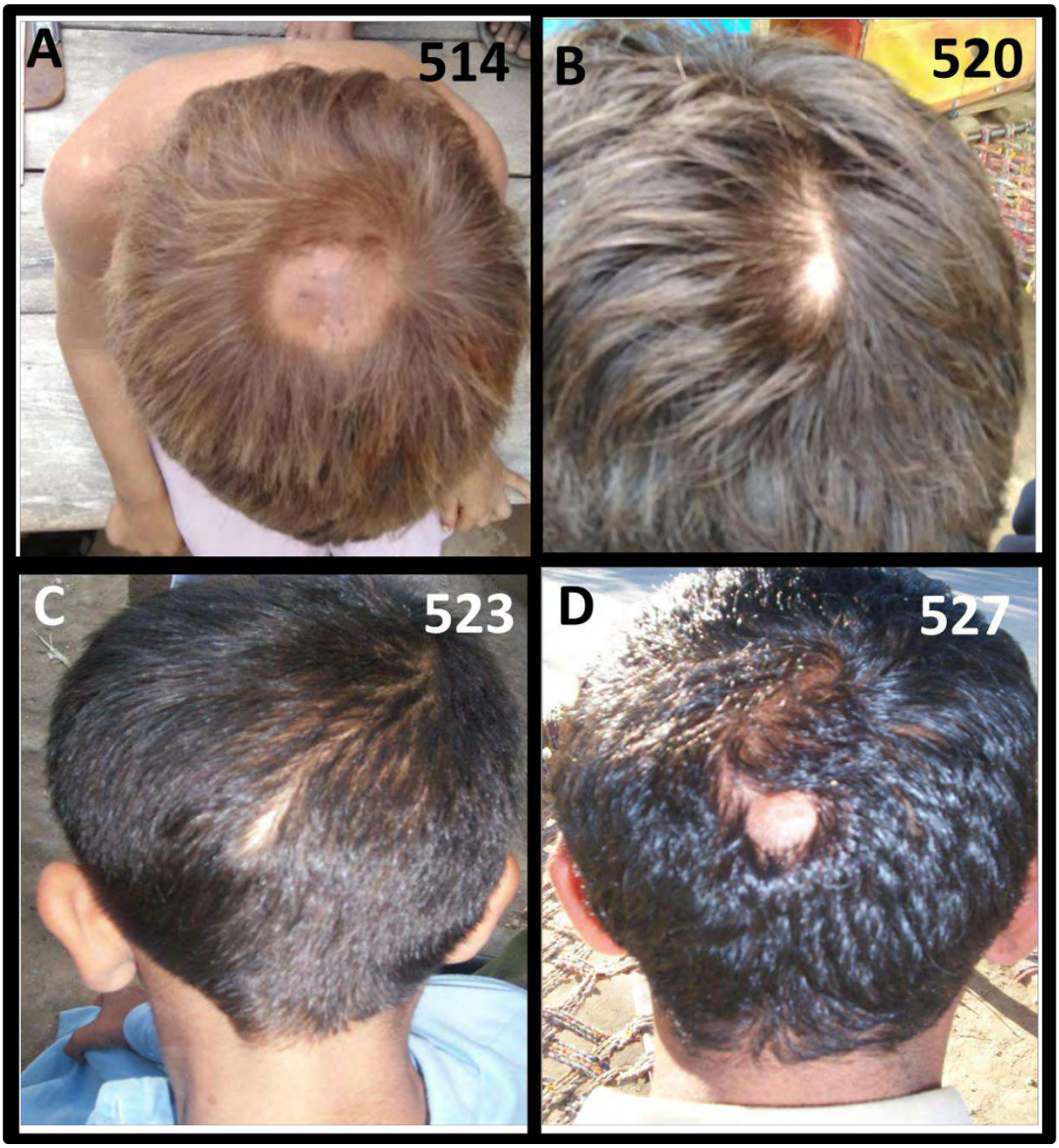

Figure 6.2: Presentation of cutis aplasia in affected subjects 514, 520, 523, and 527. Remnant scars of encephalocele evident at the dorsal (514) or posterior aspect (520, 523 and 527).

Ectodermal peculiarities evident in the affected subjects were low sweating (6/9), slow bleeding in wounds (6/9), low sensitivity to pain 2/9), and abnormal pigmentation on trunk and limbs (2/9). The skeletal abnormalities ranged from hyperflexibility of joints (5/6) and anterior chest wall defect characterized by barrel-shaped chest (3/6). The subjects were able to perform routine jobs but get tired quickly (4/8) (Table 6.1). Progressive intellectual disability was evident in two affected subjects who also had complete blindness. There had been at least six postnatal mortalities of the affected subjects. Reportedly, those children died in early infancy between 3-6 weeks and were afflicted with multiple anomalies including encephalocele, cutis aplasia, rectal closure, abnormal chest cage and talipes. They also had squint eyes, nystagmus and epilepsy. The mothers of two of the affected subjects mentioned that while weeping the affected children had swollen chest with abdominal palpation. A summary of clinical findings in the family is presented in Table 6.1.

Table 6.1: Clinical symptoms in affected subjects

Pedigree ID	**309**	**311**	**506**	**513**	**514**	**520**	**521**	**523**	**524**	**527**	**531**	**Concordance (%)**
Age (years)	**D**	**D**	**29**	**7**	**5**	**19**	**16**	**9**	**3**	**55**	**30**	
Gender	M	M	M	M	M	M	F	M	F	F	M	8M/3F
Eye												
Low vision (myopia)	+	+	+	+	-	+	+	+	+	+	+	10/11 (90.9%)
Subluxated lens	+	+	+	-	-	+	+	+	+	+	+	9/11 (81.8%)
Cataract	+	+	+	-	-	+	+	+	+	+	+	9/11 (81.8%)
Nystagmus	+	+	+	-	-	+	+	+	+	+	+	9/11 (81.8%)
Squint eyes	+	+	+	-	-	+	+	+	+	+	+	9/11 (81.8%)
Chorio-retinal atrophy	N/A	N/A	+	+	-	+	+	+	+	+	+	8/11 (72.7%)
Skull and skeleton												
Occipital encephalocele	+	+	+	-	-	+	+	+	+	+	+	9/11 (81.8%)
Protruding chest/ sternum	N/A	N/A	N/A	+	+	-	-	+	-	N/A	N/A	3/11 (27.2%)
Skin												
Cutis aplasia	+	+	+	-	+	+	+	+	+	+	+	10/11 (90.9%)
Remnant scars on head	N/A	N/A	+	-	+	+	+	+	+	+	+	8/11 (72.7%)
Recovering cutis aplasia	+	+	-	-	-	+	+	+	-	+	+	7/11 (63.6%)
Bleeding on wound	N/A	N/A	-	-	-	Low	Low	Low	Low	Low	Low	6/11 (54.5%)
Low Sweating	N/A	N/A	-	+	N/A	+	+	+	N/A	+	+	6/11 (54.5%)
Pain Insensitivity	N/A	N/A	-	-	-	-	-	-	-	+	+	2/11 (18.1%)

Abnormal skin pigmentation	N/A	N/A	-	-	+	-	-	+	-	-	-	2/11 (18.1%)
Others												
Able to perform domestic work	+	+	+	+	+	+	+	+	N/A	Low	N/A	8/11 (72.7%)
Early fatigue	N/A	N/A	+	-	-	+	+	+	N/A	+	+	6/11 (54.5%)
Schooling	N/A	N/A	-	+	+	+	-	+	-	-	-	4/11 (36.3%)
Low IQ (onset at 50s; progressive)	-	-	-	-	-	-	-	-	-	+	+	2/11 (18.1%)

D, deceased; M, male; F, female; N/A, not accessed; IQ, intelligence quotient

6.4.1.1 Index subject 520

The index subject (520) is a 19 years old male. He is a student at a religious school and learns by listening. The vision loss started in early childhood and is progressive. Currently, he is able to see only large objects from a distance of 3-4 feet. He can still discriminate between colours. On clinical examination, he was observed to have the pale optic disc, complex cataract (Fig. 6.3A), lens dislocation and nystagmus. Examination of the right eye showed right aphakia and subluxated lens. Fundoscopic examination revealed chrioratinal atrophy, large punched-out chorioretinal lens and sclera at the macular area. In the left eye, bands of keratic precipitates were observed. There was posterior synchia. The B-scan of the left eye carried out at 8-20 MHz frequency revealed echogenic opacities filling the whole of the vitreous cavity. There was vitreous haemorrhage and intra-ocular inflammation (Fig. 6.3B). The subject has cutis aplasia (Figure 6.2B) which is a remnant of occipital encephalocele (approximately 1 cm in diameter). He has low sweating and slow bleeding in the wound. He gets tired very quickly and gets headache after half an hour of study. Ultra-sonography of abdomen and chest revealed unremarkable internal vital organs.

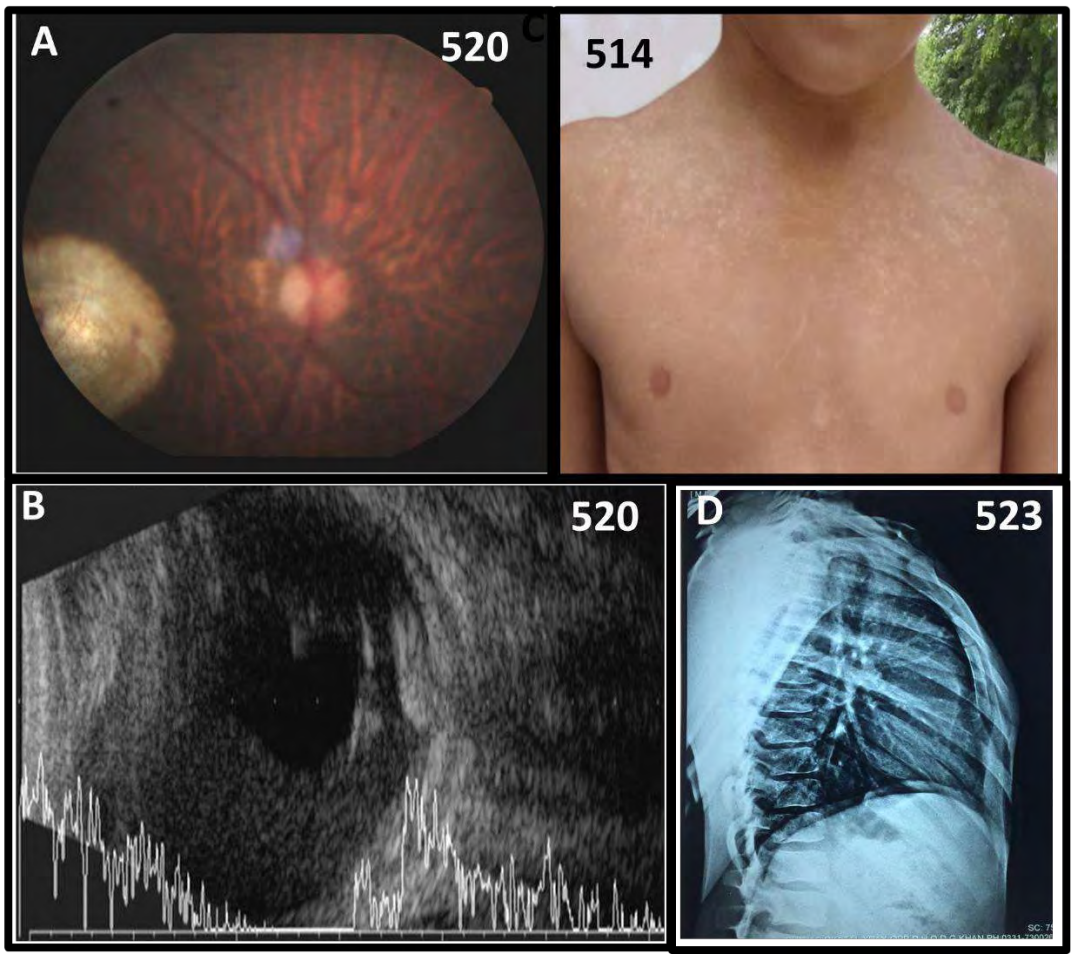

Figure 6.3: Clinical and morphological features of affected subjects 520, 514, and 523.

A: fundus photograph of left eye, B: ultrasound (Beta-scan) of right eye; C: hypopigmentation; and D: roentgenogram of chest

6.4.1.2 Subject 523

Subject 523 is 11 years boy with severe visual impairment. He was attending a special school. Clinical examination showed subluxated lens, retinal atrophy, nystagmus and squint eyes. He had congenital occipital encephalocele. He had low sweating, low pain sensitivity and pigmentation on lower limbs. Additionally, he had hyperlaxity of joints and both of his arms are bent in 15-degree outward direction. He had barrel-shaped chest and flattened diaphragm (Fig. 6.3D). Ultra-sonography of chest and abdomen did

not reveal any abnormality in vital organs. Hematological reports revealed low level of hemoglobin and high ESR (erythrocytes sedimentation rate) values (Table 6.2).

Table 6.2: Hematological assessment of patient 523.

Test	Results	Normal Range
Haemoglobin	**10.5 g/dl**	13-18 g/dl
Total WBCs count	5400 /cm^3	4000-11000/ cm^3
Poly morph	66%	40-75%
Lymphocytes	28%	20-45%
Eosinophils	2%	1-6%
Monocytes	4%	2-10%
ESR	**30 mm/h**	15 mm/h
Platelets	190000 /UL	150000-400000 /UL

WBCs: white blood cells; ESR: erythrocytes sedimentation rate; g/dl: gram per deciliter; cm^3: centimeter cube; mm/h: millimeter per hour; and UL: unit litter.

6.4.1.3. Subject 532

Subject 532 is 25 years old male. He had vision problems with cataract, nystagmus and squint eyes. He was able to recognize large objects. He also has mild to moderate intellectual disability and behavioral problems. He used to spend most of his time wondering in streets. He is sensitive to others and crowded areas and may become aggressive occasionally. However, he had excellent memory with good orientation of time and space.

6.4.2. Molecular analyses

Overall, exome sequencing captured 114498 variants from all chromosome > 23378 exonic variants > 11933 nonsynonymous variants > 2673 homozygous variants >

173 variants with less than 0.001 frequency in 1000G > 24 variants with less than 0.001 frequency in ExAC and ESP6500 > 2 pathogenic variants > 1 candidate variant (*COL18A1* on chromosome 21). The coordinates of identified mutation were *COL18A1*:NM_030582: c.4054_4055delCT: p.L1352fs in exon 40. Exome filtration strategy is given in Figure 6.4 and the results of exome analysis given in Table 6.3. Amino acids conservation across the different species is shown in Figure 6.5.

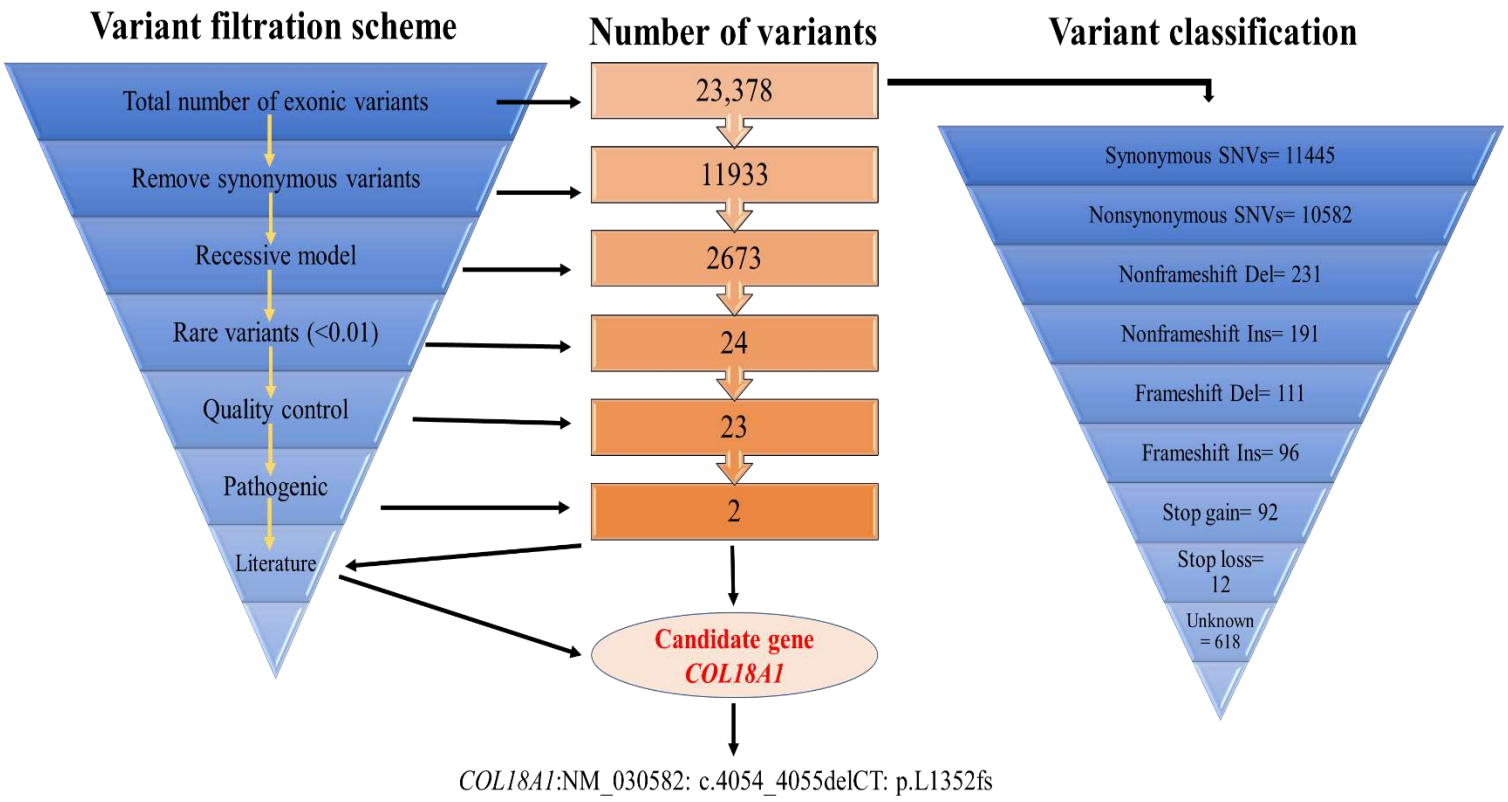

Figure 6.4: Summary of exome filtration scheme

Table 6.3. List of candidate variants as a result of exome analysis

Chr	Start	End	Ref	Alt	Func.refgene	Gene.refgene	ExonicFunc.refgene	AAChange.refgene	ClinVar_SIG	ClinVar_DIS	Other info
chr8	21966701	21966701	C	-	exonic	*NUDT18*	frameshift deletion	NUDT18:NM_024815:exon3:c.111delG:p.R37fs	.	.	Hom
chr8	87226635	87226642	CCGACATC	-	exonic	*SLC7A13*	frameshift deletion	SLC7A13:NM_138817:exon4:c.1413_1511del:p.*471fs	.	.	Hom
chr9	115216223	115216226	ATTA	-	exonic	*C9orf147*	frameshift deletion	C9orf147:NM_001350649:exon5:c.510_513del:p.I170fs	.	.	Hom
chr15	31521506	31521507	GG	-	exonic	*LOC283710*	frameshift deletion	LOC283710:NM_001243538:exon2:c.75_76del:p.P25fs	.	.	Hom
chr17	26699206	26699206	A	-	exonic	*SARM1*	frameshift deletion	SARM1:NM_015077:exon3:c.152delA:p.E51fs	.	.	Hom
chr17	26708303	26708304	GT	-	exonic	*SARM1*	frameshift deletion	SARM1:NM_015077:exon6:c.549_550del:p.G183fs	.	.	Hom
chr17	45438887	45438890	AGTG	-	exonic	*EFCAB13*	frameshift deletion	EFCAB13:NM_152347:exon10:c.805_805del:p.S269fs	.	.	Hom
chr19	52887146	52887146	A	-	exonic	*ZNF880*	frameshift deletion	ZNF880:NM_001145434:exon4:c.313delA:p.K105fs	.	.	Hom
chr20	1592151	1592152	GA	-	exonic	*SIRPB1*	frameshift deletion	SIRPB1:NM_001135844:exon2:c.284_285del:p.L95fs,SIRPB1:NM_001329157:exon2:c.284_285del:p.L95fs	.	.	Hom
chr20	1895951	1895952	CT	-	exonic	*SIRPA*	frameshift deletion	SIRPA:NM_001040023:exon2:c.286_287del:p.L96fs,SIRPA:N	.	.	Hom

								M_001040022:exon3:c.286_287del:p.L96fs,SIRPA:NM_001330728:exon3:c.286_287del:p.L96fs,SIRPA:NM_080792:exon3:c.286_287del:p.L96fs			
chr21	46930005	46930006	CT	-	exonic	*COL18A1*	frameshift deletion	COL18A1:NM_030582:exon40:c.4054_4055del:p.L1352fs,COL18A1:NM_130444:exon40:c.4759_4760del:p.L1587fs,COL18A1:NM_130445:exon41:c.3514_3515del:p.L1172fs	Pathogenic	Knobloch_syndrome_1	Hom

Species	Amino acid sequence											
Mutated *H. sapiens*	V	A	L	N	S	P	V	R	R	H	A	G
H. Sapiens	V	A	L	N	S	P	L	S	G	G	M	R
P. troglodytes	V	A	L	N	S	P	L	S	G	S	M	R
M. mulatta	V	A	L	N	S	P	L	P	G	G	M	R
M. musculus	V	A	L	N	T	P	L	S	G	G	M	R
R. norvegicus	V	A	L	N	T	P	L	S	G	G	M	R
G. gallus	V	A	L	N	T	P	L	S	G	G	M	R
X. tropicalis	V	A	L	N	T	P	L	S	G	S	M	K

Figure 6.5: Amino acid conservation of protein across the vertebrates

6.5: Discussion

KNO1 inherited in an autosomal recessive fashion (Sertie *et al.* 1996; Suzuki *et al.* 2002). Suzuki et al. recruited eight families with KNO1. The majority of the patients had severe ocular alterations. The authors observed in total six different recessive mutations in both alleles of *COL18A1* in five of the eight unrelated KNO1 patients. Among these mutations, three were compound heterozygotes and two were homozygotes. Three of the families had deletion mutation c.3514-3515delCT in exon 41. All were truncating mutations leading to deficiency of collagen XVIII isoforms (Suzuki *et al.* 2002). Likely, Caglayan et al. identified three different mutations in four families; all the patients with mutations all had structural brain abnormalities (Caglayan *et al.* 2014). Similarly, Haghighi et al. detected a frameshift deletion (c.3825_3838del: p.Ser1276Alafs*9) in an Iranian child with typical features of KNO1 (Haghighi *et al.* 2014). But none of them reported about low sweating, pain insensitivity, bleeding on wound, and recovery of cutis aplasia as mentioned in the current study due to identified mutation in exon 39. Majority of mutations cause KNO1, lie in exons 30-exon 42 (Suzuki *et al.* 2009; Joyce *et al.* 2010).

In the current study, a homozygous frameshift mutation identified in a large Pakistani family with 26 affected subjects. The same mutation reported in an Irish girl in compound heterozygosity, previously. The mutation is very rare (0.00046) in South Asian samples of ExAC, which includes many Pakistanis, but more frequent in Europeans, Finns and East Asians (>0.001). Thus, it is intriguing why the mutation is so rare in KNO1 patients. In contrary to all these, the presented study identified a homozygous 2 base pair deletion in exon 41 with unusual combination of ocular and skeletal abnormalities.

As the studied family had a large number of affected members. The combination of eye anomalies (retinal detachment, nystagmus, strabismus, myopia, and cataracts), neurological symptoms (encephalocele, seizures, cerebellar hypoplasia and intellectual disability), and cardiovascular symptoms have been reported in muscular dystrophy-dystroglycanopathy (MIM 253800). This condition however, also shows respiratory insufficiency, progressive contractures, muscular dystrophy, hypotonia, and these known to cause by *FKTN*. Rare involvement of encelphlocele

and retinal degeneration has also been observed in Joubert syndrome (MIM 615636) which is primarily characaterized by delayed psychomotor development, hypotonia, abnormal respiratory patterns in the neonatal period, oculomotor apraxia, and cerebellar ataxia, and is caused by mutations in *CSPP1*.

A characteristic feature of Knobloch syndrome is severe form of high myopia and encephalocele (Passos-Bueno *et al.* 1994). In the present family high myopia was evident in ten of the eleven studied subjects (Table 6.1). Most of the subjects also had other eye abnormalities like chorio-retinal degeneration, lens detachment, nystagmus, complex cataract and squint eyes (Table 6.1). The degenerative changes in the eye are usually progressive and lead to blindness. One of the affected subjects and two deceased individuals in the present family had developed complete blindness (Table 6.1). Progressive intellectual disability was observed in two of the subjects. However, most of the patients with KNO1 were reported to have normal intelligence (Seaver *et al.* 1993; Aldahmesh *et al.* 2013). In addition to the typical features of KNO1, the affected subjects in the present family also exhibited certain other unusual features like low sweating, slow bleeding in wounds, low sensitivity to pain, abnormal skin pigmentation. A characteristic observation was anterior chest wall defect characterized by barrel-shaped chest and mild prominence of the rib cartilage, yet a clear pectus carinatum was not evident (Table 6.3) The subjects could perform their routine jobs complained of early fatigue, which could be secondary to chest wall abnormalities. Chest wall deformities frequently are associated with systemic weakness of the connective tissues and with poor muscular development of the abdominal region and thorax (Obermeyer & Goretsky 2012). Ultra-sonographic examination of vital organs of one of the affected subjects was, however, unremarkable. The presence of skeletal and dermatological symptoms in the present family further delineate KNO1 from the above-mentioned overlapping conditions. With inclusion of this family, only two Pakistani families have been reported with KNO1 but both families were more severely affected than other reported families (Table 6.3). However, none of the family reported about low sweating, slow bleeding in wounds, low sensitivity to pain, abnormal skin pigmentation as presented in this family (Table 6.3)

Table 6.4: Phenotypic comparison of different reported families with current family.

References	(Czeizel *et al.* 1992)	(Sertie *et al.* 1996)	(Menzel *et al.* 2004)	(Keren *et al.* 2007)	(Mahajan *et al.* 2010)	(Aldahmesh *et al.* 2013)	(Caglayan *et al.* 2014)	(Paisán-Ruiz *et al.* 2009)	(Joyce *et al.* 2010)	**Current study, 2020**
Family origin	Hu	Bra	NZ	Alg	Sal	SA	Tur	Ind	Pak	Pak
Eye										
High myopia	+	+	+	+	+	+	+	-	+	+
Vitreo-retinal degeneration	-	-	+	+	-	+	-	-	+	+
Chorio-retinal atrophy	-	-	-	-	+	-	-	+	+	-
Paramacular retinal colobomas	-	-	-	+	-	-	-	-	-	-
Retinal detachment	+	-	+	+	-	+	-	-	-	+
Cataract	-	-	-	-	-	+	-	-	+	-
Ectopia lentis/ lens dislocation	-	-	-	-	-	+	-	+	+	+
Nystagmus	-	-	-	+	+	-	-	-	+	-
Night Blindness	-	-	-	-	-	-	-	-	+	-
Complete Blindness	-	-	-	+	-	-	-	-	+	+
Glaucoma	-	-	-	-	-	-	-	+	+	-
Phthisis bulbi	-	-	-	-	-	-	-	-	+	-
Choroidal sclerosis	-	-	-	-	-	-	-	-	+	-
Skin										
Cutis aplasia	-	-	-	-	-	-	-	-	+	+
Alopecia	-	-	-	-	+	-	-	-	-	-
Unusual palmar crease	+	-	-	-	-	-	-	-	-	-
Pigmentary dispersion	-	-	-	-	-	-	-	-	+	-
Skull										
Occipital encephalocele	+	+	+	+	+	+	-	-	+	+
Neurological defects	-	-	-	-	+	-	-	+	-	-
Occipital scalp defect	-	+	-	-	-	-	-	-	-	-
Large forehead	-	-	-	+	-	-	-	-	-	-
Compromised intelligence	-	-	-	+	-	-	-	+	-	-
Features not reported earlier										
Recovering cutis aplasia	-	-	-	-	-	-	-	-	-	+

Bleeding on wound	-	-	-	-	-	-	-	-	-	+
Low Sweating	-	-	-	-	-	-	-	-	-	+
Pain Insensitivity	-	-	-	-	-	-	-	-	-	+
Concordance	4/26	3/26	4/26	9/26	6/26	6/26	1/26	5/26	14/26	11/26

+, features present; -, features absent; Hu, Hungry; Bra, Brazil; NZ, New Zealand; Alg, Algeria; Sal, El Salvadorian; SA, South Africa; Tur, Turkey; Ind, India; Pak, Pakistan

The reported study presented unusual combination of skeletal abnormalities apart from primary features of Knobloch syndrome in large Pakistani kindred with 26 affected subjects. The novel features were chest abnormalities, low sweating, slow bleeding in wounds, low sensitivity to pain, and abnormal skin pigmentation. The study findings enhance the clinical spectrum of the investigated phenotype and these may be helpful to develop the genotype-phenotype correlation.

CHAPTER 7

FAMILY V

Chapter 7. Homozygous variant c.2861_2862del (p.K939Rfs*38) in *PRG4* further delineates the phenotypic spectrum in Camptodactyly-arthropathy-coxa vara-pericarditis syndrome

7.1: Abstract

Camtodactyly arthropathy coxa-vara pericarditis (CACP; MIM 208250) syndrome is congenital autosomal recessive phenotype with lack of lubricin proteoglycan 4 due to mutations in *PRG4* gene in which, at least, 98 different mutations have been reported to cause CACP syndrome. Although CACP is, a rare genetic disorder but several cases described from different ethnic populations like Korean, Chinese, Pakistan, Indian, Saudi Arabian, Egyptian, Caucasian and Europeans. This study was aimed to report a homozygous frameshift mutation in *PRG4* causing CACP syndrome in large Pakistani kindred with unreported clinically features. A large consanguineous family was studied with 12 affected subjects which were showing camptodactyly, arthropathy of joints, coxa-vara, and cardiac defects, the primary features of CACP. More importantly, some patients born with brachydactyly and small nails, which have never been reported in any previously described case of CACP. Exome analysis revealed homozygous deletion c.2861_2862del (p.Lys939Argfs*38) in coding region of *PRG4* as causative reason. Conclusively, the study described the expanded clinical spectrum of CACP syndrome in a large consanguineous family. The newly reported clinical features were brachydactyly and small nails. The study results might be helpful to establish genotype-phenotype correlation of the CACP.

7.2: Introduction

Proteoglycans (PRGs) are conjugated macromolecules of proteins and carbohydrates, which are ubiquitous components of extracellular matrix and surfaces of cells. The PRGs have multiple functions that depend on both their protein and carbohydrate constituents (Hardingham 2006). PRGs consist of protein core to which glycosaminoglycans (generally called mucopolysaccharides) of four different types like dermatan sulfate, heparin sulfate, keratin sulfate, and chondroitin sulfate. These molecules cleaved from protein core in lysosomes and then they catabolized further in lysosomes by involvement of several enzymes. Any defect in the enzymes results in different inherited disorders due to accumulation of metabolites in the lysosomes (Pyeritz 2012; Shapiro 2016).

Proteoglycan 4 (PRG4) is a chondroitin sulfate molecule found in synovial fluid that protect joints, cartilage and prevent synoviocyte overgrowth, thereby protecting the specialized acellular layer of the cartilage within the joint and any defect in PRG4 results in joints arthropathy (Jay *et al.* 2007; Jun *et al.* 2016; Thorson *et al.* 2019). Articular cartilage (to which chondrocytes are located and synthesize PRGs) is an important of the musculoskeletal system that absorbs compressive and share forces during joint movements. Therefore, dysregulation of tissues and cellular PRG4-related pathways in cartilage contributes to the age related diseases of several tissues with inclusion of bone and muscle but responsible reasons for their failure in aging need to discover (Sandri *et al.* 2004; Rached *et al.* 2010; Basit *et al.* 2011; Matsuzaki *et al.* 2018). Additionally, the PRG4 act as anti-adhesive between heart and parietal pericardium (Peters *et al.* 2016).

PRG4 gene encodes PRG4 protein and is expressed in joints, pericardial membrane, kidney, liver, and skeletal muscles (Mannurita *et al.* 2014). There are at least 98 different mutations that result in altered expression of *PRG4* and are implicated in camptodactyly–arthropathy–coxa vara–pericarditis (CACP) (Johnson *et al.* 2020).

CACP (MIM 208250) is a rare familial autosomal recessive syndromic arthropathy of childhood due to lack of glycoprotein lubricin (PRG4). Primarily, CACP

characterized by congenital or early onset of camptodactyly, noninflammatary arthropathy, synovial hyperplasia, progressive coxa vera deformity, and noninflammatary pericardial effusions (Faivre *et al.* 2000). More comprehensively, occurrence of familial cases is 64% and frequency of consanguinity is 82%. The diagnostic age ranged from 1-52 years, camptodactyly is first diagnostic feature in 68% of cases, pericarditis is evident in 30% of CACP's patients (Nadeem *et al.* 2018). Moreover, swelling of wrists, elbows, and knees begin before age of 4 years, age of joint involvement is variable, high level of pain noted above age of 10 years, and hip involvement is noted above 20 years of age. This indicates there is significant involvement between age and the number of clinical feature (Yilmaz *et al.* 2018).

Secondary features include pain, spinal abnormalities like kyphosis, scoliosis and lordosis, arhtropathy of lumbo-sacral spine, non-inflammatory synovial fluid, synovial hyperplasia, hepatomegaly, limited extension and flexion of wrist joints, bilateral flexion deformity of proximal interphalangeal joints (PIJ) and peri-articular thickening and thickened synovium. Additionally, hip dysplasia, accumulation of intra articular fluid and synovial hyperplasia, flexion deformity of fingers and toes, osteoporosis, coxa-vara, short femoral neck, enlarged femoral head, epiphyseal deformation, increased joints spaces and the smaller iliac wings (Mannurita *et al.* 2014; Nandagopalan *et al.* 2014; Peters *et al.* 2016). The recognition of CACP could be difficult not only because of its wide clinical variability but also because of its clinical resemblance to juvenile idiopathic arthritis (Peters *et al.* 2016).

This study was aimed to report the clinical spectrum of CACP in large familial Pakistani kindred due to mutation in exon 6 of *PRG4* gene. The clinical spectrum included camptodactyly, non-inflammatory arthropathy of joint, coxa-vara, pericarditis, pain in joints, low angular and limited movements, small nails and brachydactyly.

7.3: Subjects and methods

The family originates from remote area of Punjab, Pakistan. Five generation pedigree strongly illustrates the autosomal recessive inheritance pattern of the trait in the family. Fifteen subjects (9 males and 6 females) were physically examined with the help of local physician. Among examined subjects, 5 males were afflicted with CACP syndrome. During the physical and medical examination, photographs and roentgenograms were taken and whole peripheral blood was drawn from both affected and normal subjects (12 subjects) for genetic study. All materials were obtained after taking informed and written consent. In order to find the causative gene, exome sequencing was performed for patient 401. The Agilent SureSelect Target Enrichment System was used for exome capturing and the Illumina HiSeq2000 platform for sequencing. Exome file was analyzed to search for the candidate causative mutation. Detailed process is explained in Chapter 4.

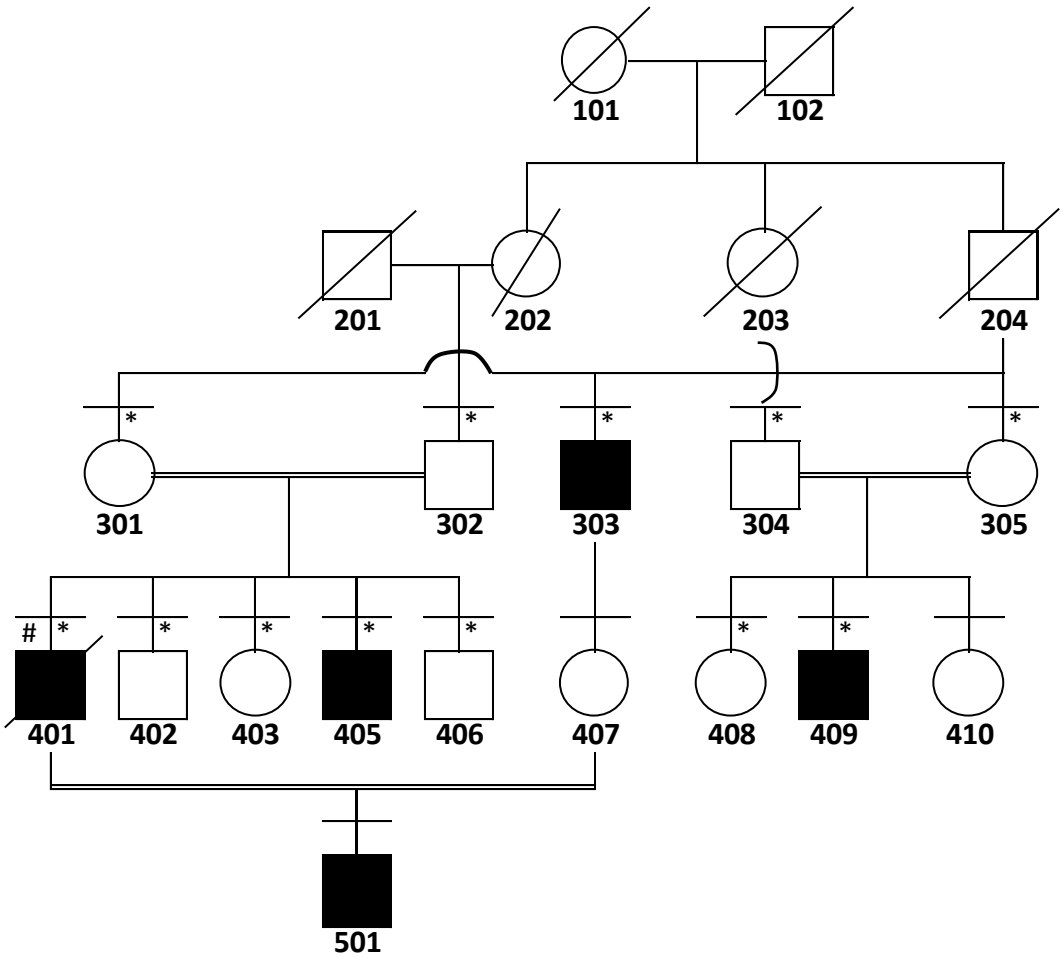

Figure 7.1: Five generations consanguineous Pakistani family pedigree in which CACP segregates. Individual with horizontal line above the symbol were physically examined, *: participated in genetic study, #: exome sequence.

7.4: Results

7.4.1: Clinical Report

Among fifteen physically observed subjects, 10 were unaffected and have no skeletal or limbs malformations. All the five patients (303, 401, 405, 409, and 501) had bilateral symmetrical skeletal defects, which preliminary affect the joints and autopods of upper and lower limbs. All the affected individuals had camptodactyly in hands/feet, arthropathy of large joints, small nails, scoliosis and brachydactyly in some members.

Limbs and large joints were the most affected parts of the body. Primary features were camptodactyly in hands/feet and arthropathy of large joints including wrist, elbow, hip, knee and ankle joints (Table 7.1). The secondary features were hallux valgus, wide space between first and second toe, morning stiffness of joints, early fatigue, cardiac and liver problems (303), depressed and barrel shape chest, swollen knee joints making sitting complicated due to the synovial fluid (405), scoliosis (405, 409). Death of the subject (401) occurred due to cardiac defects (Table 7.2).

Table 7.1: Primary features of CACP syndrome in affected subjects.

Patient ID	**303**	**401**	**405**	**409**	**501**	**Concordance (%)**
Sex, age (years)	M, 61	M, 30	M, 11	M, 26	M, 2	-
Onset	Prog.	Prog.	Prog.	Prog.	Prog.	-
Disease age on set (years)	2	1	1	1	1	-
Parental consanguinity	-	+	+	+	+	-
Primary Features						
Camptodactyly						
Hands						
index finger	+	+	+	+	-	4/5 (80%)
middle finger	+	+	+	+	-	4/5 (80%)
ring finger	+	+	+	+	-	4/5 (80%)
little finger	+	+	+	+	+	5/5 (100%)
Feet						
second toe	+	-	+	+	-	3/5 (60%)
third toe	+	+	+	+	-	4/5 (80%)
fourth toe	-	+	+	+	-	3/5 (60%)
fifth toe	-	-	+	+	-	2/5 (40%)
Arthropathy of large joints						
Wrist	+	+	+	+	+	5/5 (100%)
Elbow	+	+	+	+	-	4/5 (80%)
Hips	+	+	+	+	-	4/5 (80%)
Knees	+	+	+	+	-	4/5 (80%)
Ankle	+	+	+	+	-	4/5 (80%)
Joints complications						
Enlarged elbow	+	+	+	+	-	4/5 (80%)
Enlarged knee	+	+	+	+	-	4/5 (80%)

Pivot joint problem	+	+	+	+	-	4/5 (80%)
Joints effusion in early onset of disease	+	+	+	+	-	4/5 (80%)

+, features present; -, features absent; prog, progressive

Table 7.2: Secondary features of CACP syndrome in the affected subjects

Patient ID	**303**	**401**	**405**	**409**	**501**	**Concordance (%)**
Sex, age (years)	M, 61	M, 30	M, 11	M, 26	M, 2	-
Disease age on set (years)	2	1	1	1	1	-
Parental consanguinity	-	+	+	+	+	-
Secondary Features						
Hallux valgus	-	+	-	+	-	2/5 (40%)
Early fatigue	+	-	+	+	-	3/5 (60%)
Morning stiffness of joints	+	-	+	+	-	3/5 (60%)
Scoliosis	-	-	+	+	-	2/5 (40%)
Wide-space between 1-2 toes	+	+	-	+	-	3/5 (60%)
Joint pain	-	-	+	-	-	1/5 (20%)
Barrel shape chest	-	-	+	+	N/A	2/5 (40%)
Small nails	-	N/A	+	+	-	2/5 (40%)
Cardiac defects/ Pericarditis	+	N/A	N/A	N/A	N/A	1/5 (20%)
Swelling of joints	-	-	+	-	-	1/5 (20%)
Brachydactyly, 5th fingers	+	-	-	-	-	1/5 (20%)
Brachydactyly in feet	+	-	-	-	-	1/5 (20%)

+: features present, -: features absent, N/A, not accessed

All the individuals were having normal intellectual level. The detailed clinical reports of three patients (303, 405, 409) given below.

7.4.2: Index Subject 303

Patient reported onset of disease at age of two years. Clinical symptoms included camptodactyly in 2^{nd}-5^{th} fingers, brachydactyly in 5^{th} little finger. In feet, features were camptodactyly of 2^{nd} and 3^{rd} toes and brachydactyly in 4^{th} toe. Arthropathy of large joints included wrist, elbow, hip, knee and ankle. He had enlarged elbow and knee joints with increased joint spaces. Due to arthropathy of these joints, he was having limited flexion, extension, abduction and adduction. He had walking difficulty, which suspects the coxa-vara in this subject (no radiographic data), stiffness of joints in early morning, and small nails. He also had cardiac defect, and early exhaustiveness (Tables 7.1-7.2).

Echocardiography revealed rheumatic heart disease, moderate to severe aortic stenosis, mild to moderate aortic regurgitation, rheumatic calcified mitral valve with severe mitral stenosis, mild mitral regurgitation, mild tricuspid regurgitation, mild pulmonary hypertrophy, and concentric left ventricular hypertrophy. Good biventricular systolic function. Pericardium was normal (Figure. 7.2a-c)

Coronary arteriography of left coronary artery of main stem revealed bifurcating vessel with minor irregularities. Left anterior descending artery was good size vessel with mild disease in mid part. Left circumflex artery was non-dominant vessel with moderately severe disease just after first obtuse marginal branch. First obtuse marginal branch is fair sized vessel with moderate proximal disease. Right coronary artery was dominant vessel with mild disease in mid part. In left ventricle calcified mitral and aortic valve was observed. Ultrasonography of abdomen illustrates coarse liver echotexture parenchyma echogenicity (Fig. 7.2d).

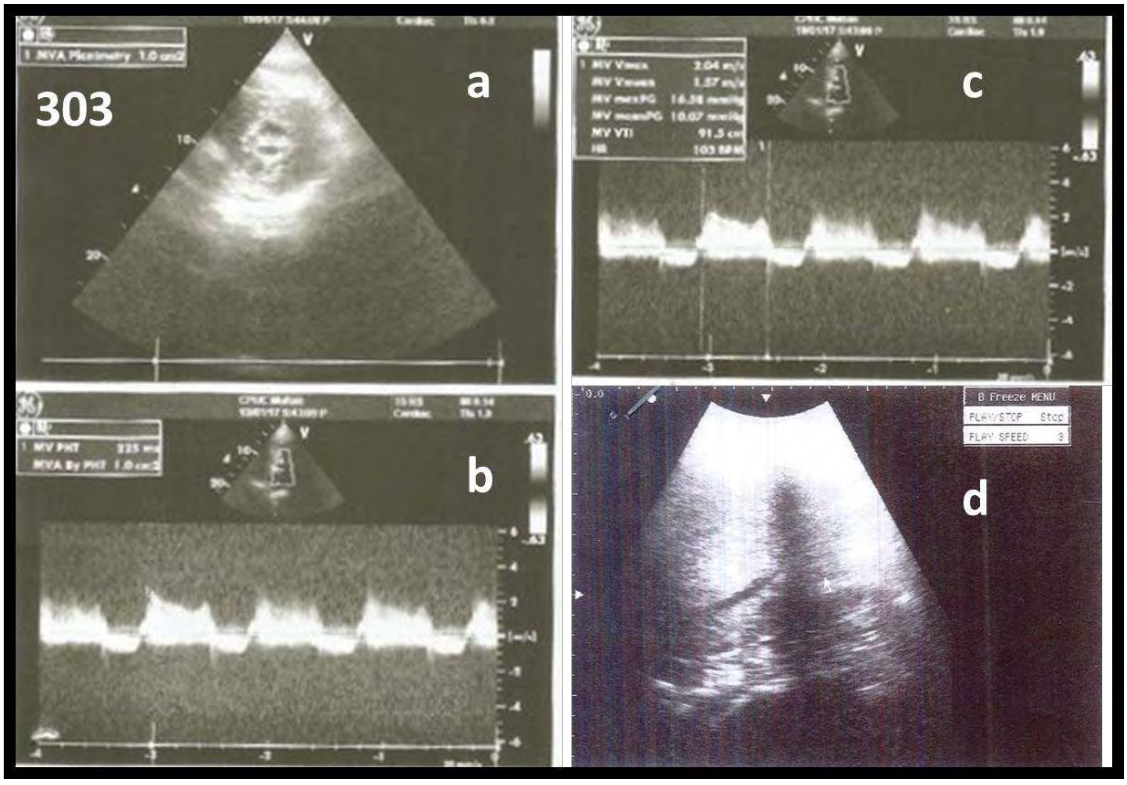

Figure 7.2: Echocardiography of subject 303 (a-c) depicting cardiac defects and ultrasonography of liver depicting liver echotexture parenchyma echogenicity (d).

7.4.3: Subject 405

Patient had bilateral camptodactyly in 2nd-to-5th fingers & in 2nd-to-5th toes, severe arthropathy of wrist, elbow, hip, knee and ankle joints, scoliosis, enlarged elbow and knee joints, increased inter joint space, swollen knee joints due to accumulation of fluid. Morning stiffness of joints, early fatigue, small nails were also observed. Depressed and Barrel shape chest was also observed (Fig. 7.3a). Ultrasonography of knee joints revealed extra articular fluid and fluid was more in left knee as compare to right (Fig. 7.3g). Ultrasound of vital organs was unremarkable (7.3h).

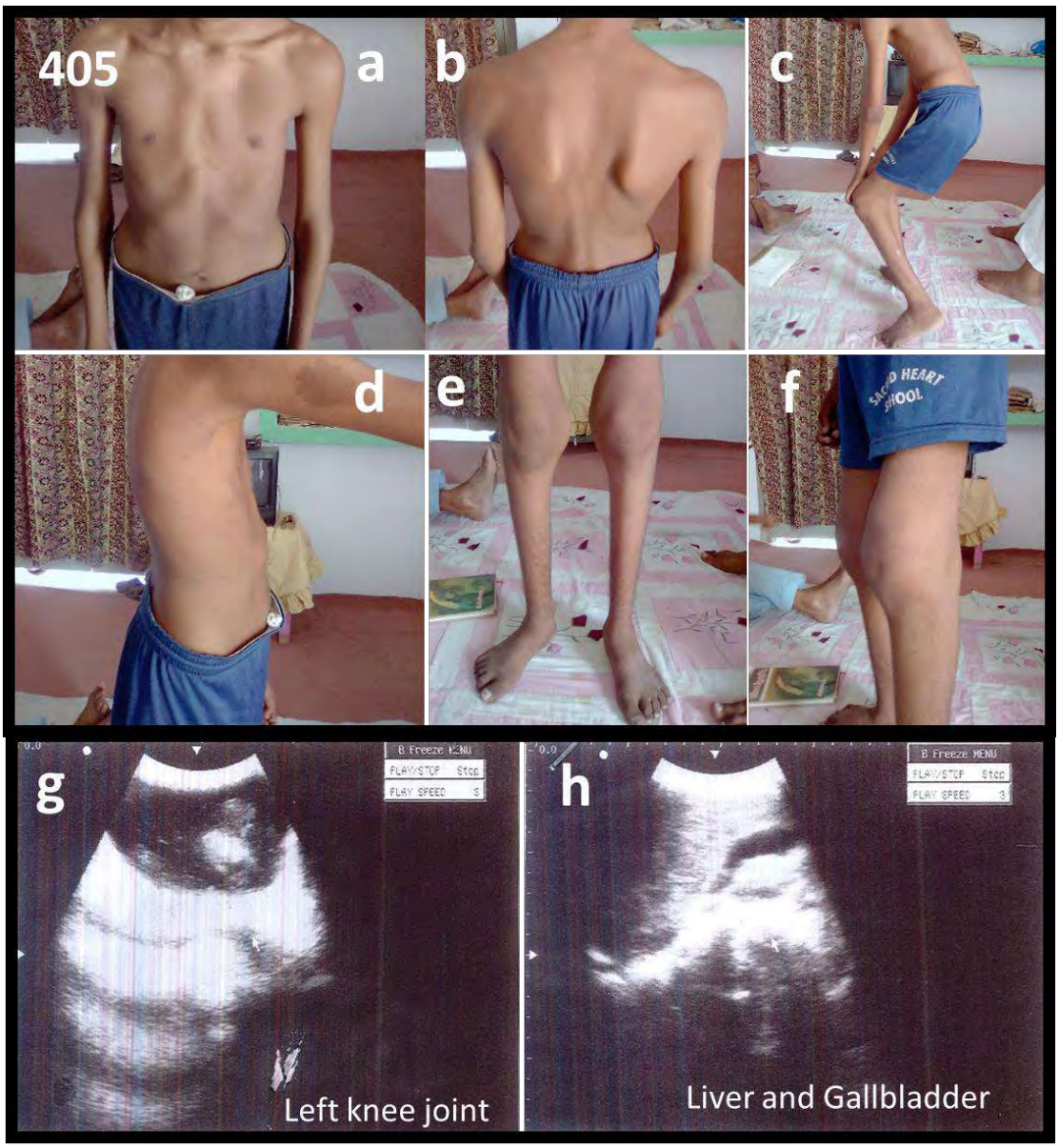

Figure 7.3: Morphological defects in subject 405. Depressed barrel shape chest (a), scoliosis (b), maximum bending position of knee (c), lateral view of chest (d), enlarged knee joints with synovial fluid frontal and lateral view (e, f), ultrasound of left knee joint (g) and liver and gallbladder (h).

7.4.3: Subject 409

Patient had bilateral camptodactyly in 1st-to-5th fingers, hallux valgus, camptodactyly in 2nd-to-4th toes, wide space between 1st and 2nd toe, arthropathy of large

joints (wrist, elbow, hip, knee and ankle), enlarged elbow and knee joints, small nails, joint stiffness in early morning, barrel shaped chest, and early exhaustiveness (Table 7.1-7.2).

Radiographs of upper limbs revealed ankyloses of proximo-distal phalangeal joints, ankyloses & osteopenia of elbow joints, narrow space between radius and ulna, anklylosis of toes joints, hallux valgus, thin & posteriorly dislocated fibulae, narrow space between tibia and fibula and osteopenic enlarged knee with increased joint space. Radiographs of pelvic girdle revealed coxa-vara, irregular femoral head, very small femoral neck, broad iliac wings, fused sacroiliac joint, unequal obturator foramen and diastasis symphysis pubis. Thorax scoliosis was also evident in roentgenograms (Fig. 7.4).

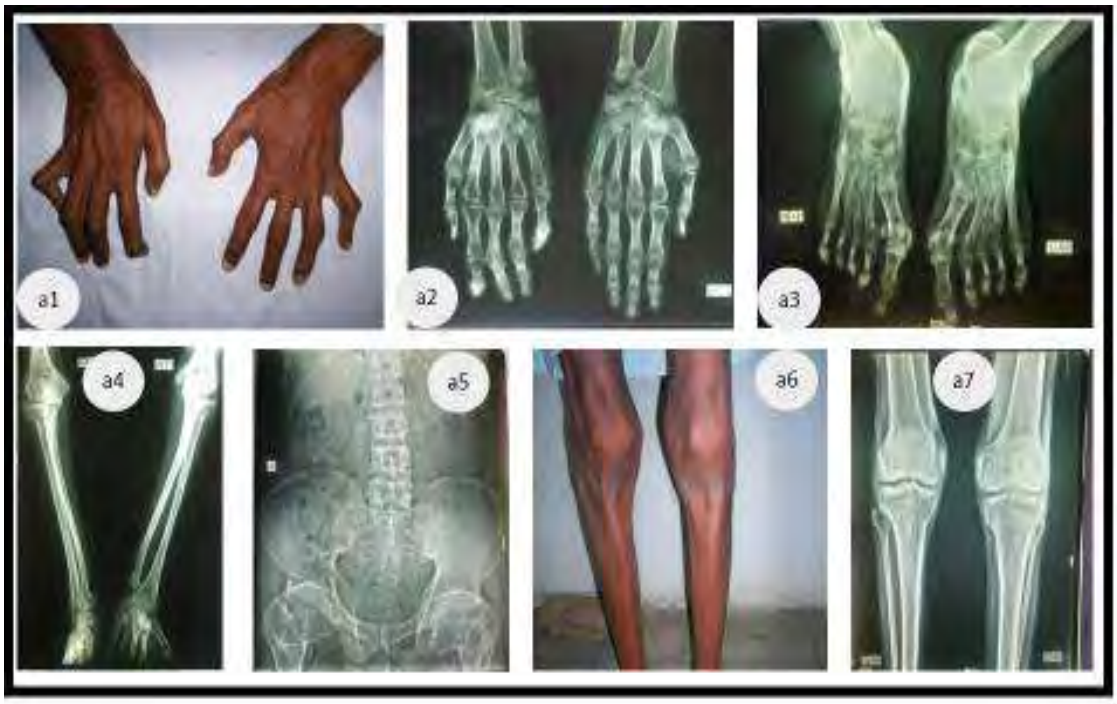

Figure 7.4: Radiographic features in affected subjects 409. Camptodactyly in hands (a), x-rays of hands depicting arthropathy of joints (a2), x-rays of feet depicting arthropathy of joints (a3), x-rays depicting arthropathy of elbow and wrist joints (a4), x-ray of spine and pelvis region clearly depicting the scoliosis and coxa vara (a5) and enlarged knee joints with arthropathy (a6-7).

7.4.4: Molecular Report

Overall, exome sequencing captured 23723 exonic variants > 12156 nonsynonymous variants > 4667 homozygous variants > 124 variants with less than 0.001 frequency in 1000G > 96 variants with less than 0.001 frequency in ExAC and ESP6500 > 26 variants left and was searched for candidate variant from literature > 1 candidate variant (*PRG4* on chromosome 1). The coordinates of identified mutation were *PRG4*:NM_005807:c.2814_2815del:p.T938fs was identified in exon 7. Exome analysis filtration strategy is given in figure 7.5 and the results of exome analysis are presented in (Table 7.3). The region is not much conserved across species and conservation across species is shown in figure 7.6.

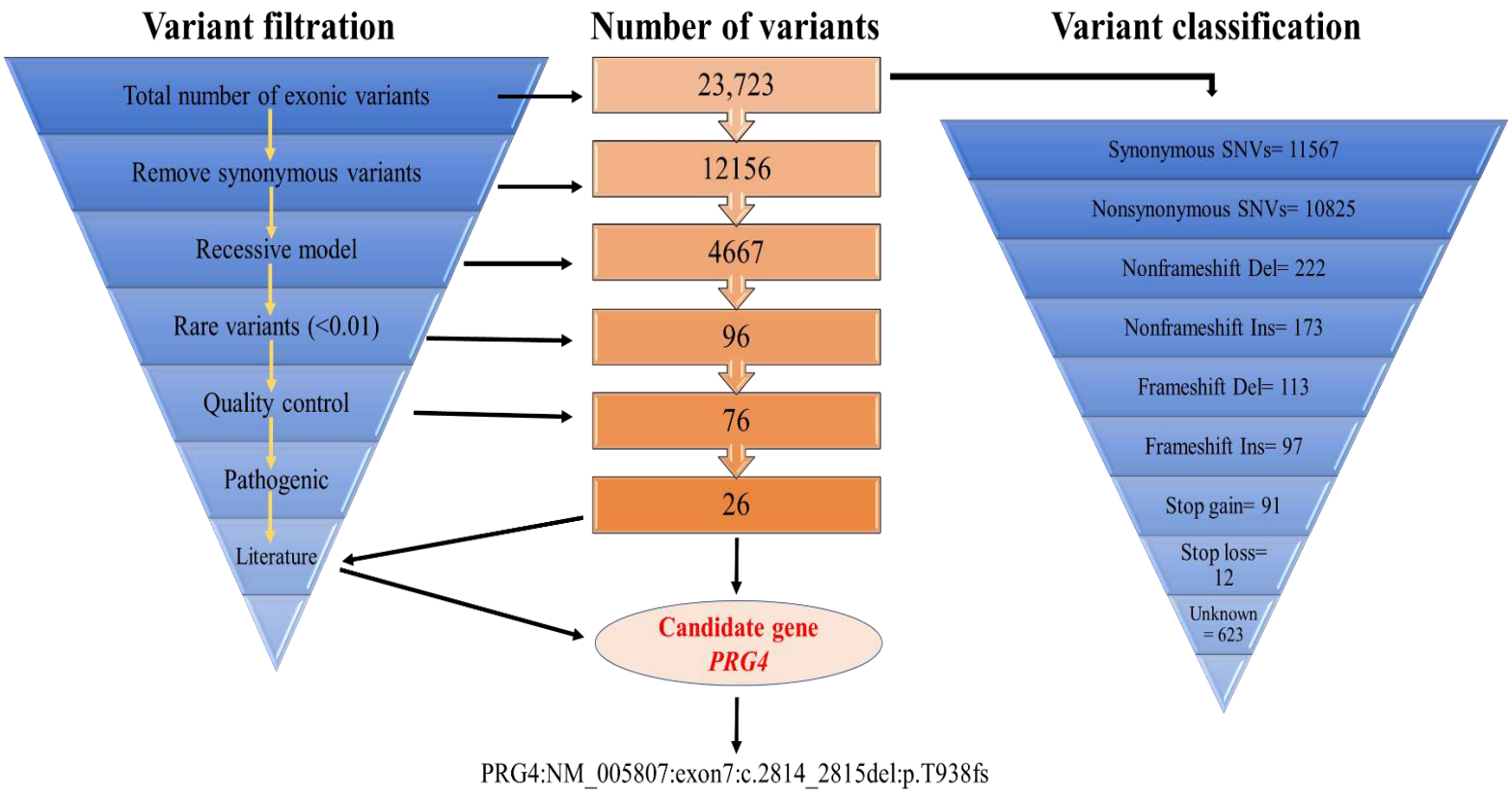

Figure 7.5. Summary of exome filtration scheme

Table 7.3: Exome sequence analysis revealed following list of rare candidate variants

Chr	Start	End	Ref	Alt	Func.refgene	Gene.refgene	ExonicFunc.refgene	AAChange.refgene	1000G_ALL
chr10	135438960	135438960	C	-	exonic	FRG2B	frameshift deletion	FRG2B:NM_001080998:exon4:c.480delG:p.R160fs	.
chr2	3743368	3743368	C	-	exonic	ALLC	frameshift deletion	ALLC:NM_018436:exon8:c.573delC:p.D191fs	0.0014
chr17	15930797	15930801	AAAGA	-	exonic	TTC19	frameshift deletion	TTC19:NM_001271420:exon10:c.783_787del:p.S261fs,TTC19:NM_017775:exon10:c.1104_1108del:p.S368fs	.
chr1	152284606	152284607	TG	-	exonic	FLG	frameshift deletion	FLG:NM_002016:exon3:c.2755_2756del:p.H919fs	.
chr4	103822483	103822484	AC	-	exonic	SLC9B1	frameshift deletion	SLC9B1:NM_139173:exon12:c.1338_1339del:p.V446fs	.
chr22	36902463	36902463	G	-	exonic	FOXRED2	frameshift deletion	FOXRED2:NM_001102371:exon2:c.7delC:p.L3fs,FOXRED2:NM_024955:exon2:c.7delC:p.L3fs	.
chr1	47685575	47685575	T	-	exonic	TAL1	frameshift deletion	TAL1:NM_001290406:exon3:c.336delA:p.G112fs,TAL1:NM_001287347:exon5:c.813delA:p.G271fs,TAL1:NM_001290403:exon5:c.813delA:p.G271fs,TAL1:NM_001290405:exon5:c.813delA:p.G271fs,TAL1:NM_001290404:exon6:c.813delA:p.G271fs,TAL1:NM_003189:exon6:c.813delA:p.G271fs	.
chr1	**186277665**	**186277666**	**AA**	**-**	**exonic**	**PRG4**	**frameshift deletion**	**PRG4:NM_001127710:exon4:c.2412_2413del:p.T804fs,PRG4:NM_001127709:exon5:c.2535_2536del:p.T845fs,PRG4:NM_001127708:exon6:c.2691_2692del:p.T897fs,PRG4:NM_001303232:exon6:c.2685_2686del:p.T895fs,PRG4:NM_005807:exon7:c.2814_2815del:p.T938fs**	.
chr2	133075479	133075479	C	-	exonic	ZNF806	frameshift deletion	ZNF806:NM_001304449:exon4:c.940delC:p.P314fs	.
chr2	133076118	133076118	A	-	exonic	ZNF806	frameshift deletion	ZNF806:NM_001304449:exon4:c.1579delA:p.N527fs	.
chr7	95125067	95125070	CAGG	-	exonic	ASB4	frameshift deletion	ASB4:NM_016116:exon2:c.188_188del:p.G63fs,ASB4:NM_145872:exon2:c.188_188del:p.G63	.

chr9	33797931	33797932	AC	-	exonic	PRSS3	frameshift deletion	fs PRSS3:NM_001197098:exon3:c.284_285del:p.D95fs,PRSS3:NM_002771:exon3:c.305_306del:p.D102fs,PRSS3:NM_007343:exon3:c.476_477del:p.D159fs,PRSS3:NM_001197097:exon4:c.347_348del:p.D116fs	.
chr9	43121655	43121658	TAAG	-	exonic	ANKRD20A2	frameshift deletion	ANKRD20A3:NM_001012419:exon6:c.775_778del:p.L259fs,ANKRD20A2:NM_001012421:exon6:c.775_778del:p.L259fs	.
chr11	55111372	55111372	T	-	exonic	OR4A16	frameshift deletion	OR4A16:NM_001005274:exon1:c.696delT:p.H232fs	.
chr11	59245732	59245733	TC	-	exonic	OR4D10	frameshift deletion	OR4D10:NM_001004705:exon1:c.830_831del:p.V277fs	.
chr11	59245746	59245747	CT	-	exonic	OR4D10	frameshift deletion	OR4D10:NM_001004705:exon1:c.844_845del:p.L282fs	.
chr13	25671273	25671273	G	-	exonic	PABPC3	frameshift deletion	PABPC3:NM_030979:exon1:c.937delG:p.A313fs	.
chr13	25671311	25671315	TATGA	-	exonic	PABPC3	frameshift deletion	PABPC3:NM_030979:exon1:c.975_979del:p.V325fs	.
chr13	25671333	25671333	A	-	exonic	PABPC3	frameshift deletion	PABPC3:NM_030979:exon1:c.997delA:p.K333fs	.
chr16	90030652	90030652	C	-	exonic	DEF8	frameshift deletion	DEF8:NM_001242817:exon10:c.897delC:p.G299fs,DEF8:NM_001242819:exon10:c.1026delC:p.G342fs,DEF8:NM_001242816:exon11:c.1047delC:p.G349fs,DEF8:NM_001242818:exon11:c.1077delC:p.G359fs,DEF8:NM_207514:exon11:c.1260delC:p.G420fs,DEF8:NM_001242820:exon12:c.1077delC:p.G359fs	.
chr16	90030657	90030669	TGGGCTGCTCGCT	-	exonic	DEF8	frameshift deletion	DEF8:NM_001242817:exon10:c.902_914del:p.L301fs,DEF8:NM_001242819:exon10:c.1031_1043del:p.L344fs,DEF8:NM_001242816:exon11:c.1052_1064del:p.L351fs,DEF8:NM_001242818:exon11:c.1082_1094del:p.L361fs,DEF8:NM_207514:exon11:c.1265_1277del:p.L422fs,DEF8:NM_001242820:exon12:c.1082_1094del:p.L361fs	.

chr18	72997849	72997850	TG	-	exonic	TSHZ1	frameshift deletion	TSHZ1:NM_001308210:exon2:c.487_488del:p.C163fs,TSHZ1:NM_005786:exon2:c.352_353del:p.C118fs	.
chr19	36212118	36212119	AG	-	exonic	KMT2B	frameshift deletion	KMT2B:NM_014727:exon3:c.1869_1870del:p.P623fs	.
chr21	41414583	41414596	TGCTGCTTCTTGCT	-	exonic	DSCAM	frameshift deletion	DSCAM:NM_001271534:exon32:c.5388_5401del:p.R1796fs,DSCAM:NM_001389:exon32:c.5388_5401del:p.R1796fs	.

Species	Amino acid sequence											
Mutated H. sapiens	A	A	P	K	M	T	R	D	S	N	Y	N
H. Sapiens	A	A	P	K	M	T	K	E	T	A	T	T
P. troglodytes	A	A	P	K	M	T	K	E	T	A	T	T
G. beringei	A	A	P	K	M	T	K	E	T	A	T	T
Hylobatidae	A	A	P	K	M	T	K	E	T	A	T	T
M. mulatta	V	A	P	K	M	T	K	E	T	A	T	T
M. musculus	-	-	P	K	P	T	K	K	P	T	K	A
G. gallus	L	E	A	-	-	-	-	-	-	-	-	-
X. tropicalis	P	A	D	E	-	S	G	D	D	G	T	S

Figure 7.6. Amino acids conservation across species

7.5: Discussion

CACP syndrome is a rare AR condition caused by mutations in *PRG4* gene. The gene is present on chromosome 1q25-q31 and have 12 exons. PRG4 encodes glycoprotein "lubricin" and is responsible for the lubrication of synovial joints. It is also present in pericardium and may be responsible for the involvement of pericardium in CACP syndrome (Alazami *et al.* 2006).

Primarily, CACP characterized by congenital or early onset of camptodactyly, noninflammatory arthropathy, synovial hyperplasia, progressive coxa vera deformity, and noninflammatory pericardial effusions (Faivre *et al.* 2000). Camptodactyly is the first symptoms to be appear with bilateral and progressive in nature. It is present about 70% of the patients (Bulutlar *et al.* 1986). Arthropathy involves mainly large joints like knee, wrist, ankle and hip in bilateral and symmetrical pattern with no inflammatory signs. Coxa-vara is observed in 50-90% of cases (Bahabri *et al.* 1998), while non-inflammatory pericarditis is reported in 6-30% of CACP patients (Yilmaz *et al.* 2018).

In coding and non-coding regions of PRG4 gene, different thirty eight mutations reported to cause CACP in almost 98 patients from different populations but mainly among the patients of Arabian origin (Mannurita *et al.* 2014).

The present study was objective to report the extended clinical spectrum of CACP syndrome due to homozygous two base pair deleltion in exon 6 of PRG4 gene in a Pakistani consangeneous family with 5 affected subjects. The identified mutation was already reported in an other Pakistani family (Basit *et al.* 2011) and this is the second Pakistani family affilicted CACP syndrome. The common mutation b/w these two family indicated founder effect that suggest that both family have their common ancestor in the remote past as the same effect has already been reported from Pakistani population but for other phenotypes not for CACP syndrome (Ijaz *et al.* 2019; Muzammal *et al.* 2019).

In that study, they reported only 12 clinical variable (Table 7.3) but in contrary to this, the present study reported 31 different clinical variables (Tables 7.1, 7.2, and 7.3) and extended the clinical spectrum of CACP sndrome. Moreover, clinical features in the family were compared with other six family (Marcelino *et al.* 1999; Basit *et al.* 2011; Albuhairan & Al-Mayouf 2013; Mannurita *et al.* 2014; Nandagopalan *et al.* 2014; Yilmaz

et al. 2018) and this comparison revealed that this is the most severe case of CACP that ever has been described and newely reported features given in table 7.3.

In the current study, congenital cataract was not evedent as reported by Akawi et al. but primary features were common (Akawi *et al.* 2012). But none of the above mentioned and other studies did not report about the brachydactyly, small nails, scoliosis, and barrel shaped chest cavity as mentioned in the current study (Mannurita *et al.* 2014; Patil *et al.* 2016; Albtoush *et al.* 2018; Yilmaz *et al.* 2018; Johnson *et al.* 2020). Addionally, the current study did nor report about the small illiac wings, increase lumber lordosis, jaoints swellings, pleuritis, and intraosseous cyst (Table 7.3).

Table 7.4: Comparison of symptoms of CACP syndrome in the present family with few of the reported studies

References	(Yilmaz *et al.* 2018)	(Nandagopalan *et al.* 2014)	(Mannurita *et al.* 2014)	(Abdulmajeed & Al-Mayouf 2013)	(Marcelino *et al.* 1999)	(Basit *et al.* 2011)	Current study
Comparative morphological, anatomical, and physiological features							
Common features among these families							
Camptodactyly in hands	+	+	+	+	+	+	+
Camptodactyly in feet	+	+	+	+	+	+	+
Arthropathy of wrist Joint	+	+	+	+	+	+	+
Arthropathy of elbow Joint	+	+	+	+	+	+	+
Arthropathy of hips Joint	+	+	+	+	+	+	+
Arthropathy of knees Joint	+	+	+	+	+	+	+
Arthropathy of ankle Joint	+	+	+	+	+	+	+
Coxa vara	+	-	+	+	+	+	+
Short/Absent femoral neck	+	-	-	+	+	+	+
Flattened/irregular femoral heads	+	-	-	+	-	+	+
Increased joint space	-	-	-	+	-	+	+
Pericarditis	+	-	+	+	-	-	?
Joint pain	+	-	-	-	+	+	+
Joints effusion in early onset of disease	-	-	+	-	-	-	+
Osteopenia of elbow joint	-	+	-	+	-	-	+
Osteoporosis of elbow joint	+	-	-	-	+	-	+
Narrow space b/w radius and ulna	-	-	-	-	-	-	+
Osteopenia of knee joint	-	+	-	+	-	-	+
Osteoporosis of knee joints	+	-	-	-	-	-	+
Features not found in the current family							
Small illiac wings	+	-	-	+	-	-	-
Intraosseous cyst	+	-	-	-	-	-	-
Pleural effusion/ Pleuritis	+	-	-	-	-	-	-

Swelling of joints	-	-	-	-	-	-	-
Increased lumbar lordosis	+	-	-	-	-	-	-
Unique Features of the current family							
Broad iliac wings	-	-	-	-	-	-	+
Sacroiliac joint gap	-	-	-	-	-	-	+
Unequal obturator foramen	-	-	-	-	-	-	+
Diastasis symphysis pubis	-	-	-	-	-	-	+
Enlarged knee joints	-	-	-	-	-	-	+
Fibulae dislocated posteriorly	-	-	-	-	-	-	+
Narrow space b/w tibia and fibula	-	-	-	-	-	-	+
Thinning of Fibula	-	-	-	-	-	-	+
Ankyloses of toes	-	-	-	-	-	-	+
Hallux valgus	-	-	-	-	-	-	+
Arthropathy of distal phalangeal joints	-	-	-	-	-	-	+
Brachydactyly in 5th finger	-	-	-	-	-	-	+
Brachydactyly in 4th toe	-	-	-	-	-	-	+
Wide-space between 1-2 toes	-	-	-	-	-	-	+
Scoliosis	-	-	-	-	-	-	+
Enlarged elbow joints	-	-	-	-	-	-	+
Enlarged knee joints	-	-	-	-	-	-	+
Pivot joint problem	-	-	-	-	-	-	+
Morning stiffness of joints	-	-	-	-	-	-	+
Early fatigue	-	-	-	-	-	-	+
Small nails	-	-	-	-	-	-	+
Ankylosis of distal phalangeal joint	-	-	-	-	-	-	+
Ankylosis of proximal phalangeal joint	-	-	-	-	-	-	+
Anklylosis of elbow joint	-	-	-	-	-	-	+
Concordance	**18/48**	**9/48**	**10/48**	**15/48**	**11/48**	**12/48**	**42/48**

The coding sequence, exon 6 account for 68% of the entire coding sequence of *PRG4* gene, suggesting that this exon form the major lubricating domain of lubricin and likely to present study, majority of the reported mutations identified in that part of the *PRG4*. This also indicates that CACP syndrome is mainly due to the complete lack of mucin like proteoglycan 4 protein (Mannurita *et al.* 2014).

Homozygous *PRG4*:NM_005807:c.2861_2862del:p.T938fs is a rare variant with 0.00003 frequency in gnomAD while in 1000G, ExAC and ESP6500si its frequency is not reported. *PRG4* consists of 12 exons and encodes highly conserved sequence of 1404 amino acids in human (Schumacher *et al.* 1999) with molecular weight of ~150kDa for unsubstituted core proteins (Flannery *et al.* 1999). Functional domains of PRG4 protein includes somatomedin B-like domain, chondroitin sulphate attachment site, mucine-like domains and hemopexin-like domain. In the current study, homozygous deletion c.2861_2862del in exon 6 is in mucine-like domain and is predicted to abolish the further protein including part of mucine-like domain and hemopexin-like domain (Basit *et al.* 2011; Mannurita *et al.* 2014). Schematic representation of PRG4 protein domains and reported mutations including this study is given in figure 7.7.

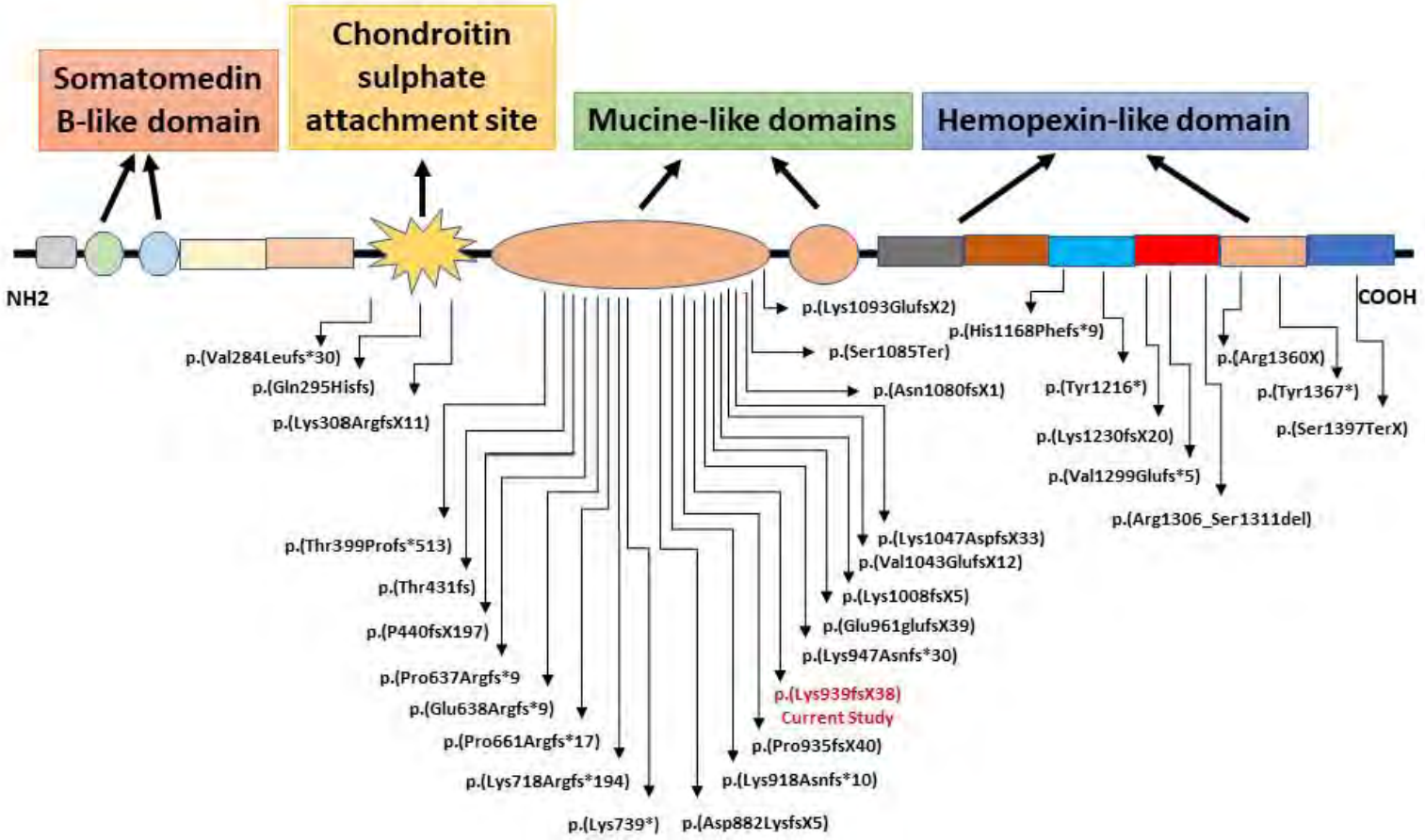

Figure 7.7: Schematic representation of PRG4 protein domains and reported mutations

The current study presented the second report of CACP syndrome as product of founder effect. The study results also extend the clinical spectrum of CACP by reporting new clinical features like brachydactyly, small nails, scoliosis, and barrel shaped chest cavity. This would be useful in establishing the genotype-phenotype correlation. However, further studies require, confirming the occurrence newly reported clinical features related to CACP syndrome.

Conclusion

The present study was conducted to identify the genetic variants in families afflicted with skeletal and ophthalmic disorders. In the current study four families with skeletal and one with ophthalmological disorders underwent detailed clinical and genetic examination. Skeletal and ophthalmological disorders had severe impact on quality of life of affected individuals. Skeletal dysplasias are group of heritable disease group that have impact on cartilage and bone growth. Hereditary ocular diseases cause damage to retina or optic nerve and may result in bilateral and although asymmetric decrease or loss in vision. Due to advancement in genotyping and sequencing technologies, molecular defects underlying many of the inherited diseases can be identified. These identifications led to novel insights in the mechanism regulating cartilage and bone growth.

The purpose of the current study was to describe in details the clinical and genetic aspects of five families afflicted with hereditary skeletal and ophthalmic disorders. Family 1 (Chapter 3), reports a novel autosomal recessive phenotype characterized by bilateral symmetrical limbs and skeletal defects in the affected individuals, was described as Osteo-chondrodysplasia-bracydactyly-malformed-digits (OCBMD; OMIM: 618167) in OMIM, in extended consanguineous Pakistani kindred due to homozygous deletion in *CHST11* gene on chromosomes 12q23.3 (Shabbir et al., 2018).

Family 2 (Chapter 4), there were five affected subjects with an unusual combination of skeletal abnormalities apart from overlapping features of cutis laxa. SNP and exome sequence analysis revealed novel homozygous deletion of exons 1-2 of *PYCR1* and exon 2 of *MYADML2*. Exons deletions were supposed to deduce the synthesis of proteins from both mutated genes. Before this, *MYADML2* has not been

associated with any kind of human phenotype but mutations in *PYCR1* caused autosomal recessive cutis laxa (ARCL). It could be hypothesized that *MYADML2* is involved in maturation and pattern formation of bones. The other unusual feature in the family like cranial asymmetry, joints dislocations, lumber lordosis, and prominent clavicles might be due to anomalous or disproportionate bone growth. In contrary to this, the rare extra transverse creases on fingers could be due to deletion in *PYCR1* that is responsible skin anomalies. The study described the family phenotype of ARCL is attributed due to deletions in *PYCR1* and unusual skeletal malformations are due to deleted exons of *MYADML2* gene.

Family 3 (Chapter 5), in which the affected subjects were afflicted with Laron syndrome (LS) or growth hormone insensitivity syndrome was described. Instead of typical features of Laron syndrome, siblings in the family had the unique features that includes the shallow eye orbits, sparse hairs, blue sclera, large ear, early fatigue during normal activities, muscle weakness, and macrocytic anemia. In the present study, a transversion mutation c.442G>C identified in exon 4 of *GHR* gene was observed to be segregating with the phenotype; this mutation has already been reported and was responsible for the phenotype. Mutation in the receptor sub-domain 2 stops the dimerization and GH-induced receptor rotation. Consequently, GH-GHR-IGF-1 axis is stopped, and inactivation of IGF-1 occurs which ultimately results in growth failure of an individual. Several mutations in *GHR* have been identified to cause dwarfism. This study expands the clinical spectrum of LS and confirm the molecular diagnosis of this rare anomaly.

Family 4 (Chapter 6), with Knobloch syndrome which is characterized by eye abnormalities like chorio-retinal degeneration, lens detachment, nystagmus, complex cataract and squint eyes. The degenerative changes in the eye are usually progressive and lead to blindness. Homozygous c.4054_4055delCT: p.L1352fs in exon 40 is a rare causative detected variant in the family. The study presents unusual combination of skeletal and ectodermal abnormalities apart from primary features of Knobloch syndrome in large Pakistani kindred with 26 affected subjects. The novel features were chest abnormalities, low sweating, slow bleeding in wounds, low sensitivity to pain, and abnormal skin pigmentation. The study findings enhance the clinical spectrum of the investigated phenotype and these may be helpful to develop the genotype-phenotype correlation.

Family 5 (Chapter 7), Pakistani kindred afflicted with camptodactyly arthropathy coxa vara pericarditis (CACP) syndrome has been described in detailed. CACP syndrome is a rare autosomal recessive condition caused by mutations in *PRG4* gene. The gene is present on chromosome 1q25-q31 and have 12 exons. PRG4 encodes glycoprotein "lubricin" and is responsible for the lubrication of synovial joints. It is also present in pericardium and may be responsible for the involvement of pericardium in CACP syndrome. Homozygous c.2861_2862del:p.T938fs is a rare causative variant detected in this family. The identified mutation was already reported in an other Pakistani family and this is the second Pakistani family affilicted CACP syndrome. The common mutation between these two family indicated founder effect that suggest that both family have their common ancestor in the remote past as the same effect has already been reported from Pakistani population but for other phenotypes not for CACP syndrome.

Future directions

Prevailed genetic disorders among individuals bring with the socio-economic burden on families leading towards social security and economic burden on whole nations as whole. Due to poverty and low possibility of complete or partial recovery from genetic disorders the families do not get proper treatment. Disability brings its adverse effects for good as they are not able to get to betterment for themselves or for others as ordinary or no opportunities are accessible like basic healthcare, education and social development. Ministry of Heath may direct health department to carry out the following measures:

- Public awareness should be initiated about close unions and its consequences in the form of hereditary genetic disorders/defects.
- Every citizen should be provided with screening and diagnoses at parental selection at government hospitals through trained geneticists to control future spread of defected gene pool.
- To conduct the research at advanced levels there should be international collaborations to make it possible to establish next generation sequencing (NGS) technologies in the country.

REFERENCES

References

Afzal M., Zaman Q., Kornak U., Mundlos S., Malik S. & Flöttmann R. (2017) Novel splice mutation in LRP4 causes severe type of Cenani-Lenz syndactyly syndrome with oro-facial and skeletal symptoms. *European journal of medical genetics* **60**, 421-5.

Ahmad M., Ul Haque M.F., Ahmad W., Abbas H., Haque S., Krakow D., Rimoin D.L., Lachman R.S. & Cohn D.H. (1998) Distinct, autosomal recessive form of spondyloepimetaphyseal dysplasia segregating in an inbred Pakistani kindred. *American journal of medical genetics* **78**, 468-73.

Ahmad T., Geffner M., Parks J., Brown M., Fisher L. & Costin G. (2011) Short stature and metabolic abnormalities in two sisters with a 7.6-kb GH1 gene deletion. *Growth Hormone & IGF Research* **21**, 37-43.

Akawi N.A., Ali B.R. & Al-Gazali L. (2012) A novel mutation in PRG4 gene underlying camptodactyly-arthropathy-coxa vara-pericarditis syndrome with the possible expansion of the phenotype to include congenital cataract. *Birth Defects Research Part A: Clinical and Molecular Teratology* **94**, 553-6.

Alazami A.M., Al-Qattan S.M., Faqeih E., Alhashem A., Alshammari M., Alzahrani F., Al-Dosari M.S., Patel N., Alsagheir A. & Binabbas B. (2016) Expanding the clinical and genetic heterogeneity of hereditary disorders of connective tissue. *Human genetics* **135**, 525-40.

Alazami A.M., Al-Mayouf S.M., Wyngaard C.A. & Meyer B. (2006) Novel PRG4 mutations underlie CACP in Saudi families. *Human Mutation* **27**, 213-.

Albtoush O.M., Taib A.A., Manzalawi K.A. & Mahafza W.S. (2018) Camptodactyly-Arthropathy-Coxa Vara-Pericarditis Syndrome with Shoulder Joint Involvement: A Case Report with Literature Review. In: *RöFo-Fortschritte auf dem Gebiet der Röntgenstrahlen und der bildgebenden Verfahren*, pp. 856-8. © Georg Thieme Verlag KG.

Albuhairan I. & Al-Mayouf S.M. (2013) Camptodactyly-arthropathy-coxavara-pericarditis syndrome in Saudi Arabia: Clinical and molecular genetic findings in 22 patients. In: *Seminars in arthritis and rheumatism*, pp. 292-6. Elsevier.

Aldahmesh M.A., Khan A.O., Mohamed J.Y., Levin A.V., Wuthisiri W., Lynch S., McCreery K. & Alkuraya F.S. (2013) No evidence for locus heterogeneity in Knobloch syndrome. *Journal of Medical Genetics* **50**, 565-6.

Amberger J., Bocchini C. & Hamosh A. (2011) A new face and new challenges for Online Mendelian Inheritance in Man (OMIM®). *Human mutation* **32**, 564-7.

Aranda J.F., Reglero-Real N., Kremer L., Marcos-Ramiro B., Ruiz-Sáenz A., Calvo M., Enrich C., Correas I., Millán J. & Alonso M.A. (2011) MYADM regulates Rac1 targeting to ordered membranes required for cell spreading and migration. *Molecular biology of the cell* **22**, 1252-62.

Argente J. & Pérez-Jurado L.A. (2018) Genetic causes of proportionate short stature. *Best Practice & Research Clinical Endocrinology & Metabolism*.

Bahabri S.A., Suwairi W.M., Laxer R.M., Polinkovsky A., Dalaan A.A. & Warman M.L. (1998) The camptodactyly-arthropathy-coxa vara-pericarditis syndrome: Clinical features and genetic mapping to human chromosome 1. *Arthritis & Rheumatism: Official Journal of the American College of Rheumatology* **41**, 730-5.

Basit S., Iqbal Z., Umicevic-Mirkov M., Naqvi S.K.U.-H., Coenen M., Ansar M., van Bokhoven H. & Ahmad W. (2011) A novel deletion mutation in proteoglycan-4 underlies camptodactyly-arthropathy-coxa-vara-pericarditis syndrome in a consanguineous pakistani family. *Archives of medical research* **42**, 110-4.

Bauman J., Wiegant J., Borst P. & Van Duijn P. (1980) A new method for fluorescence microscopical localization of specific DNA sequences by in situ hybridization of fluorochrome-labelled RNA. *Experimental cell research* **128**, 485-90.

Bermejo-Sánchez E., Botto L.D., Feldkamp M.L., Groisman B. & Mastroiacovo P. (2018) Value of sharing and networking among birth defects surveillance programs: an ICBDSR perspective. *Journal of community genetics* **9**, 411-5.

Best S., Wou K., Vora N., Van der Veyver I.B., Wapner R. & Chitty L.S. (2018) Promises, pitfalls and practicalities of prenatal whole exome sequencing. *Prenatal diagnosis* **38**, 10-9.

Bittles A.H. & Black M.L. (2010) The impact of consanguinity on neonatal and infant health. *Early human development* **86**, 737-41.

Bittles A.H., Grant J.C. & Shami S.A. (1993) Consanguinity as a determinant of reproductive behaviour and mortality in Pakistan. *International journal of epidemiology* **22**, 463-7.

Bölükbaşı E.Y., Shabbir R.M.K., Malik S. & Tolun A. (2020) Homozygous deletion of MYADML2 in cranial asymmetry, reduced bone maturation, multiple dislocations, lumbar lordosis, and prominent clavicles. *Journal of Human Genetics*, 1-9.

Bowman K.G. & Bertozzi C.R. (1999) Carbohydrate sulfotransferases: mediators of extracellular communication. *Chemistry & biology* **6**, R9-R22.

Brenner S., Johnson M., Bridgham J., Golda G., Lloyd D.H., Johnson D., Luo S., McCurdy S., Foy M. & Ewan M. (2000) Gene expression analysis by massively parallel signature sequencing (MPSS) on microbead arrays. *Nature biotechnology* **18**, 630-4.

Bulutlar G., Yazici H., Özdoğan H. & Schreuder I. (1986) A familial syndrome of pericarditis, arthritis, camptodactyly, and coxa vara. *Arthritis & Rheumatism: Official Journal of the American College of Rheumatology* **29**, 436-8.

Caglayan A.O., Baranoski J.F., Aktar F., Han W., Tuysuz B., Guzel A., Guclu B., Kaymakcalan H., Aktekin B. & Akgumus G.T. (2014) Brain malformations associated with Knobloch syndrome—review of literature, expanding clinical spectrum, and identification of novel mutations. *Pediatric neurology* **51**, 806-13. e8.

Campos D.A., Melo M.d.S.R., de Souza Medeiros B.G. & Lucena V.S. (2018) Fatores genéticos: prevalência de mortalidade neonatal e anomalias congênitas. *Journal of Biology & Pharmacy and Agricultural Management* **13**.

Cardoso-dos-Santos A.C., Magalhães V.S., Medeiros-de-Souza A.C., Bremm J.M., Alves R.F.S., Araujo V.E.M.d., Macario E.M., Oliveira W.K.d. & França G.V.A.d. (2020) International collaboration networks for the surveillance of congenital anomalies: a narrative review. *Epidemiologia e Serviços de Saúde* **29**, e2020093.

Chitty L.S. (2014) Cell-free DNA testing: An aid to prenatal sonographic diagnosis. *Best Practice & Research Clinical Obstetrics & Gynaecology* **28**, 453-66.

Chong J.X., Buckingham K.J., Jhangiani S.N., Boehm C., Sobreira N., Smith J.D., Harrell T.M., McMillin M.J., Wiszniewski W. & Gambin T. (2015) The genetic basis of Mendelian phenotypes: discoveries, challenges, and opportunities. *The American Journal of Human Genetics* **97**, 199-215.

Chopra S.S., Leshchiner I., Duzkale H., McLaughlin H., Giovanni M., Zhang C., Stitziel N., Fingeroth J., Joyce R.M. & Lebo M. (2015) Inherited CHST11/MIR3922 deletion is associated with a novel recessive syndrome presenting with skeletal malformation and malignant lymphoproliferative disease. *Molecular genetics & genomic medicine* **3**, 413-23.

Chute C.G. (2018) The rendering of human phenotype and rare diseases in ICD-11. *Journal of inherited metabolic disease* **41**, 563-9.

Collett-Solberg P.F., Ambler G., Backeljauw P.F., Bidlingmaier M., Biller B.M., Boguszewski M.C., Cheung P.T., Choong C.S.Y., Cohen L.E. & Cohen P. (2019) Diagnosis, genetics, and therapy of short stature in children: a growth hormone research Society international perspective. *Hormone Research in Paediatrics* **92**, 1-14.

Collins A.L., Levenson J.M., Vilaythong A.P., Richman R., Armstrong D.L., Noebels J.L., David Sweatt J. & Zoghbi H.Y. (2004) Mild overexpression of MeCP2 causes a progressive neurological disorder in mice. *Human molecular genetics* **13**, 2679-89.

Consortium G.O. (2019) The gene ontology resource: 20 years and still GOing strong. *Nucleic acids research* **47**, D330-D8.

Conway-Campbell B.L., Brooks A.J., Robinson P.J., Perani M. & Waters M.J. (2008) The extracellular domain of the growth hormone receptor interacts with coactivator activator to promote cell proliferation. *Molecular endocrinology* **22**, 2190-202.

Cortes M., Baria A.T. & Schwartz N.B. (2009) Sulfation of chondroitin sulfate proteoglycans is necessary for proper Indian hedgehog signaling in the developing growth plate. *Development* **136**, 1697-706.

Czeizel A., Göblyös P., Kustos G., Mester E. & Paraicz E. (1992) The second report of Knobloch syndrome. *American journal of medical genetics* **42**, 777-9.

Dauber A., Rosenfeld R.G. & Hirschhorn J.N. (2014) Genetic evaluation of short stature. *The Journal of Clinical Endocrinology & Metabolism* **99**, 3080-92.

Dawodu A., Al-Gazali L., Varady E., Varghese M., Nath K. & Rajan V. (2005) Genetic contribution to high neonatally lethal malformation rate in the United Arab Emirates. *Public Health Genomics* **8**, 31-4.

de Almeida Brasil T. & D'Angeles A.C.R. (2014) Perfil da mortalidade materna no município do Rio de Janeiro em 2010. *Gestão e Saúde* **6**, pag. 66-78.

de Leeuw N., Dijkhuizen T., Hehir-Kwa J.Y., Carter N.P., Feuk L., Firth H.V., Kuhn R.M., Ledbetter D.H., Martin C.L. & van Ravenswaaij-Arts C.M. (2012) Diagnostic interpretation of array data using public databases and internet sources. *Human mutation* **33**, 930-40.

Derr M.A., Aisenberg J., Fang P., Tenenbaum-Rakover Y., Rosenfeld R.G. & Hwa V. (2011) The growth hormone receptor (GHR) c. 899dupC mutation functions as a dominant negative: insights into the pathophysiology of intracellular GHR defects. *The Journal of Clinical Endocrinology & Metabolism* **96**, E1896-E904.

Dias C., Elzein S., Sladek R. & Goodyer C.G. (2019) Sex-specific effects of a microsatellite polymorphism on human growth hormone receptor gene expression. *Molecular and cellular endocrinology* **492**, 110442.

Dimopoulou A., Fischer B., Gardeitchik T., Schröter P., Kayserili H., Schlack C., Li Y., Brum J.M., Barisic I. & Castori M. (2013) Genotype–phenotype spectrum of PYCR1-related autosomal recessive cutis laxa. *Molecular Genetics and Metabolism* **110**, 352-61.

Ekwere E.O., McNeil R., Agim B., Jeminiwa B., Oni O. & Pam S. (2011) A retrospective study of congenital anomalies presented at tertiary health facilities in Jos, Nigeria. Journal of Physics: Conference Series (JPCS).

El Kholy M., Mella P., Rashad M., Buzi F., Meazza C., Zahra S. & Elsedfy H. (2011) Growth hormone/IGF-I axis and growth hormone receptor mutations in idiopathic short stature. *Hormone research in paediatrics* **76**, 300-6.

El Koumi M.A., Al Banna E.A. & Lebda I. (2013) Pattern of congenital anomalies in newborn: a hospital-based study. *Pediatric reports* **5**.

Fabregat A., Jupe S., Matthews L., Sidiropoulos K., Gillespie M., Garapati P., Haw R., Jassal B., Korninger F. & May B. (2018) The reactome pathway knowledgebase. *Nucleic acids research* **46**, D649-D55.

Faivre L., Prieur A.M., Le Merrer M., Hayem F., Penet C., Woo P., Hofer M., Dagoneau N., Sermet I. & Munnich A. (2000) Clinical variability and genetic homogeneity of the camptodactyly-arthropathy-coxa vara-pericarditis syndrome. *American journal of medical genetics* **95**, 233-6.

Fareed M. & Afzal M. (2017) Genetics of consanguinity and inbreeding in health and disease. *Annals of human biology* **44**, 99-107.

Fassone L., Corneli G., Bellone S., Camacho-Hübner C., Aimaretti G., Cappa M., Ubertini G. & Bona G. (2007) Growth hormone receptor gene mutations in two Italian patients with Laron Syndrome. *Journal of endocrinological investigation* **30**, 417-20.

Flannery C.R., Hughes C.E., Schumacher B.L., Tudor D., Aydelotte M.B., Kuettner K.E. & Caterson B. (1999) Articular cartilage superficial zone protein (SZP) is homologous to megakaryocyte stimulating factor precursor and is a multifunctional proteoglycan with potential growth-promoting, cytoprotective, and lubricating properties in cartilage metabolism. *Biochemical and biophysical research communications* **254**, 535-41.

Fukai N., Eklund L., Marneros A.G., Oh S.P., Keene D.R., Tamarkin L., Niemelä M., Ilves M., Li E. & Pihlajaniemi T. (2002) Lack of collagen XVIII/endostatin results in eye abnormalities. *The EMBO journal* **21**, 1535-44.

Gatseva A., Sin Y.Y., Brezzo G. & Van Agtmael T. (2019) Basement membrane collagens and disease mechanisms. *Essays in Biochemistry* **63**, 297-312.

Geister K.A. & Camper S.A. (2015) Advances in skeletal dysplasia genetics. *Annual review of genomics and human genetics* **16**, 199-227.

Gennero I., Edouard T., Rashad M., Bieth E., Conte-Auriol F., Marin F., Tauber M., Salles J.P. & El Kholy M. (2007) Identification of a novel mutation in the human

growth hormone receptor gene (GHR) in a patient with Laron syndrome. *Journal of Pediatric Endocrinology and Metabolism* **20**, 825-32.

Greisman H.A., Hoffman N.G. & Yi H.S. (2011) Rapid high-resolution mapping of balanced chromosomal rearrangements on tiling CGH arrays. *The Journal of Molecular Diagnostics* **13**, 621-33.

Guernsey D.L., Jiang H., Evans S.C., Ferguson M., Matsuoka M., Nightingale M., Rideout A.L., Provost S., Bedard K. & Orr A. (2009) Mutation in pyrroline-5-carboxylate reductase 1 gene in families with cutis laxa type 2. *The American Journal of Human Genetics* **85**, 120-9.

Guevara-Aguirre J., Guevara A., Palacios I., Pérez M., Prócel P. & Terán E. (2018) GH and GHR signaling in human disease. *Growth Hormone & IGF Research* **38**, 34-8.

Guevara-Aguirre J., Rosenbloom A.L., Fielder P.J., Diamond Jr F. & Rosenfeld R.G. (1993) Growth hormone receptor deficiency in Ecuador: clinical and biochemical phenotype in two populations. *The Journal of Clinical Endocrinology & Metabolism* **76**, 417-23.

Gulati A. & Somlo S. (2018) Whole exome sequencing: a state-of-the-art approach for defining (and exploring!) genetic landscapes in pediatric nephrology. *Pediatric Nephrology*, 1-17.

Haghighi A., Tiwari A., Piri N., Nürnberg G., Saleh-Gohari N., Haghighi A., Neidhardt J., Nürnberg P. & Berger W. (2014) Homozygosity mapping and whole exome sequencing reveal a novel homozygous COL18A1 mutation causing Knobloch syndrome. *PloS one* **9**, e112747.

Hamosh A., Scott A.F., Amberger J.S., Bocchini C.A. & McKusick V.A. (2005) Online Mendelian Inheritance in Man (OMIM), a knowledgebase of human genes and genetic disorders. *Nucleic acids research* **33**, D514-D7.

Hardingham T. (2006) Proteoglycans and glycosaminoglycans. *Dynamics of bone and cartilage metabolism* **2**, 85-98.

Hasegawa K. & Tanaka H. (2014) Children with short-limbed short stature in pediatric endocrinological services in J apan. *Pediatrics International* **56**, 809-12.

Hästbacka J., de la Chapelle A., Mahtani M.M., Clines G., Reeve-Daly M.P., Daly M., Hamilton B.A., Kusumi K., Trivedi B. & Weaver A. (1994) The diastrophic dysplasia gene encodes a novel sulfate transporter: positional cloning by fine-structure linkage disequilibrium mapping. *Cell* **78**, 1073-87.

Huang Z., Sun Y., Fan Y., Wang L., Liu H., Gong Z., Wang J., Yan H., Wang Y. & Hu G. (2018) Genetic evaluation of 114 Chinese short stature children in the next generation era: a single center study. *Cellular Physiology and Biochemistry* **49**, 295-305.

ICBDSR W. (2014) BIRTH DEFECTS SURVEILLANCE A MANUAL FOR PROGRAMME MANAGERS. World Health Organization Geneva.

Ijaz A., Basit S., Gul A., Batool L., Hussain A., Afzal S., Ramzan K., Ahmad J. & Wali A. (2019) XPC gene mutations in families with xeroderma pigmentosum from Pakistan; prevalent founder effect. *Congenital anomalies* **59**, 18-21.

Ioannidis N.M., Rothstein J.H., Pejaver V., Middha S., McDonnell S.K., Baheti S., Musolf A., Li Q., Holzinger E. & Karyadi D. (2016) REVEL: an ensemble method for predicting the pathogenicity of rare missense variants. *The American Journal of Human Genetics* **99**, 877-85.

Iozzo R.V. (1998) Matrix proteoglycans: from molecular design to cellular function. Annual Reviews 4139 El Camino Way, PO Box 10139, Palo Alto, CA 94303-0139, USA.

Iqbal Z. & Van Bokhoven H. (2014) Identifying genes responsible for intellectual disability in consanguineous families. *Human heredity* **77**, 150-60.

Ishikawa Y., Ito S., Nagata K., Sakai L.Y. & Bächinger H.P. (2016) Intracellular mechanisms of molecular recognition and sorting for transport of large extracellular matrix molecules. *Proceedings of the National Academy of Sciences* **113**, E6036-E44.

Jagadeesh K.A., Wenger A.M., Berger M.J., Guturu H., Stenson P.D., Cooper D.N., Bernstein J.A. & Bejerano G. (2016) M-CAP eliminates a majority of variants of uncertain significance in clinical exomes at high sensitivity. *Nature genetics* **48**, 1581.

Janecke A.R., Li B., Boehm M., Krabichler B., Rohrbach M., Müller T., Fuchs I., Golas G., Katagiri Y. & Ziegler S.G. (2016) The phenotype of the musculocontractural type of Ehlers-Danlos syndrome due to CHST14 mutations. *American Journal of Medical Genetics Part A* **170**, 103-15.

Janghorban R. & Azarkish F. (2016) Community Genetic Services in Iran at a Glance. *Iranian journal of public health* **45**, 1669-70.

Jay G., Torres J., Warman M., Laderer M. & Breuer K. (2007) The role of lubricin in the mechanical behavior of synovial fluid. *Proceedings of the National Academy of Sciences* **104**, 6194-9.

Johnson N., Chaudhary H., Kumrah R., Pilania R.K., Sharma Y., Sharma A., Kaur A., Mukherjee S., Kakkar N. & Vignesh P. (2020) Syndrome of progressive deforming non-inflammatory arthritis of childhood: two patients of camptodactyly-arthropathy-coxa vara-pericarditis syndrome. *Rheumatology International*, 1-8.

Joyce S., Tee L., Abid A., Khaliq S., Mehdi S.Q. & Maher E.R. (2010) Locus heterogeneity and Knobloch syndrome. *American journal of medical genetics. Part A* **152**, 2880-1.

Jun Q., Hu Z., Li Q., Zhang P., Lv Q., Lin Z. & Gu J. (2016) AB0908 A Novel Mutation in Proteoglycan-4 Underlies Camptodactyly-Arthropathy-Coxa-Vara-Pericarditis Syndrome in A Chinese Family. BMJ Publishing Group Ltd.

Kahsay R.Y., Gao G. & Liao L. (2005) An improved hidden Markov model for transmembrane protein detection and topology prediction and its applications to complete genomes. *Bioinformatics* **21**, 1853-8.

Kallioniemi A., Kallioniemi O.-P., Sudar D., Rutovitz D., Gray J.W., Waldman F. & Pinkel D. (1992) Comparative genomic hybridization for molecular cytogenetic analysis of solid tumors. *Science* **258**, 818-21.

Kanehisa M., Furumichi M., Tanabe M., Sato Y. & Morishima K. (2017) KEGG: new perspectives on genomes, pathways, diseases and drugs. *Nucleic acids research* **45**, D353-D61.

Kariminejad A., Afroozan F., Bozorgmehr B., Ghanadan A., Akbaroghli S., Khorram Khorshid H.R., Mojahedi F., Setoodeh A., Loh A. & Tan Y.X. (2017)

Discriminative features in three autosomal recessive cutis laxa syndromes: cutis laxa IIA, cutis laxa IIB, and geroderma osteoplastica. *International Journal of Molecular Sciences* **18**, 635.

Karniski L.P. (2001) Mutations in the diastrophic dysplasia sulfate transporter (DTDST) gene: correlation between sulfate transport activity and chondrodysplasia phenotype. *Human molecular genetics* **10**, 1485-90.

Karnuta J.M. & Scacheri P.C. (2018) Enhancers: Bridging the gap between gene control and human disease. *Human molecular genetics*.

Keren B., Suzuki O.T., Gérard-Blanluet M., Brémond-Gignac D., Elmaleh M., Titomanlio L., Delezoide A.L., Passos-Bueno M.R. & Verloes A. (2007) CNS malformations in Knobloch syndrome with splice mutation in COL18A1 gene. *American Journal of Medical Genetics Part A* **143**, 1514-8.

Khalid Y., Ghina M., Fadi B., Fadi C., May K., Joseph R., Makhoul G. & Hala T. (2006) Consanguineous marriage and congenital heart defects: A case-control study in the neonatal period. *American journal of medical genetics Part A* **140**, 1524-30.

KIng I. (2008) Controlling Birth Defects: Reducing the Hidden Toll of Dying and Disabled Children in Low-Income Countries.

Klaassen C.D. & Boles J.W. (1997) The importance of 3 ‘-phosphoadenosine 5 ‘-phosphosulfate (PAPS) in the regulation of sulfation. *The FASEB Journal* **11**, 404-18.

Kliemann S.E., Waetge R.T., Suzuki O.T., Passos-Bueno M.R. & Rosemberg S. (2003) Evidence of neuronal migration disorders in Knobloch syndrome: clinical and molecular analysis of two novel families. *American Journal of Medical Genetics Part A* **119**, 15-9.

Klüppel M., Wight T.N., Chan C., Hinek A. & Wrana J.L. (2005) Maintenance of chondroitin sulfation balance by chondroitin-4-sulfotransferase 1 is required for chondrocyte development and growth factor signaling during cartilage morphogenesis. *Development* **132**, 3989-4003.

Krakow D. & Rimoin D.L. (2010) The skeletal dysplasias. *Genetics in Medicine* **12**, 327-41.

Kretz R., Bozorgmehr B., Kariminejad M.H., Rohrbach M., Hausser I., Baumer A., Baumgartner M., Giunta C., Kariminejad A. & Häberle J. (2011) Defect in proline synthesis: pyrroline-5-carboxylate reductase 1 deficiency leads to a complex clinical phenotype with collagen and elastin abnormalities. *Journal of inherited metabolic disease* **34**, 731-9.

Laron Z. (2002) Growth hormone insensitivity (Laron syndrome). *Reviews in Endocrine and Metabolic Disorders* **3**, 347-55.

Laron Z. (2004) Laron syndrome (primary growth hormone resistance or insensitivity): the personal experience 1958–2003. *The Journal of Clinical Endocrinology & Metabolism* **89**, 1031-44.

Laron Z. (2015) Lessons from 50 years of study of Laron syndrome. *Endocrine Practice* **21**, 1395-402.

Laron Z. & Kauli R. (2016) Fifty seven years of follow-up of the Israeli cohort of Laron Syndrome patients—from discovery to treatment. *Growth Hormone & IGF Research* **28**, 53-6.

Laron Z., Kauli R., Lapkina L. & Werner H. (2017) IGF-I deficiency, longevity and cancer protection of patients with Laron syndrome. *Mutation Research/Reviews in Mutation Research* **772**, 123-33.

Laron Z. & Klinger B. (1994) IGF-I treatment of adult patients with Laron syndrome: preliminary results. *Clinical endocrinology* **41**, 631-8.

Laron Z., Lilos P. & Klinger B. (1993) Growth curves for Laron syndrome. *Archives of disease in childhood* **68**, 768-70.

Lewis R. (2009) Cell and Molecular Biology: Human Genetics: Concepts and Applications. McGraw-Hill USA.

Li Z., Zhou C., Tan L., Chen P., Cao Y., Li C., Li X., Yan J., Zeng H. & Wang D.-W. (2017) Variants of genes encoding collagens and matrix metalloproteinase system increased the risk of aortic dissection. *Science China Life Sciences* **60**, 57-65.

Lin D.S., Chang J.H., Liu H.L., Wei C.H., Yeung C.Y., Ho C.S., Shu C.H., Chiang M.F., Chuang C.K. & Huang Y.W. (2011) Compound heterozygous mutations in PYCR1 further expand the phenotypic spectrum of De Barsy syndrome. *American Journal of Medical Genetics Part A* **155**, 3095-9.

Lin S., Li C., Li C. & Zhang X. (2018) Growth hormone receptor mutations related to individual dwarfism. *International journal of molecular sciences* **19**, 1433.

Lin S., Li H., Mu H., Luo W., Li Y., Jia X., Wang S., Jia X., Nie Q. & Li Y. (2012) Let-7b regulates the expression of the growth hormone receptor gene in deletion-type dwarf chickens. *BMC genomics* **13**, 1-10.

Liu L., Oza S., Hogan D., Perin J., Rudan I., Lawn J.E., Cousens S., Mathers C. & Black R.E. (2015) Global, regional, and national causes of child mortality in 2000–13, with projections to inform post-2015 priorities: an updated systematic analysis. *The Lancet* **385**, 430-40.

Mahajan V.B., Olney A.H., Garrett P., Chary A., Dragan E., Lerner G., Murray J. & Bassuk A.G. (2010) Collagen XVIII mutation in Knobloch syndrome with acute lymphoblastic leukemia. *American Journal of Medical Genetics Part A* **152**, 2875-9.

Maizels N. & Lupski J.R. (2013) Molecular and genetic bases of disease. Elsevier.

Malla B. (2007) One year review study of congenital anatomical malformation at birth in Maternity Hospital (Prasutigriha), Thapathali, Kathmandu. *Kathmandu Univ Med J* **5**, 557-60.

Mannurita S.C., Vignoli M., Bianchi L., Kondi A., Gerloni V., Breda L., Ten Cate R., Alessio M., Ravelli A. & Falcini F. (2014) CACP syndrome: identification of five novel mutations and of the first case of UPD in the largest European cohort. *European Journal of Human Genetics* **22**, 197-201.

Marcelino J., Carpten J.D., Suwairi W.M., Gutierrez O.M., Schwartz S., Robbins C., Sood R., Makalowska I., Baxevanis A. & Johnstone B. (1999) CACP, encoding a secreted proteoglycan, is mutated in camptodactyly-arthropathy-coxa vara-pericarditis syndrome. *Nature genetics* **23**, 319-22.

Marian A.J. (2012) Challenges in medical applications of whole exome/genome sequencing discoveries. *Trends in cardiovascular medicine* **22**, 219-23.

Martínez-Moreno C.G., Calderón-Vallejo D., Harvey S., Arámburo C. & Quintanar J.L. (2018) Growth hormone (GH) and gonadotropin-releasing hormone (GnRH) in the central nervous system: a potential neurological combinatory therapy? *International journal of molecular sciences* **19**, 375.

Matsuzaki T., Alvarez-Garcia O., Mokuda S., Nagira K., Olmer M., Gamini R., Miyata K., Akasaki Y., Su A.I. & Asahara H. (2018) FoxO transcription factors modulate autophagy and proteoglycan 4 in cartilage homeostasis and osteoarthritis. *Science translational medicine* **10**.

Mazzucato M., Visonà Dalla Pozza L., Minichiello C., Manea S., Barbieri S., Toto E., Vianello A. & Facchin P. (2018) The Epidemiology of Transition into Adulthood of Rare Diseases Patients: Results from a Population-Based Registry. *International journal of environmental research and public health* **15**, 2212.

McMurray C.T. & Vijg J. (2014) Editorial overview: Molecular and genetic bases of disease: the double life of DNA. Elsevier.

MEHREGAN A.H., CHUAN LEE S. & NABAI H. (1978) Cutis laxa (generalized elastolysis) a report of four cases with autopsy findings. *Journal of cutaneous pathology* **5**, 116-26.

Menzel O., Bekkeheien R.C., Reymond A., Fukai N., Boye E., Kosztolanyi G., Aftimos S., Deutsch S., Scott H.S. & Olsen B.R. (2004) Knobloch syndrome: novel mutations in COL18A1, evidence for genetic heterogeneity, and a functionally impaired polymorphism in endostatin. *Human mutation* **23**, 77-84.

Metzker M. (2005) Emerging Technologies in DNA Sequencing. Genome Research.

Mikami T. & Kitagawa H. (2013) Biosynthesis and function of chondroitin sulfate. *Biochimica et Biophysica Acta (BBA)-General Subjects* **1830**, 4719-33.

Modell B. & Darr A. (2002) Genetic counselling and customary consanguineous marriage. *Nature Reviews Genetics* **3**, 225-9.

Moia S., Tessaris D., Einaudi S., De Sanctis L., Bona G., Bellone S. & Prodam F. (2017) Compound heterozygosity for two GHR missense mutations in a patient affected by Laron Syndrome: a case report. *Italian Journal of Pediatrics* **43**, 1-4.

Mone F., Jones E.Q. & Kilby M.D. (2018) CLINICAL UTILITY OF EXOME SEQUENCING IN THE PRENATAL DIAGNOSIS OF CONGENITAL ANOMALIES: A REVIEW. *European Journal of Obstetrics & Gynecology and Reproductive Biology*.

Monti L., Paganini C., Lecci S., De Leonardis F., Hay E., Cohen-Solal M., Villani S., Superti-Furga A., Tenni R. & Forlino A. (2015) N-acetylcysteine treatment

ameliorates the skeletal phenotype of a mouse model of diastrophic dysplasia. *Human molecular genetics* **24**, 5570-80.

Moore K., Persaud T. & Torchia M. (2013) Human birth defects. *The Developing Human: Clinically Oriented Embryology. 9th edition. Saunders/Elsevier, Philadelphia, PA*, 471-501.

Moorhead P.S., Nowell P.C., Mellman W.J., Battips D.t. & Hungerford D.A. (1960) Chromosome preparations of leukocytes cultured from human peripheral blood. *Experimental cell research* **20**, 613-6.

Morava E., Guillard M., Lefeber D.J. & Wevers R.A. (2009) Autosomal recessive cutis laxa syndrome revisited. *European Journal of Human Genetics* **17**, 1099-110.

Morris J.K., Springett A.L., Greenlees R., Loane M., Addor M.-C., Arriola L., Barisic I., Bergman J.E., Csaky-Szunyogh M. & Dias C. (2018) Trends in congenital anomalies in Europe from 1980 to 2012. *PloS one* **13**, e0194986.

Mortier G.R., Cohn D.H., Cormier-Daire V., Hall C., Krakow D., Mundlos S., Nishimura G., Robertson S., Sangiorgi L. & Savarirayan R. (2019) Nosology and classification of genetic skeletal disorders: 2019 revision. *American Journal of Medical Genetics Part A* **179**, 2393-419.

Moseley C.T. & Phillips III J.A. (2000) Pituitary gene mutations and the growth hormone pathway. In: *Seminars in reproductive medicine*, pp. 021-30. Copyright© 2000 by Thieme Medical Publishers, Inc., 333 Seventh Avenue, New ….

Mourão P.A., Kato S. & Donnelly P.V. (1981) Spondyloepiphyseal dysplasia, chondroitin sulfate type: a possible defect of PAPS—chondroitin sulfate sulfotransferase in humans. *Biochemical and biophysical research communications* **98**, 388-96.

Muzammal M., Zubair M., Bierbaumer S., Blatterer J., Graf R., Gul A., Abbas S., Badar M., Abbasi A.A. & Khan M.A. (2019) Exome sequence analysis in consanguineous Pakistani families inheriting Bardet-Biedle syndrome determined founder effect of mutation c. 299delC (p. Ser100Leufs* 24) in BBS9 gene. *Molecular genetics & genomic medicine* **7**, e834.

Nadeem M.T., Tabassum K., Imroze F.R., Ahmed S.U. & Vindhya K. (2018) Camptodactyly-arthropathy-coxa-vara-pericarditis syndrome: A rare childhood syndrome. *The Journal of Medical Research* **4**, 204-6.

Nandagopalan R.S., Phadke S.R., Dalal A.B. & Ranganath P. (2014) Novel mutations in PRG4 gene in two Indian families with camptodactyly-arthropathy-coxa vara-pericarditis (CACP) syndrome. *The Indian journal of medical research* **140**, 221.

Narasimhan V.M., Hunt K.A., Mason D., Baker C.L., Karczewski K.J., Barnes M.R., Barnett A.H., Bates C., Bellary S. & Bockett N.A. (2016) Health and population effects of rare gene knockouts in adult humans with related parents. *Science* **352**, 474-7.

Ndibazza J., Lule S., Nampijja M., Mpairwe H., Oduru G., Kiggundu M., Akello M., Muhangi L. & Elliott A.M. (2011) A description of congenital anomalies among infants in Entebbe, Uganda. *Birth Defects Research Part A: Clinical and Molecular Teratology* **91**, 857-61.

Numabe H. (2018) 58th Annual Meeting of the Japanese Teratology Society: Congenital anomalies as variants. *Congenital anomalies*.

O'CONNELL A.C., Toner M. & Murphy S. (2009) Knobloch syndrome: novel intra-oral findings. *International journal of paediatric dentistry* **19**, 213-5.

Obermeyer R.J. & Goretsky M.J. (2012) Chest wall deformities in pediatric surgery. *Surgical Clinics* **92**, 669-84.

Oestergaard M.Z., Inoue M., Yoshida S., Mahanani W.R., Gore F.M., Cousens S., Lawn J.E. & Mathers C.D. (2011) Neonatal mortality levels for 193 countries in 2009 with trends since 1990: a systematic analysis of progress, projections, and priorities. *PLoS Med* **8**, e1001080.

Onoufriadis A., Nanda A., Sheriff A., Tomita K., Gomaa N.S., Simpson M.A. & McGrath J.A. (2019) Consanguinity and Double Recessive Gene Pathology: Cutis Laxa (PYCR1) and Nephrotic Syndrome (PLCE1). *JAMA dermatology* **155**, 257-9.

Organization W.H. (2009) *Infant and young child feeding: model chapter for textbooks for medical students and allied health professionals*. World Health Organization.

Pagani S., Petkovic V., Messini B., Meazza C., Bozzola E., Mullis P.-E. & Bozzola M. (2014) Heterozygous GHR gene mutation in a child with idiopathic short stature. *Journal of Pediatric Endocrinology and Metabolism* **27**, 329-34.

Paganini C., Costantini R., Superti-Furga A. & Rossi A. (2019) Bone and connective tissue disorders caused by defects in glycosaminoglycan biosynthesis: A panoramic view. *The FEBS journal* **286**, 3008-32.

Paganini C., Gramegna Tota C., Superti-Furga A. & Rossi A. (2020) Skeletal Dysplasias Caused by Sulfation Defects. *International Journal of Molecular Sciences* **21**, 2710.

Paisán-Ruiz C., Scopes G., Lee P. & Houlden H. (2009) Homozygosity mapping through whole genome analysis identifies a COL18A1 mutation in an Indian family presenting with an autosomal recessive neurological disorder. *American Journal of Medical Genetics Part B: Neuropsychiatric Genetics* **150**, 993-7.

Parmar A., Rathod S., Patel S. & Patel S. (2010) A study of congenital anomalies in newborn. *NJIRM* **1**, 13-7.

Passos-Bueno M.R., Suzuki O.T., Armelin-Correa L.M., Sertié A.L., Errera F.I., Bagatini K., Kok F. & Leite K.R. (2006) Mutations in Collagen 18A1 (COL18A1) and their relevance to the human phenotype. *Anais da Academia Brasileira de Ciencias* **78**, 123-31.

Passos-Bueno M.R., Marie S.K., Monteiro M., Neustein I., Whittle M.R., Vainzof M. & Zatz M. (1994) Knobloch syndrome in a large Brazilian consanguineous family: confirmation of autosomal recessive inheritance. *American journal of medical genetics* **52**, 170-3.

Patil D.V., Phadke M.S., Pahwa J.S. & Dalal A.B. (2016) Brothers with constrictive pericarditis–A novel mutation in a rare disease. *indian heart journal* **68**, S284-S7.

Peters B., Schuurs-Hoeijmakers J.H., Fuijkschot J., Reimer A., van der Flier M., Lugtenberg D. & Hoppenreijs E.P. (2016) Protein-losing enteropathy in camptodactyly-arthropathy-coxa vara-pericarditis (CACP) syndrome. *Pediatric Rheumatology* **14**, 1-6.

Porto W.F., Marques F.A., Pogue H.B., de Oliveira Cardoso M.T., do Vale M.G.R., da Silva Pires Á., Franco O.L., de Alencar S.A. & Pogue R. (2017) Computational

Investigation of Growth Hormone Receptor Trp169Arg Heterozygous Mutation in a Child With Short Stature. *Journal of Cellular Biochemistry* **118**, 4762-71.

Pyeritz R.E. (2012) Inherited diseases of connective tissue. In: *Goldman's Cecil Medicine* (pp. 1662-7. Elsevier.

Rached M.-T., Kode A., Xu L., Yoshikawa Y., Paik J.-H., DePinho R.A. & Kousteni S. (2010) FoxO1 is a positive regulator of bone formation by favoring protein synthesis and resistance to oxidative stress in osteoblasts. *Cell metabolism* **11**, 147-60.

Rajab A., Vaishnav A., Freeman N. & Patton M. (1998) Neural tube defects and congenital hydrocephalus in the Sultanate of Oman. *Journal of tropical pediatrics* **44**, 300-3.

Randles M.J., Humphries M.J. & Lennon R. (2017) Proteomic definitions of basement membrane composition in health and disease. *Matrix Biology* **57**, 12-28.

Redin C., Brand H., Collins R.L., Kammin T., Mitchell E., Hodge J.C., Hanscom C., Pillalamarri V., Seabra C.M. & Abbott M.-A. (2017) The genomic landscape of balanced cytogenetic abnormalities associated with human congenital anomalies. *Nature genetics* **49**, 36-45.

Rentzsch P., Witten D., Cooper G.M., Shendure J. & Kircher M. (2019) CADD: predicting the deleteriousness of variants throughout the human genome. *Nucleic acids research* **47**, D886-D94.

Reversade B., Escande-Beillard N., Dimopoulou A., Fischer B., Chng S.C., Li Y., Shboul M., Tham P.-Y., Kayserili H. & Al-Gazali L. (2009) Mutations in PYCR1 cause cutis laxa with progeroid features. *Nature genetics* **41**, 1016-21.

Ritelli M., Palit A., Giacopuzzi E., Inamadar A.C., Dordoni C., Mujja A., Murgude M.S. & Colombi M. (2017) Clinical and molecular characterization of a 13-year-old Indian boy with cutis laxa type 2B: Identification of two novel PYCR1 mutations by amplicon-based semiconductor exome sequencing. *Journal of dermatological science* **88**, 141-3.

Rittler M., Liascovich R., López-Camelo J. & Castilla E.E. (2001) Parental consanguinity in specific types of congenital anomalies. *American journal of medical genetics* **102**, 36-43.

Rosenbloom A.L. (2016) A half-century of studies of growth hormone insensitivity/Laron syndrome: a historical perspective. *Growth Hormone & IGF Research* **28**, 46-50.

Rossi A. & Superti-Furga A. (2001) Mutations in the diastrophic dysplasia sulfate transporter (DTDST) gene (SLC26A2): 22 novel mutations, mutation review, associated skeletal phenotypes, and diagnostic relevance. *Human mutation* **17**, 159-71.

Saengkaew T., McNeil E. & Jaruratanasirikul S. (2017) Etiologies of short stature in a pediatric endocrine clinic in Southern Thailand. *Journal of Pediatric Endocrinology and Metabolism* **30**, 1265-70.

Saleheen D., Natarajan P., Armean I.M., Zhao W., Rasheed A., Khetarpal S.A., Won H.-H., Karczewski K.J., O'Donnell-Luria A.H. & Samocha K.E. (2017) Human knockouts and phenotypic analysis in a cohort with a high rate of consanguinity. *Nature* **544**, 235-9.

Sandri M., Sandri C., Gilbert A., Skurk C., Calabria E., Picard A., Walsh K., Schiaffino S., Lecker S.H. & Goldberg A.L. (2004) Foxo transcription factors induce the atrophy-related ubiquitin ligase atrogin-1 and cause skeletal muscle atrophy. *Cell* **117**, 399-412.

Sanger F., Nicklen S. & Coulson A.R. (1977) DNA sequencing with chain-terminating inhibitors. *Proceedings of the national academy of sciences* **74**, 5463-7.

Scherrer D., Baptista M., Matos A., Maurer-Morelli C. & Steiner C. (2013) Mutations in PYCR1 gene in three families with autosomal recessive cutis laxa, type 2. *European Journal of Medical Genetics* **6**, 336-9.

Schumacher B.L., Hughes C.E., Kuettner K.E., Caterson B. & Aydelotte M.B. (1999) Immunodetection and partial cDNA sequence of the proteoglycan, superficial zone protein, synthesized by cells lining synovial joints. *Journal of Orthopaedic Research* **17**, 110-20.

Seaver L.H., Joffe L., Spark R.P., Smith B.L. & Hoyme H.E. (1993) Congenital scalp defects and vitreoretinal degeneration: redefining the Knobloch syndrome. *American journal of medical genetics* **46**, 203-8.

Sekhobo J.P. & Druschel C.M. (2001) An evaluation of congenital malformations surveillance in New York State: an application of Centers for Disease Control and Prevention (CDC) guidelines for evaluating surveillance systems. *Public health reports* **116**, 296.

Sertie A., Quimby M., Moreira E., Murray J., Zatz M., Antonarakis S. & Passos-Bueno M. (1996) A gene which causes severe ocular alterations and occipital encephalocele (Knobloch syndrome) is mapped to 21q22. 3. *Human molecular genetics* **5**, 843-7.

Sertié A.L., Sossi V., Camargo A.A., Zatz M., Brahe C. & Passos-Bueno M.R. (2000) Collagen XVIII, containing an endogenous inhibitor of angiogenesis and tumor growth, plays a critical role in the maintenance of retinal structure and in neural tube closure (Knobloch syndrome). *Human molecular genetics* **9**, 2051-8.

Shabbir R.M.K., Nalbant G., Ahmad N., Malik S. & Tolun A. (2018) Homozygous CHST11 mutation in chondrodysplasia, brachydactyly, overriding digits, clino-symphalangism and synpolydactyly. *Journal of medical genetics* **55**, 489-96.

Shapiro F. (2016) Developmental bone biology. In: *Pediatric Orthopedic Deformities, Volume 1* (pp. 1-158. Springer.

Silva J.H.d., Terças A.C.P., Pinheiro L.C.B., França G.V.A.d., Atanaka M. & Schüler-Faccini L. (2018) Perfil das anomalias congênitas em nascidos vivos de Tangará da Serra, Mato Grosso, 2006-2016. *Epidemiologia e Serviços de Saúde* **27**, e2018008.

Singh A. & Gupta R.K. (2009) Pattern of Congenital Anomalies in Newborn: A Hospital Based Prospective Study. *JK science* **11**.

Singh K., Krishnamurthy K., Greaves C., Kandamaran L., Nielsen A.L. & Kumar A. (2014) Major congenital malformations in Barbados: the prevalence, the pattern, and the resulting morbidity and mortality. *International Scholarly Research Notices* **2014**.

Small N., Bittles A.H., Petherick E.S. & Wright J. (2016) Endogamy, consanguinity and the health implications of changing marital choices in the UK Pakistani community. *Jour-nal of Biosocial Science* **49**, 435-46.

Somale A.K. & Ahmed M. (2016) An unusual cause of short stature-Laron syndrome. *International Journal of Advances in Medicine* **3**, 435.

Stoll C., Alembik Y., Roth M. & Dott B. (1999) Parental consanguinity as a cause for increased incidence of births defects in a study of 238,942 consecutive births. In: *Annales de genetique*, pp. 133-9.

Superti-Furga A., Neumann L., Riebel T., Eich G., Steinmann B., Spranger J. & Kunze J. (1999) Recessively inherited multiple epiphyseal dysplasia with normal stature, club foot, and double layered patella caused by a DTDST mutation. *Journal of medical genetics* **36**, 621-4.

Suzuki O., Kague E., Bagatini K., Tu H., Heljasvaara R., Carvalhaes L., Gava E., de Oliveira G., Godoi P. & Oliva G. (2009) Novel pathogenic mutations and skin biopsy analysis in Knobloch syndrome. *Molecular vision* **15**, 801.

Suzuki O., Sertie A., Der Kaloustian V., Kok F., Carpenter M., Murray J., Czeizel A., Kliemann S., Rosemberg S. & Monteiro M. (2002) Molecular analysis of collagen XVIII reveals novel mutations, presence of a third isoform, and possible genetic heterogeneity in Knobloch syndrome. *The American Journal of Human Genetics* **71**, 1320-9.

Tadmouri G.O., Nair P., Obeid T., Al Ali M.T., Al Khaja N. & Hamamy H.A. (2009) Consanguinity and reproductive health among Arabs. *Reproductive health* **6**, 17.

Taksande A., Vilhekar K., Chaturvedi P. & Jain M. (2010) Congenital malformations at birth in Central India: A rural medical college hospital based data. *Indian journal of human genetics* **16**, 159.

Taye M., Afework M., Fantaye W., Diro E. & Worku A. (2019) Congenital anomalies prevalence in Addis Ababa and the Amhara region, Ethiopia: a descriptive cross-sectional study. *BMC pediatrics* **19**, 234.

Thorson C., Galicia K., Burleson A., Bouchard O., Hoppensteadt D., Fareed J. & Hopkinson W. (2019) Matrix metalloproteinases and their inhibitors and proteoglycan 4 in patients undergoing total joint arthroplasty. *Clinical and Applied Thrombosis/Hemostasis* **25**, 1076029619828113.

Unger S., Lausch E., Rossi A., Mégarbané A., Sillence D., Alcausin M., Aytes A., Mendoza-Londono R., Nampoothiri S. & Afroze B. (2010) Phenotypic features of

carbohydrate sulfotransferase 3 (CHST3) deficiency in 24 patients: congenital dislocations and vertebral changes as principal diagnostic features. *American journal of medical genetics Part A* **152**, 2543-9.

Vatankhah S., Jalilvand M., Sarkhosh S., Azarmi M. & Mohseni M. (2017) Prevalence of congenital anomalies in Iran: A review article. *Iranian journal of public health* **46**, 733.

Vissers L.E., Lausch E., Unger S., Campos-Xavier A.B., Gilissen C., Rossi A., Del Rosario M., Venselaar H., Knoll U. & Nampoothiri S. (2011) Chondrodysplasia and abnormal joint development associated with mutations in IMPAD1, encoding the Golgi-resident nucleotide phosphatase, gPAPP. *The American Journal of Human Genetics* **88**, 608-15.

Waters M.J. (2016) The growth hormone receptor. *Growth Hormone & IGF Research* **28**, 6-10.

Watson J.D. & Crick F.H. (1953) The structure of DNA. In: *Cold Spring Harbor symposia on quantitative biology*, pp. 123-31. Cold Spring Harbor Laboratory Press.

Wilson C., Aftimos S., Pereira A. & McKay R. (1998) Report of two sibs with Knobloch syndrome (encephalocoele and viteroretinal degeneration) and other anomalies. *American journal of medical genetics* **78**, 286-90.

Wit J.M., Oostdijk W., Losekoot M., van Duyvenvoorde H.A., Ruivenkamp C.A. & Kant S.G. (2016) Mechanisms in endocrinology: novel genetic causes of short stature. *European Journal of Endocrinology* **174**, R145-R73.

Yadav S. & Dabas A. (2015) Approach to short stature. *The Indian Journal of Pediatrics* **82**, 462-70.

Yan D., Kannan-Sundhari A., Vishwanath S., Qing J., Mittal R., Kameswaran M. & Liu X.Z. (2015) The genetic basis of nonsyndromic hearing loss in Indian and Pakistani populations. *Genetic testing and molecular biomarkers* **19**, 512-27.

Yilmaz S., Uludağ Alkaya D., Kasapçopur Ö., Barut K., Akdemir E.S., Celen C., Youngblood M.W., Yasuno K., Bilguvar K. & Günel M. (2018) Genotype–phenotype investigation of 35 patients from 11 unrelated families with

camptodactyly–arthropathy–coxa vara–pericarditis (CACP) syndrome. *Molecular genetics & genomic medicine* **6**, 230-48.

Yunis J.J. (1976) High resolution of human chromosomes. *Science*, 1268-70.

Turnitin Originality Report

Identification of disease causing genes in families with skeletal and ophthalmological disorders by Rana Muhammad Kamran Shabbir .

From DRSM (DRSM L)

- Processed on 21-Oct-2020 15:10 PKT
- ID: 1421930920
- Word Count: 31939

Similarity Index
17%
Similarity by Source

Internet Sources:
9%
Publications:
11%
Student Papers:
6%

sources:

1 2% match (student papers from 18-Dec-2017)
Submitted to Higher Education Commission Pakistan on 2017-12-18

2 1% match (Internet from 25-Jul-2020)
https://www.mdpi.com/1422-0067/21/8/2710/htm

3 1% match (Internet from 13-Oct-2020)
https://www.hindawi.com/journals/bmri/2015/461524/

4 1% match (student papers from 04-Jan-2017)
Submitted to Higher Education Commission Pakistan on 2017-01-04

5 < 1% match (Internet from 14-Dec-2019)
https://www.mdpi.com/1422-0067/19/5/1433/html

6 < 1% match (publications)
Sara Mumtaz, Gökhan Nalbant, Esra Yıldız Bölükbaşı, Zele Huma, Nafees Ahmad, Aslıhan Tolun, Sajid Malik. "Novel EDAR mutation in tooth agenesis and variable associated features", European Journal of Medical Genetics, 2020

7 < 1% match (publications)
Nameirakpam Johnson, Himanshi Chaudhary, Rajni Kumrah, Rakesh Kumar Pilania et al. "Syndrome of progressive deforming non-inflammatory arthritis of childhood: two patients of camptodactyly-arthropathy-coxa vara-pericarditis syndrome", Rheumatology International, 2020

8 < 1% match (publications)
Éva Morava, Maïlys Guillard, Dirk J Lefeber, Ron A Wevers. "Autosomal recessive cutis laxa syndrome revisited", European Journal of Human Genetics, 2009

9 < 1% match (publications)
"Abstracts from the 51st European Society of Human Genetics Conference: Posters",

ORIGINAL ARTICLE

Homozygous *CHST11* mutation in chondrodysplasia, brachydactyly, overriding digits, clino-symphalangism and synpolydactyly

Rana Muhammad Kamran Shabbir,[1] Gökhan Nalbant,[2] Nafees Ahmad,[3] Sajid Malik,[1] Aslıhan Tolun[2]

ABSTRACT

Background Carbohydrate sulfotransferase 11 (CHST11) is a membrane protein of Golgi that catalyses the transfer of sulfate to position 4 of the N-acetylgalactosamine residues of chondroitin. Chondroitin sulfate is the predominant proteoglycan in cartilage, and its sulfation is important in the developing growth plate of cartilage. A homozygous deletion encompassing part of the gene and the embedded miRNA *MIR3922* had been detected in a woman with hand/foot malformation and malignant lymphoproliferative disease. Chst11-deficient mouse has severe chondrodysplasia, congenital arthritis and neonatal lethality. We searched for the causative variant for the unusual combination of limb malformations with variable expressivity accompanied by skeletal defects in a consanguineous Pakistani kindred.

Methods We performed detailed clinical investigations in family members. Homozygosity mapping using SNP genotype data was performed to map the disease locus and exome sequencing to identify the underlying molecular defect.

Results The limb malformations include brachydactyly, overriding digits and clino-symphalangism in hands and feet and syndactyly and hexadactyly in feet. Skeletal defects include scoliosis, dislocated patellae and fibulae and pectus excavatum. The disease locus is mapped to a 1.6 Mb region at 12q23, harbouring a homozygous in-frame deletion of 15 nucleotides in *CHST11.* Novel variant c.467_481del (p.L156_N160del) is deduced to lead to the deletion of five evolutionarily highly conserved amino acids and predicted as damaging to protein by in silico analysis. Our findings confirm the crucial role of CHST11 in skeletal morphogenesis and show that *CHST11* defects have variable manifestations that include a variety of limb malformations and skeletal defects.

INTRODUCTION

Carbohydrate sulfotransferases catalyse the transfer of sulfate to the carbohydrate groups in glycoproteins and glycolipids. The glycosaminoglycan chondroitin sulfate is attached to the surface of certain cells, and proper sulfation of the molecule is essential for its roles in the extracellular matrix of several tissues such as cartilage, bone, ligaments and tendons. Carbohydrate sulfotransferase protein family has 15 members (CHST1-15). Carbohydrate sulfotransferase 11 (CHST11), also known as chondroitin-4-sulfotransferase-1 (C4ST-1), is a membrane enzyme of the Golgi complex and the primary enzyme for 4-O-sulfation of N-acetylgalactosamine residues of chondroitin.[1] It regulates the chain length of chondroitin sulfate.[2] The crucial role of the enzyme in skeletal morphogenesis has been shown first in mice.[3] Mouse orthologue *Chst11* has a highly specific temporal and spatial expression pattern in embryogenesis. Mice with Chst11 deficit die within hours after birth and have severe dwarfism and other skeletal defects resulting from chondrodysplasia, indicating that the protein is required for the growth and morphogenesis of only those bones that grow by endochondrial bone formation (ossification).[3] A 55 kb homozygous deletion encompassing *CHST11* exon 2 and the embedded miRNA *MIR3922* was identified in a woman with mildly short stature, hand/foot malformation encompassing brachydactyly, campto-clinodactyly and hyperphalangy as well as malignant lymphoproliferative disease, and her deceased sister was similarly affected.[4]

We report the detailed clinical findings in a family afflicted with an unusual combination of highly variable skeletal defects in vertebrae and leg bones and additionally hand and foot malformations (predominantly brachydactyly), and a homozygous damaging variant in *CHST11*. Our results delineate the phenotype of CHST11 deficiency and show that the deficiency has several clinical manifestations with variable expressivity.

MATERIALS AND METHODS

All information was obtained according to the Declaration of Helsinki II.

Family

The family originates from Punjab, Pakistan and was first investigated in 2005. The six-generation pedigree strongly suggested an autosomal recessive inheritance pattern (figure 1). Ten members (eight males and two females) of the family were affected. In total, 21 family members (9 affected and 12 unaffected) were physically examined with the help of local physicians. Photographs of nine affected members and roentgenograms of three of those individuals were obtained.

Genetic study

Seven affected and 11 unaffected members of the family participated in the genetic study (figure 1).

► Additional material is published online only. To view, please visit the journal online (http://dx.doi.org/10.1136/jmedgenet-2017-105003).

[1]Human Genetics Program, Department of Animal Sciences, Faculty of Biological Sciences, Quaid-i-Azam University, Islamabad, Pakistan
[2]Department of Molecular Biology and Genetics, Boğaziçi University, Istanbul, Turkey
[3]Institute of Biomedical and Genetic Engineering, Islamabad, Pakistan

Correspondence to
Dr. Sajid Malik, Human Genetics Program, Department of Animal Sciences Faculty of Biological Sciences, Quaid-i-Azam University Islamabad Pakistan ; malik@qau.edu.pk and Professor Aslıhan Tolun, Department of Molecular Biology and Genetics, Boğaziçi University, Istanbul 34342, Turkey; tolun@boun.edu.tr

Received 23 August 2017
Revised 18 January 2018
Accepted 15 February 2018

To cite: Shabbir RMK, Nalbant G, Ahmad N, *et al*. *J Med Genet* Epub ahead of print: [please include Day Month Year]. doi:10.1136/jmedgenet-2017-105003

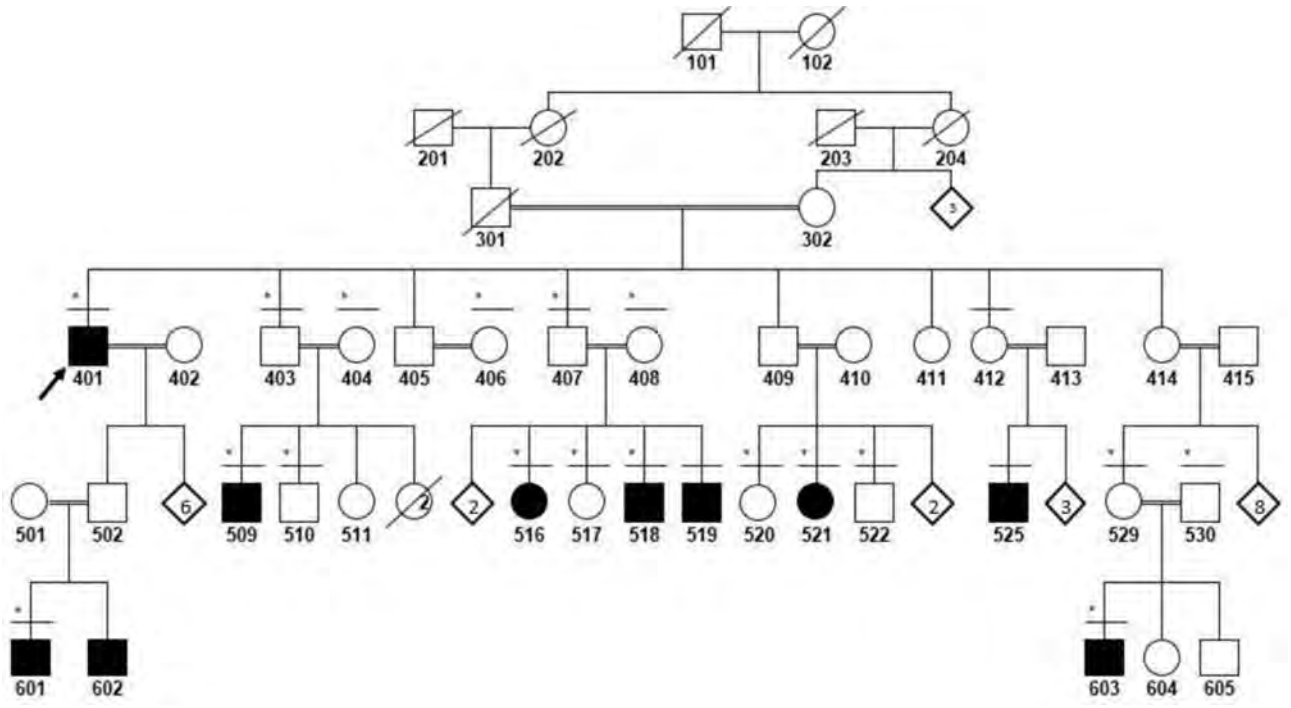

Figure 1 Pedigree. A horizontal line above the symbol indicates that the individual was physically examined. *DNA available.

SNP genotype data of four affected individuals (401, 509, 516 and 603) from different branches of the kindred were generated using Illumina Human OmniExpress-24 BeadChip and used to detect shared homozygosity regions by Homozygosity Mapper (www.homozygositymapper.org). 'Broad' regions (where small decreases of the score are neglected) in the output were considered because the patients were from different branches of the family and thus mutations could have occurred in regions of shared homozygosity in a branch. Regions with scores >80% of the maximum score were further investigated. Genotypes were compared on Excel sheets to verify that the homozygosity at the identified gene locus was shared by the patients. Genomic deletions and duplications were detected through cnvPartition (V.3.2.0) CNV Analysis Plug-in for Genome Studio.

Exome sequencing library for affected individual 516 was prepared using IDT xGen Exome Research Panel V.1.0 that targets 98% of bases in RefSeq database and sequencing was performed using Illumina HiSeq2500. The generated reads were aligned to reference sequence GRCh37/hg19 using BWA-0.7.12-r1039. Exome sequencing yielded a mean depth of 104X with approximately 99.68% of the targeted bases read with at least 20X depth. Variants were called with SAMtools-1.6. After annotation of the variants by ANNOVAR, we considered those variants that are novel or have frequencies <0.01 in all populations reported in databases ExAC and 1000 Genomes, residing in the identified gene region, having number of reads to the total reads ratios >0.5 and possibly damaging to protein. Sanger sequencing was carried out to validate the single candidate variant detected, and its segregation in 18 family members was investigated by electrophoresis on an 8% polyacrylamide gel to resolve fragments for wild-type allele (283 bp) and variant allele (268 bp). Sequences of the primers for PCR amplifications are F: CATCTACTGCTACGTGCCCA and R: GTACCGCTTGTGGAAGGAGA. The variant is submitted to ClinVar with submission number SUB3259126.

In silico analysis

Human reference sequence GRCh38 was retrieved from NCBI database (https://www.ncbi.nlm.nih.gov). Conservation of the genomic region of interest across species was visualised by HomoloGene (https://www.ncbi.nlm.nih.gov/homologene). Computational algorithms Mutation Taster and Protein Variation Effect Analyzer (PROVEAN) were used to predict the effect of the identified deletion on the protein.[5 6] We used Predict Protein Server (https://www.predictprotein.org) to predict and compare the secondary structures of the reference and variant proteins. To visualise the effect of the deletion on CHST11, we predicted tertiary (three-dimensional (3D)) structures for the reference and variant proteins encoded by the two splice variants by using I-TASSER,[7 8] predicting the 3D structures based on threading approach and assembling the structural fragments using Monte Carlo simulations. For evaluation and overlay of 3D models, RAMPAGE (http://mordred.bioc.cam.ac.uk/~rapper/rampage.php) and VMD tools were used.[9]

RESULTS

Clinical findings

None of the 12 unaffected relatives examined had any skeletal defects or limb malformations. All affected individuals have skeletal defects, generally bilateral and symmetrical, which primarily affect the limbs. Clinical findings are compiled in table 1 and radiological findings in table 2. Shortened lower leg bones have led to mild short stature in the patients investigated (see online supplementary table S1). The average of the heights of three of the adult patients (509, 525 and 603) was somewhat but not significantly shorter than the average of the heights of the three available parents (one for each patient). The hand/foot malformation can be summarised as short and adducted thumbs, overriding fingers (most often third over fourth), short second fingers with ulnar curvature and short and campto-clinodactylous 3–5 fingers in hands, and as short and broad halluces with

Table 1 Characteristics of affected family members

Patient	401	509	516	518	519	521	525	601	603	Chopra *et al*[4]
Sex, age (years)	M, 50	M, 20	F, 10	M, 8	M, 4	F, 13	M, 24	M, 6	M, 18	F, 46
Hands										
Thumb: adducted and short	+, broad	–	+	+ (R)	+	–	–	–	–	–
Index finger: ulnar curved	+, short	+, short	+, short	+, short	+, short, overriding third finger	+, short	+	+	+	+ (R), radial curved (L)
Middle finger: curved	Ulnar, short	Ulnar	Radial, elongated, camptodactyly	–	Ulnar, overriding the fourth finger	Radial	Ulnar	Ulnar	Ulnar, short	Ulnar, short
Ring finger: campto-clionodactylous, curved	+, ulnar	+, radial	+, radial	–, –	+, radial	+, –	+, radial	+, –	-, ulnar	–
Fifth finger: campto-clinodactyly	+, short	+, short	+, short, radial curved	+	–	+	+	+	+, ulnar curved	+
Overriding finger	–	+, 3–4	+, 2–3	–	+, 3–4, 2–3	–	+, 3–4	+, 3–4	–	–
Flexion creases on fingers	Missing	Missing	Extra	Missing, extra	Extra	Extra	Extra	Extra	Missing, extra	NA
Feet										
Hallux: varus inclination	+, short, broad	+	+, short, broad	+	+	–	+	+, short, broad	–	–
Second toe overriding third	+	–	+	–	+, overriding toes	–	+	+	+	–
Third toe: campto-clinodactyly	–	+	+	–	–	–	–	–	+	–
Fourth toe: short	–	–	–	–	–	–	–	+, camptodactylous	+, camptodactylous	+
Fifth toe: short	+	+	–	+	–	–	+	+	+	+
Postaxial polydactyly	+	–	–	–	–	–	+, synpolydactyly (L)	–	+, synpolydactyly (R)	–
Wide-space between 1 and 2 toes	–	–	–	+	–	–	+	+	+	–
Skeletal and other findings										
Scoliosis	+	+	NA	+	NA	NA	+	NA	+	–
Lumber lordosis	+	–	NA	+	NA	NA	–	NA	+	–
Pectus excavatum	–	+	–	–	–	–	–	–	+	–
Prominent clavicle	+	–	NA	–	–	NA	+	–	+	–
Pain in running	+	+	–	+	–	–	–	–	+	–
Joint pain	+, knee	+, backbone, lumbar region	NA	NA	NA	NA	NA	NA	NA	–
Swelling of joints	–	–	NA	NA	NA	NA	NA	NA	NA	–
Morning stiffness of joints	+	+	NA	NA	NA	NA	NA	NA	NA	–
Early fatigue	+	+	NA	NA	NA	NA	NA	NA	NA	–

All findings are bilateral unless specified otherwise.
+, feature present; -, feature absent; R, right limb; L, left limb; NA, not assessed.

Table 2 Radiological findings in affected family members

Patient	401	509	519	Chopra *et al*.[4]
Sex, age (years)	M, 50	M, 20	M, 4	F, 46
Upper limbs				
Hypertrophic first digital rays	+	–	–	–
Short proximal phalanx	2–4 fingers	2–4 fingers	–	Third finger; long proximal phalanx in second finger
Hypoplastic distal phalanges	+	–	+	–
Delta phalanx	–	–	2–3	–
Extra osseous elements in fingers	4–5	2–4	2–4	2–3
Symphalangism in fingers	4	5	–	2
Fifth finger with two phalanges	+	+	–	–
Carpals	Crowding	Crowding	Immature/missing	Crowding, hypoplastic index metacarpal
Radii and ulnae	Short	Short, narrow spaces	Wide spaces	NA
Humerae curved	–	+	–	NA
Lower limbs				
Hypertrophic first digital rays	+	+	+	–, symphalangism in first digital ray
Dysmorphic and short proximal and distal phalanges	+	+	+	+, short midphalanx of 2–3 toes
Duplication of fifth phalanges	+	–	–	–
Crowding of tarsals	+	+	–	–
Laterally displaced calcanei	+	–	+	–
Narrow aligned femora and tibiae	+	+	NA	–
Thinning of tibiae and fibulae	+	+	–	–
Dislocated patellae	+	+	NA	–
Latero-ventrally displaced fibulae	+	+	–	–
Skeletal				
Scoliosis	Thoracic and lumbar vertebrae	Thoracic vertebrae	NA	–
Sacroiliac joint gap	+	–	NA	–

NA, not assessed.

varus inclinations, second toes overriding the third, short fifth toes and postaxial polydactyly in feet (figure 2 and figure 3). There was no restriction in movement in wrists or ankles despite the crowding of carpals and tarsals. Three of the elder patients complained of exhausting easily and being not able to carry heavy loads. Both of the adult patients interrogated (401 and 509) complained of joint pain indicative of osteoarthritis, but the current knee and ankle X-ray images did not show any degenerative changes characteristic for osteoarthritis (figure 2). All patients had normal mental status, and the adult males were engaged in manual jobs. Asymmetric face was observed in one patient (603). Another patient (525) and two of his siblings without skeletal defects (526 and 527) were deaf-mute. Details of the clinical findings for three of the elder patients are given below.

Index patient 401

He is the eldest and the most severely affected patient. He was aged 50 years at the time of the most recent clinical examination. His mildly short stature was due to short lower leg bones, and clavicles were prominent. Radiographs revealed mild scoliosis in the thoracic and pelvic vertebrae with an impression of lumbar lordosis (table 1). Spaces between femurs and tibiae/fibulae were narrow, and fibulae displayed posterior dislocation. Patellae were dorsolaterally displaced, and spaces in knee joints were narrow. A slight curvature was noted in left femur. Patient had a slow gait and difficulty in running. He complained of joint pain, morning stiffness of joints and early fatigue, which are symptoms reminiscent of osteoarthritis. Left ear was prominent.

Mild shortening of hands and feet was noted. Fingers were short and odd-shaped, and thumbs were broad and adducted (figure 2). Second, third and fifth fingers were short, and camp-to-clinodactyly was evident at the distal phalangeal joints of fourth and fifth fingers. All fingers were with ulnar deflections. Radiographic investigations revealed that in 2–4 fingers proximal phalanges were short and dysplastic, whereas distal phalanges were hypoplastic. There were signs of symphalangism at proximal phalangeal joint of fourth fingers. Fifth fingers had only two phalanges, and proximal phalanges were enlarged. There were extra osseous elements at the distal phalangeal joints of 4–5 fingers. The first digital rays appeared hypertrophic. Mild shortening of radii and ulnae and crowding of carpals were noted.

Both feet had a supernumerary postaxial toe. Halluces were short, hypertrophic and displayed varus inclinations (figure 2). Second toes were overriding the third. Shortening of fifth and sixth toes was evident. Radiographs revealed five metatarsals with hypoplastic ends and bearing six phalanges. Proximal and distal phalanges of all toes were dysmorphic and dwarfed. Tarsals were crowded and overriding each other, whereas calcanei were laterally displaced.

Ultrasonographic examination of the chest and abdomen and biochemical analyses of urine and blood were unremarkable.

Patient 509

Skeletal findings in the man aged 20 years were mildly short stature, scoliosis and pectus excavatum (figure 2). Spaces between radii and ulnae were narrow. He had recurrent joint pain particularly in the lumbar vertebrae, morning stiffness of

Figure 2 Malformations of hands and feet and scoliosis in three patients.

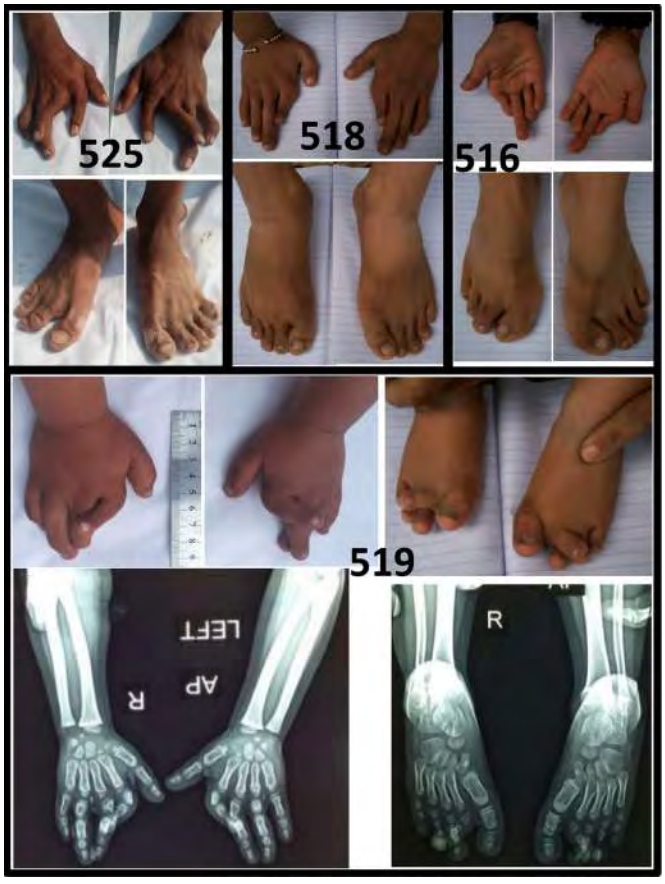

Figure 3 Malformations of hands and feet in four patients.

joints and early fatigue. He had length discrepancy of forearms, with left arm approximately 17% shorter than the right. He had brachydactyly of second fingers, third fingers overriding fourth and campto-clinodactyly of fifth fingers. Radiographs of hands revealed short proximal phalanges in 2–4 fingers, hypoplastic terminal phalanges in 2–5 fingers and symphalangism of fifth fingers. In the feet, bilateral campto-clinodactyly of third toes and shortening of fifth toes as well as cutaneous fusion in left 1–2 toes were noted.

Patient 603

The young man aged 18 years had mildly short stature, scoliosis, pectus excavatum, prominent clavicle and scapula, lumbar lordosis and mildly asymmetric face (figure 2). He also had disproportionate and short fingers with a camptodactylous and symphalangus presentation. Fingers had missing and/or supernumerary flexion creases, indicative of symphalangism and hyperphalangism, respectively. Second and fifth toes were short, and third toes were campto-clinodactylous. Postaxial synpolydactyly was noted in the right foot.

Genetic findings

Homozygosity mapping using SNP genotype data of four patients from different branches of the family detected two loci (figure 4). Alignment of the SNP data on an Excel sheet revealed that the maximal shared homozygosity in the larger region (at 12q23.3) was 1.6 Mb, between rs1922261 (nucleotide 104 854 011) and rs6539247 (nucleotide 106 459 902). Homozygosity in the region was identical in the four patients, and two of the patients (401 and 516) shared homozygosity for 11.5 Mb. Shared homozygosity in the smaller region (at 17q23.2) was <0.7 Mb. At the time no similar phenotype was associated with any gene in either region, and thus we launched exome sequencing.

In the exome file of a patient, rare and novel homozygous variants possibly affecting the protein were investigated within the two regions mentioned above. All rare (frequency <0.01) variants within the candidate region at 17q23.2 were heterozygous, indicating that the kindred was non-informative for the SNPs used and hence the homozygosity was not due to identity by descent, excluding the region. The region at 12q23.3 was thus identified as the disease locus, and it harboured a single candidate variant (see online supplementary table S2). This in-frame deletion of 15 nucleotides in *CHST11* exon 3 affects both transcript isoforms: c.467_481del (p.L156_N160del; NM_001173982.1) or c.482_496del (p.L161_N165del; NM_018413.5). The variant is deduced to lead to the deletion of five amino acids (figure 4), and not reported in databases ExAC, 1000 Genomes or ESP6500. Unaffected relatives tested were either heterozygous or non-carriers (see online supplementary figure S1). This novel variant was an excellent candidate to underlie the disease in the family, considering the function of the encoded protein.

Lastly, to rule out any contribution to this unusual phenotype, we evaluated all variants in known brachydactyly genes, that is, *BMP2, BMPR1B, CHSY1, GDF5, HOXD13, IHH, NOG, PRMT7, PTHLH, ROR2, RUNX2* and *TRPV4*. The targeted regions were adequately covered (see online supplementary table S3). No variant with a frequency <0.01, number of read to total reads ratios >0.25 and predicted to be possibly damaging to the protein was found (see online supplementary table S3).

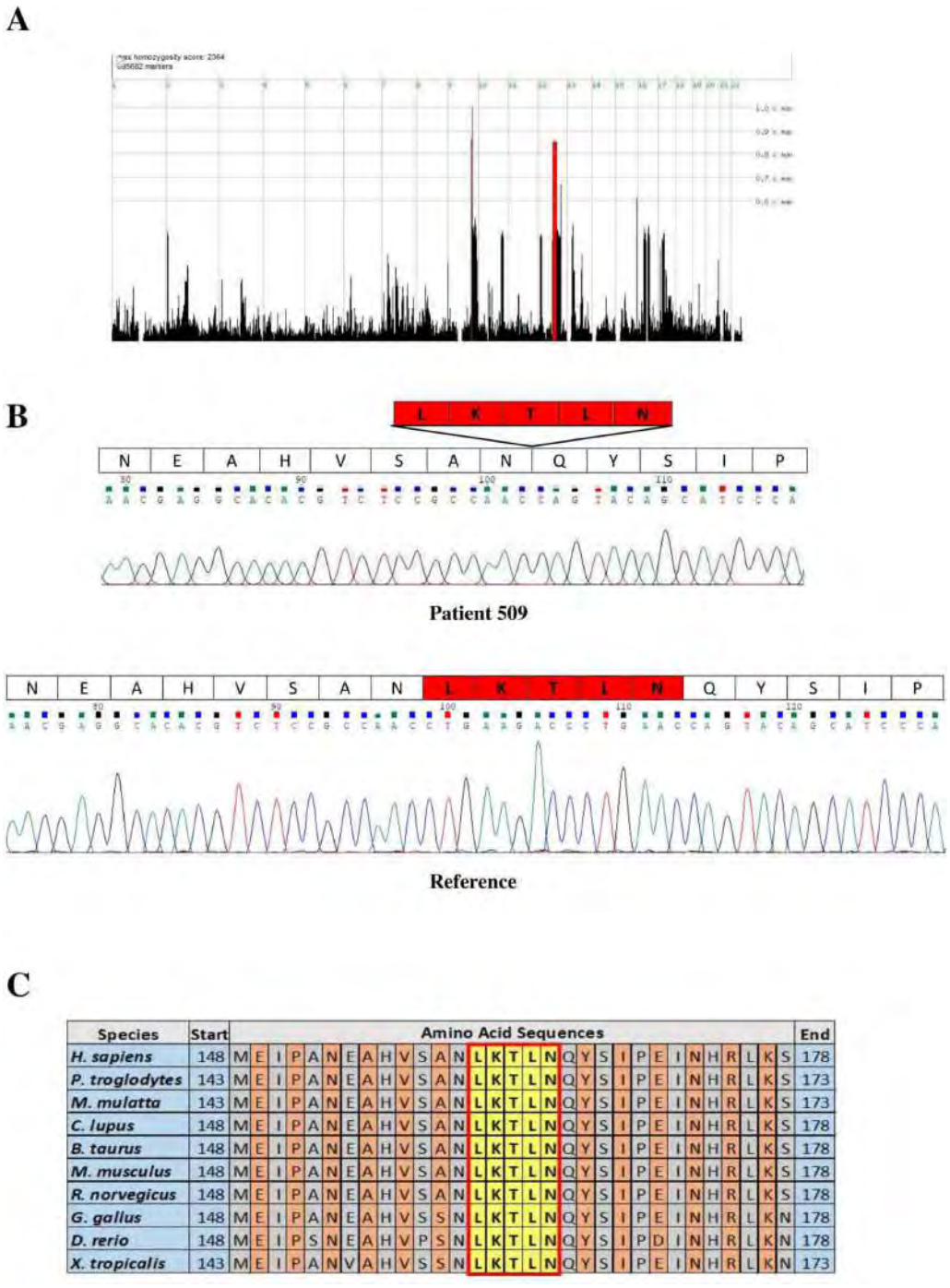

Species	Start	Amino Acid Sequences	End
H. sapiens	148	M E I P A N E A H V S A N **L K T L N** Q Y S I P E I N H R L K S	178
P. troglodytes	143	M E I P A N E A H V S A N **L K T L N** Q Y S I P E I N H R L K S	173
M. mulatta	143	M E I P A N E A H V S A N **L K T L N** Q Y S I P E I N H R L K S	173
C. lupus	148	M E I P A N E A H V S A N **L K T L N** Q Y S I P E I N H R L K S	178
B. taurus	148	M E I P A N E A H V S A N **L K T L N** Q Y S I P E I N H R L K S	178
M. musculus	148	M E I P A N E A H V S A N **L K T L N** Q Y S I P E I N H R L K S	178
R. norvegicus	148	M E I P A N E A H V S A N **L K T L N** Q Y S I P E I N H R L K S	178
G. gallus	148	M E I P A N E A H V S S N **L K T L N** Q Y S I P E I N H R L K N	178
D. rerio	148	M E I P S N E A H V P S N **L K T L N** Q Y S I P D I N H R L K N	178
X. tropicalis	143	M E I P A N V A H V S S N **L K T L N** Q Y S I P E I N H R L K N	173

Figure 4 Mapping and variant identification. (A) Homozygosity mapping. (B) Electrophoretograms showing *CHST11* c.467_481del (p.L156_N160del; NM_001173982.1). (C) Evolutionary conservation of the amino acids deleted in patients (boxed).

Protein analysis

CHST11 is encoded as a 352 or a 347-amino acid protein by the two transcript isoforms. It has a cytoplasmic topological domain, a transmembrane domain and a luminal domain.[10] The luminal domain is catalytic and has a phosphosulfate binding site and a phosphate binding site. The deletion we identified lies in the luminal topological domain, in a region where the amino acid sequence is highly conserved across species (figure 4). To investigate whether the variant is damaging to the protein, we first employed online computational algorithms. Mutation Taster predicted the variant as disease causing (score 0.98) and PROVEAN as highly deleterious (score −20.03). Next, we applied protein modelling using threading approach. I-TASSER predicted five models for each version of the protein, and for comparison one model was selected for each version, based on the C-scores, Exp. TM-scores and Exp. RMSD. The values of these parameters for selected models are presented in supplementary table S4. Comparison of reference and variant protein models using RAMPAGE revealed differences in the number of favoured and outlier regions (see online supplementary table S5). The superimposed structures of the reference (NP_060883.1; NP_001167453.1) and variant protein models for both of the splice variants showed differences in protein folding, especially in the cytoplasmic and transmembrane domains (see online supplementary figure S2).

DISCUSSION

We performed clinical investigations in a family afflicted with skeletal defects that include scoliosis, dislocated patellae and fibulae and pectus excavatum as well as limb malformations that include brachydactyly. We mapped the disease locus and identified a 5-amino acid deletion in the catalytic, luminal domain of CHST11. Chopra *et al*[4] reported a woman of Irish descent with a deletion of 55 kb that encompasses *CHST11* exon 2 and the embedded *MIR3922*. She had brachydactyly with disproportionately short index fingers and radial or ulnar deviations of fingers and toes at the interphalangeal joints, long proximal phalanx in the second fingers, a fused distal phalanx and subluxation of the index metacarpophalangeal joint, third finger with four phalanges and a horizontal articulation at the base of proximal phalanx, fourth and fifth fingers with long proximal phalanges, and fifth finger middle phalanx with a curved articulation. Features she shared with our patients are brachydactyly, hyperphalangy and radial and ulnar deviation of fingers and toes. However, unlike our patients she also had symphalangism of first toe, short middle phalanges of second and third toes, loss of phalanx in fourth toes and normal thumbs and wrist bones (no crowding of carpals or tarsals). Our patients had additional features such as adducted thumbs, overriding-fingers, campto-clinodactyly of third and fourth fingers, missing or extra flexion creases in certain fingers, hallux varus, overriding toes and postaxial polydactyly in feet. However, our patients had skeletal defects as well, including scoliosis, dislocated patellae and fibulae, pectus excavatum and predilection of mild osteoarthritis. Also, the Irish-descent woman had a history of acute respiratory distress syndrome which was not observed in any of our patients. Mouse *Chst11*-knockout embryos had severely shortened limbs, small rib cage, kinked vertebral column and dome-shaped skull. Additional findings included absence of second and third phalanges in both fore limbs and hind limbs, impaired segmentation of cartilage in the digits and misshapen vertebrae with poorly formed dorsal arches.[3] The similarities of the phenotypes of our patients to those of the Irish-descent woman and the mouse knockout as well as the results of our bioinformatics analyses make it highly likely that the variant we identified in *CHST11* is the molecular defect underlying the disease in the presented family. The variant is in a protein region that is highly conserved across species indicating the functional importance of the region and predicted to be harmful to the protein. The site of the deletion is not close to any of the four N-glycosylation sites necessary for the activity of the enzyme;[11] however, the deletion is predicted to considerably alter the tertiary structure of the protein and thus probably influence its integration into the Golgi membrane and/or its binding with ligand.

It has been hypothesised that if CHST11 has a role in cancer, the role is the suppression of the proliferation of tumour but not the development of the tumour.[12] The Irish-descent woman and her similarly affected deceased sister additionally had malignant lymphoproliferative disease.[4] The sisters developed the disease by the ages of 36 and 17 years, respectively, and so did their father, at the age of 59. The family we present has no cancer history, verifying the hypothesis. Chopra *et al*[4] suggested that alternatively *MIR3922*, deleted in their patients, could be the gene with the tumour suppressor role in the lymphocyte lineage.

[3]Mice deficient for Chst11 had severe dwarfism and died shortly after birth. They had severe skeletal and limb malformations and severely shortened facial bones that included the maxilla, mandible and nasal bones. Hence, the Chst11-deficient mice were much more severely affected than the humans, as is generally not the case for mouse knockouts. The deletion of exon 2 in the woman described by Chopra *et al*[4] is deduced to shift the translational reading frame and thus expected to be a much more severe variant than the one in our patients. However, her clinical features we attributed to CHST11 deficit seem to be not more severe than those in our patients (tables 1 and 2), assuming that the additional symptoms of respiratory and immunological systems, skin lesions, tachypnoea and lymphoproliferative disease she had are likely not related to the CHST11 deletion. Hence, there seems to be no apparent genotype-phenotype correlation for CHST11 variants.

The pattern of short fingers in the family was not fully concordant with any of the well-characterised brachydactylies but appeared to be closest to brachydactyly type C (BDC), caused by heterozygous *GDF5* mutation.[13] BDC is characterised by shortening of 2–5 fingers with fourth finger affected the least. BDC may exhibit additional features such as hyperphalangism of second and third fingers together with ulnar deviation of second fingers.[14 15] Limb anomalies in the family we present are more complex considering the additional overriding fingers/overriding toes, campto-clino-symphalangus digits and polydactylous and syndactylous toes. Additionally, patients have other skeletal findings. The similarities in the phenotypes could be due to the fact that the function of growth/differentiation factor 5 (GDF5) is related to the expression of *CHST11*. GDF5 is the secreted ligand of the transforming growth factor-β superfamily. Its binding to the receptor leads to the activation of chondrogenic transcription factor Sox9 through Smad3 in rat.[16 17] Sox9/SOX9 was shown to regulate the expression of *Chst11*/*CHST11* in a rat chondrosarcoma cell line, mouse chondrocytes and human dermal fibroblasts.[18 19] Transcription factors SOX9 and SOX5/SOX6 cooperate through super-enhancers to drive chondrogenesis.[19] Also, *GDF5* is a very strong candidate gene associated with osteoarthritis, as *CHST11* is.[20 21]

One of the paralogs of *CHST11* is *CHST3 (C6ST-1),* encoding the chondroitin 6-O-sulfotransferase. A homozygous missense variant (p.R304Q) was identified in an Omani kindred with severe chondrodysplasia with progressive spinal involvement.[22] Limb involvement included rhizomelic shortening, genu valgum, cubitus valgus, mild brachydactyly and camptodactyly. Considering also that variants in *CHSY1*, encoding chondroitin synthase 1, cause Temtamy preaxial brachydactyly syndrome (MIM 605282), with some features overlapping with the disease in our patients (brachydactyly, short thumb, clinodactyly, symphalangism, phalangeal duplication together with syndactyly, scoliosis and pectus excavatum),[23 24] defects in other chondroitin-related proteins could be expected to manifest with skeletal defects and limb malformations.

Congenital osteoarthritis-like symptoms in Chst11-deficient mice is discordant with human phenotype. Degenerative changes in joints typical for osteoarthritis were not evident in the roentgenographs of the two elder patients we investigated (401 and 509) at the ages of 50 and 20 years (figure 3). However, both patients complained of joint pain, morning stiffness of joints and early fatigue, indicative of early symptoms of the disease. In the Irish-descent woman, no sign of osteoarthritis was mentioned.[4] Of note, genome-wide association studies have identified *CHST11* locus as a susceptibility locus for osteoarthritis and found intronic SNP rs835487 to be significantly associated with knee osteoarthritis.[21]

In summary, this is the first report of a family with a variant affecting *CHST11* only. Extensive clinical investigations in nine affected individuals defined the variable phenotype of a *CHST11* damaging variant. We propose that patients with

skeletal chondrodysplasia, especially in concurrence with limb malformations be screened for causative variants in *CHST11* and other chondroitin-related genes.

Acknowledgements The authors would like to thank the family members for their cooperation.

Contributors AT and SM were responsible for the concept and design of the study. GN and NA generated and interpreted the data. SM and RMKS contributed the clinical data. AT, SM, GN and NA drafted the manuscript. All authors revised the manuscript.

Funding This study was supported by the Scientific and Technological Research Council of Turkey (TÜBİTAK 114Z829 to AT) and URF-QAU, Pakistan (2013-2014 to SM).

Competing interests None declared.

Patient consent Parental/guardian consent obtained.

Ethics approval The ethical review committee of Quaid-i-Azam University and the Boğaziçi University Institutional Review Board for Research with Human Participants.

Provenance and peer review Not commissioned; externally peer reviewed.

REFERENCES

1. Mikami T, Kitagawa H. Biosynthesis and function of chondroitin sulfate. *Biochim Biophys Acta* 1830;2013:4719–33.
2. Izumikawa T, Okuura Y, Koike T, Sakoda N, Kitagawa H. Chondroitin 4-O-sulfotransferase-1 regulates the chain length of chondroitin sulfate in co-operation with chondroitin N-acetylgalactosaminyltransferase-2. *Biochem J* 2011;434:321–31.
3. Klüppel M, Wight TN, Chan C, Hinek A, Wrana JL. Maintenance of chondroitin sulfation balance by chondroitin-4-sulfotransferase 1 is required for chondrocyte development and growth factor signaling during cartilage morphogenesis. *Development* 2005;132:3989–4003.
4. Chopra SS, Leshchiner I, Duzkale H, McLaughlin H, Giovanni M, Zhang C, Stitziel N, Fingeroth J, Joyce RM, Lebo M, Rehm H, Vuzman D, Maas R, Sunyaev SR, Murray M, Cassa CA. Inherited CHST11/MIR3922 deletion is associated with a novel recessive syndrome presenting with skeletal malformation and malignant lymphoproliferative disease. *Mol Genet Genomic Med* 2015;3:413–23.
5. Schwarz JM, Rödelsperger C, Schuelke M, Seelow D. MutationTaster evaluates disease-causing potential of sequence alterations. *Nat Methods* 2010;7:575–6.
6. Choi Y, Chan AP. PROVEAN web server: a tool to predict the functional effect of amino acid substitutions and indels. *Bioinformatics* 2015;31:2745–7.
7. Zhang Y. I-TASSER server for protein 3D structure prediction. *BMC Bioinformatics* 2008;9:40.
8. Yang J, Yan R, Roy A, Xu D, Poisson J, Zhang Y. The I-TASSER Suite: protein structure and function prediction. *Nat Methods* 2015;12:7–8.
9. Humphrey W, Dalke A, Schulten K. VMD: visual molecular dynamics. *J Mol Graph* 1996;14:33–8.
10. Kahsay RY, Gao G, Liao L. An improved hidden Markov model for transmembrane protein detection and topology prediction and its applications to complete genomes. *Bioinformatics* 2005;21:1853–8.
11. Yusa A, Kitajima K, Habuchi O. N-linked oligosaccharides are required to produce and stabilize the active form of chondroitin 4-sulphotransferase-1. *Biochem J* 2005;388(Pt 1):115–21.
12. Cooney CA, Jousheghany F, Yao-Borengasser A, Phanavanh B, Gomes T, Kieber-Emmons AM, Siegel ER, Suva LJ, Ferrone S, Kieber-Emmons T, Monzavi-Karbassi B. Chondroitin sulfates play a major role in breast cancer metastasis: a role for CSPG4 and CHST11 gene expression in forming surface P-selectin ligands in aggressive breast cancer cells. *Breast Cancer Res* 2011;13:R58.
13. Farooq M, Nakai H, Fujimoto A, Fujikawa H, Kjaer KW, Baig SM, Shimomura Y. Characterization of a novel missense mutation in the prodomain of GDF5, which underlies brachydactyly type C and mild Grebe type chondrodysplasia in a large Pakistani family. *Hum Genet* 2013;132:1253–64.
14. Castriota-Scanderbeg A, Garaci FG, Beluffi G. Angel-shaped phalanges in brachydactyly C: a case report, and speculation on pathogenesis. *Pediatr Radiol* 2005;35:535–8.
15. Gutiérrez-Amavizca BE, Brambila-Tapia AJ, Juárez-Vázquez CI, Holder-Espinasse M, Manouvrier-Hanu S, Escande F, Barros-Núñez P. A novel mutation in CDMP1 causes brachydactyly type C with "angel-shaped phalanx". A genotype-phenotype correlation in the mutational spectrum. *Eur J Med Genet* 2012;55:611–4.
16. Furumatsu T, Ozaki T, Asahara H. Smad3 activates the Sox9-dependent transcription on chromatin. *Int J Biochem Cell Biol* 2009;41:1198–204.
17. Hatakeyama Y, Tuan RS, Shum L. Distinct functions of BMP4 and GDF5 in the regulation of chondrogenesis. *J Cell Biochem* 2004;91:1204–17.
18. Ohba S, He X, Hojo H, McMahon AP. Distinct Transcriptional Programs Underlie Sox9 Regulation of the Mammalian Chondrocyte. *Cell Rep* 2015;12:229–43.
19. Liu CF, Lefebvre V. The transcription factors SOX9 and SOX5/SOX6 cooperate genome-wide through super-enhancers to drive chondrogenesis. *Nucleic Acids Res* 2015;43:8183–203.
20. Miyamoto Y, Mabuchi A, Shi D, Kubo T, Takatori Y, Saito S, Fujioka M, Sudo A, Uchida A, Yamamoto S, Ozaki K, Takigawa M, Tanaka T, Nakamura Y, Jiang Q, Ikegawa S. A functional polymorphism in the 5′ UTR of GDF5 is associated with susceptibility to osteoarthritis. *Nat Genet* 2007;39:529–33.
21. Yau MS, Yerges-Armstrong LM, Liu Y, Lewis CE, Duggan DJ, Renner JB, Torner J, Felson DT, McCulloch CE, Kwoh CK, Nevitt MC, Hochberg MC, Mitchell BD, Jordan JM, Jackson RD. Genome-Wide Association Study of Radiographic Knee Osteoarthritis in North American Caucasians. *Arthritis Rheumatol* 2017;69:343–51.
22. Thiele H, Sakano M, Kitagawa H, Sugahara K, Rajab A, Höhne W, Ritter H, Leschik G, Nürnberg P, Mundlos S. Loss of chondroitin 6-O-sulfotransferase-1 function results in severe human chondrodysplasia with progressive spinal involvement. *Proc Natl Acad Sci U S A* 2004;101:10155–60.
23. Temtamy SA, Meguid NA, Ismail SI, Ramzy MI. A new multiple congenital anomaly, mental retardation syndrome with preaxial brachydactyly, hyperphalangism, deafness and orodental anomalies. *Clin Dysmorphol* 1998;7:249–55.
24. Li Y, Laue K, Temtamy S, Aglan M, Kotan LD, Yigit G, Canan H, Pawlik B, Nürnberg G, Wakeling EL, Quarrell OW, Baessmann I, Lanktree MB, Yilmaz M, Hegele RA, Amr K, May KW, Nürnberg P, Topaloglu AK, Hammerschmidt M, Wollnik B. Temtamy preaxial brachydactyly syndrome is caused by loss-of-function mutations in chondroitin synthase 1, a potential target of BMP signaling. *Am J Hum Genet* 2010;87:757–67.

Journal of Human Genetics
https://doi.org/10.1038/s10038-020-0817-8

ARTICLE

Homozygous deletion of *MYADML2* in cranial asymmetry, reduced bone maturation, multiple dislocations, lumbar lordosis, and prominent clavicles

Esra Yıldız Bölükbaşı[1] · Rana Muhammad Kamran Shabbir[2] · Sajid Malik[2] · Aslıhan Tolun[3]

Received: 29 January 2020 / Revised: 28 May 2020 / Accepted: 27 July 2020

Abstract

A null mutation in a patient can facilitate phenotype assignment and uncovers the function of that specific gene. We present five sibs of a consanguineous Pakistani family afflicted with a new syndrome with an unusual combination of skeletal anomalies including cranial asymmetry, fused sagittal sutures deviating from the medial axis, mandibular prognathia, maxillary hypoplasia, misaligned and crowded teeth, delayed bone age, multiple dislocations, hypoplastic and malpositioned patellae, humeral intracondylar fissures, scapular dyskinesis, long limbs, lumbar lordosis, protruding chest, prominent clavicles, short 5th digital rays, and ventral transverse digital creases plus features of cutis laxa. We mapped the disease gene locus to a 3.62-Mb region at 17q25.3 and identified a homozygous deletion of maximal 7.3 kb deduced to totally inactivate *MYADML2* and downstream gene *PYCR1*, biallelic variants in which cause autosomal recessive cutis laxa (ARCL). All five affected sibs had the most common features of ARCL but not many of the less common ones. We attributed the anomalies not typical for ARCL to MYADML2 deficit, because no other genetic defect possibly a candidate to underlie the skeletal phenotype was found. *MYADML2* is a gene of unknown function, has not been studied, and has not been associated with disease. Our findings present a possible phenotype for MYADML2 deficit that includes impaired bone patterning and maturation, definitely show that the gene is not essential for survival, and provide a start point for future studies on the function of MYADML2 protein. Detection of new patients is needed to confirm and delineate MYADML2-deficiency phenotype.

Introduction

Phenotypes have been assigned to only 5798 of our 25424 genes covered by OMIM, and many of the genes are not listed at all in the database. There are no reports on some genes, such as *MYADML2* (PubMed), indicating that the gene has not been studied much. Identification of a null mutation in a gene as the molecular basis of a disease defines the clinical manifestations of the deficit of the encoded protein and can unravel the function of the protein.

We present five siblings born to consanguineous parents and afflicted with cutis laxa plus an unusual combination of various skeletal and other anomalies. The homozygous deletion identified in the siblings is deduced to totally inactivate both of the genes it encompasses. Those adjacent genes are transcribed in the same direction. One of them is *PYCR1*, encoding pyrroline-5-carboxylate reductase 1, and biallelic variants in the gene cause cutis laxa [1–14]. Cutis laxa is inelastic and sagging skin that tends to form loose folds, giving an appearance of premature ageing or progeria

These authors contributed equally: Esra Yıldız Bölükbaşı, Rana Muhammad Kamran Shabbir

Supplementary information The online version of this article (https://doi.org/10.1038/s10038-020-0817-8) contains supplementary material, which is available to authorized users.

✉ Sajid Malik
malik@qau.edu.pk

✉ Aslıhan Tolun
tolunasli@itu.edu.tr

[1] Department of Molecular Biology and Genetics, Boğaziçi University, Istanbul, Turkey

[2] Human Genetics Program, Department of Zoology, Faculty of Biological Sciences, Quaid-i-Azam University, Islamabad, Pakistan

[3] Department of Molecular Biology and Genetics, Istanbul Technical University, Istanbul, Turkey

Published online: 10 August 2020

[15]. Numerous variable clinical symptoms accompany the skin anomaly. The disease is also genetically highly heterogeneous. ARCL2B (MIM 612940) and ARCL3B (MIM 614438) caused by biallelic *PYCR1* variants have variable, overlapping features, and therefore they are referred together as *PYCR1*-related autosomal recessive cutis laxa (ARCL), the most common features of which are wrinkled skin, intrauterine growth retardation (IUGR), intellectual disability, aged appearance, visible veins under the skin particularly on the chest and limbs, hyperextensible joints, and hypotonia [6, 15, 16]. Less common features include postnatal growth delay, microcephaly, and osteopenia (low bone density usually in the bone shaft).

As we did not find any possibly causative variant for the features unusual for cutis laxa in the affected siblings, we hypothesized that those features result from the deletion of *MYADML2*, a gene that has not been linked to any disease.

Materials and methods

Family

Family originates from a remote area of Punjab, Pakistan. Grandmothers are sisters and grandfathers are uncle-nephew (Fig. 1). Causes of the three prenatal deaths are unknown. The five affected sibs plus five unaffected family members participating in the study were physically examined with the help of local physicians. All participants or their parents gave informed consent prior to initiation of the study, and the study protocol was approved by the Ethical Review Committee of Quaid-i-Azam University (DAS-1070) and the Istanbul Technical University Human Research Ethical Committee (MBG.22/2014).

Genetic analyses

DNA samples of father and four affected and one unaffected sib were available for genetic studies. First, we attempted to identify the disease gene locus. Genotype data for 710K SNP markers for father and three affected sibs were generated using Illumina Human OmniExpress-24 BeadChip. Multipoint linkage analysis for all autosomes plus the pseudo-autosomal regions was performed using Allegro in easyLINKAGE v.5.08, assuming autosomal recessive inheritance and a disease allele frequency of 0.001.

To search for the gene defect underlying the disease afflicting the family, we performed exome sequencing for patient 502. The Agilent SureSelect Target Enrichment System was used for exome capturing and the Illumina HiSeq2000 platform for sequencing. Exome file was analyzed to search for the putative causative variant. Rare variants with no reported homozygotes and with frequencies <0.01 in all

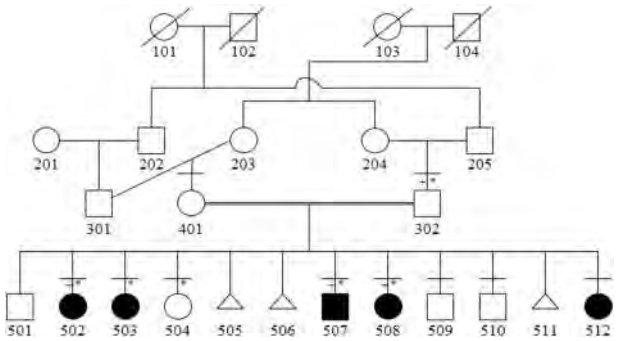

Fig. 1 Pedigree. DNA was available for individuals marked *. SNP genotype data were generated for individuals marked +. Participants clinically evaluated are marked with horizontal lines

populations listed in ESP6500, 1000 Genomes and gnomAD that includes 10,000 Pakistani exomes in the South Asian samples were selected. Those assessed as possibly homozygous (reads with the variant to total reads ratio >0.6), predicted as damaging to the protein, not found in our 56 in-lab exome files and is in a possibly relevant gene were considered as candidates to underlie the disease. Hg19 map was used throughout the study.

In order to validate the homozygous deletion identified in patients and in addition to test whether *MYADML2* exon 2 was also deleted, PCR amplification was performed targeting exons 2 and 3 of the two genes involved. Primer sequences for *MYADML2* exon 2 were F: AACCCTGTG AACCCCAGG and R: CCCAACATTTATCTCACCCCT and exon 3 were F: CTGGCCACCCTGCTATG and R: AAGGCCTGGACGATCTTG, and for *PYCR1* exon 2 were F: CCTAACTTGCTCTCGATCCT and R: GCCAGTCT CTCCCACTG and exon 3 were F: AAGAACTGAAGA GGAACTGTTT and R: GTCTCCTTTCTCCCTTTCATC.

Results

Clinical findings

The five unaffected members (parents and three sibs) clinically evaluated had no facial dysmorphism, skeletal malformation or skin anomaly. All five affected sibs were similarly affected, as we assessed by physical examination and X-ray imaging (Fig. 2a, Tables 1, 2, and Supplementary Fig. 1). Cranial asymmetry, mandibular prognathia, maxillary hypoplasia, and misaligned and crowded teeth were observed. 3D reconstructions of cranial CT (of sib 503) revealed cranial anomalies including incompletely fused sagittal sutures deviating from the medial axis, and asymmetry evident as depressions in the frontal and occipital aspects of the skull (Fig. 2b). X-ray imaging revealed osteopenia and gross skeletal anomalies affecting

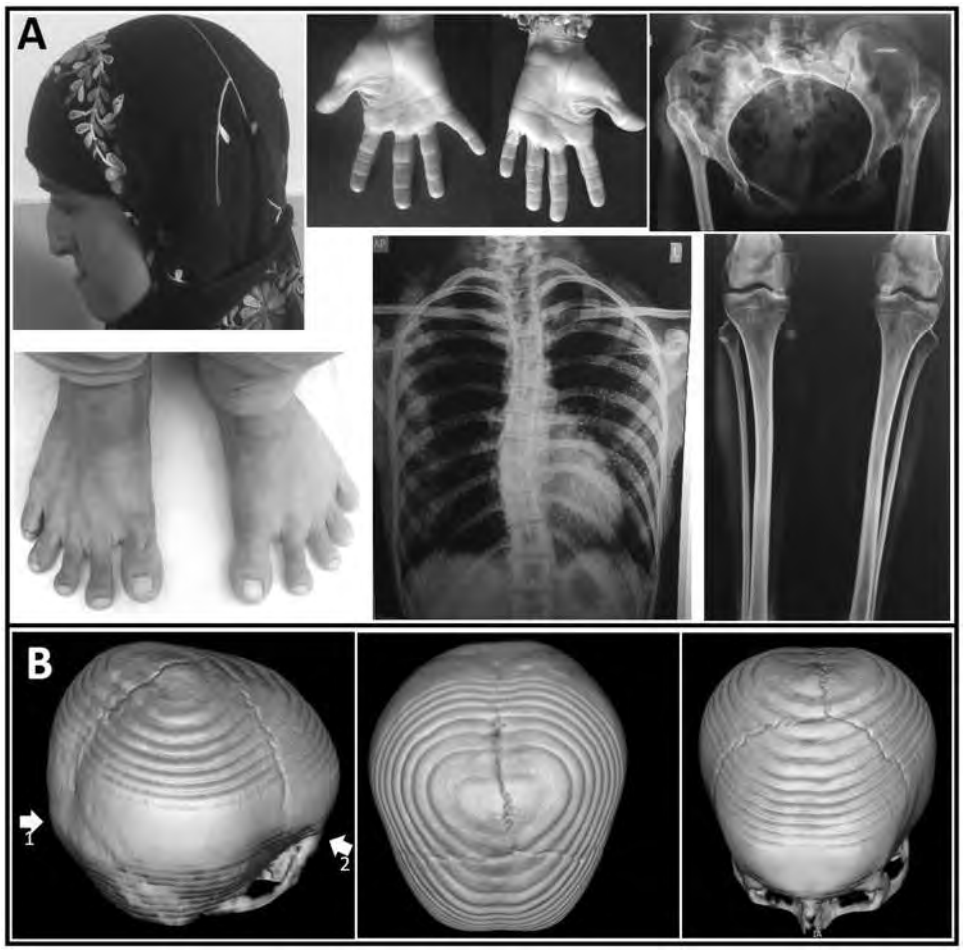

Fig. 2 Findings in patients. **a** Pictures and X-ray images of affected sib 502. Clockwise from upper left: mandibular prognathia, maxillary hypoplasia, and prominent nose bridge; thin cylindrical fingers with extra ventral phalangeal creases and shortening of fifth fingers; hypoplasia of pelvic girdle with short iliac wings, malformation of acetabula and asymmetrically and posteriorly dislocated femoral heads that articulated with the posterior aspects of iliac crests; narrowly aligned tibiae and fibulae, and hypoplastic and malpositioned patellae; general osteopenia and lack of maturation of tubular bones as evidenced by visible metaphyseal lines, unfused metaphyseal lines and poor bone mineralization; general delayed bone age indicated by the epiphyseal gaps at the end of long bones and delayed closure of epiphyseal lines; scoliosis of thoracic and lumbar spines and dislocated and hypoplastic clavicles; splayfoot; **b** 3D reconstructions of cranial CT of 503, showing cranial anomalies including incompletely fused sagittal sutures deviating from the medial axis, and asymmetry evident as depressions in the frontal and occipital aspects of the skull (arrows)

craniofacial, axial, and appendicular bones (Table 3, Fig. 2, and Supplementary Fig. 1). In the axial skeleton we noted variable scoliosis of thoracic and/or lumbar spines as well as hypoplastic and asymmetrical pelvic girdles, dislocation of proximal femoral heads, posteriorly dislocated fibulae, hypoplastic and malpositioned patellae, and splayfoot. Bilateral marked malformation of acetabula and dislocated femoral heads were mostly asymmetric. Femoral heads were completely dislocated and articulating with the posterior aspects of iliac crests. Malformations in upper limbs included dislocated and hypoplastic clavicles, scapular dyskinesis, humeral intracondylar fissures, dislocation of proximal ulnar heads, shortening of 5th digital rays, and in the youngest patient (508) additionally narrowly aligned radii and ulnae. Lack of maturation of tubular bones including those in hands, as evidenced by visible metaphyseal lines, unfused metaphyseal lines and poor bone mineralization, were indicative of osteopenia. General delayed bone age was evidenced by the epiphyseal gaps at the end of long bones and delayed closure of epiphyseal lines. Skeletal findings were also rather invariant and included short stature, joint hyperlaxity, scoliosis, lumbar lordosis, protruding sternum, prominent clavicles, flat feet, scapular dyskinesis, and cylindrical and elongated fingers and toes. On some fingers ventral transverse digital creases were present in addition to the normal flexion creases. Those extra transverse creases were not due to supernumerary osseous elements, as X-ray imaging showed that the phalangeal elements under the creases were of normal quantity.

Table 1 Clinical features of affected sibs as compared to reported *PYCR1*-related ARCL cases

Features	This study					Reported cases	
	502	503	507	508	512		
Sex, age (years)	F, 18	F, 16	M, 12	F, 10	F, 4	Total[a]	%
Wrinkled skin	+	+	+	+	+	105/106	99
IUGR	+	+	+	+	+	90/95	95
Intellectual disability	+	+	+	+	+	91/97	94
Hyperextensibility of joints	+	+	+	+	+	85/91	94
Aged appearance	+	+	+	+	+	94/102	92
Visible veins on the chest	+	+	+	+	+	59/66	89
Hypotonia	+	+	+	+	+	43/58	74
Postnatal growth delay	+	+	+	+	+	52/75	69
Microcephaly	−	−	−	+	−	42/61	69
Osteopenia	+	+	+	+	+	41/61	67
Wormian bones	NA	NA	NA	NA	NA	20/32	63
Persistent open fontanel	−	−	−	−	NA	31/50	62
Adducted thumbs	−	−	−	−	−	35/58	60
Congenital hip dislocation	+	+	+	+	NA	56/99	57
Flat feet	+	+	+	+	+	11/20	55
Corpus callosum dysgenesis	NA	−	NA	NA	NA	30/59	51
Blue sclera	−	−	−	−	−	25/58	43
Hernia	−	−	−	−	−	39/96	41
Dislocations (elbow, patella)	+	+	+	+	NA	4/12	33
Strabismus	+	+	+	+	−	19/59	32
Seizures	−	−	−	−	−	15/74	20
Athetoid or dystonic movements	−	−	−	−	−	17/89	19
Cataract or corneal clouding	−	−	−	−	−	14/99	14
Fractures	−	−	−	−	−	3/36	8

[a]Total, number of patients having the trait among those investigated for the trait, as reported in the literature

NA not assessed

Parents mentioned IUGR for all five affected sibs. Anthropometric measurements performed for four patients indicated poor developmental landmarks and in sister 508 microcephaly (severe) (Supplementary Table 1). Sibs attended normal schools but with low performance, indicative of mildly low IQ. Eldest four had developed strabismus in late childhood. All five had features reminiscent of cutis laxa, with marked progeroid features including dysmorphic facial appearance, loose wrinkled skin, and skeletal defects. Gait was abnormal, apparently due to the joint dislocations. Affected sibs had elongated and triangular face with protruding forehead, splayed eyebrows, and down slanting eyes (Fig. 2 and Supplementary Fig. 1). Ears were large and prominent, and hairline was low. Ectodermal features included sparse hair and wrinkled skin with thin, translucent appearance (Supplementary Table 1). Veins under the skin were visible throughout the body but more prominent on the abdomen and limbs. Sibs suffered from osteopenia and hypotonia, and complained of shortness of breath and early fatigue during physical activity. Ophthalmologic examination revealed alternative esotropia with normal refractive error and normal vision. Brain computed tomography scan of affected sib 503 showed normal sulci, gyri, differentiation of gray matter, brain parenchyma density, ventricles, posterior fossa, paranasal sinuses, orbits, and mastoids; hence, a normal result was concluded.

As the clinical findings were not typical of a known disease, we launched disease gene search. After our genetic studies uncovered deletions in *PYCR1* and *MYADML2*, we re-evaluated the clinical findings and assessed which phenotypic features could be attributed to PYCR1 deficit (Table 1); the remaining were attributed to MYADML2 deficit (Table 2).

Genetic findings

Linkage analysis was performed to map the putative gene defect underlying the disease in the family. We considered all regions yielding maximal multipoint LOD scores >2 and

Table 2 Clinical features of affected sibs not typical for *PYCR1*-related ARCL

Features	502	503	507	508	512
Age (years), sex	18, F	16, F	12, M	10, F	4, F
Cranial asymmetry	+	+	+	+	+
Mandibular prognathia	+	+	+	+	+
Maxillary hypoplasia	+	+	+	+	+
Misaligned/crowded teeth	+	+	+	+	NA
Dislocations of hips, knees and elbows	+	+	+	+	NA
Scoliosis[a]	+	+	+	+	NA
Lumbar lordosis[a]	+	+	+	+	NA
Protruding sternum[a]	+	+	+	+	NA
Prominent clavicles[a]	+	+	+	+	NA
Posteriorly dislocated fibulae	+	+	+	+	NA
Hypoplastic and dislocated patellae	+	+	+	+	NA
Splayed tarsal bones	+	+	−	−	NA
Dislocated and hypoplastic clavicles	+	+	+	+	NA
Scapulae winged and dyskinesis[a]	+	+	+	+	NA
Humeral intracondylar fissures	+	+	+	+	NA
Shortening of 5th digital rays	+	+	+	+	+
Cylindrical and elongated digits[a]	+	+	+	+	+
Extra flexion creases on fingers	+	+	+	+	+
Alternative esotropia	+	+	+	+	−

NA, could not be assessed due to too young age

[a]Reported for only a few cases of *PYCR1*-related ARCL

Table 3 Radiologic findings in affected sibs

Variables	502	503	507	508
Age (years), sex	18, F	16, F	12, M	10, F
Skull and orofacial				
Mandibular prognathia	+	+	+	+
Maxillary hypoplasia	+	+	+	+
Dental crowding	+	+	+	+
Cranial asymmetry	+	+	+	+
Axial skeleton and lower limbs				
Protruding chest	+	+	+	+
Scoliosis	+	+	+	+
Hypoplastic and asymmetrical pelvic girdle	+	+	+	+
Hip dislocation	+	+	+	+
Hypoplastic iliac shaft	+	+	+	+
Femoral head hypoplasia/dislocation	+	+, left	+	+
Hypoplastic and posteriorly dislocated fibulae	+	+	+	+
Hypoplastic and malpositioned patellae	+	+	+	+
Splayed tarsal bones	+	+	−	−
Upper limbs				
Dislocated and hypoplastic clavicle	+	+	+	+
Scapular dyskinesis	+	+	+	+
Humeral intracondylar fissure	+	+	+	+
Dislocation of proximal ulnar heads	+	+	+	+
Narrow spaces between radii and ulnae	−	−	−	+
Brachydactyly of 5th finger	+	+	+	+
Generally delayed bone age	+	+	+	+

+ feature present, − feature absent. Features are present bilaterally unless mentioned otherwise

with shared homozygous genotypes that were possibly due to identity by descent in the three patients with generated SNP data as candidates to harbor the disease gene (Supplementary Fig. 2). Regions with LOD scores >2 were all <1 Mb, except for the 3.62-Mb region at 17q25.3 between rs2612778 (nucleotide 77,150,807) and rs2677919 (80,774,148). Later, the remaining patient 503 without SNP data was found to be homozygous for the deletion in the region whereas unaffected sister 504 was found to be not homozygous, increasing the LOD score from 2.69 to 3.43. This region was thus identified as the disease gene locus.

In the exome file all candidate variants throughout the genome were selected. Only eight of those falls in a region of homozygosity (of any length) shared by patients only. They are all intronic and predicted as polymorphism by Mutation Taster2, the only computational algorithm that could be applied (Supplementary Table 2).

SNP genotype data in the identified gene region aligned in Microsoft Excel listed two SNPs annotated as homozygous in father and no-call in affected sibs, indicative of a homozygous deletion in sibs. Those no-call SNPs rs36101864 (nucleotide 79,898,644) and rs34319293 (79,899,900) are flanked by rs34575645 (79,891,184) and rs35810039 (79,901,665) which were read in all SNP genotype files (Fig. 3). Inspection with Integrative Genome Viewer (IGV) revealed that the two no-call SNPs indeed had not been read. Between the flanking SNPs reside some exons of *PYCR1* and *MYADML2*. Exome sequence data for the region were evaluated (Fig. 3). Inspection with IGV revealed that no reads had been aligned to exons 2 and 1 (both coding) of *PYCR1* (NM_001282281) and the upstream regulatory regions of the gene as well as to exon 3 (the sole coding exon) of *MYADML2* (NM_001145113). *MYADML2* non-coding exons 1 and 2 were not covered by exome sequencing and thus not read in any exome file including the control exome files generated in the same sequencing batch. Exons 3–8 of *PYCR1* have been covered in the patient exome file, 20X–36X. The three exons included in the exome sequencing but not read in the affected sib sample had been covered 20X–70X in the control exome files.

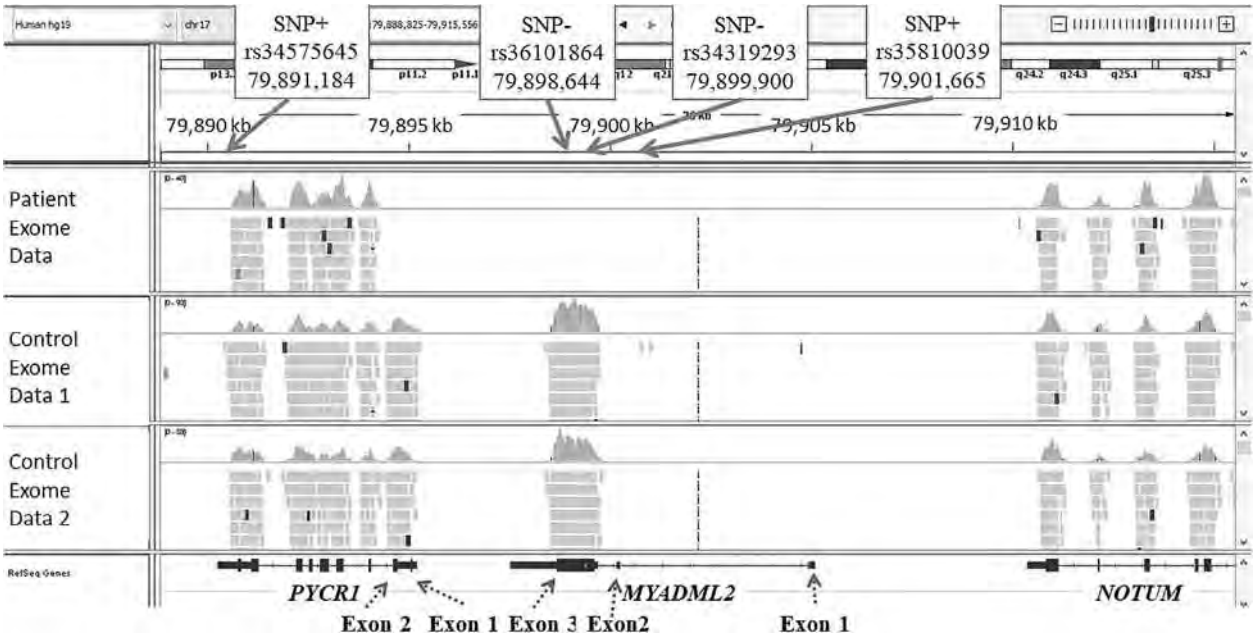

Fig. 3 The deletion. Comparison in IGV of the reads in the deleted region with the exome data of two unrelated individuals. SNP+ and SNP− are read SNPs and no-call SNPs, respectively

We attempted to amplify across the deletion junction to identify the breakpoints. However, only a few oligo primers for long-range PCR reaction could be designed around the deletion region using computational tool PrimerQuest Tool (Integrated DNA Technologies), and many attempts using those primers to amplify across the junction failed. We then attempted to PCR amplify exons 2 and 3 of the two genes of interest. We obtained products for all those exons for the DNA samples of father, unaffected sister, and control individuals. As for patient samples, we obtained product for exon 3 of *PYCR1* but not for the other three exons, validating the deletion and showing that it encompasses also exon 2 of *MYADML2*. Hence, the SNP genotype and exome data plus the PCR amplification results together indicated that the deletion extended maximally from 79,894,278 (where exome reads in patient file end) to 79,901,665 bp (rs35810039) and minimally again from 79,894,278 to 79,900,249 bp (*MYADML2* exon 2 reverse primer starts), with a length of 7.3 and 5.9 kb, respectively (Fig. 3).

We evaluated the exome data also for rare variants in genes that are responsible for multiple dislocations. The list of those genes as well as the two rare variants in exome file are presented in Supplementary Table 3. Variants were in *FLNB* and *ALDH18A1*, both heterozygous and intronic, and predicted as polymorphism by Mutation Taster2. Likewise, we evaluated for any rare variants in progeria-related genes other than *PYCR1*, namely, *BANF1, LMNA, SLC25A24, ZMPSTE24, ERCC8, NAT10, SUN2, ALDH18A1, B4GALT7, FOXM1, NAMPT, PIK3R1, SOD2, PTDSS1,* and *GH1* and telomere genes *TERT, TERC, RTEL1*, *PARN, DKC1,* and *TINF2*, as biallelic variants in all and heterozygous variants in some can cause progeria or progeria-like syndromes. Only one variant was found, the same in *ALDH18A1* mentioned above.

Discussion

The five affected sibs had a similar syndrome of an unusual combination of skeletal features and cutis laxa. Both the SNP genotype data and the exome file indicated the presence of a novel homozygous deletion encompassing the first two of the total eight exons of *PYCR1*, all coding, as well as the only coding exon (of the total three exons) of *MYADML2* [17]. By PCR amplification assay we validated the deletion and further showed that exon 2 of *MYADML2* was also deleted. The deletion of minimal 5.9 kb is deduced to completely prevent the synthesis of the proteins encoded by the two genes. *MYADML2* has not been implicated in any disease whereas biallelic variants in *PYCR1* are known to cause ARCL. In order to access the clinical manifestations of MYADML2 deficit, we evaluated our clinical findings with respect to the features in the over 100 reported cases of *PYCR1*-related ARCL and hypothesized that the non-concordant skeletal findings were due to MYADML2 deficit. The findings atypical for *PYCR1*-related ARCL are a unique combination of skeletal defects including delayed bone age, multiple dislocations, cranial asymmetry, humeral intracondylar fissures, scapular dyskinesis, and in the youngest narrow spaces between radii and ulnae.

Dislocations have been reported for *PYCR1*-related ARCL as well [14], but our patients have dislocations in all major joints of long bones, scapula, and clavicles. Our patients additionally have several features reported in only one or few *PYCR1*-related ARCL cases, such as cylindrical digits, long digits, lumbar lordosis, protruding sternum, winged scapulae, and scoliosis [2, 5, 8, 10]. Because these features are very rare and variable for *PYCR1*-related ARCL and all our patients have these features, we attributed them also to the MYADML2 deficit. However, whether those very rare features developed invariably in all of our patients due to a combined effect of the deficits of the two proteins remains to be seen when new families with MYADML2 deficit are described. We propose that MYADML2 has a role in bone maturation as well as pattern formation, as cranial asymmetry, multiple dislocations, lumbar lordosis, and prominent clavicles could be due to abnormal or disproportionate bone growth. The rare feature of extra transverse finger creases does not seem to arise from underlying bone anomalies. Could it be due to PYCR1 deficiency which manifests with skin anomalies? Perhaps it could, but such creases have not been reported for any individual with PYCR1 deficit.

Evaluation of the clinical findings in our patients with respect to all reported cases with *PYCR1*-related ARCL is presented in Table 1. Reversade et al. reported 22 families with total 35 affected individuals, evaluating patients in a family together and not individually; thus, whether all related patients have the same particular finding is not clear [3]. The largest group of patients is reported by Dimopoulou et al., 33 patients from 27 families [7]. Kariminejad et al. reviewed all reported cases plus four new patients they evaluated [16]. To their Table we added the ten patients in the most recent three reports and compared the findings in all published reports to those of our patients (Table 1) [12–14]. While our patients have all the most common features (frequency >0.73 in all reported patients, as presented in Table 1) of wrinkled skin, IUGR, ID, joint hyperlaxity, aged appearance, visible veins, hypotonia and postnatal growth delay, no patient has some of the less common features (frequency < 0.70) such as persistent open fontanel, adducted thumb, blue sclera, or hernia. In our patients clinical features are not variable, possibly because of the rather uniform genetic background expected in communities with high consanguinity, as in the village.

We attributed the features unusual for cutis laxa in the family to the deletion of *MYADML2* (Table 2), as we did not find any other possible causative variant. The gene has not been linked to any disease and is located 2406 nucleotides telomeric to *PYCR1* exon 1. It encodes myeloid-associated differentiation marker-like 2, a protein of 307 amino acids with seven transmembrane domains, each of which is 21 residues (UniProt). The protein is an integral component of the cell membrane, and its function is not known. It is not listed in OMIM or PubMed, and in ClinVar no mutation is reported. Its sequence is highly conserved in jawed vertebrates; sequence homology of human MYADML2 with chimpanzee is 99.7%, macaque 97.1%, mouse 91.5%, bird 73.4%, frog 62.8%, and zebrafish 62.3%. The gene is highly expressed in skeletal muscles and weakly in brain (Genotype Genome Expression-GTEx; the Human Protein Atlas), but bone tissue is not included in databases. MYADML2 is not involved in any of the reported pathways in KEGG, Reactome, or GO databases [17–20]. Paralog protein MYADM has a role in cell spreading and migration [17].

Our findings suggest that total MYADML2 deficit is compatible with life in humans, i.e., the encoded protein is not vital but instead most likely essential for bone maturation and morphogenesis, and the deficit manifests with a novel skeletal phenotype. Our hypothesis that MYADML2 deficit most likely underlies the findings unusual for ARCL in patients is based on several evidences: by extensive bioinformatics analysis we did not find any other candidate genetic defect in the rather small disease gene region we had identified, the deletion is novel and deleterious, the amino acid sequence of the gene is highly conserved across species, no homozygous loss-of-function variant is reported in individuals with consanguineous parents [21–23], gnomAD does not list any protein loss-of-function variant detected in homozygous state and reports that the frequencies of all such variants are <0.000038, and there is no evidence that the gene is not relevant to bone development. We propose that total MYADML2 deficit can be deleterious in contrast to the inactivation of some genes with no obvious effect on phenotype, even though gnomAD reports a pLI of 0 for the gene, indicating that it is tolerant to loss-of-function variants, and the five missense variants predicted as deleterious by computational algorithms have frequencies ranging from 0.00098 to 0.0347 and are reported in homozygous state in many individuals (gnomAD; Supplementary Table 4). However, predictions for missense variants by computational algorithms are not always reliable. One example is a variant in *GLI3*, responsible for AD polydactyly. c.2179G>A (p.Gly727Arg; rs121917710) affects both of the protein-coding transcripts, and six of the seven computational algorithms predict it as damaging to the protein: SIFT, damaging (0.01); PolyPhen-2, possibly damaging (0.8); PROVEAN, damaging (−7.34); Mutation Taster2, damaging; M-CAP, possibly damaging; and REVEL [24] benign (score is 0.505, somewhat below the recommended pathogenicity threshold of 0.6). Also, the CADD score for the variant is 26.8, indicating that the variant is at the top 0.2% of the deleterious variants predicted by CADD [25]. The gene is highly loss-of-function intolerant with pLI of 1 and o/e ratio of 0.09 (gnomAD). The altered amino acid is

totally conserved across species, down to zebrafish. gnomAD lists the frequency of the variant as highest (>0.007) in Europeans and Finns, and six homozygotes, all Europeans. Yet the variant is benign in contrast to some heterozygous damaging variants in the same gene that manifest with isolated or syndromic polydactyly (OMIM 165240). Even after manual curation it is classified as disease causing for polydactyly (UniProt). In contrast, some disease-causing missense variants are predicted as benign: Jagadeesh et al. reported that SIFT, PolyPhen-2, and CADD misclassified pathogenic variants from HGMD as benign at a rate of 38%, 31%, and 26%, respectively [26].

Amino acid sequence of PYCR1 is rather well conserved across species. Homology of human protein with chimpanzee is 99.7%, macaque 95.4%, and mouse 91.6% (HomoloGene). Twenty-nine biallelic *PYCR1* variants are known to cause ARCL (ClinVar, OMIM and references 3–5, 7–9, 12, 14). Some of the homozygous *PYCR1* variants are severe, including a 22-bp deletion (c.617_633 + 6del; NM_006907.2), c.28C>T (p.Gln10*) and a full deletion that did not extend to *MYADML2* [3, 4, 8]. There is no phenotype–genotype correlation. For example, the full deletion did not lead to a severe phenotype similarly to the deletion we identified [4]. We have mapped the disease and did not find any other candidate gene defect in the gene region.

In conclusion, we report a homozygous deletion of the coding sequences of *MYADML2* as the first disease-causing variant in the gene together with a deletion in *PYCR1*. The five affected siblings have several clinical features that are in common with *PYCR1*-related ARCL. The skeletal findings that have not been reported to date or reported as very rare in patients with biallelic *PYCR1* variant are likely due to the MYADML2 deficit. Our findings provide a start point for future studies on the function of MYADML2. Testing individuals with skeletal findings similar to those in our patients for *MYADML2* variant could validate the pathology of MYADML2 deficit and delineate its clinical manifestations.

Web resources

The URLs for data presented herein are as follows:

OMIM (Online Mendelian Inheritance in Man), http://www.ncbi.nlm.nih.gov/Omim/

UniProt (Universal Protein Resource), http://www.uniprot.org/

NCBI PubMed, https://www.ncbi.nlm.nih.gov/pubmed/ ClinVar

GeneCards, https://www.genecards.org/

NCBI-BioProject, https://www.ncbi.nlm.nih.gov/bioproject

KEGG (Kyoto Encyclopedia of Genes and Genomes), https://www.genome.jp/kegg/

Reactome, https://reactome.org/

GO (Gene Ontology) databases, http://geneontology.org/

ESP6500 (Exome Sequencing Project), https://evs.gs.washington.edu/EVS/

1000Genomes, http://www.internationalgenome.org/1000-genomes-browsers

gnomAD (Genome Aggregation Database), http://gnomad.broadinstitute.org/

HomoloGene, https://www.ncbi.nlm.nih.gov/homologene 1000Genomes

Mutation Taster2, http://www.mutationtaster.org/

SIFT (Sorting Intolerant From Tolerant), https://sift.bii.a-star.edu.sg

PolyPhen-2 (Polymorphism Phenotyping v2), http://genetics.bwh.harvard.edu/pph2/

PROVEAN (Protein Variation Effect Analyzer), http://provean.jcvi.org/index.php

M-CAP (Mendelian Clinically Applicable Pathogenicity), http://bejerano.stanford.edu/mcap/

Data availability

Additional data that support the findings of this study are available from the corresponding authors upon request.

Acknowledgements We thank the family members for their cooperation. This study was supported by the Scientific and Technological Research Council of Turkey (114Z829 to AT) and URF-QAU Pakistan (QAU-URF-2017-18 to SM).

Author contributions Conception and design: AT and SM. Analysis and interpretation: EYB, SM, and AT. Clinical data collection: RMKS and SM. Obtained funding: AT and SM.

Compliance with ethical standards

Conflict of interest The authors declare that they have no conflict of interest.

Publisher's note Springer Nature remains neutral with regard to jurisdictional claims in published maps and institutional affiliations.

References

1. Dougherty KM, Brandriss MC, Valle D. Cloning human pyrroline-5-carboxylate reductase cDNA by complementation in *Saccharomyces cerevisiae*. J Biol Chem. 1992;15:871–5.
2. Guernsey DL, Jiang H, Evans SC, Ferguson M, Matsuoka M, Nightingale M, et al. Mutation in pyrroline-5-carboxylate reductase 1 gene in families with cutis laxa type 2. Am J Hum Genet. 2009;85:120–9.
3. Reversade B, Escande-Beillard N, Dimopoulou A, Fischer B, Chng SC, Li Y, et al. Mutations in PYCR1 cause cutis laxa with progeroid features. Nat Genet. 2009;41:1016–21.

4. Kretz R, Bozorgmehr B, Kariminejad MH, Rohrbach M, Hausser I, Baumer A, et al. Defect in proline synthesis: pyrroline-5-carboxylate reductase 1 deficiency leads to a complex clinical phenotype with collagen and elastin abnormalities. J Inherit Metab Dis. 2011;34:731–9.
5. Lin DS, Chang JH, Liu HL, Wei CH, Yeung CY, Ho CS, et al. Compound heterozygous mutations in PYCR1 further expand the phenotypic spectrum of De Barsy syndrome. Am J Med Genet A. 2011;155A:3095–9.
6. Lin DS, Yeung CY, Liu HL, Ho CS, Shu CH, Chuang CK, et al. A novel mutation in PYCR1 causes an autosomal recessive cutis laxa with premature aging features in a family. Am J Med Genet A. 2011;155A:1285–9.
7. Dimopoulou A, Fischer B, Gardeitchik T, Schroter P, Kayserili H, Schlack C, et al. Genotype-phenotype spectrum of PYCR1-related autosomal recessive cutis laxa. Mol Genet Metab. 2013;110:352–61.
8. Scherrer DZ, Baptista MB, Matos AH, Maurer-Morelli CV, Steiner CE. Mutations in PYCR1 gene in three families with autosomal recessive cutis laxa, type 2. Eur J Med Genet. 2013;56:336–9.
9. Gardeitchik T, Mohamed M, Fischer B, Lammens M, Lefeber D, Lace B, et al. Clinical and biochemical features guiding the diagnostics in neurometabolic cutis laxa. Eur J Hum Genet. 2014;22:888–95.
10. Alazami AM, Al-Qattan SM, Faqeih E, Alhashem A, Alshammari M, Alzahrani F, et al. Expanding the clinical and genetic heterogeneity of hereditary disorders of connective tissue. Hum Genet. 2016;135:525–40.
11. Vahidnezhad H, Karamzadeh R, Saeidian AH, Youssefian L, Sotoudeh S, Zeinali S, et al. Molecular dynamics simulation of the consequences of a PYCR1 mutation (p.Ala189Val) in patients with complex connective tissue disorder and severe intellectual disability. J Investig Dermatol. 2017;137:525–8.
12. Ritelli M, Palit A, Giacopuzzi E, Inamadar AC, Dordoni C, Mujja A, et al. Clinical and molecular characterization of a 13-year-old Indian boy with cutis laxa type 2B: Identification of two novel PYCR1 mutations by amplicon-based semiconductor exome sequencing. J Dermatol Sci. 2017;88:141–3.
13. Lessel D, Ozel AB, Campbell SE, Saadi A, Arlt MF, McSweeney KM, et al. Analyses of LMNA-negative juvenile progeroid cases confirms biallelic POLR3A mutations in Wiedemann-Rautenstrauch-like syndrome and expands the phenotypic spectrum of PYCR1 mutations. Hum Genet. 2018;137:921–39.
14. Onoufriadis A, Nanda A, Sheriff A, Tomita K, Gomaa NS, Simpson MA, et al. Consanguinity and double recessive gene pathology: cutis laxa (PYCR1) and nephrotic syndrome (PLCE1). JAMA Dermotol. 2019;155:257–9.
15. Morava E, Guillard M, Lefeber DJ, Wevers RA. Autosomal recessive cutis laxa syndrome revisited. Eur J Hum Genet. 2009;17:1099–110.
16. Kariminejad A, Afroozan F, Bozorgmehr B, Ghanadan A, Akbaroghli S, Khorram Khorshid HR, et al. Discriminative features in three autosomal recessive cutis laxa syndromes: cutis laxa IIA, cutis laxa IIB, and geroderma osteoplastica. Int J Mol Sci. 2017;18:E635.
17. Aranda JF, Reglero-Real N, Kremer L, Marcos-Ramiro B, Ruiz-Saenz A, Calvo M, et al. MYADM regulates Rac1 targeting to ordered membranes required for cell spreading and migration. Mol Biol Cell. 2011;22:1252–62.
18. Kanehisa M, Furumichi M, Tanabe M, Sato Y, Morishima K. KEGG: new perspectives on genomes, pathways, diseases and drugs. Nucleic Acids Res. 2017;45:D353–61.
19. Fabregat A, Jupe S, Matthews L, Sidiropoulos K, Gillespie M, Garapati P, et al. The reactome pathway knowledgebase. Nucleic Acids Res. 2018;46:D649–55.
20. The Gene Ontology C. The Gene Ontology Resource: 20 years and still GOing strong. Nucleic Acids Res. 2019;47:D330–8.
21. Gudbjartsson DF, Sulem P, Helgason H, Gylfason A, Gudjonsson SA, et al. Sequence variants from whole genome sequencing a large group of Icelanders. Sci Data. 2015;2:150011.
22. Narasimhan VM, Hunt KA, Mason D, Baker CL, Karczewski KJ, Barnes MR, et al. Health and population effects of rare gene knockouts in adult humans with related parents. Science. 2016;352:474–7.
23. Saleheen D, Natarajan P, Armean IM, Zhao W, Rasheed A, Khetarpal SA, et al. Human knockouts and phenotypic analysis in a cohort with a high rate of consanguinity. Nature. 2017;544:235–9.
24. Ioannidis NM, Rothstein JH, Pejaver V, Middha S, McDonnell SK, Baheti S, et al. REVEL: an ensemble method for predicting the pathogenicity of rare missense variants. Am J Hum Genet. 2016;9:877–85.
25. Rentzsch P, Witten D, Cooper GM, Shendure J, Kircher M. CADD: predicting the deleteriousness of variants throughout the human genome. Nucleic Acids Res. 2019;47:D886–94.
26. Jagadeesh KA, Wenger AM, Berger MJ, Guturu H, Stenson PD, Cooper DN, et al. M-CAP eliminates a majority of variants of uncertain significance in clinical exomes at high sensitivity. Nat Genet. 2016;48:1581–6.